Analysis of the spore formation process in *Myxococcus xanthus*

D I S S E R T A T I O N

zur Erlangung des Doktorgrades der Naturwissenschaften
(Dr. rer. nat.)

dem
Fachbereich Biologie
der Philipps-Universität Marburg

vorgelegt von

Frank-Dietrich MÜLLER

aus Zwickau

Marburg/Lahn im Januar 2009

Vom Fachbereich Biologie der Philipps-Universität Marburg als Dissertation am

_____ angenommen.

Erstgutachter:	Prof. Dr. MD Lotte Søgaard-Andersen
Zweitgutachter:	Prof. Dr. Renate Renkawitz-Pohl
Tag der mündlichen Prüfung:	31.03.2009

Die Untersuchungen zur vorliegenden Arbeit wurden von Dezember 2005 bis November 2008 am Max-Planck-Institut für terrestrische Mikrobiologie Marburg unter der Leitung von Dr. Penelope I. Higgs durchgeführt.

*

Die während der Promotion erzielten Ergebnisse wurden und werden in folgenden Originalpublikationen veröffentlicht:

Müller, F.-D. & Jakobsen, J. S. (2008). Expression analysis. In: Myxobacteria. Multicellularity and Differentiation. D. E. Whitworth (ed). Washington, D.C.: ASM Press, pp. 479 - 489.

Müller, F.-D. & Higgs, P. I. (2009). Identification of a novel locus involved in spore formation in *Myxococcus xanthus* by transcriptome profiling. *In preparation.*

*

Ergebnisse aus in dieser Dissertation nicht erwähnten Projekten sind in folgenden Originalpublikationen veröffentlicht:

Kleinsteuber, S., Müller, F.-D., Chatzinotas, A., Wendt-Potthoff, K., Harms, H. (2008). Diversity and *in situ* quantification of Acidobacteria subdivision 1 in an acidic mining lake. FEMS Microbiol Ecol. 63(1): 107-17.

KURZFASSUNG

Myxococcus xanthus ist ein Vertreter Gram-negativer Bakterien, die die Fähigkeit besitzen, als Antwort auf sich verschlechternde Umweltbedingungen widerstandsfähige und metabolisch inaktive Sporen zu bilden. Im Gegensatz zu bereits gut untersuchten Gram-positiven Modellorganismen, die Sporen durch spezialisierte Zellteilung hervorbringen, werden *M. xanthus*–Sporen durch Abrunden vollständiger, stäbchenförmiger Zellen gebildet. Die Sporulation erfolgt normalerweise innerhalb multizellulärer Fruchtkörper als letztes Stadium eines komplizierten, durch Nährstoffmangel induzierten Entwicklungsprogramms. Die Analyse des Sporulationsprozesses wird durch das Auftreten nicht sporulierender Teilpopulationen innerhalb einer sich differenzierenden Kolonie sowie den geringen Anteil der tatsächlich sporenbildenden Zellen und die hohe Widerstandsfähigkeit der Sporen nachhaltig erschwert. Deshalb wurde in der vorliegenden Arbeit die glycerininduzierte, synchrone Sporulation als Modell für den Differenzierungsprozess vegetativer *M. xanthus*-Zellen in resistente, sphärische Sporen genutzt. Eine Transkriptomanalyse der glycerin-induzierten Zellen mit Hilfe von Microarrays ergab, dass während der ersten vier Stunden nach erfolgter Induktion 1.596 Gene mindestens zweifach höher oder niedriger transkribiert werden, als in vegetativen Zellen. Es konnte gezeigt werden, dass die Gruppe der differentiell regulierten Gene die meisten der bisher beschriebenen sporulationsspezifischen Markergene enthält, nicht jedoch Gene, die für Aggregation und Fruchtkörperbildung spezifisch sind. Diese Ergebnisse zeigen, dass die Glycerininduktion speziell den Sporulationsprozess aktiviert und als Modellsystem für die Differenzierung vegetativer *M. xanthus*-Zellen geeignet ist.

Die Analyse der Microarraydaten führte zur Identifikation eines bisher unbeschriebenen Genclusters, der als *nfs* (*n*ecessary *f*or *s*porulation) bezeichnet wurde. Alle acht hier codierten Proteine besitzen keine Homologie zu bereits charakterisierten Proteinen. *In-frame*-Deletion aller acht Gene führte zu einem Defekt sowohl in glycerin- als auch in nährstoffmangelinduzierter Sporenbildung, während Aggregation und Fruchtkörperbildung nicht beeinträchtigt waren. Von der *nfs*-Promotorregion ausgehende Transkription war 30 Minuten nach Glycerininduktion und während nährstoffmangelinduzierter Sporulation ausschließlich in der sporenbildenden Subpopulation nachweisbar. Diese Ergebnisse lassen darauf schließen, dass die *nfs*-Gene den zentralen Sporulationsgenen zugehören. Die glycerininduzierte Sporulation führte zu vorübergehendem Auftreten morphologisch aberranter Zellen. Die Analyse verschiedener Entwicklungsmutanten weist außerdem darauf hin, dass die Expression der *nfs*-Gene während nährstoffmangelinduzierter Sporulation C-Signal abhängig ist und durch FruA kontrolliert wird. Zellfraktionierung, Bioinformatik- und Immunoblot-Analysen legen nahe, dass die Nfs-Proteine mit der Zellhülle assoziiert sind und interagieren. Die Ergebnisse lassen insgesamt darauf schließen, dass die Nfs-Proteine für die Bildung widerstands- und lebensfähiger Sporen essentiell sind und einen speziell während der Sporulation gebildeten und in der Zellhülle verankerten Komplex bilden.

Darüber hinaus wurde die Rolle des filament- und cytoskelettbildenden Proteins MreB bei der Zellform-Konversion während der Sporenbildung und Sporenkeimung in *M. xanthus* untersucht. MreB ist in den meisten stäbchenförmigen Bakterien maßgeblich an der Aufrechterhaltung der Zellform sowie an Wachstums- und Zellteilungsprozessen beteiligt. Immunoblot-Analysen legen nahe, dass MreB während glycerininduzierter Sporenbildung in vergleichbaren Mengen erhalten bleibt, während nährstoffmangel-induzierter Sporenbildung jedoch abgebaut wird. Dies deutet an, dass alternative Mechanismen der Zellformkonversion in *M. xanthus* existieren. Ferner weist die Analyse der Sporenkeimung in Gegenwart der MreB-destabilisierenden Verbindung A22 darauf hin, dass die Bildung polymerer MreB-Filamente einen wesentlichen Schritt während des Keimungsprozesses, also während der Konversion sphärischer Zellen in stäbchenförmige, darstellt.

Die in dieser Arbeit erzielten Ergebnisse eröffnen die Möglichkeit, mit Hilfe von *M. xanthus* als Modellorganismus fundamentale Mechanismen der Entstehung bakterieller Zellmorphologie, gesteuerter Konversion der Zellform, Zellwandsynthese und Bildung resistenter Sporen in Gram-negativen Bakterien zu entschlüsseln.

ABSTRACT

Myxococcus xanthus is a representative of Gram-negative bacteria that are able to form quiescent, environmentally-resistant spores in response to changes in environmental conditions, such as nutrient depletion. *M. xanthus* spores are formed inside fruiting bodies as final stage of an elaborate developmental program. In contrast to well studied Gram-positive spore formers, where sporulation is linked to cell division, *M. xanthus* spores are formed by rounding up of an entire rod-shaped cell. Studies on the core sporulation process in *M. xanthus* are impeded by the complexity of the starvation induced developmental program, subpopulations within a developing colony, the low proportion of cells that convert into spores, and their high mechanical resistance. We took advantage of the glycerol induced spore formation process and performed micro array analysis. This study revealed that 1,596 genes are significantly at least two-fold up- or down-regulated within four hours after addition of the inducer. Most of the genes that previously have been identified to play a role during starvation induced sporulation were found to be up-regulated indicating that the glycerol induced sporulation is an appropriate model to study the core sporulation process in *M. xanthus*.

The array data analysis led to identification of a novel and highly up-regulated genomic locus termed *nfs* (*n*ecessary *f*or *s*porulation). The *nfs* locus encodes for eight proteins that show no homology to characterized proteins. Bioinformatics, mutational and immunoblot analysis suggest that the Nfs-proteins localize to the cell envelope and form a complex. In-frame deletion of the *nfs*-genes led to a severe defect both in glycerol and starvation induced sporulation, whereas aggregation was not affected. In response to glycerol induction, the Δ*nfs* mutant displayed transiently aberrant cell morphology. Transcription from the *nfs*-promoter was detectable 30 minutes after induction with glycerol. Translational fusion of the putative promoter region to *mcherry* as reporter suggests that the *nfs*-genes only accumulate in spores. Analysis of *nfs*-expression in developmental mutant backgrounds suggests that *nfs*-expression is dependent on C-signaling and controlled by FruA. Based on this observation it is hypothesized that the Nfs proteins are specifically expressed during spore formation, that they form a cell envelope-associated complex and that they play a crucial role in generating viable spores.

In addition, the role of the filament-forming cytoskeletal protein MreB was analyzed in respect to spore formation using genetic and biochemical approaches. MreB plays a crucial role in maintaining a rod-like cell shape in most known rod-shaped bacteria and has been shown to be a key-organizer of cell wall synthesis. The results suggest that the protein stays present during glycerol induced spore formation but becomes degraded during starvation induced spore formation suggesting two alternative ways of sphere formation in *M. xanthus*. Assays of spore germination with the MreB perturbing compound A22 revealed that MreB polymerization is an important precondition for germination of spherical spores, i.e. when cells re-establish rod-like cell morphology.

The results of this work could provide a set of tools that can be used to reveal fundamental mechanisms of cell shape determination and coordinated cell shape conversion during spore formation as well as peptidoglycan synthesis with respect to cell morphogenic events in Gram-negative bacteria.

ACKNOWLEDGEMENTS

I am deeply indebted to my supervisor Dr. Penelope I. Higgs for her guidance, suggestions and encouragement throughout my research and thesis.

I wish to express my sincere gratitude and appreciation to my thesis committee members, Prof. Dr. MD Lotte Søgaard-Andersen, Prof. Dr. Renate Renkawitz-Pohl, Prof. Dr. Martin Thanbichler and PD Dr. Michael Feldbrügge and my IMPRS thesis committee for their invaluable time for ideas, and comments.

A special thanks to Petra Mann for her excellent technical assistance throughout my work in Marburg. Moreover, I would like to thank Dr. Sigrun Wegener-Feldbrügge for help in micro array data analysis and constructive discussions and I am grateful to Dr. Kai Thormann for collaboration in confocal laser scanning microscopy. I also thank Dr. Stuart Huntley for his help in bioinformatics. I would also like to thank Anna-Lena Müller and Emöke Cserti for their technical help in the lab. I would like to extend my thanks to IMPRS coordinators Dr. Juliane Dörr (former), Dr. Ronald Brudler (present) and Susanne Rommel for their help in official issues.

I would like to gratefully acknowledge all colleagues from the Higgs lab for productive discussions. I thank all past and present members of the Department of Ecophysiology for providing a friendly working environment; and I would like to thank Dr. Jimmy Jakobsen and Steffi Lindow for their support at the beginning of my work.

In a special way, I would like to express my deepest gratitude to my family, for their encouragement and unconditional support throughout my life and in particular during my studies. In addition, I express my sincere thanks to all those who contributed to this thesis in one way or the other.

TABLE OF CONTENTS

ABBREVIATIONS

A22	*S*-(3,4-dichlorbenzyl)isothiourea
APS	Ammonium persulfate
bp	Base pairs
CTT	Casitone Tris medium
CTTYE	Casitone Tris Yeast Exctract medium
CYE	Casitone Yeast Extract medium
cDNA	single stranded complementary DNA
DMF	Dimethylformamide
DTT	Dithiothreitol
EDTA	Ethylendiamine tetraacetic acid
gDNA	genomic DNA
HEPES	4-(2-hydroxyethyl)-1-piperazineethanesulfonic acid
IPTG	Isopropyl β-D-1-thiogalactopyranoside
kb	Kilo base pairs
LB	Luria-Bertani medium
MOPS	Morpholinepropanesulfonic acid
Ni-NTA	Nickel-nitriloacetic acid
PMSF	Phenylmethylsulfonylfluoride
rpm	rounds per minute
rt	room temperature
SDS	Sodium dodecylsulfate
TE	Tris-EDTA
TEMED	*N,N,N',N'*-Tetramethylethylendiamine
Tris	Tris-(hydroxymethyl)-aminomethane
wt	wild type
X-Gal	5-bromo-4-chloro-3-indolyl- β -D-galactopyranoside

1 INTRODUCTION

1.1 Spore forming bacteria

Free living bacteria are exposed to changes of environmental conditions such as pH- or osmotic shifts, nutrient limitation and predation. These changes can exert physical or biochemical stresses. To survive under unfavorable conditions, many species have developed the ability to form resistant dormant stages as an adaptive response. These stages are characterized by decreased metabolical activity and increased resistance to harmful environmental traits such as desiccation, heat, UV-irradiation and enzymatic or mechanical disintegration (Sonenshein *et al.*, 1993, Whitworth, 2008). The most robust entities displaying large changes in metabolism, cell envelope structure and -shape are spores. The spore envelope forms the first and most important barrier against the detrimental factors acting from the surrounding milieu. A characteristic feature of spores is therefore an enhanced cell envelope consisting of modified call wall and membranes, and they are surrounded by polymeric surface layers that are not found in vegetative cells.

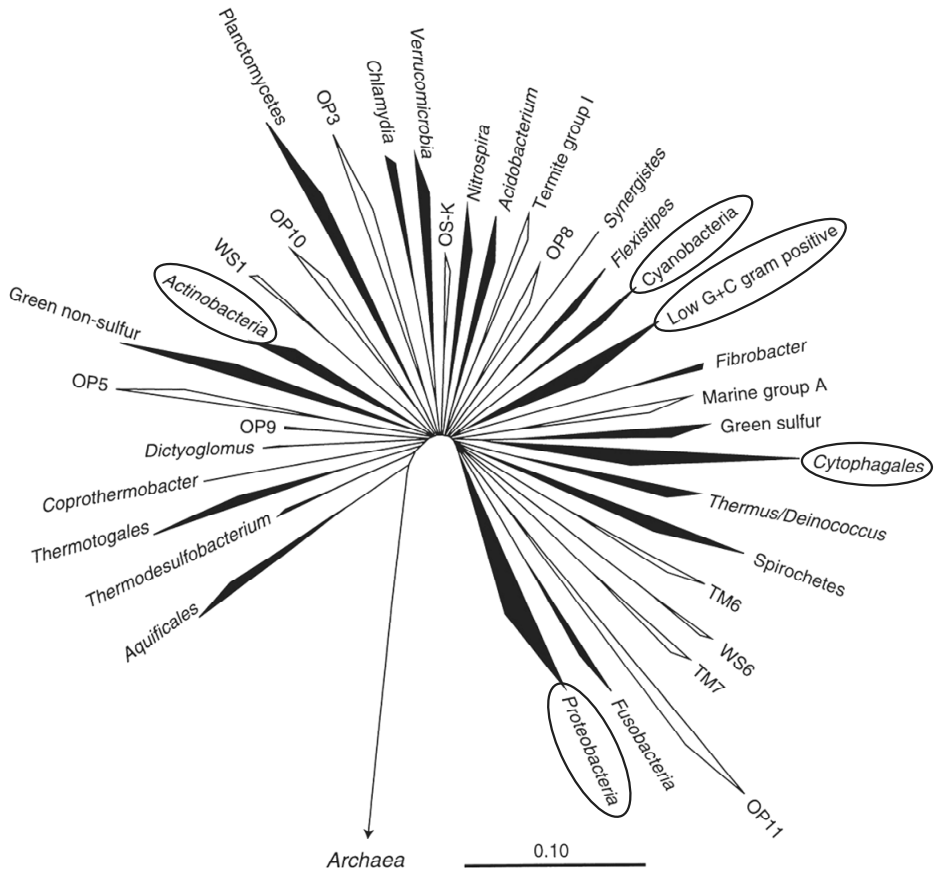

Figure 1-1 Proposed evolutionary distance tree of the bacterial domain showing recognized divisions and candidate divisions (taken from (Hugenholtz *et al.*, 1998)). Phyla containing characterized spore-forming species are circled.

The ability to form spores is known from a variety of bacteria. To date, the best studied model systems for bacterial spore formation are found in the Gram-positive *Bacillus*, *Clostridium* and *Streptomyces* species. In these bacteria, spore formation is accomplished by progression through distinct stages including initiation, chromosome segregation, sporulation-specific cell division (asymmetric in rod-shaped bacteria), differential gene expression and specific signal transduction mechanisms. This means that in Gram-positives, sporulation is generally connected to a distinct mechanism of cell division (Barak *et al.*, 2005). Interestingly however, resistant dormant stages are also known from Gram-negative bacteria such as *Sporocytophaga* sp. (Bacteroidetes/Cytophagales), Cyanobacteria, *Methylosinus*, *Methanobacterium*, *Rhodospirillum* and *Azospirillum* (Alphaproteobacteria), *Azotobacter* (Gammaproteobacteria) or Myxococcales species (Deltaproteobacteria) (**Figure 1-1**). Whereas the spore formation process in Gram-positives has been successfully studied for decades, sporulation in Gram-negative bacteria is poorly understood.

1.1.1 *Bacillus subtilis*

In *B. subtilis* (and similarly in *Clostridium sp.*), a complex set of inter- and intracellular signals is evaluated before a cell enters the sporulation pathway. Such signals are nutrient availability, glucose utilization and activity of the citrate and glyoxylate cycles, DNA integrity and state of chromosome replication. Initial key regulators are σ^H and the transcriptional regulator Spo0A whose activity is controlled by a phospho-relay system. Both factors control the expression of more than 500 genes (Barak *et al.*, 2005). If the sporulation process has been initiated, the cell is committed to proceed. A current round of chromosome replication is finished and initiation of a new cycle is prevented. The origin regions of the chromosomes are separated by moving and tethering them to opposite cell poles (**Figure 1-2 a**). Septum formation is initiated by the FtsZ protein that assembles into the Z ring which recruits the machinery necessary for cytokinesis (Carballido-Lopez & Formstone, 2007, Pichoff & Lutkenhaus, 2007). In contrast to vegetative cell division, the FtsZ-ring does not localize at midcell but instead asymmetrically at a polar site leading to transient trapping of one chromosome in the forming septum and placement of specific genes inside the forespore. To ensure that the emerging spore later contains one complete DNA molecule, the trapped DNA is actively pumped into the forespore by SpoIIIE. Further Spo0A~P accumulation is subsequently inhibited in the forespore but continues in the mother cell. This initiates unequal gene expression cascades in both compartments but there exists also a crosstalk between mother cell and the developing spore. Spo0A~P triggers indirectly expression of σ^E in the mother cell, whereas Spo0A~P disappears in the forespore leading to synthesis of σ^F (**Figure 1-2 a**). σ^F becomes active after the septum has formed, and generates a signal that activates σ^E in the mother cell. The forespore subsequently gets engulfed by the mother cell's membrane leading to a second membrane-layer surrounding the forespore. σ^G is subsequently activated in the spore and generates a signal that produces active σ^K in the mother cell. Subsequently, cortex material consisting of weakly cross-linked peptidoglycan is synthesized between the two spore membranes and deposited as spore cortex. The spore coat proteins are then synthesized in the mother cell and assembled on the cortex. Finally, the mother cell undergoes

autolysis and the spore is set free (reviewed in (Piggot & Losick, 2002), (Piggot & Hilbert, 2004) and (Errington, 2003)). The whole endospore forming process in *B. subtilis* takes about eight hours.

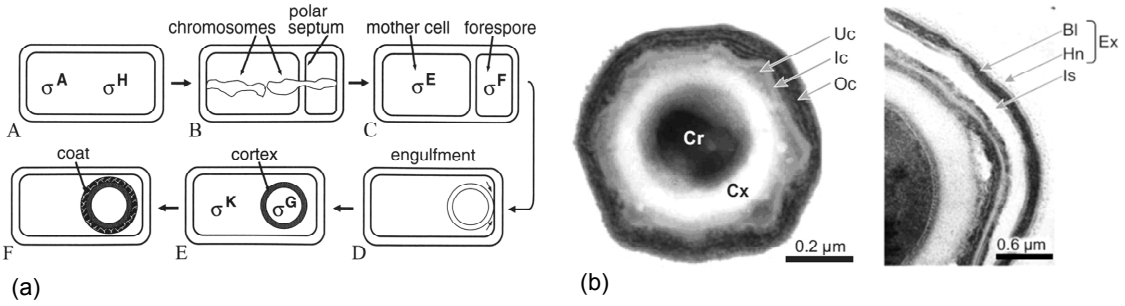

Figure 1-2 (a) Schematic view of spore formation in *Bacillus*, taken from (Kroos *et al.*, 2008). (b) Spore ultra structure. Cr: core, Cx: cortex, Uc: undercoat, Ic: inner coat, Oc: outer coat, Ex: exosporium, Bl: basal layer, Hn: glycoprotein nap, Is: inter space. Taken from (Waller *et al.*, 2004). See text for details.

1.1.2 The *Bacillus* endospore

The endospore is a complex, multi-layered structure (**Figure 1-2 b**). The DNA-containing core is surrounded by the inner spore membrane. This membrane is covered by two distinct layers of peptidoglycan, called cortex. The cortex is covered by a triple-layered coat consisting of peptides and proteins. Finally, the coat is enclosed in a loose-fitting glycoprotein structure termed exosporium. Both external layers encase an interspace compartment. Interestingly, all envelope components above the inner layer of the cortex are synthesized and deposited by the mother cell (Henriques & Moran, 2007). Hardening the spore against environmental traits involves desiccation and accumulation of small acid soluble proteins (Sasp's) that protect the spore DNA and serve as amino acid source during germination. Incorporation of dipicolinic acid in the cortex is also essential for resistance and germination (Magge *et al.*, 2008).

It appears that most proteins detected in the spore coat are structural proteins controlling their own multimeric assembly and that of the whole coat (Kim *et al.*, 2006). Interestingly, the coat proteins and peptides are frequently post-translationally modified by glycosylation, cross-linking, proteolytic processing or they are assembled in the mature coat in either homo- or heteromultimeric forms (Isticato *et al.*, 2004, Zilhao *et al.*, 2004). The function of the coat proteins is partially understood. Their major role in *B. subtilis* is to protect the spore from enzymatic and chemical attacks such as from hydrogen peroxide, chlorine dioxide or ozone (Setlow, 2006). A defective spore coat also compromises the spore cortex to lysozyme and renders the spore prone to digestion by protozoans (Klobutcher *et al.*, 2006). The exosporium known from other *Bacillus* species may help to escape phagocytosis in eukaryotic hosts (Henriques & Moran, 2007). Some of the spore coat proteins display enzymatic activities and are probably involved in sensing environmental conditions (Enguita *et al.*, 2002, Costa *et al.*, 2004). The coat proteins are also involved in control of germination (Bagyan & Setlow, 2002, Moir, 2006). Moreover, the entire coat structure can fold and unfold allowing adaptation to a changing spore volume such as shrinking during desiccation and swelling during germination.

1.1.3 Spore formation in *Streptomyces* spp.

A second model system for spore formation is the filamentous growing Gram-positive genus *Streptomyces*. In these bacteria, chains of spores are formed at the tips of distinct filaments that rise from the substrate. This means, in contrast to *Bacillus*, *Streptomyces* cells need to grow to form compartments that differentiate into spores.

The signals that initiate the differentiation process are not yet well characterized. Nutrient limitation as well as intercellular signaling plays a role. Detachment of the differentiating filaments from the substrate is facilitated by secretion of hydrophobic proteins. Upon spore formation, growth of these filaments ceases and single chromosomes are separated into pre-spore compartments (**Figure 1-3**). At least two distinct complex gene expression cascades have been identified to regulate the process (Ausmees *et al.*, 2007). The *bld* cascade regulates initiation of aerial growth (*bld* stands for *bald* because of the missing aerial hyphae), whereas the *whi* genes control later steps such as chromosome segregation and septum formation (*whi* stands for *white* because of abolished pigment synthesis) (Chater, 2001, Claessen *et al.*, 2006).

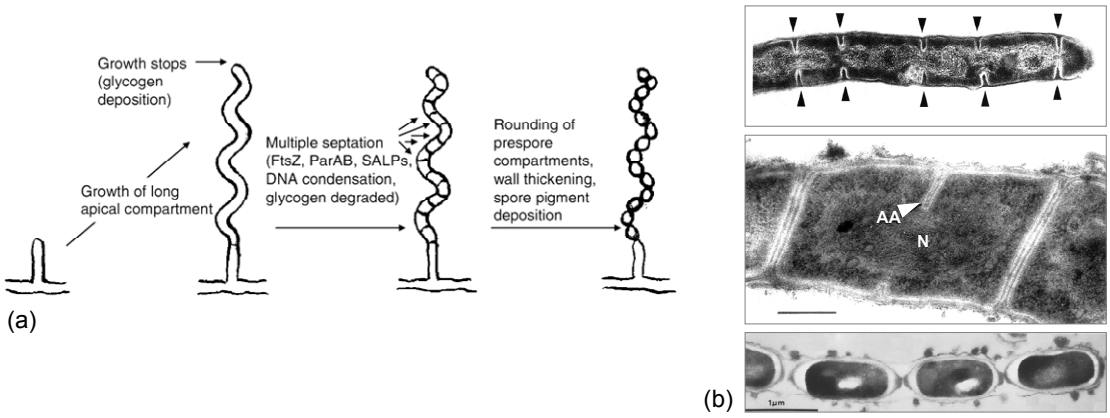

Figure 1-3 (a) Schematic view of spore formation in the Gram-positive filamentous *S. coelicolor* (taken from (Chater & Chandra, 2006)). (b) Process of spore formation in *Streptomyces* sp. shown by electron micrographs. Single spores are separated by growing sporulation septa. AA: Double edge of ingrowing annulus, N: nucleoid. Taken from (Hardisson & Manzanal, 1976) and (Vobis & Zimmermann, 1984).

Interestingly, *Streptomyces* lacks many cell division related genes essential for other bacteria such as *ftsA*, *minCD*, *ftsB*, *N* and others. Vegetative filaments septate only occasionally and even mutants unable to form septa are still viable. Therefore, the filamentous vegetative cells contain an unspecific number of chromosomes. Furthermore, the conserved cell division proteins *ftsZ*, *ftsQ* and *mreB* are dispensable for vegetative growth, but they are essential to septate and therefore to form spores (Mazza *et al.*, 2006). This means, in *Streptomyces*, chromosome replication is independent of cell division but chromosome segregation and cell division are essential for proper spore formation. This is underlined by the role of *ftsZ*. Although dispensable for vegetative growth, *ftsZ* plays a crucial role in sporulation. In *S. coelicolor*, *ftsZ* possesses three promoters that allow a tightly controlled gene expression. The amount of FtsZ in aerial hyphae was found to be much higher than in vegetative filaments probably supporting the high number of septa necessary for spore formation.

1.1.4 Gram-negative spore formers

In contrast to the model Gram-positive spore formers, sporulation in Gram-negative bacteria is not well understood. Not only the overall cell envelope architecture of vegetative cells and, as far as known, of spores differs largely, but the whole process of spore formation is very different. Characterized spores of Gram-negative bacteria are resistant to desiccation, detergents, ultrasound and UV-radiation but they display less heat resistance than spores from Gram-positives (Whittenbury & Dow, 1977, Titus *et al.*, 1982).

(a) 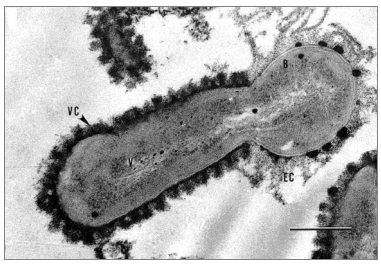

(b) 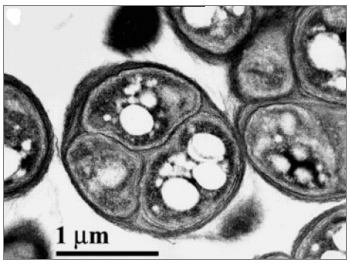

Figure 1-4 Electron micrographs of a spore-budding *Methylosinus* cell (a) (Titus *et al.*, 1982) and *Rhodospirillum* cysts (b) (Berleman & Bauer, 2004).

Spores from *Methylosinus* species (Alphaproteobacteria) are termed exospores. These entities are budded off from vegetative cells (**Figure 1-4 a**). Therefore, a cell-division event seems to be involved in exospore formation. In contrast, *Rhodospirillum* forms resting states termed cysts directly from vegetative cells, apparently circumventing cell division. Occasionally, few cysts can be enclosed in a common envelope (**Figure 1-4 b**). The nitrogen fixing genus *Azotobacter* (Gammaproteobacteria) has been studied in more detail. Desiccation-resistant cysts of these bacteria are enclosed by carbohydrate capsules that mainly consist of alginate. AlgU, an alternative sigma factor, plays an essential role in capsule formation and encystment (Gaona *et al.*, 2004). A common characteristic of Gram-negative resting cells seems to be accumulation of carbohydrates in the cell envelope (Sutherland & Mackenzie, 1977). However, the molecular mechanisms that enable vegetative cells to differentiate into resistant stages with large changes in morphology and metabolism are mainly unknown.

1.2 Spore formation in *Myxococcus xanthus*

1.2.1 Starvation-induced development

The most intriguing group of Gram-negative spore formers belongs to the Myxococcales order within the Deltaproteobacteria. Most known species within this order are characterized by a complex, multicellular lifecycle that culminates in formation of spherical myxospores (Kaiser, 2004). A model organism in this group is *Myxococcus xanthus*. The vegetative growing rod-shaped cells are common in soils and on decaying organic matter. They are able to move by gliding and form swarms that feed cooperatively on organic compounds or other microorganisms by secretion and pooling of lytic enzymes (Reichenbach, 1999). When nutrients are depleted, *M. xanthus*

swarms initiate an elaborate developmental program. Rod-shaped cells aggregate into mounds containing approximately 100,000 cells. The mounds compact into fruiting bodies and only the cells inside these fruiting bodies undergo distinct morphological changes, i.e. they differentiate into spherical, thick walled, resistant and metabolically quiescent spores. Non-aggregating cells form at least two more distinct subpopulations: Peripheral rods and cells that undergo programmed cell death. The latter fraction accounts for up to 90% of the entire population (Nariya & Inouye, 2008). The whole process of sporulation takes at least 72 hours. Mature myxospores are viable for several years (Harris & Singer, 1998). Upon sensing nutrient-rich conditions, spores germinate and re-enter the vegetative cycle (**Figure 1-5**).

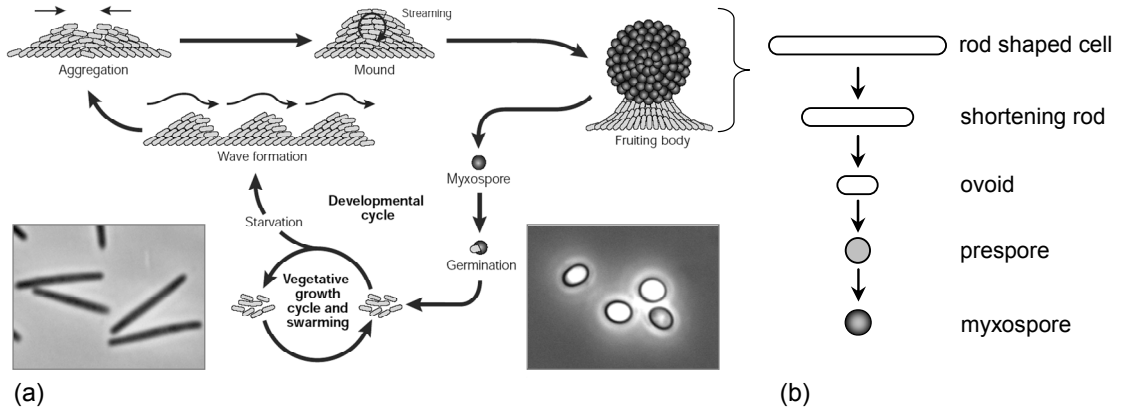

Figure 1-5 (a) Life cycle of *M. xanthus*. (taken from (Kaiser, 2003), modified). Phase contrast images of vegetative, rod-shaped *M. xanthus* cells and starvation-induced spores obtained from fruiting bodies illustrate the differentiation. (b) Schematic view of morphological changes during differentiation into myxospores that normally occurs inside fruiting bodies. Rod shaped cells shorten until they form ovoids and non-refractile spherical pre-spores. The pre-spores maturate into resistant myxospores.

The starvation-induced developmental process is controlled by a series of intra- and intercellular signaling and temporal and spatially coordinated gene expression (Kaiser, 2004). A number of regulatory genes and enzymatic activities have been identified to play a crucial role during the starvation-induced development.

Current models (Søgaard-Andersen, 2004, Kaiser, 2004, Nariya & Inouye, 2008) suggest that the developmental program is initiated by sensing of nutrient limitation. Synthesis of (p)pGpp triggers A-signaling. The A-signal consists of specific amino acids and short peptides and is thought to serve as a quorum sensing messenger. Development only proceeds if a certain minimal population density is present (Plamann & Kaplan, 1999). The A-signal is probably perceived by SasS, a membrane bound histidine kinase that transduces the signal to SasR, its cognate response regulator. SasR is proposed to trigger expression of A-signal dependent genes (Kaiser, 2004) such as *mrpAB* and *C*. MrpC is a transcriptional regulator of the cyclic AMP receptor family. To activate downstream developmental genes, MrpC needs to be cleaved and its proteolytic product MrpC2 activates the key developmental transcriptional regulator gene, *fruA* (Nariya & Inouye, 2006) (**Figure 1-6**). *fruA* encodes for an orphan response regulator containing an N-terminal receiver and a C-terminal DNA binding domain. The

fruA-mutant is unable to aggregate (Ellehauge *et al.*, 1998, Horiuchi *et al.*, 2002, Ogawa *et al.*, 1996).

Activation of FruA by phosphorylation is thought to occur in response to the C-signal pathway (Ellehauge *et al.*, 1998). The C-signal is a 17 kDa cell surface exposed protein (p17) that is generated by proteolytic cleavage of its inactive precursor p25. p25 is encoded by *csgA* and synthesized in vegetative cells but up-regulated during starvation-induced development (Kruse *et al.*, 2001). The protein is essential for aggregation and fruiting body formation. It is exported to the cell surface by an as yet unidentified mechanism (Lobedanz & Søgaard-Andersen, 2003). Upon starvation, the cell surface anchored p25 becomes cleaved by PopC and thereby converted into its truncated active form (Rolbetzki *et al.*, 2008). By an unknown receptor, the 17 kDa protein of neighboring cells is recognized and the signal is transduced to the DNA-binding response regulator FruA (Søgaard-Andersen, 2004) leading to FruA-activation by phosphorylation.

The phosphorylated active FruA-protein is proposed to allow progression of development through a branched pathway (Søgaard-Andersen & Kaiser, 1996). One branch controls cell movement by methylation of the FrzCD methyl-accepting chemotaxis protein. Changes in FrzCD methylation during development diminishes the frequency of cell movement reversals and directs cells to aggregate into mounds (Zusman *et al.*, 2007). By a feed back loop, higher cell densities inside the mounds are thought to increase the contact dependent C-signaling and therefore phosphorylation of FruA.

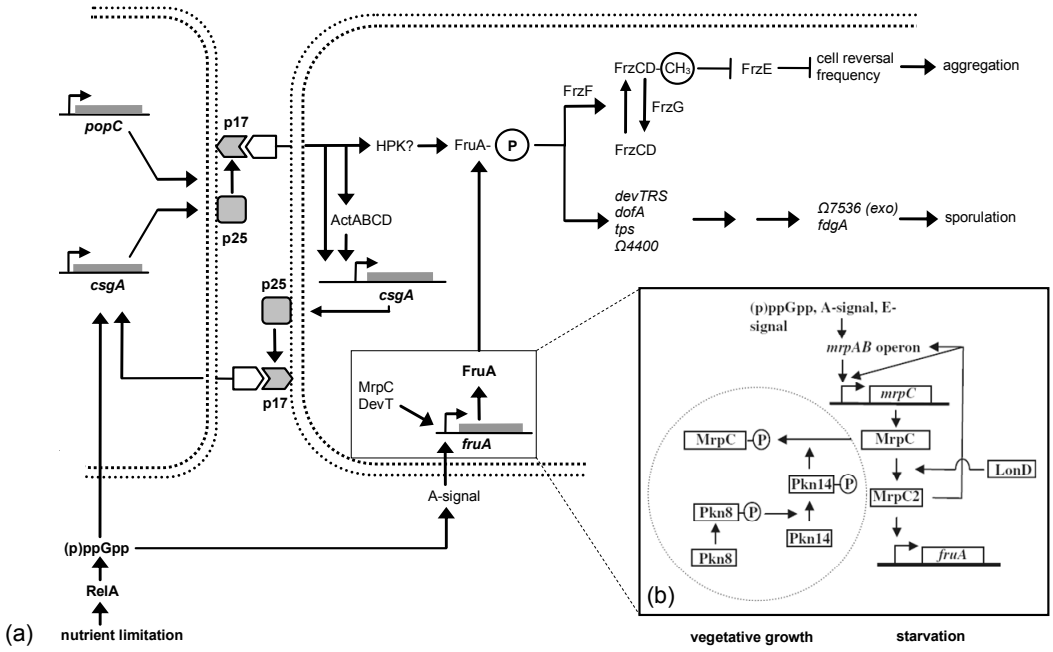

Figure 1-6 (a) Schematic view of proposed signal transduction pathways during *M. xanthus* starvation-induced development. The inset (b) depicts control of *fruA*-expression by MrpC2 in more detail (taken from (Søgaard-Andersen, 2008)), modified.

High levels of phosphorylated FruA are proposed to activate transcription of the *dev* locus inside the mounds (Viswanathan *et al.*, 2007) as part of the second branch. The *dev* genes are expressed inside fruiting bodies and are likely necessary for induction of sporulation (Thony-Meyer & Kaiser, 1993). Finally, late sporulation specific genes are expressed such as Ω7536 (*exo*). *exo* is essential to form mature spores (Licking *et al.*, 2000). The final stage of the sophisticated developmental program is the formation of resistant, spherical spores.

1.2.2 *M. xanthus* spores

Unlike in Gram-positive spore formers, *M. xanthus* spores are not formed by specific cell division processes nor by budding as in alphaproteobacterial species. Instead, an entire rod shaped cell converts into a spherical spore that matures and acquires resistance not inside a mother cell, but rather inside a multicellular fruiting body or, under certain circumstances, detached and freely. Myxospores do not possess the high resistance properties known from many Gram-positive spores. However, in contrast to vegetative cells, myxospores survive heat treatment up to 60°C and they are resistant to desiccation, UV-radiation, sonication and treatment with detergents such as SDS (Reichenbach, 1999, Sudo & Dworkin, 1969).

However, to examine the processes that developing *M. xanthus* cells undergo inside fruiting bodies has proven difficult. Genome wide transcriptional profiling, for example, is hampered by the fact that a developing culture divides into subpopulations with very different cellular fates. To identify genes involved in the late stage of spore formation is additionally hindered by the small proportion of emerging spores and by their high mechanical resistance.

Interestingly, a second means to rapidly generate spores is to add certain chemicals such as 0.5 M glycerol (Dworkin & Gibson, 1964), 0.7 M DMSO (Komano *et al.*, 1980), beta-lactam antibiotics, D-amino-acids (O'Connor & Zusman, 1997) and secondary alcohols (Dworkin & Gibson, 1964) to exponentially growing liquid cultures. The most effective inducers that have been identified are glycerol and DMSO (Komano *et al.*, 1980). In this case, resistant spores are formed within hours and virtually every cell converts into a resistant spore without forming fruiting bodies (Dworkin & Gibson, 1964). In contrast to starvation-induced sporulation, this process takes place in the presence of nutrients, is independent of cell density, it obviates the need of aggregation and most likely, no subpopulations are formed. Instead, it leads to a synchronized sporulating culture. However, glycerol- and starvation-induced spores are not identical as seen in electron microscopic images (**Figure 1-7**). The envelope layers of glycerol-induced spores are thinner and they contain apparently more ribosomes. Additionally, some spore specific proteins are detectable in starvation-induced, but not in glycerol-induced spores.

Importantly however, the two types of spores share many characteristics such as spherical shape, refractivity in phase contrast, and resistance to heat, sonication and detergents (Sudo & Dworkin, 1969) and both pathways induce a β-lactamase activity (O'Connor & Zusman, 1997).

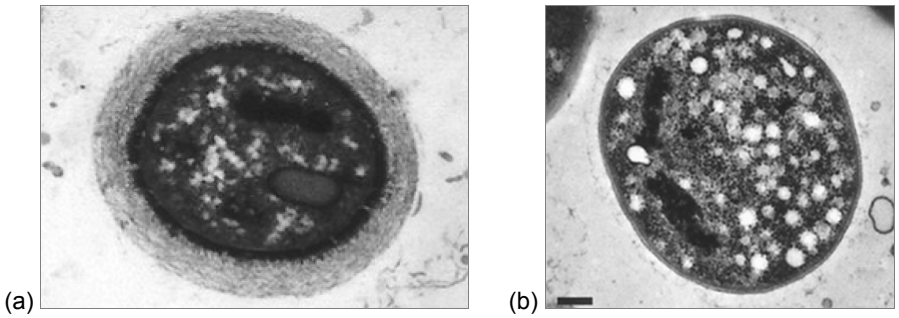

Figure 1-7 Electron micrographs of starvation-induced (a) and glycerol-induced (b) spores of *M. xanthus* (taken from (O'Connor & Zusman, 1999)).

Numerous proteins that are differentially expressed during *M. xanthus*' spore formation were found by early 1-D and 2-D SDS-PAGE approaches (Komano *et al.*, 1980, Inouye *et al.*, 1979b). However, most of these proteins have not been characterized except for few spore coat associated proteins. In particular, the spore coat proteins S and its homologue S1 have been studied in more detail. During starvation-induced development, synthesis of both proteins is differentially regulated. Protein S is synthesized soon after onset of starvation (Inouye *et al.*, 1979a), but protein S1 accumulates much later, when spores are formed (Downard & Zusman, 1985). Up to 15% of the total cellular protein synthesis during starvation-induced development is devoted to the early synthesized protein S (Komano *et al.*, 1980, Inouye *et al.*, 1979b) which is considered as the major spore coat protein. The mRNA of protein S has been shown to possess an unusually long half life of 15 to 30 minutes (Nelson & Zusman, 1983) which probably accounts for the high ratio of protein S synthesis. Protein S possesses the ability to self-assemble on starvation-induced spores (Inouye *et al.*, 1979a). However, it is yet unknown how the protein is exported from developing cells since the protein sequence lacks an obvious secretion signal. One model proposes that the protein first accumulates inside cells that have initiated the developmental program and is later set free by autolysis of non-sporulating cells. The free protein then may assemble on starvation-induced spores (Teintze *et al.*, 1985). The role of protein S is not yet clear since it seems not to be essential for spore resistance and viability (Komano *et al.*, 1984). A proposed function of this abundant protein is to mediate spore adhesion. Protein S is not detectable in glycerol-induced spores but its homologue and later synthesized protein S1 is detectable in both spore types (Downard & Zusman, 1985). Other spore-specific proteins that have been analyzed are protein U, W and C. Protein U is synthesized late during starvation-induced development and known from both starvation and glycerol-induced spores (Gollop *et al.*, 1991). Protein U is synthesized as signal-peptide containing precursor, secreted, and assembled on the spore surface. In contrast, protein W is detected only inside starvation-induced spores and is proposed to be involved in poly-phosphate storage (Otani *et al.*, 1998). Finally, protein C was shown to be early expressed during starvation-induced development and to be spore coat associated (McCleary *et al.*, 1991). Its sequence has not yet been published.

A recent 2-D gel proteomics approach has identified three more spore proteins (major spore proteins, MspA, B and C). Deletion of the according genes results in less resistant spores and structural defects (Dahl *et al.*, 2007). Furthermore, CbgA was identified to play a role in spore formation based on its homology to SpoVR, a *B. subtilis* protein that

is involved in the formation of the endospore cortex. The *cbgA* mutant also displays structural defects in the spore envelope and decreased spore resistance properties (Tengra *et al.*, 2006), and its fruiting bodies are of aberrant shape. However, the function of the proteins S, S1, U, C, the Msp's and CbgA has not yet been demonstrated.

Furthermore, some regulatory genes have been identified to cause a sporulation defect upon deletion. Inactivation of four of the *M. xanthus* NtrC-like activators (*nla4*, *6*, *18*, and *24*) leads to starvation and glycerol-induced sporulation defects (Caberoy *et al.*, 2003). Additionally, the alternative sigma factors B and C are involved in sporulation. Expression of the late stage sigma factor B starts at the onset of sporulation and only inside spores. The spores of the *sigB* mutant are viable but not stable. Therefore, SigB is proposed to be involved in spore maturation and maintenance of spore dormancy. Sigma factor C has been shown to be synthesized during sporulation but inactivation does not elicit an obvious sporulation defect. However, the *sigC* mutant forms fruiting bodies and spores on semi-rich media suggesting that SigC controls genes involved in repression of fruiting body formation in the presence of nutrients.

An interesting gene that has been identified by Tn5-*lacZ* insertion during starvation-induced development is *Mxan_3227* (Ω7536 or *exo*) (Licking *et al.*, 2000). *exo* stands for 'exopolysaccharide synthesis and export' and refers to its proposed function. The *exo*-gene is part of a cluster of nine genes consisting of four hypothetical genes, a putative tyrosine-kinase, an amino-transferase and three genes involved in carbohydrate metabolism and trafficking. Interestingly, the *exo*-mutant is blocked very late in starvation-induced spore formation. The mutant forms normal fruiting bodies but the cells inside are unable to finish shape conversion into spheres (**Figure 1-8**). Mature glycerol-induced spores are not formed suggesting that the *exo* gene is essential to form resistant, spherical spores, i.e. it is part of the core sporulation process. However, the function of this gene has also not been demonstrated. Interestingly, the same locus has been identified later again. Its first gene, *Mxan_3325*, is now termed *fdgA* (Ueki & Inouye, 2005). The *fdgA* mutant forms non-darkening fruiting bodies and spores with strongly reduced resistance but its glycerol spore-induction phenotype has not been reported.

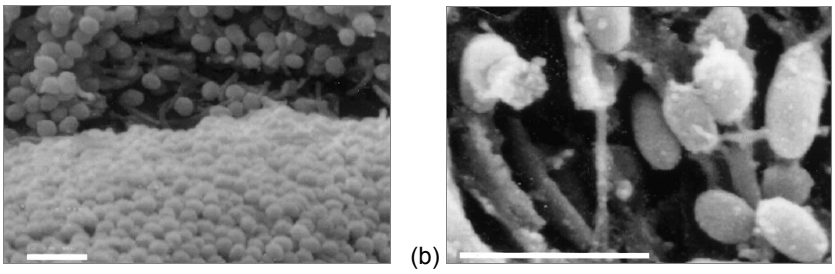

Figure 1-8 Scanning electron micrographs of starvation-induced wild type (DK1622) (a) and *exo* mutant (b) spores inside fruiting bodies (taken from (Licking *et al.*, 2000)).

In summary, the overall picture of spore formation in *M. xanthus* remains vague since the function of most spore-specific proteins has not been determined. Compared to the large regulons and signaling networks involved in *Bacillus*' spore formation, little is known about the processes in the Gram-negative *M. xanthus*.

Assays for specific enzyme activities suggest that upon spore formation, trehalose is synthesized and carbohydrate synthesis is activated (McBride & Zusman, 1989, Orlowski *et al.*, 1972). Intriguingly, a recent study demonstrated that glycerol spores do not contain peptidoglycan (Bui *et al.*, 2008). This is in sharp contrast to spores from Gram-positive bacteria and raises the question of what the *M. xanthus* spore envelope consists of. Besides the above mentioned spore coat proteins that only account for 14% of the spore coat dry weight and whose function is not yet clear, large amounts of glucose, galactosamine and glycine have been found (Kottel *et al.*, 1975). However, yet it is unknown how the carbohydrates become exported and assembled on the spores, if and how this material is cross-linked, and how it contributes to spore resistance. Deposition of the spore envelope material needs to be tightly controlled to avoid cell lysis during simultaneous peptidoglycan degradation. Additionally, the large structural changes in the spore envelope need to be tightly coordinated with the cell shape change process.

1.3 Cell shape control during spore formation and germination

One of the most interesting aspects of spore formation in bacilli is the shape transition from rod to sphere. As discussed previously, spore formation in *Bacillus* and *Streptomyces* arises from an unequal cell division. In case of *M. xanthus* however, the entire cell rounds up suggesting re-arrangements of cell wall and cytoskeleton. The cytoskeleton is largely the result of the actin-like MreB protein. This protein is highly conserved in most rod-shaped bacteria. It polymerizes into twisted filaments that are attached to the cytoplasmic membrane and traverse the longitudinal axis of the cell (Varley & Stewart, 1992, Figge *et al.*, 2004). It has been proposed that one task of the spiral-like MreB filaments is to indirectly position and to guide peptidoglycan synthases and lytic enzymes during growth (**Figure 1-9**) (Figge *et al.*, 2004) (Carballido-Lopez, 2006). By that means, the assembly of cell wall precursors occurs not at random positions but is highly coordinated and distinctly localized. Some related proteins have been shown to co-localize with the MreB filaments (Divakaruni *et al.*, 2005) but to date, besides RNA-polymerase and RodZ no direct interaction partners of MreB have been identified *in vivo* (Bendezu *et al.*, 2008, Kruse *et al.*, 2006).

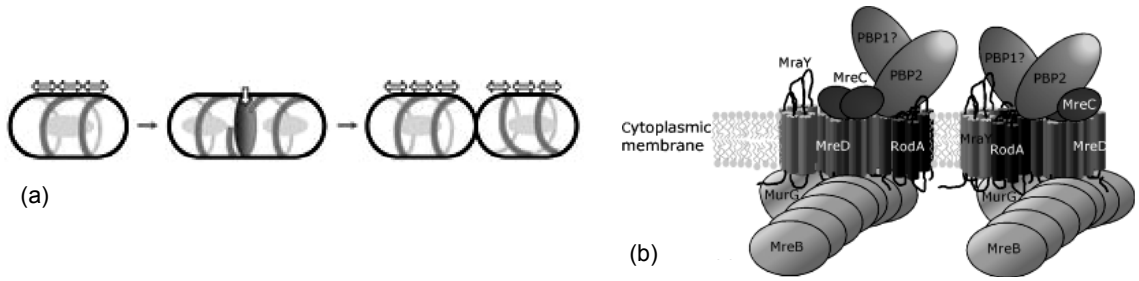

Figure 1-9 (a) Organization of MreB spirals in rod-shaped bacteria during vegetative growth and cell division (taken from (Carballido-Lopez, 2006)). (b) Proposed interaction partners of MreB forming the "elongase" complex, essential for lateral vegetative growth (from (den Blaauwen *et al.*, 2008)).

In the transition from vegetative cells to spores, *M. xanthus* must posses a means to regulate cell shape from rod to sphere and, during germination, back from sphere into rod. Therefore, the entire cell envelope needs to be extensively remodelled. A good candidate for regulation of this process is the structural protein, MreB. In various model organisms, such as *B. subtilis*, *C. crescentus* and *E. coli*, depletion of MreB turns the rod-like cells into spheres and repletion of the protein reconstitutes normal rod cell shape (Figge *et al.*, 2004, Carballido-Lopez & Formstone, 2007, den Blaauwen *et al.*, 2008). Additionally, MreB polymerization can be inhibited by addition of the chemical compound A22 (Iwai *et al.*, 2002b). In this case, existing MreB filaments are disassembled and rod-shaped cells turn also into spheres. Interestingly, in *E. coli*, inhibition of penicillin binding proteins (PBP's) involved in lateral cell wall growth, likewise leads to formation of spherical cells. Spiral-like MreB-filaments are still detectable in these spheres (Karczmarek *et al.*, 2007, den Blaauwen *et al.*, 2008). Therefore, different ways to form a sphere from a rod-shaped cell are possible. During shape change in *M. xanthus*, MreB may either be degraded or the MreB-filaments are disassembled to enable sphere formation. A third possibility is that the control of MreB on cell shape is interrupted by an unknown mechanism.

1.4 Scope

This thesis research focused on identification of not only single genes but whole clusters and functional groups likely to be involved in spore formation. This aim was approached by transcriptome profiling of a synchronized sporulating *M. xanthus* culture using micro arrays. The glycerol-induced spore formation process served as model for the spore formation process in general. The data set of significantly regulated genes was screened for both known and putatively novel core sporulation genes. Novel candidate genes were selected for more detailed analysis based on their ratio of up-regulation, their regulation pattern compared to known sporulation markers and their predicted subcellular localization. The role of a selected cluster of candidate genes in spore formation was analyzed by mutagenesis, genetic and biochemical approaches.

Simultaneously, the role of MreB during spore formation and germination was studied. Inhibition of MreB polymerization by A22 was investigated to analyze how *M. xanthus* accomplishes co-ordinated cell shape conversion.

2 RESULTS

2.1 Identification of the sporulation-specific transcriptome by micro array analysis

2.1.1 Genes significantly regulated in response to glycerol-induced spore formation

To identify genes involved in the *M. xanthus* sporulation process, micro array analysis was performed on a time course of cells sporulating in response to glycerol. The micro array chips used were provided by The Institute for Genomic Research (TIGR, http://www.tigr.org/TIGRFAMs/). Until the beginning of this work, this type of array had not been applied successfully. Thus, the experimental conditions had to be determined. The results of this optimization procedure are published (Müller & Jakobsen, 2008).

The arrays are based on the genome annotation from September 9, 2005 and comprise 7,200 of 7,380 *M. xanthus* protein coding sequences. Each sequence is represented by three spots of specific, identical 70-mers of single stranded DNA. Due to potential cross-hybridization, 472 of the sequences are termed 'not reliable' resulting in 6,728 reliable open reading frames (orfs) represented on the chips which accounts for approximately 91% of the *M. xanthus* protein coding sequences (B. Nierman, unpublished).

The time course experiment was carried out in three independent biological replicates. Samples were taken at 0.5, 1, 2, 4, 8 and 16 hours after addition of glycerol, processed as described in Materials and Methods (**Section 4.8**) and hybridized on the arrays together with samples from uninduced cells as reference (**Figure 2-1**). The tighter sample sequence at the beginning was chosen because major morphological and metabolic changes take place within the first four hours of induction (Sadler & Dworkin, 1966, Komano *et al.*, 1980, Orlowski *et al.*, 1972). After scanning and normalization, the data of each time course were pre-filtered applying an intensity criterion of signal minus background ≥ 100 in at least one channel and in at least one time point.

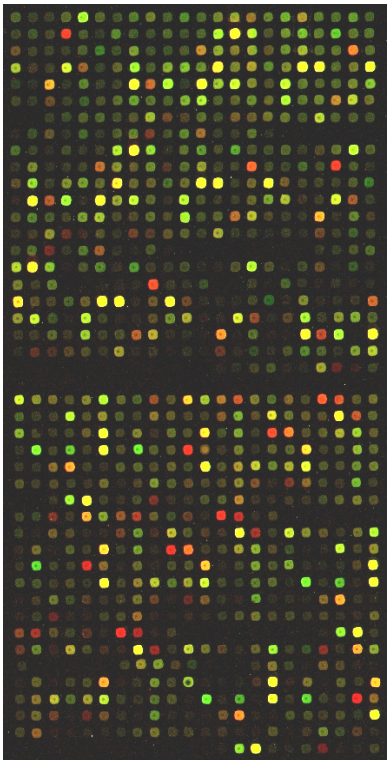

Figure 2-1 Representative section of a TIGR micro array displaying two blocks of spots. Hybridized are labeled cDNAs of vegetative cells (green) and cells that have been exposed to glycerol for 0.5 hours (red). Yellow color is the result of a red and green overlay and corresponds to genes that are expressed in both cell types.

These data were analyzed for significantly regulated genes by SAM (Statistical Analysis of Microarrays, Stanford University) applying a median false discovery rate (FDR) of 5%. A cut off criterion of two-fold up- or down-regulation was applied to this data set, resulting in 976 genes considered as significantly regulated above threshold. More detailed analysis of the array data revealed that from the eight hours time point on the number of detected regulated genes decreased. This phenomenon is probably not due to gene expression levels that drop below detection limits in sporulating cells, but was instead caused by the increasing resistance of the emerging spores. Spores at this stage do not lyse during the hot phenol RNA isolation method (data not shown) which resulted in loss of signals from some genes that were detected as up-regulated in the earlier time points. One of the applied quality criteria to call a gene significantly regulated was to only consider genes where data are present for each time point. Therefore, the samples until four hours were analyzed separately resulting in 1,596 significantly regulated genes (**Table 2-1**) which are listed together with their annotation in the Appendix (**Table A-15**).

Table 2-1 Numbers of regulated genes considering 4 hours and 16 hours time course (data present for all time points).

Time course	4 h	16 h
Significantly regulated genes	4,506	1,977
At least 2-fold up- or down-regulated genes	1,596	976

2.1.2 Previously described core sporulation genes are up-regulated

As a first step to analyze the micro array data, genes encoding for proteins known to be involved in the core sporulation process were searched. Genes that are obviously involved in other processes, such as motility or core metabolism, were not considered. For example, defects in motility can cause sporulation defects since cells are not able to form proper fruiting bodies. Likewise, mutations that interfere with parts of the central metabolism may evoke pleiotropic effects and also influence sporulation indirectly.

The known core sporulation related proteins were divided into groups. The first group contains structural proteins that have been detected specifically in the spore coat of either starvation- or glycerol-induced spores, or both. The second group contains regulatory proteins that have been shown to cause sporulation defects upon deletion. The third group contains metabolic enzymes whose activity has been shown to be highly increased during glycerol-induced sporulation and the fourth group contains proteins that are necessary to form resistant and viable starvation- or glycerol-induced spores but whose detailed function has not yet been characterized. **Table 2-2** lists these genes and the associated regulation in the microarray analysis.

The data suggest that 19 of the 26 listed sporulation marker genes are found to be up-regulated. Those that were not significantly regulated include the specifically in fruiting bodies expressed *devTRS* locus, tree transcriptional regulators (*nla4*, *18*, *24*), and the gene for protein W (*prW*), known to be not present in glycerol spores (**Table 2-2**).

Table 2-2 Known core sporulation process related genes.

Gene	Product	Mxan	Detected in Glycerol/Starvation spores	Fold upregulation (max.)	Cluster	Spore formation or viability impaired by Glycerol/Starvation induced sporulation	Reference
Structural or spore coat associated proteins							
tps	Protein S	5432	S	3.7	2	-/-	(Komano et al., 1984, Downard & Zusman, 1985)
ops	Protein S-1	5430	G/S	2.7	2	-/-	
pru	Protein U	3885	G/S	93.5	2	?/-	(Gollop et al., 1991)
unknown	Protein C	?	S	?	?	?/?	(McCleary et al., 1991)
prw	Protein W	2491	S			?/-	(Otani et al., 1998)
Regulatory proteins							
actA	C-signal amplification proteins	3213	S	4.6	1	G[a]/S	(Gronewold & Kaiser, 2001, Gronewold & Kaiser, 2007)
actB		3214	S	23.2	2	G[a]/S	
actD		3216	S	2.1	2	G[a] (reduced)/S	
sigB	Sigma factor B	3357	S	50.5	2	-/S[c]	(Apelian & Inouye, 1990)
sigC	Sigma factor C	6209	S	140.5	2	-/-[d]	(Apelian & Inouye, 1993)
nla4	Enhancer binding proteins	2516	S			G/S	(Caberoy et al., 2003)
nla6		4042	S	20.6	1	G/S	
nla18		3692	S			G/S	
nla24		7440	S			G/S	
Metabolism							
aceA	Isocitrate lyase	6442	G	126.1	1	?[b]/?	(Orlowski et al., 1972)
aceB	Malate synthase	6441	G	36.3	1	?[b]/?	(Orlowski et al., 1972)
treS	Trehalose synthase	3684	G	9.5	2	?/?	(McBride & Zusman, 1989)
Other Proteins							
fdgA	FdgA	3225	S	12.3	1	?/S	(Ueki & Inouye, 2005)
Ω7536 (*exo*)	Exo	3227	G/S	57.4	1	G/S	(Licking et al., 2000)
mspA	Major spore proteins	2269	S	3.6	1	?/S	(Dahl et al., 2007)
mspB		2432	S			?/S	
mspC		6969	S	203.0	2	?/S	
cbgA	CbgA	5828	S	5.7	1	?/S	(Tengra et al., 2006)
dev	Dev	7267-7258	S			-/S	(Thony-Meyer & Kaiser, 1993)
		3026		22.7	1	G[a] /?	
		1101		124.8	1	G[a] /?	

G: glycerol spores, S: starvation spores, -: sporulation not affected, ?: unknown
[a]Inactivation affects glycerol sporulation (Müller & Higgs, unpublished).
[b]No increased enzyme activity in a non-inducible mutant.
[c]Viability defect after 12 days.
[d]*sigB*/*sigC* double mutant may have a sporulation defect (Ueki & Inouye, 2001).

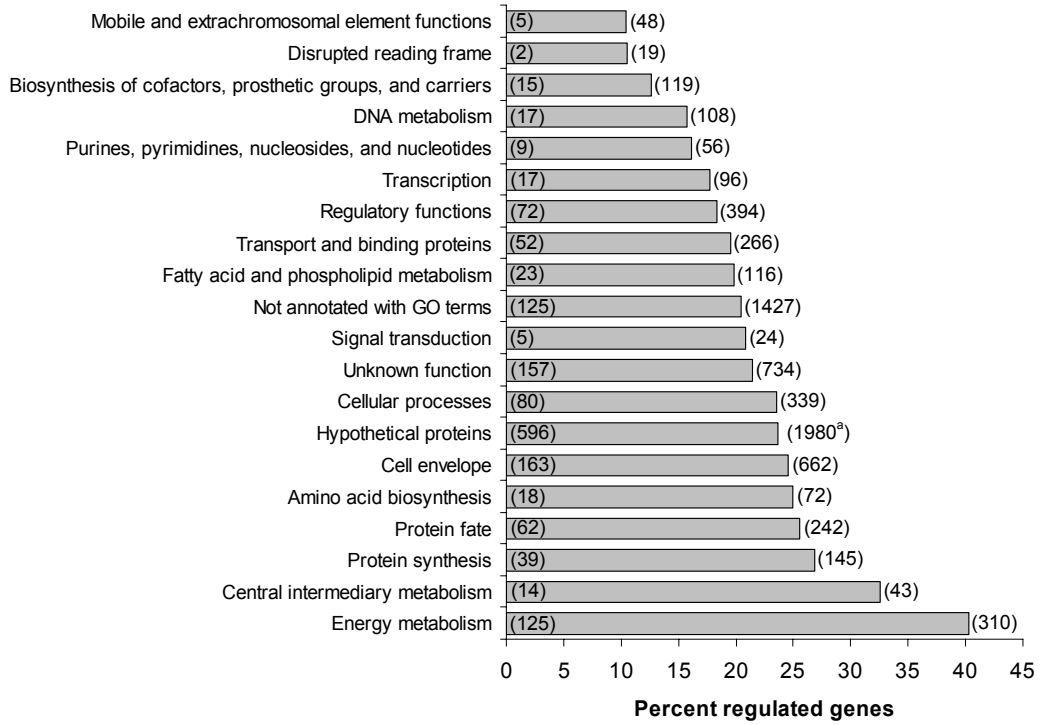

Figure 2-2 Percent of significantly regulated genes were sorted into the functional categories (bars) assigned by TIGR annotation. The functional categories are grouped based on their percentage of regulated genes. Numbers in brackets inside the bars indicate the regulated genes. The total number of genes in each category is indicated on the right. [a]1923 of the hypothetical proteins are also unannotated with gene ontology (GO) terms.

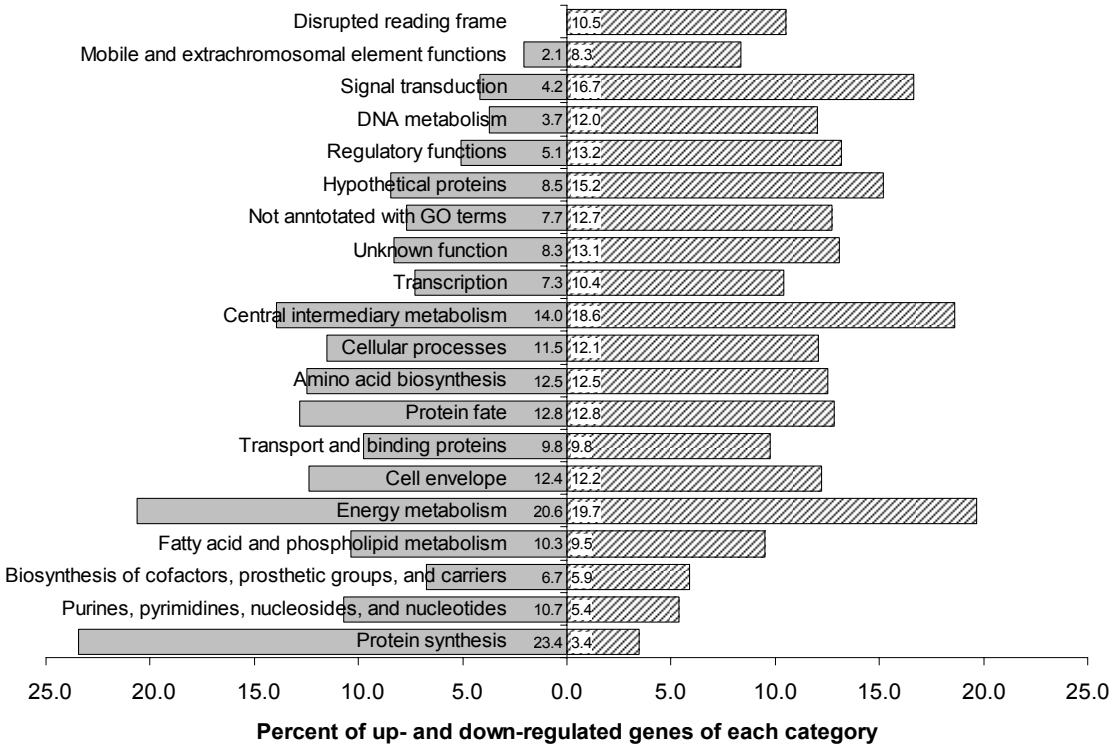

Figure 2-3 Proportions of up- and down-regulated genes in each functional category. Genes in each category were divided into up- (shaded) and down-regulated (gray) genes. The categories were sorted by the ratio of up- and down-regulated genes.

2.1.3 Functional categories

To determine whether the data are consistent with previous reports on sporulation genes and to study which cellular processes are most affected by glycerol induction, the regulated genes were first analyzed and grouped based on the genome annotation from TIGR that also assigns functional categories to most of the predicted gene products. For this purpose, the percentage of genes that change their expression level was calculated for each category (**Figure 2-2**). The data suggest that the major influenced functional groups are energy metabolism (40.3% genes of this category are either up-or down-regulated) and central intermediary metabolism (32.6%). Large changes in gene expression are also found in the categories protein synthesis (26.8%) and protein fate (25.6%).

To determine how the majority of genes in distinct categories are affected, the genes were further divided into up- and down-regulated genes (**Figure 2-3**). Interestingly, the proportion of up- and down-regulated genes is very different for distinct categories. More than 40% of all genes in the energy metabolism category change their expression level, but equal proportions are up- and down-regulated suggesting that the cells exchange large parts of their energy metabolism proteins. For example, all seven regulated genes for enzymes involved in glycolysis or gluconeogenesis are up-regulated as well as the genes for glyoxylate cycle enzymes whereas genes for seven TCA cycle associated enzymes are down-regulated. Down-regulated are also all six genes encoding for ATP-synthase subunits, twelve genes encoding cytochromes or cytochrome oxidase subunits and all ten genes encoding NADH dehydrogenase subunits consistent with the observation that respiration decreases by 80% during glycerol induction (Bacon *et al.*, 1975).

However, of the 26.8% regulated genes in the category protein synthesis, the vast majority are down-regulated including 28 genes encoding ribosomal proteins. This result is consistent with the observation that in glycerol-induced spores protein synthesis is reduced (Komano *et al.*, 1980, Sadler & Dworkin, 1966).

2.1.4 Grouping of the regulated genes by their expression profiles reveals distinct expression patterns

Co-regulated genes (regulons) are often involved in the same processes. The microarray technique allows monitoring expression levels of thousands of genes in parallel and is therefore particularly powerful to identify co-regulated genes (DeRisi *et al.*, 1997, Eisen *et al.*, 1998, Tavazoie *et al.*, 1999, Terai *et al.*, 2001). This approach can also provide information on processes in which novel genes might be involved.

To determine if all groups of core sporulation genes (**Table 2-2**) share the same expression profile or if there exist distinct patterns for specific groups, the significantly regulated genes were analyzed for genes with similar expression profiles. **Figure 2-4 a** displays a heat map where the genes are sorted by their regulation at 0.5 hours after addition of glycerol. As indicated by the intense yellow color, the genes at top of the map are highly expressed at the beginning of the experiment. However, their expression levels decrease towards the end of the time course as emphasized by the upper bracket.

The map also suggests that there exists a second group of highly expressed genes but with peak expression levels at two to four hours (lower bracket).

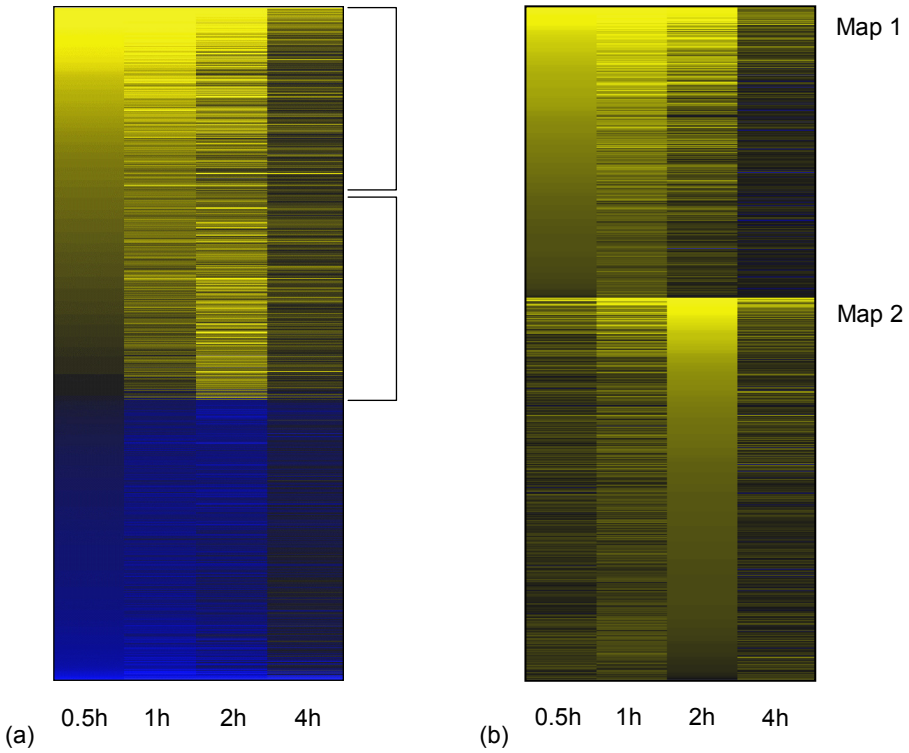

Figure 2-4 Heat maps of significantly regulated genes. Each column corresponds to one time point and each row corresponds to one regulated gene. Yellow colour indicates up-regulation, blue indicates down-regulation. The colour intensity matches the magnitude of regulation compared to uninduced cells. (a) The genes are sorted by their expression levels at 0.5 hours. (b) The set of up-regulated genes was grouped into two maps by hierarchical clustering resulting in one map containing early peaking genes (Map 1) and in one map containing later peaking genes (Map 2). The genes are sorted by expression levels at 0.5 and 2 hours.

To verify that the genes follow different regulation patterns, hierarchical clustering was applied to group the genes according to their specific expression profiles. Additionally, for this analysis only genes were considered that are up-regulated in at least one time point. These analyses revealed that the array data fit best if divided into two groups (**Figure 2-4 b**).

The previously described sporulation marker genes (**Table 2-2**) were then analyzed for their placement in the first or second set of up-regulated genes. The genes for the spore coat associated proteins S, S1 and U are found in Map 2. However, *actA, nla6*, *fdgA*, Ω7536 (*exo), mspA*, *cbgA*, *Mxan_1101* and *Mxan_3026* cluster in Map 1. Interestingly, inactivation of the former genes for spore coat proteins does not affect spore viability, but deletion of the latter sporulation markers in Map 1 interferes with glycerol-induced and/or starvation-induced sporulation. These results suggest that the array data can be organized into groups to enrich for essential sporulation genes.

2.1.5 Real time PCR on sporulation marker genes confirms the array-based regulation patterns

To confirm the regulation patterns determined by micro array analysis, real time PCR analysis on selected genes was performed. For this study, highly up-regulated as well as some known sporulation marker genes were selected. Additionally, the expression pattern of one down-regulated gene was analyzed. Sigma factors B (*sigB*) and C (*sigB*) are examples for highly transcribed regulatory genes, *atpE* and *devR* are examples for weakly or unregulated genes. *Mxan_5543* was chosen to represent down-regulated genes. *mspC, prU* and Ω7536 (*exo*) are highly activated sporulation markers.

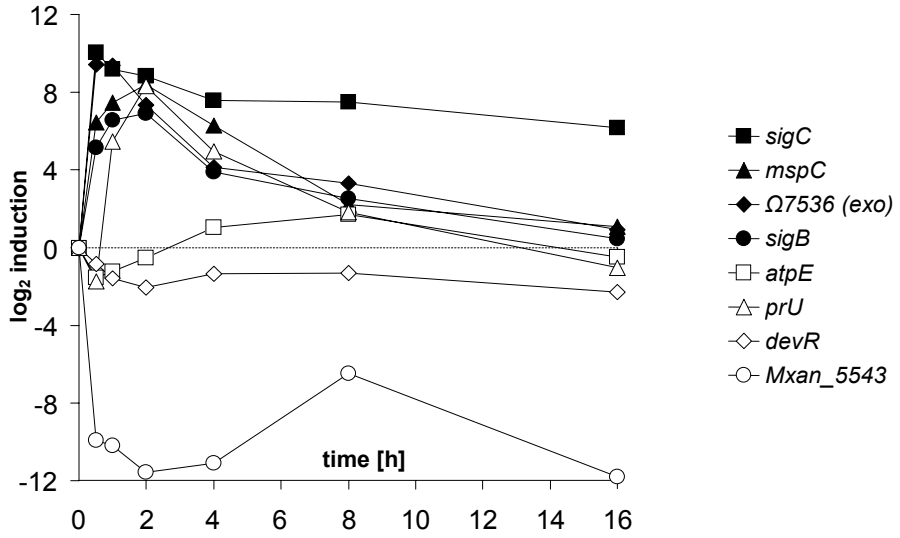

Figure 2-5 Real time PCR analysis of representative genes. Primers specific for *sigC*, *mspC*, Ω7536 (*exo*), *sigB*, *atpE*, *prU*, *devR* and *Mxan_5543* were used to amplify cDNA templates generated from RNA used in the microarray experiments.

Table 2-3 Comparison of maximum fold induction rates of marker genes.

Gene	*sigC*	*mspC*	Ω7536 (*exo*)	*sigB*	*atpE*	*prU*	*devR*	*Mxan_ 5543*
Fold induction								
Micro array	140.5	203	57.4	50.5	-3.7	93.5	-	-154.2
Real time PCR	1058.9	340.5	676.9	119.7	-2.9	322.2	-4.9	-3535.2

The array-based regulation patterns as well as the time points of peak expression / repression are confirmed by real time PCR analysis. The only exception is *sigC* which was placed in the group of later peaking genes (**Figure 2-4 b**). Real time PCR suggests that expression of this gene is highest at 0.5 hours (**Figure 2-5**). However, the changes in *sigC* expression are only minor as this gene stays highly activated during the whole time course. The differences in the calculated fold-changes between array and real time PCR are due to characteristics of the different methods such as the much higher sensitivity of the amplification-based PCR (**Table 2-3**).

2.1.6 Insertion mutagenesis in several up-regulated loci generated mutants defective in glycerol-induced sporulation

One approach to identify genes essential for spore formation is to inactivate candidate genes by insertion mutagenesis. Most of the known sporulation marker genes were found to be up-regulated. However, these genes belong to different gene ontology categories. To study if the up-regulated genes of different categories contain additional putative uncharacterized sporulation genes, the data were screened for up-regulated genes in different categories that could also be involved in spore formation. In this study, 14 open reading frames were selected for inactivation. Eight are predicted to reside in an operon such that inactivation of these genes likely causes polar effects.

Nine of the mutants displayed no obvious glycerol sporulation defect; three mutants could not be obtained suggesting that the genes are essential. Two mutants were deficient in glycerol spore formation (**Table 2-4**).

Both mutants defective in glycerol sporulation are affected in genes that are up-regulated highly and immediately. Additionally, the predicted gene products of *Mxan_1101* and *Mxan_3026* are probably involved in cell envelope modifications during sporulation. This suggests that these properties provide reasonable criteria to select additional candidates for mutagenesis.

2.1.7 Identification of the *nfs* locus

The simultaneous second approach was to search for genes likely to be involved in spore formation based on the following criteria:

Criterion #1: ≥ *16-fold up-regulation*

High up-regulation suggests that the according gene products are important for conversion of vegetative cells into spores. Notably, genes for synthesis, modification and export of abundant structural proteins are expected to be highly activated. Applying this criterion yielded 122 candidate genes.

Criterion # 2: *Predicted to localize to the cell envelope*

Major changes during spore formation involve the cell envelope. In contrast to vegetative cells, spores contain an enhanced, resistant envelope with an electron dense cortex and a prominent protein layer (Rosenbluh & Rosenberg, 1989, Kottel *et al.*, 1975, Dahl *et al.*, 2007). Additionally, the cell shape itself is altered suggesting changes in cell wall synthesis and composition. Moreover, sporulation mutants either display spore envelope defects (such as *mspA* and *mspC*) or the according proteins are predicted to localize or to act in the cell envelope (such as Ω7536 (*exo*), *fdgA* and the two newly identified genes from this study *Mxan_1101* and *Mxan_3026*).

Table 2-4 Loci selected for insertion mutagenesis.

Name[a]	Annotation	Map	Max. log induction	In putative operon	Glycerol spore formation affected
Mxan_0110	Fatty acid synthase	1	10.6	No	No mutant
Mxan_0434	Glycogen debranching enzyme	1	12.1	Yes	No
Mxan_0433	Hypothetical protein	1	2.5		
Mxan_0524	Response regulator	1	30.0	Yes	No
Mxan_0525	Serine/threonine protein kinase	2	2.5		
Mxan_0526	Hypothetical protein	1	43.4		
Mxan_0527	Efflux transporter	1	15.1		
Mxan_0528	Efflux transporter	1	13.4		
Mxan_0529	Glucano transferase	1	4.3		
Mxan_0646	Nuclease/phosphatase of unknown specificity	1	9.2	No	No
Mxan_0690	Lipoprotein of unknown function	2	18.4	No	No
Mxan_0781	Glycosyltransferase	2	9.8	Yes	No mutant
Mxan_0780	Putative membrane protein		-		
Mxan_0797	Protein of unknown function	2	3.0		
Mxan_0862	Pyrophosphatase	1	14.9	Yes	No
Mxan_0861	Protein of unknown function	1	3.9		
Mxan_0888	Serine/threonine phosphatase	1	3.1	Yes	No
Mxan_0887	Transcriptional regulator	1	19.7		
Mxan_0912	Glutamate/ammonia ligase	2	4.9	No	No mutant
Mxan_0994	Hypothetical protein	1	18.4	Yes	No
Mxan_0995	ABC transporter	1	3.0		
Mxan_1065	Translation factor	2	4.9	No	No
Mxan_1092	Heat shock protein	1	4.9	No	No
Mxan_1101	UDP-N-acetylglucosamine 2-epimerase	1 1	124.8	Yes	Yes
Mxan_1102	RNA modifying enzyme		7.4		
Mxan_3026	O-antigen polymerase	1	22.7	Yes	Yes
Mxan_3027	Glycosyltransferase	1	97.8		

[a]Genes in bold were selected as targets for insertion mutagenesis. Genes putatively influenced by polar effects are following.

The subcellular localization of the selected candidate genes was predicted by CELLO (Yu *et al.*, 2004). Only genes for proteins with predicted cell envelope localization (cytoplasmic membrane, periplasm or outer membrane) were considered. Applying this criterion left 41 candidate genes.

Criterion # 3: *The role of the gene products is not yet characterized.*

Since spore formation in *M. xanthus* is unique compared to other bacteria, it is likely that proteins without characterized homologues are involved. For that reason, hypothetical or conserved hypothetical proteins that fit the two above criteria were searched leading to a set of 20 candidate genes.

By this means, a genomic region consisting of consecutive genes was identified. As shown below, this gene cluster is one of the most intriguing loci identified and will subsequently be termed *nfs* (*n*ecessary *f*or *s*porulation).

2.1.8 The *nfs* locus consists of eight consecutive, highly up-regulated genes that cluster in Map 1.

The genes of the *nfs* locus are highly up-regulated. According to microarray data, the first gene *Mxan_3371* is the highest up-regulated gene at 0.5 hours (150-fold) and the following seven genes (*Mxan_3372* - *Mxan_3378*) belong to the 50 highest activated genes in this group (**Table 2-5**). Additionally, all *nfs* genes are activated early and cluster in Map 1 (**Figure 2-4 b**) together with *actA, fdgA,* Ω7536 (*exo*)*, mspA, cbgA, Mxan_1101* and *Mxan_3026* which cause sporulation defects when mutated (**Table 2-2**).

The locus consists of eight predicted genes (*Mxan_3371 – Mxan_3378*) oriented in the same direction (**Figure 2-6**).

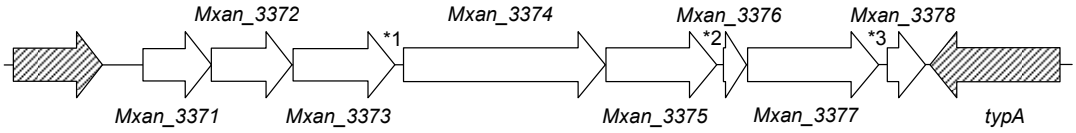

Figure 2-6 Genetic organization of the *nfs* locus. Arrows represent each predicted gene; stars indicate intergenic regions of *1: 163, *2: 201 and *3: 152 bp.

Table 2-5 Maximum fold up-regulation of the eight nfs genes determined by micro array analysis.

Gene (*Mxan_*)	3371	3372	3373	3374	3375	3376	3377	3378
Fold up-regulation	153	17	78	55	51	87	64	36

The gene *Mxan_3370* upstream of *nfs* is oriented in the same direction and annotated as protein of the large ribosomal subunit (*rplC*). The *nfs* locus is separated from *rplC* by 323 bp non-coding sequence. *rplC* is not significantly regulated as shown by micro array analysis and real time PCR (**Figure 2-9 a**). The gene downstream of *nfs* (*Mxan_3379*) is annotated as *typA*, a GTP-binding translational regulator. This gene is also not significantly regulated and is oriented in the opposite direction. Therefore, both flanking genes are not part of the *nfs* locus.

2.1.9 The *nfs* locus encodes for proteins with uncharacterized functions

All eight Nfs proteins are annotated as hypothetical or conserved hypothetical which means that they do not contain any catalytic domains of known function. Therefore, the predicted sequences were analyzed by bioinformatics tools in detail to gain information about their probable subcellular localization, possible protein interactions and distribution in other species. Several structural domains were found in the *nfs* proteins. A survey of the results is outlined below.

Table 2-6 Predicted subcellular localization of the Nfs proteins.

	Prediction algorithm/server			
Protein	**CELLO**[a]	**PSORTb**[b]	**Phobius**[c]	**Subloc**[d]
NfsA	Outer membrane/ Cytoplasm/Periplasm	Outer membrane	Non-cytoplasmic	Cytoplasmic (63%)
NfsB	Outer membrane	Non-cytoplasmic	Non-cytoplasmic	Periplasmic (92%)
NfsC	Outer membrane	Non-cytoplasmic	Non-cytoplasmic	Cytoplasmic (63%)
NfsD	Cytoplasmic/Periplasmic	Non-cytoplasmic	Non-cytoplasmic	Periplasmic (85%)
NfsE	Periplasmic	Non-cytoplasmic	Non-cytoplasmic	Periplasmic (98%)
NfsF	Cytoplasmic/Periplasmic	Non-cytoplasmic	Non-cytoplasmic	Periplasmic (85%)
NfsG	Periplasmic	Non-cytoplasmic	Inner membrane	Periplasmic (91%)
NfsH	Outer membrane	Non-cytoplasmic	Non-cytoplasmic	Cytoplasmic (63%)

[a]only significant results are shown
[b](Gardy *et al.*, 2005)
[c](Kall *et al.*, 2007)
[d](Hua & Sun, 2001)

Table 2-7 Predicted signal peptides in the Nfs proteins.

	Prediction algorithm/server			
Protein	**SignalP**	**LipoP**	**PSORTb v. 2.0.4**	**Phobius**
NfsA	?	-	+	?
NfsB	+	+	+	+
NfsC	+	+	+	+
NfsD	-	-	-	-
NfsE	+	+[a]	+	+
NfsF	+	+	+	+
NfsG	-	-	-	-
NfsH	+	+	+	+

[a]Peptide is predicted to be signal protease II cleavable suggesting that the protein is anchored to the membrane by a lipid modification.

Subcellular localization prediction programs suggest that the Nfs proteins are non-cytoplasmic. The CELLO-predictions are supported by results of PSORTb and Subloc where highest scores are found for predicted periplasmic or outer membrane localization (**Table 2-6**). Export of proteins from the cytoplasm is often mediated by N-terminal signal peptides and membrane localization can be determined by structural motifs such as hydrophobic transmembrane domains, lipid modifications or beta barrel folds. For that reason, the protein sequences were screened for signal peptides and additional structural domains (**Table 2-7** and **Table 2-8**).

Table 2-8 Predicted structural motifs in the Nfs proteins.

Protein	COG-Domains[c]	Pfam-motifs	3D-structures	Catalytic domains	Post-translational modification sites
NfsA			Beta-barrel[e]		
NfsB	COG4982 (acyl-carrier protein) PRK05648 (DNA polymerase III subunits gamma and tau)				
NfsC	COG1729 (uncharacterized domain)			Prenylyl[a]-transferase	
NfsD	PRK10803 (hypothetical protein) COG1729 (uncharacterized domain)	TPR[b,c,d] Trans[d]-membrane			
NfsE	COG3063 (cell motility and secretion / Intracellular trafficking and secretion) COG2956 (N-acetyl-glucosamin transferase / carbohydrate transport and metabolism) PRK11447 (cellulose synthase subunit) PRK11788 (hypothetical protein) PRK12370 (invasion protein regulator)[f]	TPR[b,c,d]			Lipid attachment[b]
NfsF					
NfsG	COG1716 (FHA domain / signal transduction)[b,c,d]	FHA[b,c,d]			
NfsH			Beta-barrel[e]		N-glycosylation[b]

[a]detected by SCOP (Murzin *et al.*, 1995) [b]detected by Prosite (Sigrist *et al.*, 2002)
[c]COG: domains from Clusters of Orthologous Genes, detected by BLASTp (Altschul *et al.*, 1997)
[d]detected by SMART (Letunic *et al.*, 2006)
[e]detected by Phyre (protein 3D modeling) (Bennett-Lovsey *et al.*, 2008)
[f]further domains were aligned based on TPR motifs

The results suggest that at least five of the eight Nsf proteins possess signal peptides and are exported from the cytoplasm. For NfsA and H there are predictions for beta-barrel structures which suggests that these proteins reside in the outer membrane. NfsD may be attached to the inner membrane via a transmembrane domain and NfsE is predicted to be membrane anchored by a lipid modification. The remaining proteins NfsB, C, F and G do not possess a predicted membrane attachment structure. However, besides NfsG they all possess signal peptides.

NfsD and E contain multiple tetratrico peptide repeat (TPR) domains; NfsG contains a putative fork head-associated (FHA) domain. TPR domains are abundant motifs in several proteins and mediate molecular recognition in protein interactions (D'Andrea & Regan, 2003). FHA domains bind phospho-threonine containing proteins (Durocher *et al.*, 2000) and also predicted to be involved in protein interactions.

Blast searches against to date available annotated bacterial genomes revealed that some of the Nfs proteins have homologues in other bacteria. Notably, the entire locus seems to be conserved in the closely related species *Stigmatella aurantiaca (Stiau2471 - 78)* suggesting that the Nfs proteins provide functions not only restricted to *M. xanthus*. In particular, *S. aurantiaca* is able to form spores as *M. xanthus*. *Sorangium cellulosum* and *Bdellovibrio bacterivorus* are more distantly related species but both are able to form spores or cysts (Qualls *et al.*, 1978, Tudor & Conti, 1977b, Tudor & Conti, 1977a, Vasquez *et al.*, 1985). Moreover, there exist paralogues in *M. xanthus* itself (**Table 2-9**). However, these proteins seem to have different functions since the respective genes are not up-regulated in the micro array studies. NfsC, D and G have homologues in other Deltaproteobacteria. The high number of related sequences for NfsD, E and G in species of other phyla is probably due to the presence of TPR repeats in NfsD and E and the FHA-domain in NfsG.

Table 2-9 Distribution of Nfs homologues in other bacterial species. The protein sequences were analyzed with the FastBlast algorithm (E-value below 0.003) of Microbesonline (Alm *et al.*, 2005) containing 747 bacterial genomes.

Protein	*M. xanthus*	*S. aurantiaca*	*A. dehalo-genans*	*B. bacteri-vorus*	*S. cellulosum*	Other Deltaproteo-bacteria	Other phyla
NfsA	-	1	-	-	-	-	-
NfsB	-	1	-	-	-	-	-
NfsC	3	3	1	5	1	-	2
NfsD	5	5	2	3	1	2	17
NfsE	3	3	1	-	-	-	72
NfsF	-	1	-	-	-	-	-
NfsG	6	12	4	6	13	3	29
NfsH	-	1	-	-	-	-	-

2.1.10 Analysis of functional predictions

As mentioned above, except for NfsC there are no predictions for catalytic activity or a structural role for the Nfs proteins. However, iterative PsiBlastp analysis can be applied to find proteins with similar partial sequence architecture and distantly related proteins or new members of a protein family (Altschul *et al.*, 1997). This analysis was used to gain more information about the processes in which the proteins might be involved.

Table 2-10 Position specific iteration Blastp results. Only proteins with known or predicted function / localization that were aligned more than once are shown.

Protein	Putative function	No. of aligned sequences
NfsA	OmpW/OmpA related outer membrane protein, porin	>300
NfsB	Cell surface or secreted protein / Glucan binding	>100[b]
NfsC	Glycosyltransferase	6
	O-linked N-acetylglucosamintransferase	6
	Prenylyltransferase	2
NfsD	Glycosyltransferase	5
	Glucosamintransferase	6
	TPR-repeat containing proteins of unknown function	>400
NfsE	Glycosyltransferase	5
	O-linked N-acetylglucosamintransferase	9
	Sulfotransferase	10
NfsF	-	-
NfsG	ABC-transporter / Efflux pump	>100
	Sigma54 dependent responseregulator	>40
	Adenylate / Guanylatecyclase	>20
NfsH	OmpA-related outer membrane protein, porin	>100
	OmpW related outer membrane protein, channel[a] , stress response	>20
	OprF, porin	>20

[a](Hong *et al.*, 2006)
[b]after five iterations, inconclusive results after ten iterations

PsiBlastp iterations were run with a maximum of 500 sequences against all bacterial non-redundant GenBank CDS translations including PDB (Protein Data Bank), SwissProt, PIR (Protein Information Resource) and PRF (Protein Research Foundation) excluding environmental samples from WGS (Whole Genome Shotgun Submission) projects. Sequences were included with an E-value threshold below 0.005. After two to three iteration steps, hypothetical or conserved hypothetical proteins of Myxobacteria and other bacterial species were aligned. Further iterations also raised protein sequences with predicted function for most of the Nfs proteins and after nine to ten steps no new sequences were found indicating saturation of the alignments. Exceptions are the small proteins NfsF and H. For NfsF, saturation with hypothetical protein sequences was

observed after five iterations and for NfsH after four iterations. In case of NfsH, increasing of the cut-off E-value for new detected sequences led to rapid alignment of OmpA/OmpW-related outer membrane proteins. Due to TPR motifs in NsfD and E, PsiBlastp searches were also carried out with truncated sequences lacking the TPR motifs to avoid artificial selection for TPR-related sequences. Nevertheless, the algorithm aligned mainly TPR motif-containing sequences to the truncated versions.

2.2 The *nfs* locus is necessary for sporulation

To determine if the *nfs* genes are necessary for the core sporulation process, a Δ*nfs* mutant was generated. The markerless in-frame deletion of all eight genes (12.5 kb) was accomplished by fusion of the six 5'-terminal codons of *nfsA* to the six 3'-terminal codons of *nfsH*. A schematic overview of the in-frame deletion procedure is shown in Materials and Methods (**Section 4.4.4**).

The Δ*nfs* strain was analyzed for its ability to form both glycerol- and starvation-induced spores.

2.2.1 The Δ*nfs* mutant does not form glycerol-induced spores

To study if the Δ*nfs* mutant is impaired in glycerol spore formation, liquid cultures of both wild type and Δ*nfs* mutant were induced with glycerol for 24 hours and assayed for the formation of heat and sonication resistant spores. After heat and sonication, no spores of the mutant were observed by phase contrast microscopy. The treated samples were also plated and allowed to form colonies for seven days. The results indicate that the Δ*nfs* mutant is not able to form resistant glycerol-induced spores suggesting that the *nfs* genes are indeed involved in the sporulation process (**Table 2-11**).

Table 2-11 Viability of glycerol-induced spores in wild type and Δ*nfs* strain. Equivalent cell numbers induced with glycerol were treated with heat and sonication and then plated on rich media. Values are recorded as percent of wild type (wt) cfu.

Strain	Sporulation efficiency [% of wt]	Spore viability [% of wt]
wt (DK1622)	100	100
Δ*nfs*	0	0.001

2.2.2 Δ*nfs* displays aberrant cell morphologies upon glycerol induction

To analyze the sporulation defect in more detail, a time course experiment was carried out where Δ*nfs* and wild type cells were induced with glycerol and imaged at distinct time points. Up to four hours after induction, no differences were visible (**Figure 2-7**). Both strains started to shorten and to form ovoids and spheres. After eight hours, wild type cells were mostly spherical and bright in phase contrast suggesting dehydration and acquisition of an enhanced cell envelope. However, Δ*nfs* cells failed to turn bright in phase contrast. Instead, the translucent cells started to gain in size and after approximately twelve hours, the cells converted back into rods. During this process, a

transient malformed, spiral like cell morphology was visible. After an additional six hours of incubation, all Δ*nfs* cells showed a normal rod shape even in the presence of glycerol.

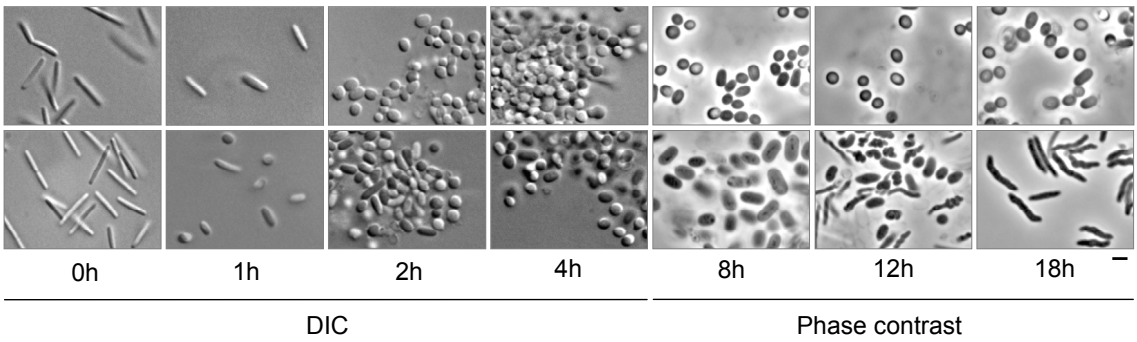

Figure 2-7 Time course analysis of glycerol-induced spore formation. Wild type (upper panel) and Δ*nfs* (lower panel) were induced with glycerol and imaged at the indicated time points at 1000-fold magnification. After eight hours, cells were imaged with phase contrast to better visualize the differences between wild type and Δ*nfs*. Bar: 1 µm.

2.2.3 Δ*nfs* forms fruiting bodies but less resistant starvation-induced spores

To determine if the *nfs* genes are necessary for starvation-induced development, the Δ*nfs* mutant was tested for its ability to form fruiting bodies and resistant spores under several nutrient limited conditions.

Analysis of starvation-induced development indicated that the Δ*nfs* mutant behaved as wild type with respect to timing and morphology of aggregation centers under submerged culture conditions (**Figure 2-8 a**), on CF nutrient limited plates (**Figure 2-8 b**) and on TPM strict starvation plates (data not shown). However, while wild type aggregation centres darken after approximately 48 hours development, Δ*nfs* failed to darken even after 120 hours (**Figure 2-8**) suggesting that spores of the deletion strain do not mature (Morrison & Zusman, 1979).

To determine if spores can be isolated from the mutant, cultures were harvested after 120 hours, and heat and sonication resistant spores were enumerated using a counting chamber. Surprisingly, in submerged culture, equal numbers of heat and sonication resistant spores could be isolated from the Δ*nfs* mutant as from wild type (**Table 2-12**). However, these spores were not refractile (**Figure 2-8 a**) and unable to germinate efficiently (only 2.6% of wild type ± 16%). Cells grown on CF produced fewer heat and sonication resistant spores (28.2% of wild type ± 15%) that also failed to germinate. The results suggest that the Δ*nfs* mutant does not have a defect in aggregation and timing of development but in formation of viable spores.

Table 2-12 Efficiency and viability of starvation-induced spores in wild type and Δ*nfs* strain. Numbers are recorded as percent of wild type.

Condition	Strain	Sporulation efficiency [% of wt]	Spore viability [% of wt]
Submerged	wt (DK1622)	100 ± 7	100 ± 16
	Δ*nfs*	103.3 ± 12	2.6 ± 16
CF	wt (DK1622)	100 ± 12	100 ± 30
	Δ*nfs*	28.2 ± 16	5.4 ± 35

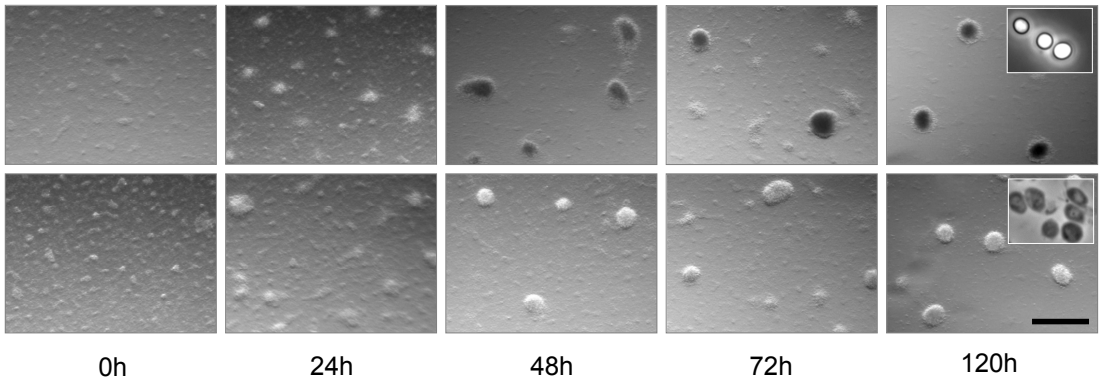

(a)

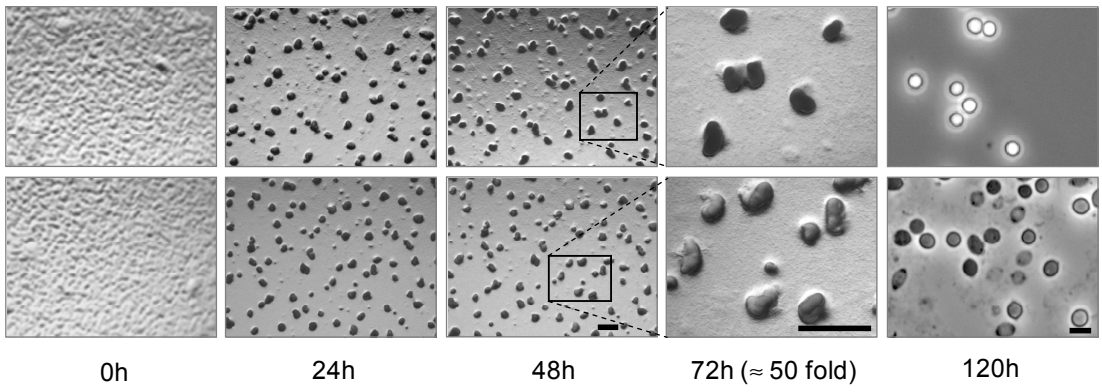

(b)

Figure 2-8 Stereo microscope and phase contrast images of wild type and Δ*nfs* developed for five days. (a) Submerged culture. Bar: 1 mm. Insets: Phase contrast micrographs of isolated spores. (b) CF agar. Bar: 0.5 mm. Last images in each row are phase contrast micrographs. Bar: 1 µm.

2.3 The *nfs* locus becomes activated when rod-shaped cells convert into spheres

To characterize the *nfs* locus in more detail, we confirmed the *nfs* gene expression pattern during glycerol induction, and examined the pattern during a developmental time course.

2.3.1 *nfs* gene expression and protein accumulation during glycerol-induced sporulation

To confirm the *nfs* expression pattern observed in the microarray analysis, the cDNA from a glycerol-induced time course was tested by real time PCR. Consistent with the micro array data, *nfsA*, *D* and *H* as well as Ω7536 (*exo*) were highly up-regulated at 0.5 to two hours and *Mxan_3370* (*rplC*) upstream of *nfs* appears to be not regulated (**Figure 2-9 a**).

To determine the pattern of protein accumulation, the glycerol-induced cultures were next examined by immunoblot analysis using anti peptide antibodies (Eurogentec) generated against NfsA to H (**Figure 2-9 b**). The apparent molecular masses of the Nfs proteins approximately matched the predicted masses (**Table 2-13**).

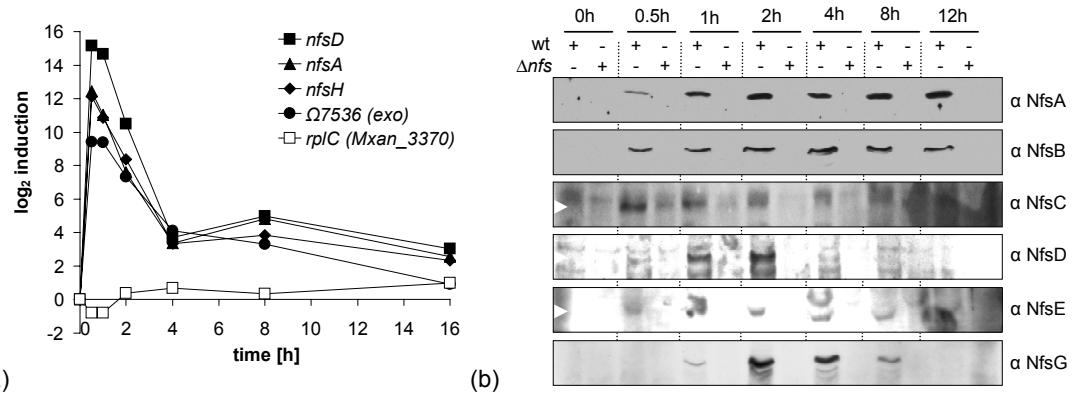

Figure 2-9 *nfs* gene expression and protein accumulation. (a) Real time PCR analysis on three selected *nfs* genes. Ω7536 (*exo*) was used as a highly up-regulated sporulation marker gene. The expression profile of *Mxan_3370* (upstream of the *nfs* locus) was also determined. (b) Anti-Nfs immunoblots on protein samples from glycerol-induced cultures. Equal culture proportions were harvested at the indicated times after induction with glycerol, proteins were released by bead beating, resolved by SDS-PAGE, and probed with anti-sera specific to NfsA - H.

Table 2-13 Number of amino acids, calculated and observed molecular weight of the Nfs proteins.

Protein	Amino acids	Calculated molecular mass [kDa]	Apparent molecular mass (SDS-PAGE) [kDa]
NfsA	294	32.3	30
NfsB	442	47	53
NfsC	512	57.5	57
NfsD	1219	137	140
NfsE	499	52	55
NfsF	96	10.8	-
NfsG	682	70.4	73
NfsH	200	21.3	-

Antibodies against NfsF and NfsH failed to recognize a specific protein in cell lysates (data not shown). NfsA, B, C, D, E, and G could not be detected in vegetative cells but

started to accumulate 0.5 hours after induction with glycerol. Interestingly, however, while NfsA, B and C were stably accumulated from 0.5 to twelve hours, accumulation of NfsD, E and G began to reduce after two hours and the proteins were absent after eight hours. Since the mRNA transcription profiles of all eight *nfs* genes are very similar, this may reflect differences in protein stability controlled by proteolysis.

As shown above, the *nfs* genes are immediately up-regulated during glycerol induction. To see if every cell activates expression of the *nfs* locus, a fusion of the putative *nfs* promoter region with *mcherry* was generated and the vector introduced into the Mx8 phage attachment site of *M. xanthus* DK1622. As control strain, *mcherry* was also fused to the *pilA*-promoter in order to express the reporter constitutively while the wild type bearing the empty vector served as negative control. The strains were induced with glycerol and imaged by fluorescence microscopy (**Figure 2-10**).

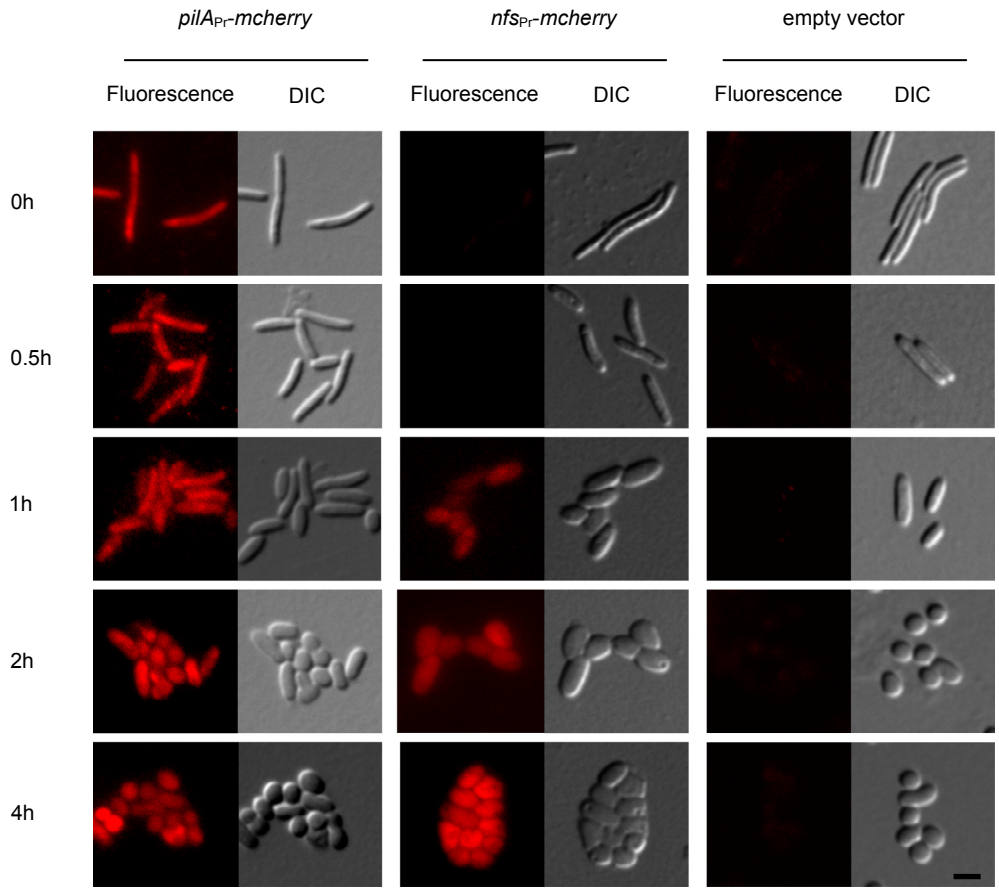

Figure 2-10 Expression analysis of PH1221 (*pilA*$_{Pr}$-*mcherry*, left), PH1220 (*nfs*$_{Pr}$-*mcherry*, center), and PH1222 (empty vector control, right) strains grown in CTT and induced with glycerol. Samples were taken at indicated time points, spotted on Agar slides and imaged with a fluorescence microscope. Bar: 1 µm.

The experiment covers the time in which glycerol-induced vegetative cells convert into spheres as seen in the DIC images. *mcherry* under control of the *pilA*-promoter is constitutively expressed as seen for strain PH1221. Both rod shaped cells, shortening rods and spherical spores fluoresce. For strain PH1222 (empty vector control) only weak autofluorescence signals are detectable at any time point. However, in PH1220 where *mcherry* is fused to the *nsf*-promoter, fluorescence signals become detectable

after approximately one hour when cells are shortening. The signal is detectable from all cells that round up and increases until four hours. This suggests that *nfs* expression is below detection limits in vegetative cells but that proteins of *nfs* promoter controlled genes accumulate one hour after addition of glycerol.

2.3.2 Activation during starvation-induced sporulation

To determine *nfs* promoter activation during starvation-induced development, quantitative fluorescence measurements of developing submerged cultures were performed on the above strains.

Strains containing no *mcherry* display an approximately 2.9-fold gain in signal intensity over time which correlates with increasing autofluorescence of developing cultures (data not shown). Signal intensity of Mcherry derived from the *pilA*-promoter starts approximately twofold higher than in the control strain. The signal intensity increases and peaks at 36 hours 2.7-fold higher than at 0 hours. *nfs* promoter driven *mcherry*-expression starts at same levels as the negative control but increases 6.6-fold at 36 hours (**Figure 2-11 a**) correlating with darkening of the fruiting bodies (**Figure 2-11 b**).

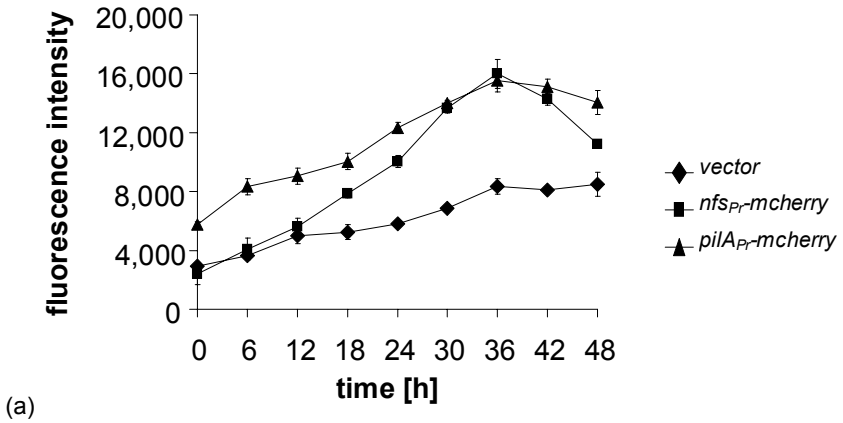

(a)

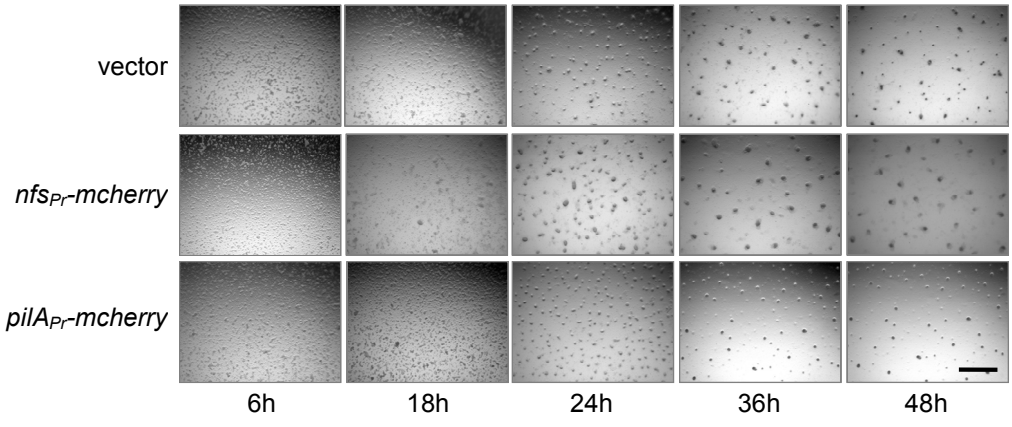

(b)

Figure 2-11 Quantitative fluorescence measurements of developing cultures. $2.5 \cdot 10^8$ cells were developed in black 24-well glass bottom dishes in submerged culture. (a) Mcherry specific fluorescence was determined every six hours. Experiments were carried out in triplicate. (b) Stereo microscope images of the developing cultures. The strains were imaged to confirm proper development (selected time points are shown). Bar: 1 mm.

These results suggest that *nfs* promoter driven proteins start to accumulate after 18 hours of development and reach highest levels at 36 hours reflecting continued expression. Otherwise, the curve of the signal intensity would adopt the slope of the control strain or decrease.

To distinguish which subpopulations of developing cells express *nfs* promoted *mcherry*, cultures that have developed for 36 hours were harvested and fruiting bodies were separated from peripheral rods by centrifugation (O'Connor & Zusman, 1991). The separated populations were then imaged with a fluorescence microscope.

While both rods and spores of the empty vector control strain displayed only weak autofluorescence signals, rods and spores from PH1221 (*pilA*$_{Pr}$-*mcherry*) produced strong fluorescence signals. In PH1220 (*nfs*$_{Pr}$-*mcherry*), only the background signal is detected from rods whereas spores emitted strong fluorescence suggesting that *nfs* is only expressed in the spore forming subpopulation of developing cells. This observation was confirmed by confocal laser microscopy of fruiting bodies. Fluorescing rods were only visible in strain PH1221 (*pilA*$_{Pr}$-*mcherry*) but not in PH1220 (*nfs*$_{Pr}$-*mcherry*) and the empty vector control (**Figure 2-12 a**).

We next sought to determine the patterns of Nfs protein accumulation during a starvation-induced time course. Only NfsA and B could be detected by immunoblot analysis (**Figure 2-12 b**). The proteins could be observed after 24 hours of development and they are still detected after one week. NfsC - H were not detectable by immunoblot. Therefore, it cannot be ruled out that these proteins display different expression and stability patterns during starvation-induced development.

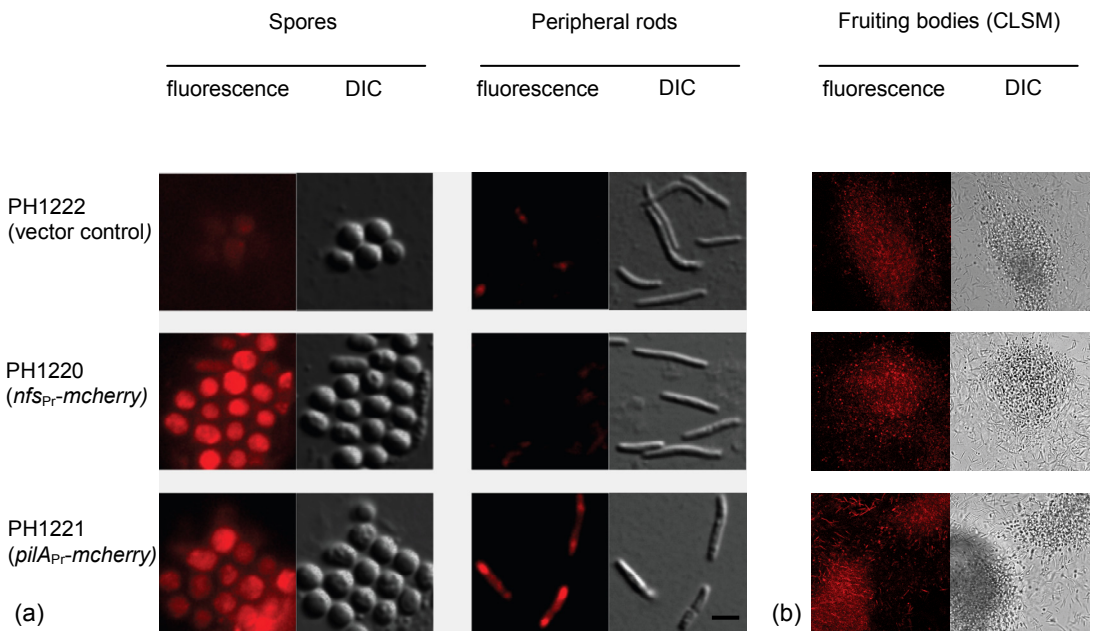

Figure 2-12 Fluorescence micrographs of cells from submerged culture. (a) Separated spores (left) and peripheral rods (right) after 36 hours development. Bar: 1 µm. (b) Confocal laser scanning microscope images of fruiting bodies after 48 hours (microscopy was performed by Dr. Kai Thormann).

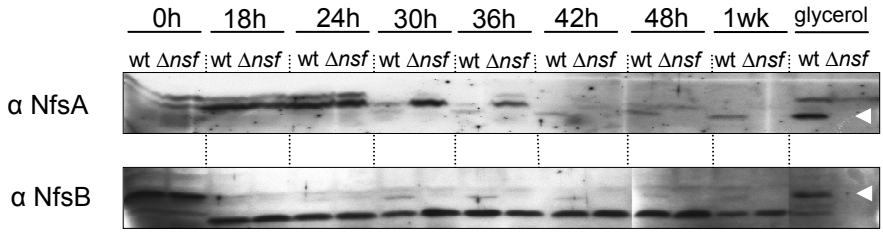

Figure 2-13 Anti-Nfs immunoblots on samples from developing cultures. Equal culture volumes were harvested at the indicated times of development, proteins were released by bead beating, resolved by poly-acrylamide gel electrophoresis, and probed with anti-sera specific to NfsA - H.

2.4 The Nfs proteins likely function together

2.4.1 Single *nfs* in-frame deletion mutants do not form glycerol-induced spores

To investigate whether all eight Nfs proteins are part of one functional unit, single *nfs* in-frame deletion mutants were generated with intact genes for the remaining *nfs* genes. The strains were characterized in terms of their ability to form glycerol spores. None of the mutants was able to form phase contrast bright spores but displayed a phenotype similar to the Δ*nfs* mutant (**Figure 2-14**).

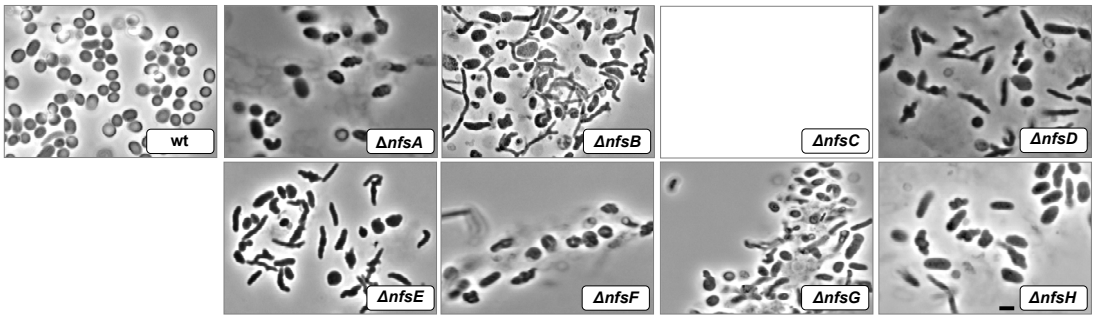

Figure 2-14 Phenotype of *nfs* single gene in-frame deletion mutants. Exponentially growing liquid cultures were induced with glycerol for twelve hours and imaged with phase contrast at 1000-fold magnification. Bar: 1 µm.

The phenotypes of the seven single mutants are similar to the Δ*nfs* mutant suggesting that each of the *nfs* genes is essential to form refractile spores and that the proteins may function together.

Several attempts to delete *nfsC* failed. We were not able to delete the entire gene or an internal fragment of 790 bp length. Recombining into up- or downstream regions as necessary precondition for a deletion was also not successful. Deletion by a recombineering approach using the existing *M. xanthus* cosmid library (Nils Hamann *et al*., unpublished) was not possible because the *nfs* locus is not part of this library.

2.4.2 The Nfs proteins localize to the cell envelope

To assay the predicted subcellular localization of the Nfs proteins, cell fractionation experiments were performed and the separated fractions of soluble and insoluble proteins probed with Nfs antisera.

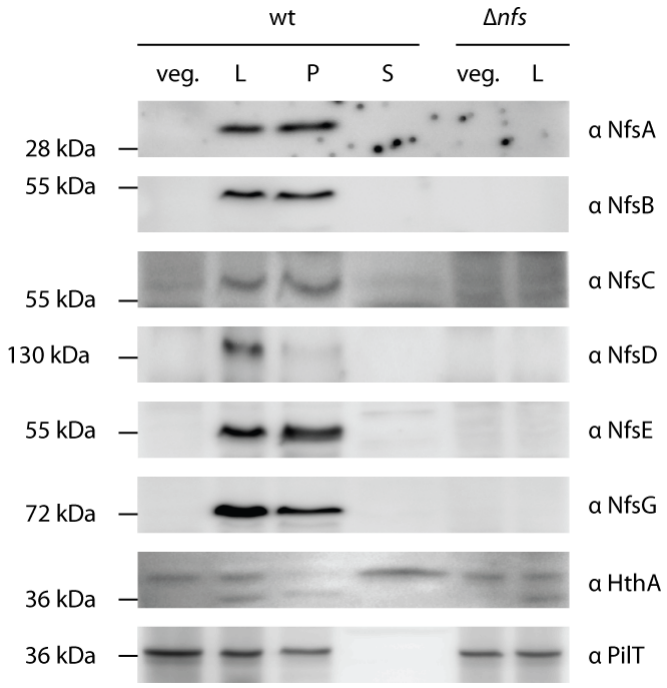

Figure 2-15 Subcellular localization of the Nfs proteins. Wild type (wt) and Δ*nsf* liquid cultures were induced with glycerol for two hours. Cells were harvested, lysed by bead beating and ultracentrifuged to separate soluble proteins from insoluble proteins with membranes. The proteins were further separated by SDS-PAGE and probed with Nsf-antibodies. veg: uninduced control, L: whole cell lysate, P: insoluble pellet fraction, S: soluble supernatant fraction.

The DNA-binding protein HthA (Nielsen *et al.*, 2004) served as example for soluble proteins and PilT as control for membrane associated proteins. Interestingly, the Nfs proteins can be detected in the fraction of insoluble proteins which suggests that the proteins are membrane associated and agrees with the predicted cell envelope localization.

2.4.3 Stability of the Nfs proteins is reduced in single in-frame deletion backgrounds

The predicted interaction domains in NfsD, E and G suggest that the proteins may be part of a larger complex and act together. In that case, loss of one of the proteins may destabilize the putative complex. Proteins that are not longer part of the complex may then be less stable, i.e. they are subjected to proteolysis. To test this hypothesis, the mutants with single *nfs* in-frame deletions were induced with glycerol, lysed and the cell lysates probed with Nfs antibodies (**Figure 2-16**).

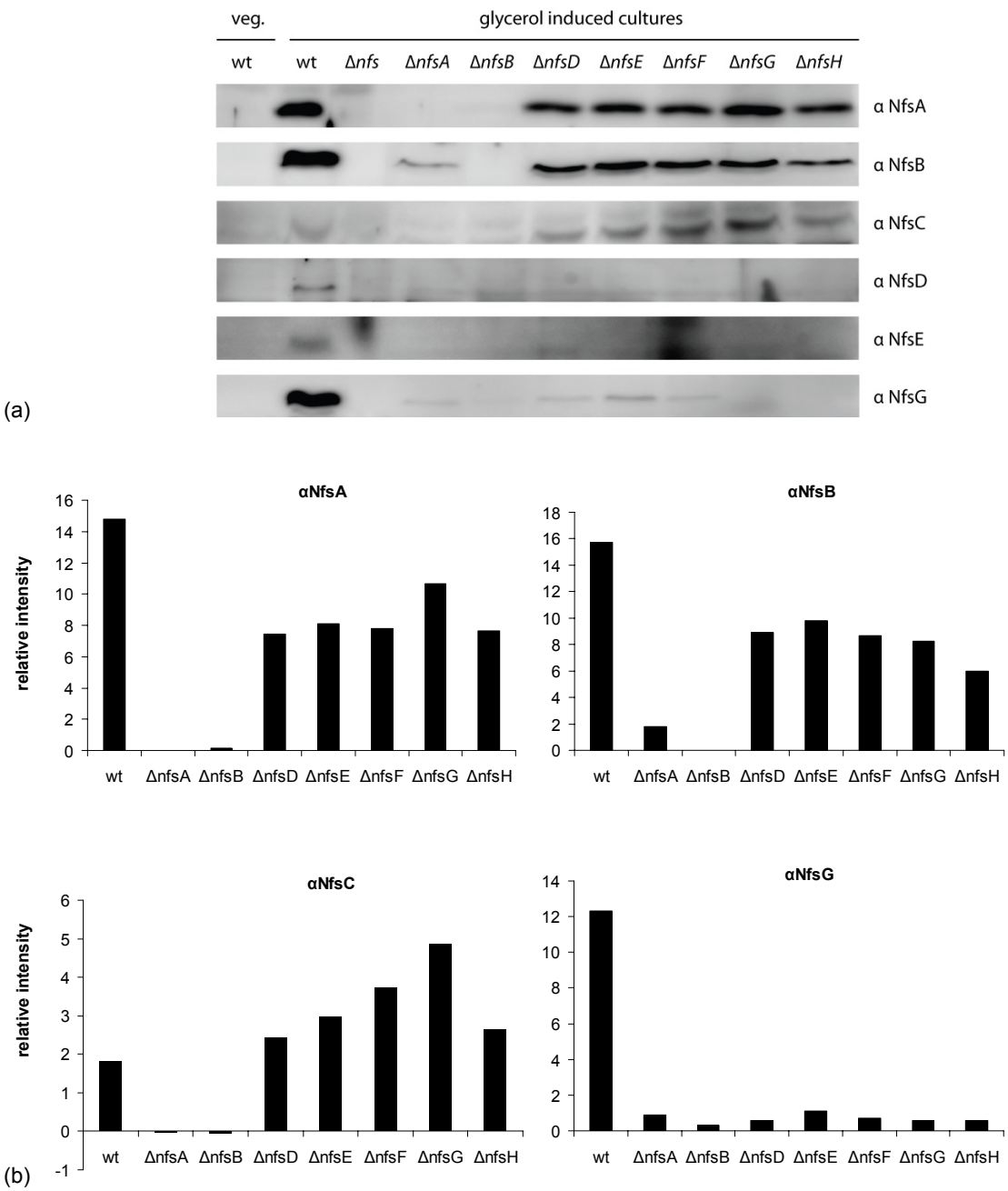

Figure 2-16 Western blot analysis on single in-frame deletion mutants. (a) Nfs immunoblots. Protein from cells that were induced with glycerol for two hours was released by bead beating. Equal protein concentrations were loaded on SDS-PA gels. Samples of uninduced (veg.) and induced wild type and induced Δ*nfs* served as control. (b) Bar graphs represent signal intensities as determined by densiometric analyses.

The immunoblot results suggest that NfsA, B and C are affected by loss of any of NfsD, E and G proteins since NfsA, B and C are still detectable but with reduced signal intensities compared to wild type. However, the signal of NfsB is strongly reduced in the *nfsA* background. Likewise, NfsA cannot be detected in the *nfsB* background. NfsC is also not detectable in *nfsA* and *nfsB* backgrounds suggesting that stability of these three proteins depends on each other.

However, NfsD and E cannot be detected in any of the single mutants; and the signal of NfsG is strongly reduced. These results indicate that Nfs D, E and G are unstable if any of the remaining Nfs proteins is absent.

2.4.4 The *nfs* locus consists of two transcriptional units

As outlined in **Section 2.1.8**, the *nfs* locus consists of eight genes oriented in the same direction. However, between NfsC and D as well as NfsE and F and NfsG and H exist non-coding sequences that could contain additional promoter elements. To test if the whole 12.5 kB locus forms one single transcriptional unit, PCR on cDNA generated from glycerol-induced cells was performed. Negative controls included samples without added reverse transcriptase to verify absence of contaminating genomic DNA and samples without added template. The results suggest that the locus is transcribed in two separate units consisting of *nfsA* to *C* and *nfsD* to *H*.

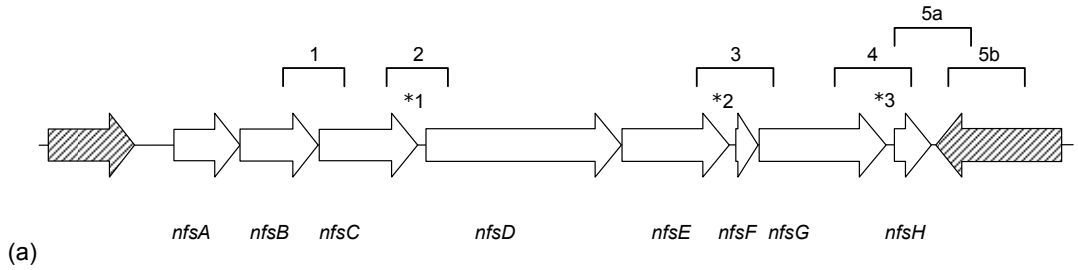

(a)

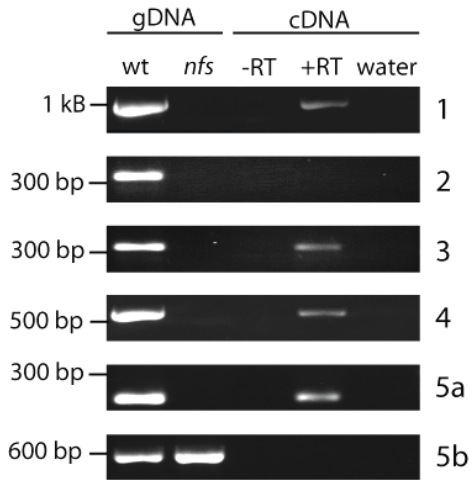

(b)

Figure 2-17 The *nfs* locus forms two transcriptional units. (a) Genetic organization of the *nfs* locus. Numbered brackets indicate the regions that were tested for presence of a continuous transcript. (b) PCR results. cDNA from glycerol-induced wild type cells was analyzed by PCR using oligonucleotide primers flanking the regions to be tested. Genomic DNA of wild type and Δ*nfs* served as control. wt: wild type, *nfs*: *nfs* deletion strain, -RT: control reaction without added reverse transcriptase, +RT: reaction with reverse transcriptase, water: template-free control.

Notably, a transcript could be amplified with an oligonucleotide that bound 183 bases downstream of the *nfsH* stop codon (**Figure 2-17 a**, Bracket 5a). However, no PCR product was obtained with an oligonucleotide that bound 506 bases downstream (**Figure**

2-17 a, Bracket 5b) suggesting that the terminator region of the second transcript is located in between these two binding sites.

Interestingly, the two transcriptional units detected by PCR coincide with the two patterns of protein stability (**Section 2.4.3**) and protein accumulation (**Section 2.3.1**).

2.5 Expression of the Nfs proteins is changed in the *fruA* developmental mutant background

It has been shown that the developmental process in *M. xanthus* is controlled by a gene expression cascade and that later key or marker genes are not expressed if the development is blocked earlier by inactivation of a key regulator (Kroos, 2007) (**Figure 1-6**). Therefore, genes involved in development can be classified by their dependency on certain developmental key regulators.

To test if *nfs* expression depends on key developmental proteins, the *nfs* promoter-*mcherry* fusion was introduced into specific developmental mutant backgrounds. These strains were developed and fluorescence intensities were measured at distinct time points.

Figure 2-18 a suggests that fluorescence intensities of all four strains are about equal levels at the beginning of the time course. The signal of the vector control is slightly increasing due to growing autofluorescence during development. However, fluorescence signals of PH1220 (nfs_{Pr}-*mcherry*) and Ω7536 (*exo*) with nfs_{Pr}-*mcherry* increase strongly by 6.6- and 5.4-fold until 36 hours. Fluorescence intensity of the *dev* mutant also increases but does not reach the level of the PH1220 and Ω7536 (*exo*). However, fluorescence signals of *csgA* stay low and close to control levels (**Figure 2-18 b**). Interestingly, in the *fruA* mutant, fluorescence intensity increases 6.2-fold already at 24 hours (**Figure 2-18 b**). This transcriptional activation of *nfs* in the *fruA* mutant background was confirmed by an NfsB-immunoblot on samples from a developing culture of an independent *fruA* mutant (data not shown).

These results suggest that *nfs* expression is independent of *exo* and *dev* but dependent on the C-signal. Interestingly, the genes are expressed in the *fruA*-mutant. FruA is a central regulator of developmental gene expression. The *fruA* mutant is blocked in developmental progression during early mound formation. Beta-galactosidase assays have shown that several genes are deregulated in a *fruA* mutant (Ogawa *et al.*, 1996). The data suggest that FruA may be involved in *nfs* repression during early stages of development.

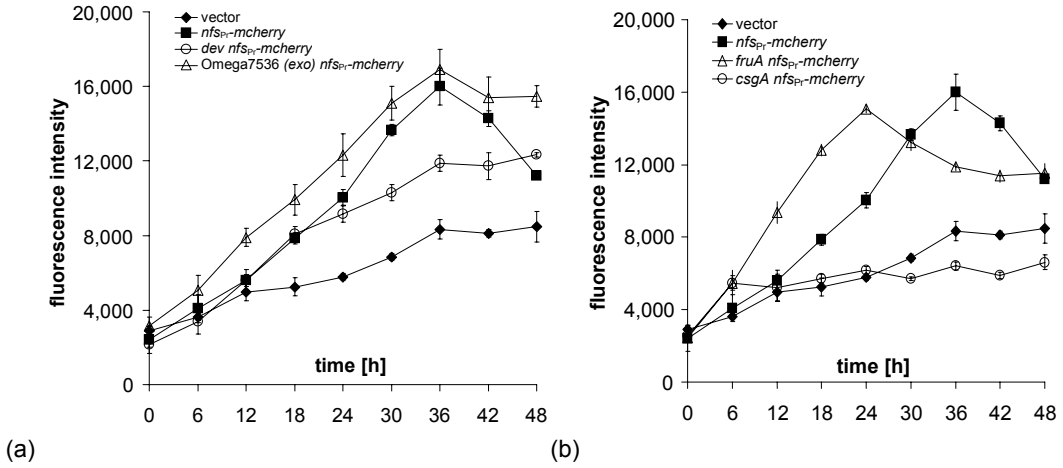

(a) (b)

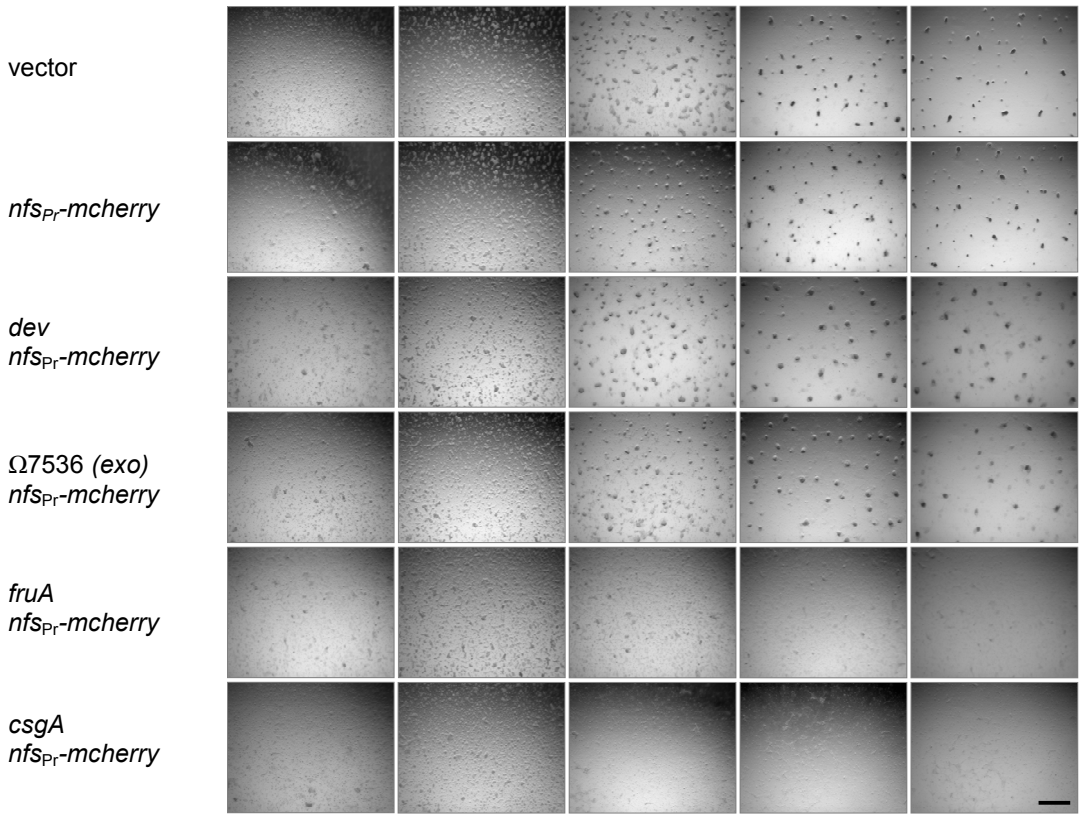

(c)

Figure 2-18 Quantitative fluorescence measurements of developmental mutants in submerged culture. Equal cell numbers were developed in 24-well black glass bottom dishes. *mcherry* specific fluorescence was determined at indicated time points. Experiments were carried out in triplicate. (a) Fluorescence intensities of the aggregating but not spore forming *dev* and Ω7536 (*exo*) mutants are plotted together with the empty vector control and PH1220 where *mcherry* is under control of the *nfs* promoter. (b) Fluorescence intensities of the non-aggregating *fruA* and *csgA* mutants with the same controls as in (a). (c) Stereo microscope images of the cultures. Selected time points are shown. Bar: 1 mm.

2.6 Differences in protein glycosylation patterns of wild type and Δ*nfs* were not detectable

Sequence analyses suggested that NfsC and E may be involved in protein glycosylation and NfsH may be a target for glycosylation. Glycosyltransferases are a large protein family involved in numerous processes mainly known from eukaryotic systems. Many of the characterized proteins play a role in cell wall associated polysaccharide metabolism (Iwai *et al.*, 2002a, Coutinho *et al.*, 2003). In bacteria, an increasing number of glycosylated proteins are known. In *B. subtilis*, spore coat proteins are glycosylated and in Gram-negative bacteria, exported or surface anchored proteins such as pili, adhesins and surface-layer proteins have been reported to be glycosylated (Power & Jennings, 2003, Messner, 2004, Schaffer & Messner, 2004). In *E. coli*, glycosylation of the exported cell adhesion mediating protein Ag43 by the action of the Aah and TibC glycosyltransferases has been observed. This protein modification takes place in the periplasm (Sherlock *et al.*, 2006). Since upon sporulation in *M. xanthus* spore-specific proteins are synthesized, and since spores of the *nfs* mutant appear less resistant and refractile, protein glycosylation patterns of wild type and the *nsf* mutant were analyzed. Ω7536 (*exo*) was also assayed because of its similar phenotype and putative function in carbohydrate metabolism and trafficking. For this purpose, cells were grown in liquid culture and induced with glycerol for four hours. Proteins were released by bead beating and separated by SDS-PAGE. The separated proteins were assayed for glycosylation. The protein glycosylation assay revealed no clear differences in protein glycosylation patterns between wild type and Δ*nsf*. Likewise, between wild type and Ω7536 (*exo*) no clear differences were visible.

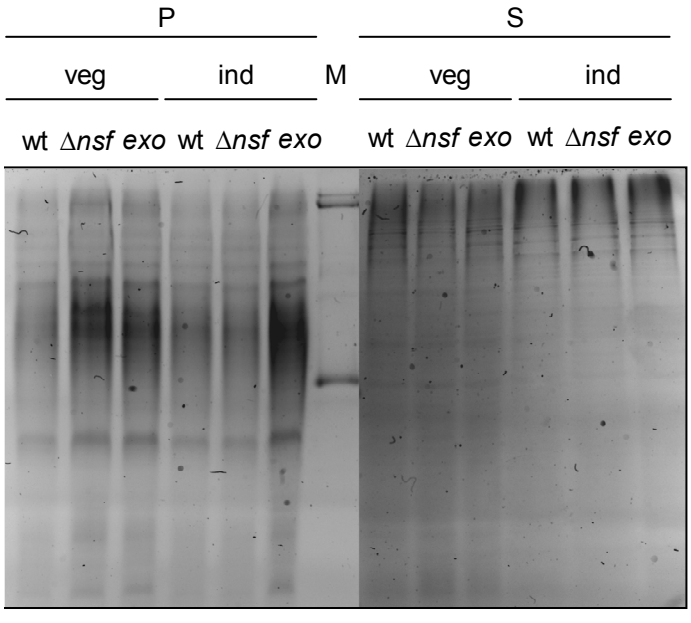

Figure 2-19 SDS-PA-gel stained for glycosylated proteins. Wild type, Δ*nsf* and Ω7536 (*exo*) were induced with glycerol for four hours. Cells were harvested and disintegrated by bead beating. The cell lysates were divided into soluble and insoluble fractions by ultracentrifugation and proteins were separated by SDS-PAGE. The fixed gel was stained for glycosylated proteins and imaged at excitation of 300 nm wavelength. P: cell envelope fractions, S: soluble fractions, veg: uninduced cells, ind: glycerol-induced cells, M: glycosylation marker.

2.7 Cell wall synthesis

The *nfs* mutant displays an aberrant spiral like cell morphology during elongation. Spiral-like structures in rod-shaped cells have been identified before. For example, the filament forming protein MreB was identified to assemble in spiral-like structures and as one key organizer of bacterial cell shape and cell wall synthesis. To test the hypothesis that the Nfs proteins are involved in co-ordinated cell shape remodelling and cell wall synthesis during outgrowth, peptidoglycan synthesis was studied by fluorescence labelling with vancomycin.

Vancomycin inhibits cell wall synthesis by forming stable complexes with the C-terminal d-Ala-d-Ala residues present in the lipid II-linked disaccharide pentapeptide cell wall precursors and in the nascent, un-cross-linked peptidoglycan. This blocks access of cell wall synthesizing penicillin binding proteins (PBPs) to their substrates, resulting in the inhibition of cell wall biosynthesis (Reynolds, 1989). Fluorescently labeled Vancomycin (VanFL) can therefore be used to identify places in the bacterial cell wall where new peptidoglycan is synthesized (Pereira *et al.*, 2007).

Exponentially grown wild type and mutant cells were stained as described in Materials and Methods (**Section 4.10**). As control and to test if the staining is specific to nascent peptidoglycan, cells were also grown to stationary phase. Since cells in stationary phase do almost not grow anymore, their rate of peptidoglycan synthesis was expected to be much lower compared to exponentially growing cells.

The signal of logarithmic growing cells appeared as patches dispersed over the entire cell. Cells of stationary phase displayed strong fluorescence signals towards the cell poles and sometimes at mid-cell (**Figure 2-20**). Since it is unlikely that stationary phase cells have strong turnover of peptidoglycan at the cell poles, the intense signal may be due to autofluorescence of storage compounds and unspecific binding of the stain. The background signals towards the cell poles can also be observed in unstained control cells but to lesser extend. Application of the staining technique to germinating wild type spores or re-elongating induced Δ*nfs* cells led to occurrence of patchy fluorescence signals sometimes with intense spots at the tips of outgrowing spheres (**Figure 2-20**) but these cells were fragile and prone to lysis after fixation.

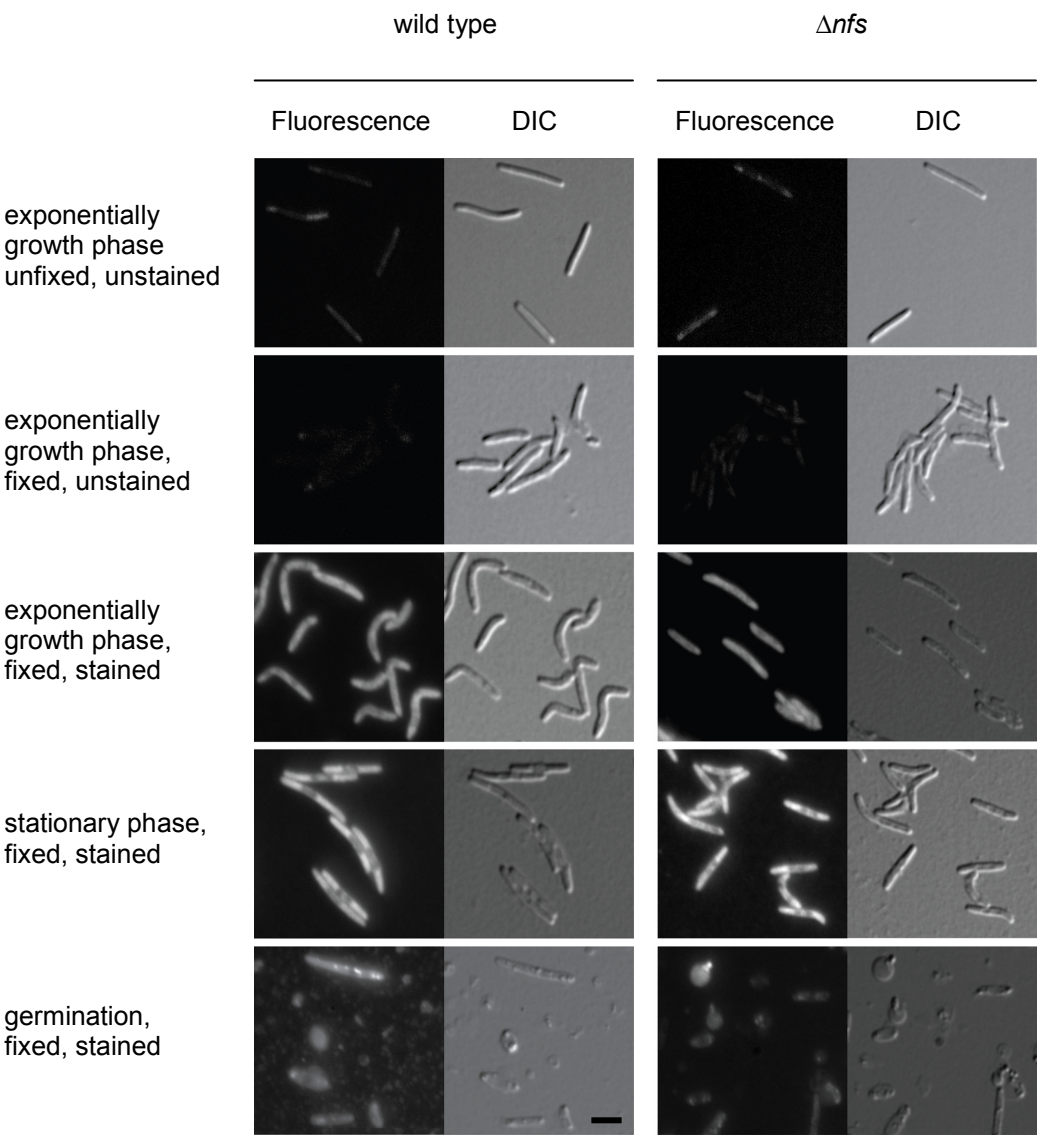

Figure 2-20 Fluorescence images of VanFL stained cells. Wild type and Δ*nsf* was grown in liquid culture and 1 ml samples were taken from logarithmic and stationary phase. Additionally, samples of germinating glycerol spores were used. Cells were fixed, stained and imaged under the fluorescence microscope. Bar: 1 µm.

2.8 Role of MreB during spore formation and germination

In most non-coccoid bacteria, certain proteins are present and responsible for maintenance of a distinct cell shape. In most cases, these proteins are highly conserved and essential or, if there are several homologues in one genome, at least important for a normal cell shape.

One of these proteins is the actin-like MreB. This protein is able to polymerize into twisted filaments that are attached to the cell membrane and traverse the longitudinal axis of the cell (Varley & Stewart, 1992, Figge *et al.*, 2004). Depletion of MreB in *Caulobacter crescentus* turns the rod-like cells into spheres and repletion of the protein reconstitutes normal rod cell shape (Figge *et al.*, 2004).

It is thought that the spiral-like MreB filaments localize the peptidoglycan synthesizing enzyme complexes during lateral growth and cell division (Figge *et al.*, 2004) (Carballido-Lopez, 2006) (den Blaauwen *et al.*, 2008). Therefore, assembly of new cell wall material occurs at distinct positions and coordinated by the cytoskeleton. To date, some proteins have been shown to co-localize with the MreB filaments (Divakaruni *et al.*, 2005, den Blaauwen *et al.*, 2008) and likely interact directly or indirectly (Kruse *et al.*, 2006, Bendezu *et al.*, 2008).

The observed phenotype of the *nfs* deletion mutants during glycerol induction suggests that there could be an uncoupling between the cytoskeleton protein MreB scaffolds and rapid cell wall conversion. Hence, the *nfs* genes may encode proteins that directly or indirectly interact with MreB and coordinate cell wall remodelling during sporulation and germination. To characterize the behaviour of MreB during the transition from rods to spherical spores and, during germination, back again to rods with respect to MreB synthesis and degradation as well as localization and its polymeric state could serve as a tool to understand how coordinated cell shape changes in *M. xanthus* are accomplished.

2.8.1 *In-vivo* labelling of MreB

To analyze the role of *M. xanthus'* MreB in cell morphogenesis and to visualize the behaviour of MreB during spore formation and cell elongation *in vivo*, the protein was fused both N- and C-terminal to the green fluorescent protein (Gfp) and the enhanced Gfp (March *et al.*, 2003, Chudakov *et al.*, 2005). To avoid the natural green autofluorescence background signal, the protein was also fused to Venus, a yellow fluorescing Gfp derivative.

In *M. xanthus*, MreB is likely essential under standard growth conditions. Several attempts to recombine in the *mreB* gene were not successful. Notably, high magnesium concentrations in the medium did not support growth of *M. xanthus mreB*-mutants (data not shown) as contrasted by *B. subtilis* (Formstone & Errington, 2005). To introduce a C-terminal label by homologous recombination likewise failed suggesting that the C-terminal labelled MreB is not functional (**Table 2-14**).

Mutants only were obtained for N-terminal fusions that were introduced at the Mx8 phage attachment site leaving the native *mreB* intact. However, distinct fluorescence signals above background were not detectable in these strains (**Figure 2-21**). A possible reason for this result is that the labelled MreB is not as efficiently assembled into the filaments as the simultaneously present native protein.

Table 2-14 Results of in vivo fluorescent labelling of MreB

Construct	Integration	Results
mreB (C-term)-*venus*	homologous	no colonies
$mreB_{Pr}$-*gfp-mreB*	Mx8-att	no specific fluorescence
$mreB_{Pr}$-*egfp-mreB*	Mx8-att	no specific fluorescence
$mreB_{Pr}$-*venus-mreB*	Mx8-att	no specific fluorescence
$mreB_{Pr}$-*gfp*	Mx8-att	no specific fluorescence
$mreB_{Pr}$-*egfp*	Mx8-att	no specific fluorescence
$pilA_{Pr}$-*gfp-mreB*	Mx8-att	multiple phenotypes

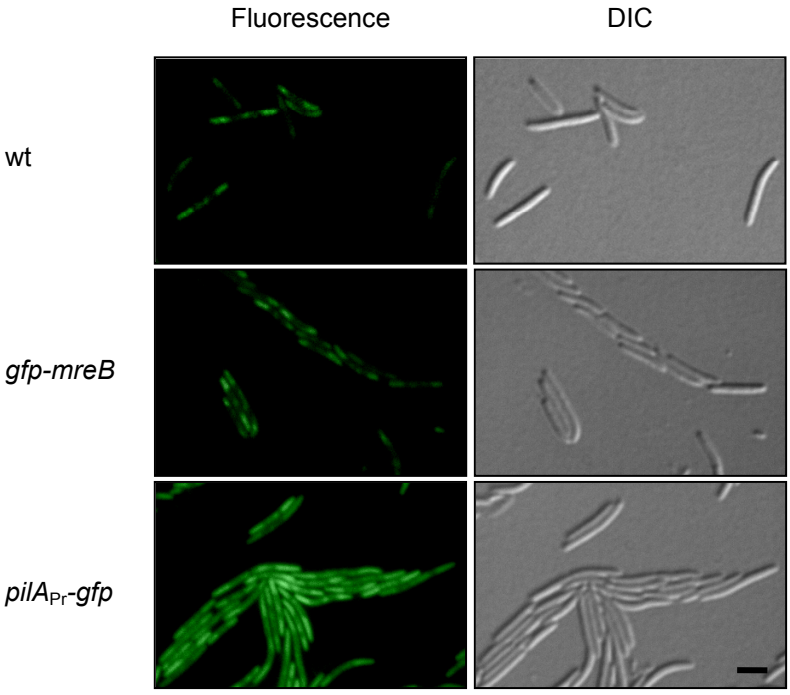

Figure 2-21 Fluorescence images of wild type, PH1250 (*gfp-mreB*) and PH1251 where *gfp* is under control of the *pilA*-promoter. Vegetatively growing cells were spotted on agarose pads and imaged with a fluorescence microscope. Bar: 1 µm.

2.8.2 Overexpression of MreB leads to cell shape defects

To increase the amount of labelled MreB per cell, a mutant was generated containing *gfp-mreB* under control of the strong *pilA*-promoter leading to overexpression of the fusion protein. Overexpression was confirmed by immunoblot (**Figure 2-25**). The obtained mutants grew slowly, colonies were tan and cells were non-motile. However, after incubation for several days, motile revertant cells spread from colony edges. The microscopic image revealed that many cells displayed severe cell shape defects such as spherical cells of various sizes (**Figure 2-22 a**).

The florescence images suggest that some cells contain bright fluorescing filaments associated with cell shape defects (**Figure 2-22 b**). These fluorescing filaments are also known from other studies (Karczmarek *et al.*, 2007). Furthermore, some single cells displayed an alternate punctuate fluorescence pattern along the cell axis as expected for the spiral forming MreB (**Figure 2-22 c**). Both the fluorescing filaments and the occasionally observed punctuate fluorescence pattern of *mreB* overexpressing cells suggest that *in vivo* labelling of MreB in *M. xanthus* is in principle possible, but expression of the labeled *mreB* needs a tight control as, for example, by an inducible promoter.

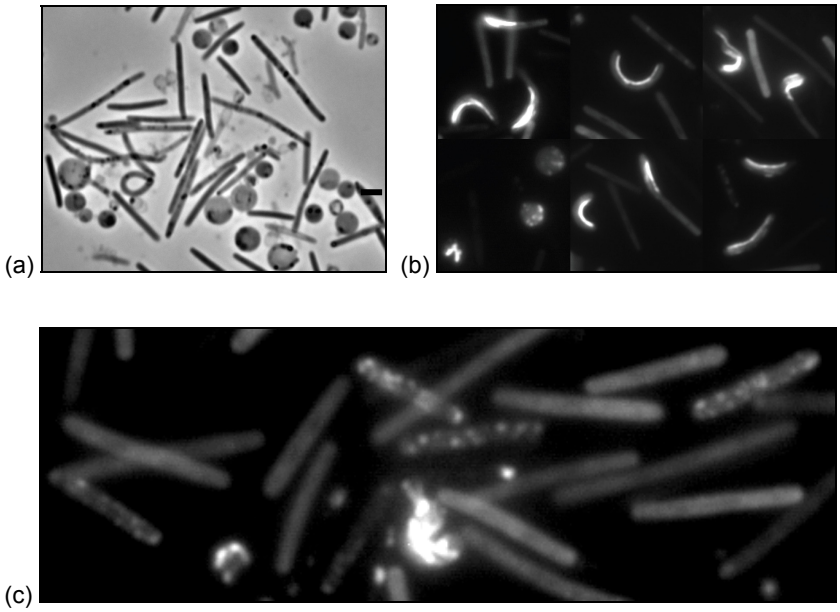

Figure 2-22 Phase contrast and fluorescence images of PH1252 (*pilA*$_{Pr}$-*mreB*). (a) Cells were grown in liquid, spotted on an agarose pad and imaged at 1000-fold magnification. (b) Malformed cells with bright fluorescent filaments are visible (combined image). (c) Single cells with punctuate fluorescence patterns.

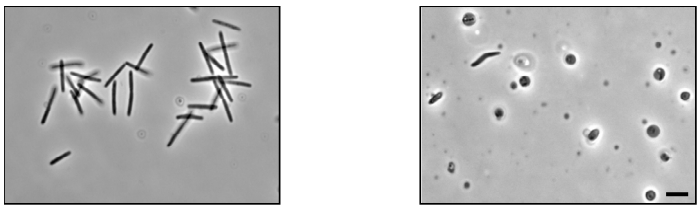

Figure 2-23 Phase contrast images of wt cells treated with 20 µg/ml A22 (dissolved in methanol) for 12 hours. The left image shows a control were the equal volume of methanol was added. Bar: 1 µm.

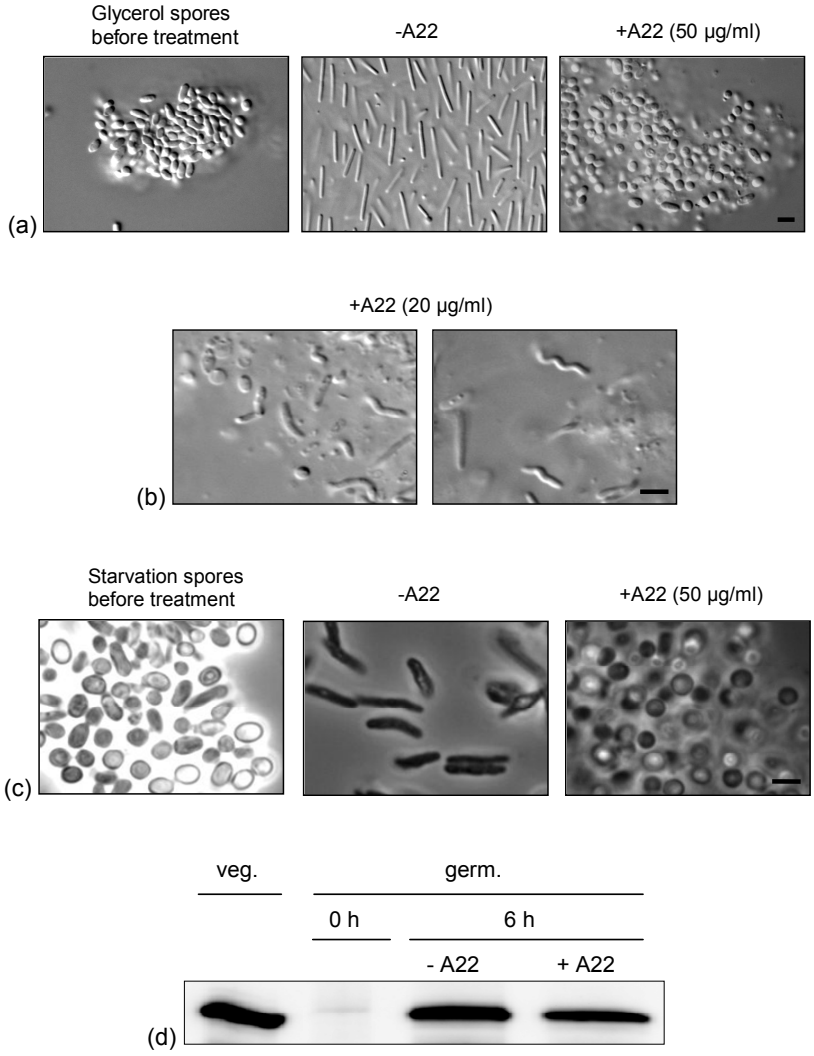

Figure 2-24 Micrographs of wild type spores in CTT treated with A22. (a) Glycerol spores were harvested, washed and resuspended in CTT medium. The suspension was split and A22 was added to a final concentration of 50 µg/ml. Cultures were incubated for twelve hours shaking at 32°C. Cells were imaged at 600-fold magnification with DIC. (b) Glycerol spores were treated as in (a) but A22 was applied to a final concentration of 20 µg/ml. (c) Starvation-induced spores were harvested after five days development in submerged culture. Samples were sonicated to disrupt fruiting bodies and peripheral rods and centrifuged to pellet the spores. Spores were resuspended in CTT medium and the suspension split into two samples and treated as in (a). Cells were imaged after six hours with phase contrast at 1000-fold magnification. Bar: 1 µm. (d) MreB immunoblots on samples from (c). Spores were germinated in CTT for 6 hours. veg.: vegetative cells (control), germ.: spores germinating in CTT with and without A22 (50 µg/µl) added.

2.8.3 *M. xanthus* cells are susceptible to A22 treatment

A second approach to manipulate MreB and cell shape is to add *S*-(3,4-dichlorbenzyl)isothiourea (A22) to growing cells (Iwai *et al.*, 2002b). Upon addition of A22, MreB filaments disappear and cells round up and lyse as shown for *E. coli*, *B. subtilis* and *C. crescentus* (Figge *et al.*, 2004, Carballido-Lopez & Formstone, 2007, den Blaauwen *et al.*, 2008) To test if A22 also affects *M. xanthus,* vegetative cells were incubated with the compound.

The results show that *M. xanthus* cells round up upon addition of A22. This suggests that *M. xanthus* MreB is susceptible to A22 and essential to maintain a rod shaped cell morphology (**Figure 2-23**).

2.8.4 A22 inhibits spore germination

To test the hypothesis that MreB polymerization is not only essential to maintain rod-like cell morphology but that is also crucial to generate rod-shaped cells from spheres in *M. xanthus*, A22 was added to both glycerol and starvation spores in rich medium.

The results of this experiment suggest that A22 inhibits spore germination at a concentration of 50 µg/ml and above (**Figure 2-24 a** and **c**), data for higher concentrations not shown). Interestingly, at a concentration of 20 µg/ml, glycerol spores start to germinate after 12 hours and most of the cells lyse. During this state, few spiral-formed cells are visible (**Figure 2-24 b**). However, since A22 is not stable in aqueous solutions, the concentration may have dropped below 20 µg/ml at this time.

The phase contrast images of developmental spores suggest that spores do not germinate in presence of 50 µg/ml A22 but their refractivity decreases. This probably means that spores turn into spherical cells when A22 is present in rich medium (**Figure 2-24 c**).

2.8.5 Overexpression and purification of MreB for antibody generation

To generate specific tools to study MreB in more detail, the *M. xanthus mreB*-gene was cloned into pET32a^{+} (Invitrogen) resulting in plasmid pFM50 containing several tags for protein affinity purification. This plasmid was transferred into different *E. coli* strains optimized for heterologous protein expression. The purified protein was to serve as antigen to generate anti-MreB antibodies in rabbits (Eurogentec).

Several attempts to obtain the protein soluble were not successful. Therefore, the protein was harvested and purified from inclusion bodies. Obtained antisera were tested for specificity against *M. xanthus* cell lysates and the inclusion body fraction from induced *E. coli* cells. These tests revealed that the antisera needed to be affinity purified (data not shown). After purification, the antisera were of sufficient sensitivity and specificity as shown by immunoblot (**Figure 2-25**).

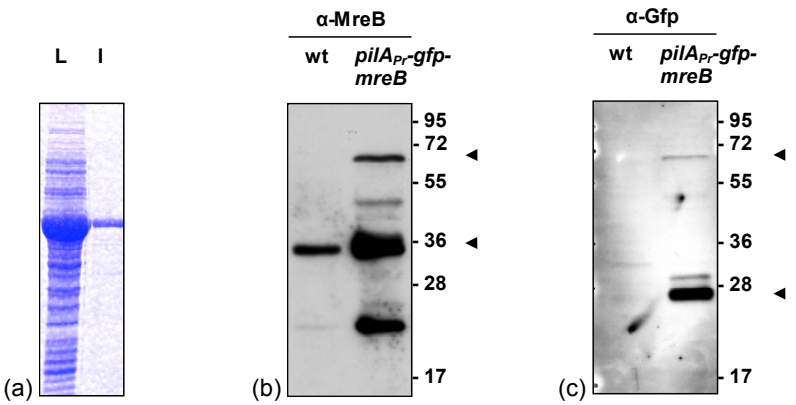

Figure 2-25 Purification of anti MreB antisera. (a) Cell lysate of *mreB* overexpressing *E. coli* BLλDE3 pLysS loaded on a SDS-PA gel. The MreB containing inclusion bodies were separated by centrifugation at 600 x g. L: whole cell lysate, I: separated inclusion bodies. (b) Test of purified antiserum against *M. xanthus* cell lysates. Samples of a *gfp-mreB* overexpressing strain were probed as control. wt: *M. xanthus* wild type, *pilA*$_{Pr}$*-gfp-mreB*: *gfp-mreB* overexpressing strain PH1252. (c): Same samples as in (b) but probed with anti Gfp antibodies. Calculated molecular weights: MreB: 36.5 kDa, Gfp: 26.9 kDa, Gfp-MreB: 65 kDa.

2.8.6 The fate of MreB depends on the sporulation pathway

To test if MreB becomes degraded or only depolymerized upon spore formation, a time course experiment of both glycerol- and starvation-induced spore formation was carried out. Cells and spores were lysed by bead beating and equal protein concentrations for each time point were separated by SDS-PAGE. The samples were blotted and probed with MreB antibodies. Both wild type and Δ*nfs* were tested to determine if MreB is regulated differently in the deletion mutant.

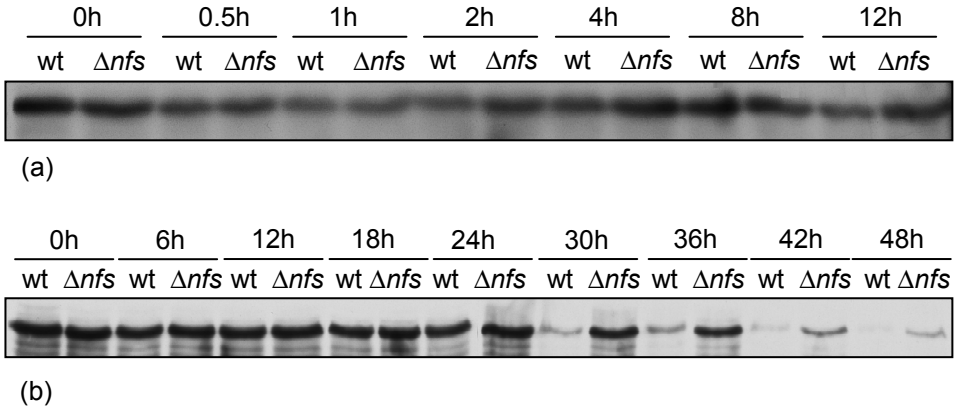

Figure 2-26 Anti MreB immunoblots on glycerol- and starvation-induced sporulating cells. (a) Glycerol induction time course. Wild type and Δ*nfs* were induced with glycerol and samples were taken at indicated time points. Proteins were released by bead beating and separated by SDS-PAGE. (b) The same strains as in (a) were developed in submerged culture and lysed as the glycerol-induced cells. To distinguish relative MreB levels at distinct time points, all samples were adjusted to equal protein concentrations.

The immunoblots suggest that MreB can be detected during the whole glycerol spore induction time course in similar amounts. This means that the protein is not degraded although cells round up and form spores. However, during starvation-induced development, MreB specific signals start to decrease after 30 hours suggesting that the protein becomes degraded. Additionally, the timing of this degradation is slightly different in the Δ*nfs* mutant. In this strain, the MreB signal decreases after 42 hours. Since developmental spores of the Δ*nfs* mutant are less refractile and display reduced viability, this may reflect perturbed cell wall reorganization.

Interestingly, immunoblot results suggest that starvation-induced spores synthesize MreB *de novo* upon germination but do not elongate in the presence of A22 (**Figure 2-24 c** and **d**). This result suggests that MreB polymerization is essential for spore germination.

2.8.7 MreB subcellular localization

Sequence analysis of MreB suggests that the protein is cytoplasmic. However, it has been reported that MreB has a strong membrane affinity (Chiu *et al.*, 2008). The mechanism by which MreB is directly or indirectly attached to the membrane is not yet known. Under native conditions, most of MreB is present in its polymerized form as filaments, protofilaments or oligomers. These polymers are sedimented by ultra-centrifugation together with the insoluble cell envelope fraction.

As shown above, the protein seems not to be degraded during glycerol-induced sporulation. Therefore, it is likely that the MreB filaments are disassembled and the protein is kept in its monomeric or in an oligomeric state. These mono- or oligomers then could detach from the membrane allowing cells to round up.

Immunoblot analysis on separated soluble and cell envelope fractions of glycerol-induced cells suggest that MreB is still associated with the membrane when cells form glycerol spores. This suggests that MreB stays in its polymeric and/or membrane attached state during glycerol spore formation and is not cytoplasmic dispersed.

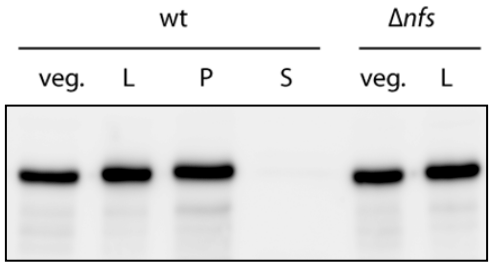

Figure 2-27 Subcellular localization of MreB after glycerol induction. Wild type (wt) and Δ*nsf* liquid cultures were induced with glycerol for two hours; harvested, lysed by bead beating and ultracentrifuged to separate soluble proteins from insoluble proteins with membranes. Samples are the same as in **Figure 2-15**. Proteins were separated on a SDS-PA-gel and probed with MreB antibodies. veg: uninduced control, L: whole cell lysate, P: insoluble pellet fraction, S: soluble supernatant fraction.

3 DISCUSSION

3.1 Micro array analysis

3.1.1 Up-regulation of sporulation markers indicates that glycerol- and starvation-induced spore formation share core processes

To better understand the process of spore formation in *M. xanthus,* we applied transcriptome profiling of glycerol induced spore formation by micro array analysis. This approach to use the glycerol-induced sporulation as model for *M. xanthus*' spore formation in general has been previously proposed (Dworkin & Gibson, 1964) and was applied in several early studies. However, the model system became disregarded mainly because of differences in thickness of the spore envelope seen in electron micrographs (O'Connor & Zusman, 1999). Additionally, proteins S, W and C, present in starvation induced spores, are absent in glycerol spores. Interestingly however, deletion of the gene encoding for protein S has no effect on spore formation (Komano *et al.*, 1984). Moreover, both spore types share many characteristics such as resistance to heat, sonication and detergents (Sudo & Dworkin, 1969), spherical shape and refractivity in phase contrast, and both spore types contain protein U. Additionally, both pathways induce a β-lactamase activity (O'Connor & Zusman, 1997).

Analysis of our micro array data suggests that most of the described sporulation marker genes are up-regulated such as *prU* (encoding for protein U) which is one of the most highly activated genes, *ops* (encoding for protein S1), *fdgA*, *exo*, *sigB* and *C*, *nla6*, *mspA* and *C* (where *mspC* represents also one of the most highly activated genes), *aceA* and *B* (encoding for glyoxylate cycle enzymes), *treS* (encoding for trehalose synthase). Conversely, genes that have been described to play a role in signaling, aggregation and non-spore forming subpopulations during starvation-induced development such as *asg* (encoding for A-signaling genes), *csg* (encoding for the C-signal), *popC*, *frzCD* and *devTSR* as well as the gene for myxobacterial hemagglutinin (MBHA) which is known from non-aggregating peripheral rods, are not regulated. This indicates that glycerol induction specifically activates the core sporulation process.

Interestingly, we also found *tps* (encoding for spore coat protein S) weakly up-regulated as contrasted by a previous beta galactosidase assay based report that suggests that *tps* is not transcribed during glycerol spore formation (Downard & Zusman, 1985). The reason for this difference may be the unequal sensitivity of both methods. Unexpectedly, we found three genes up-regulated which to date are only known to play a role in aggregation during starvation-induced development. These genes are *fruA*, *mrpC* and *actB*. Interestingly, all three genes are thought to act as transcriptional regulators during starvation-induced development, but intriguingly, *mrpC* and the *actB* mutant seem to have a glycerol-induced sporulation defect whereas the *fruA* mutant forms normal refractile glycerol spores (Müller & Higgs, unpublished data and (Ogawa *et al.*, 1996)). These results suggest that the regulated target genes of MrpC, ActB and

maybe FruA are not only involved in early stages of aggregation and formation of fruiting bodies but also directly in spore formation. Since the *mrpC*, *actB* and *fruA* mutants are defective in starvation-induced aggregation, the role of these genes in spore formation may be masked by the inability of the mutants to form fruiting bodies. Glycerol-induced spore formation would provide an appropriate tool to analyze putative targets of these regulators during spore formation.

The genes for the alternative sigma factors B (*sigB*) and C (*sigC*) are highly up-regulated. Target sequences for these sigma factors have not been published. However, deletion of *sigB* affects stability of mature spores. Therefore, *sigB* is proposed to be involved in maintaining the dormant stage of spores (Apelian & Inouye, 1990). Up-regulation of the late-stage sigma factor B supports this idea in particular, since peak expression of *sigB* is not at the beginning of the time course but after two hours. *sigC* is highly transcribed throughout the whole time course. Expression of *sigC* during glycerol-induced sporulation has been reported (Apelian & Inouye, 1993) but inactivation of *sigC* alone likely does not interfere with both glycerol- and starvation-induced spore formation. However, the mutant forms fruiting bodies on semi-rich media (Apelian & Inouye, 1993). Therefore, it is thought that SigC is involved in repression of fruiting body formation but not sporulation in the presence of nutrients, which also matches the conditions of glycerol-induced spore formation. This suggests that *sigC*, although consistently and highly activated, is not actually a core sporulation gene.

NtrC-like transcriptional activators are a second group of regulatory proteins that have been demonstrated to play a role in development. At least four of these genes (*nla4*, *6, 18* and *24*) have been reported to cause both a glycerol- and a starvation-induced sporulation defect upon deletion (Caberoy *et al.*, 2003). However, target DNA binding consensus sequences of the regulatory proteins have not yet been published. We found *nla6* up-regulated while *nla4*, *18* and *24* were not regulated. NtrC-like activators mostly act as response regulators in signal transduction systems. Therefore, the genes do not necessarily need to be up-regulated to function. More likely, the proteins are constitutively synthesized and are activated by respective signaling systems. *nla6* seems to be an exception. It has been studied in more detail and a putative binding consensus sequence for the protein has been proposed (K. Giglio, 34th International Conference on the Biology of the Myxobacteria). One of the predicted binding sites lies upstream of *Mxan_3259*, the leading gene of a highly activated gene cluster encoding for putative membrane associated proteins involved in polysaccharide metabolism (**Table A-15**). Other putative targets of Nla6 are genes *Mxan_2688* through *Mxan_2690* which are also up-regulated in our data and might be involved in lipo- or exopolysaccharide synthesis. Notably, *Mxan_2689* may be involved in synthesis of alginate, an exopolysaccharide essential for cyst-formation in *Azotobacter* (Nunez *et al.*, 1999) (Moreno *et al.*, 1998). Therefore, these gene clusters represent excellent candidates for further study of spore envelope biogenesis. These data also may suggest that Nla6 acts as an activator of sporulation-specific genes involved in spore envelope synthesis. Real-time PCR analysis of sporulation marker genes, immunoblot analysis on spore-specific proteins in the *nla6* mutant and more detailed analysis of the target DNA-binding sequence could test this hypothesis.

The observation that most sporulation marker genes are up-regulated in the micro array data suggests that the oligomer-based micro arrays from the TIGR institute and the optimized hybridization protocol which we employed provide reliable data. In summary, analysis of the micro array results revealed that the glycerol-induced sporulation process is a suitable model for the core sporulation pathway in *M. xanthus*. Our transcriptional profiling may also be advantageous over proteomics approaches that largely depend on solubilization and mobility of the isolated proteins.

3.1.2 Regulated processes and regulation patterns

Genes of all functional categories are represented in the large number of significantly regulated genes. To analyze which functional groups of genes and which putative processes are mostly subjected to differential regulation, the genes were first grouped based on their assigned functional category and the genes in each category were divided into up- and down-regulated genes. We found that genes involved in 'protein synthesis' (such as ribosomal proteins) and genes encoding for proteins involved in respiration and electron transport (**Figure 2-3** and **Table A-15**) are down-regulated suggesting that that glycerol-induced cells reduce metabolism and synthesis of macromolecules. However, transcription of these genes does not appear to be completely shut down which suggests that they are still transcribed or their mRNA stays stable during glycerol-induced spore formation. These results are consistent with previous biochemical analyses showing that respiration rates of glycerol-induced cells decrease. Likewise, net synthesis of protein, DNA and RNA was found to decline (but not cease) within the first two hours after addition of glycerol (Bacon *et al.*, 1975).

The surprisingly high proportion of up-regulated genes reflects the fact that glycerol-induced sporulating cells do not simply convert into dormant vegetative cells, but instead form distinct entities which acquire very different structural and metabolical properties. This is emphasized by the high proportion of regulated genes in the categories 'energy metabolism' and 'central intermediate metabolism'. Similar numbers of genes in these categories are up- and downregulated suggesting that sporulating cells switch from actively growing to a non-growing but still active state as new spore specific proteins and envelope material need to be synthesized. For example, all seven of the genes encoding for enzymes involved in glycolysis or gluconeogenesis are found up-regulated. Another interesting result is the high up-regulation of the genes encoding for glyoxylate cycle enzymes (*Mxan_6441* and *Mxan_6442*, **Table A-15**). These results suggest activation of carbohydrate synthesis during spore formation. Previous reports have shown that 75% of the glycerol-induced spore coat consists of glucose and galactosamine (Kottel *et al.*, 1975). *M. xanthus* cannot not utilize carbohydrates as a carbon source (Bretscher & Kaiser, 1978) and the growth medium does not contain significant amounts of sugars. The glycerol added to induce sporulation does not serve as precursor for the carbohydrates in the spore coat because it has been reported that only minor amounts are incorporated (Sadler & Dworkin, 1966). Previous analyses of enzymatic activities have also shown that gluconeogenesis and glyoxylate cycle enzymes are much more active during glycerol-induced spore formation (Filer *et al.*, 1977). Together, these observations suggest that synthesis and export of large amounts

of carbohydrates necessary for spore formation may be due to up-regulation of the related genes.

Similarly, *treS*, encoding for trehalose synthase, was found to be up-regulated. Trehalose is a common bacterial carbohydrate storage compound, but is also synthesized during adaptation to osmotic shifts (Elbein *et al.*, 2003). Therefore, the up-regulation could be a side effect of adding glycerol which leads to changes of the osmotic conditions. However, it has been reported that also starvation-induced spores accumulate trehalose to even higher amounts than glycerol-induced spores (McBride & Zusman, 1989). Our data suggest that the trehalose accumulation is not only due to increased enzyme activity but also up-regulation of the gene for trehalose synthase.

To gain insight into patterns of gene expression during glycerol-induced development, the up-regulated genes were clustered based on their expression profile. Interestingly, this hierarchical clustering revealed two distinct regulation patterns suggesting two waves of gene expression. Distribution of known sporulation marker genes in the two generated heat maps (**Figure 2-4 b**) suggests that most genes essential for conversion into resistant, viable spores (such as *exo*, *fdgA*, *cbgA*, *Mxan_3026* and *Mxan_1101*) are enriched in Map 1 containing immediately up-regulated genes. Genes that are necessary for spore maturation (such as genes for spore coat proteins U, S and S1) are enriched in Map 2 together with later expressed genes. We cannot rule out that there are subsequent groups of genes expressed since data from later time points were excluded from the analysis. Our findings are supported by a proteomics approach using SDS-PAGE (Komano *et al.*, 1980) where distinct patterns of protein synthesis during glycerol-induced spore formation were observed, although sequence and function of the proteins were not determined. Quantitative measurements of DNA-, RNA- and protein synthesis during glycerol spore formation also identified a biphasic profile (Sadler & Dworkin, 1966). These results suggest that not only the starvation-induced developmental program requires tightly controlled gene expression cascades (Kroos, 2007), but also the core spore formation process itself is divided into early and later stages.

3.1.3 Genes involved in cell envelope related processes likely are important for spore formation

Spore formation in *M. xanthus* is very distinct from spore formation in Gram-positives. This is emphasized by the fact that *cbgA* is the only sporulation-related gene in *M. xanthus* that has been identified by sequence homology to a *Bacillus sp*. spore cortex protein. Approaches to identify *M. xanthus* spore formation genes by homology to genes of other Gram-negative spore formers are not successful since the sporulation process in Gram-negative bacteria is not understood.

The most obvious differences between *M. xanthus* spores and vegetative cells are found in the cell envelope. Shape, ultrastructure, and composition are very different which is emphasized by the recent finding that glycerol-induced spores do not contain significant amounts of peptidoglycan (Bui *et al.*, 2008). The spore envelope is largely responsible for the increased resistance properties since less resistant sporulation mutants often display defects in their spore envelopes (such as *fdgA*, *exo*, *cbgA*, *mspA* and *C* mutants). Likewise, the results of our small-scale mutagenesis approach support this assumption.

We selected up-regulated genes from different functional categories for inactivation by insertion mutagenesis. Although this mutagenesis was not saturating, the surprising result was that the both mutants which displayed defects in glycerol-induced spore formation are putatively affected in envelope modifications.

Therefore, up-regulated hypothetical genes encoding for proteins that likely localize to the cell envelope appear to be good candidates to identify novel core sporulation genes in *M. xanthus*. Our transcriptional profiling data indicate that almost 25% of the cell envelope associated proteins were differentially regulated (**Figures 2-2** and **2-3**) which also suggests large changes in envelope associated proteins. However, the role of many of these proteins is unknown because their assignment to this particular category is often only due to a predicted lipid modification or alpha-helix fold (**Table A-15**). This means, from a functional point of view, these genes are of unknown function.

3.2 The *nfs* locus consists of hypothetical genes encoding for proteins involved in the core sporulation process

The identified *nfs* locus supports the conclusion that sporulation-specific expressed hypothetical genes that are predicted to localize to the cell envelope form a sufficiently defined group to search for novel core sporulation genes. Deletion of the *nfs* genes does not affect vegetative growth or fruiting body formation. However, the fruiting bodies fail to darken and the spores inside are less viable. Additionally, the mutant is not able to form refractile, resistant glycerol spores. This suggests that the *nfs* genes represent core sporulation genes.

The phenotype of the Δ*nfs* strain during glycerol spore formation is intriguing. Upon glycerol-induction, cells shorten but seem unable to acquire refractivity or an optical dense spore envelope. Refractivity in phase contrast indicates spore maturation by desiccation suggesting that *nfs* mutants are not able to complete the process. Instead, the translucent ovoids convert back into rod-shaped cells. This re-elongation is accompanied by transient formation of malformed, spiral-like cells. Interestingly, mutants in *exo* likewise do not form glycerol- and starvation-induced spores, whereas fruiting body formation is not affected. Like in the Δ*nfs* mutant, glycerol-induced *exo* cells shorten but do not form spores and convert back into rod-shaped cells (Licking *et al.*, 2000). Because of this similar phenotype, it is possible that *nfs* and *exo* are involved in the same cellular process.

exo resides in a locus consisting of nine genes likely involved in carbohydrate synthesis and trafficking (**Table A-15**). Glycerol spores do not contain peptidoglycan (Bui *et al.*, 2008). Assuming that *exo* and Δ*nfs* cells degrade their cell walls too but fail to modify the cell envelope correctly (for example by export and cross-linking of carbohydrates or deposition of coat proteins) this could explain formation of non-refractile, translucent and enlarged ovoids approximately six to eight hours after addition of glycerol when wild type spores gain refractivity.

By an unknown mechanism, the cells unable to finish spore formation convert back into rod-shaped cells which could suggest that there exists check points or sensing mechanisms that monitor progress of the spore formation and are able relieve cells from

this developmental pathway if they cannot pass through the next stage. This contrasts spore formation in *Bacillus*, where the process cannot be interrupted after certain stages have been passed. In *M. xanthus* however, also starvation-induced sporulation can be interrupted at any stage by repletion of nutrients. The Δ*nfs* mutant forms non-refractile spores also inside fruiting bodies suggesting that cells that undergo starvation-induced development are likewise unable to finish the sporulation process. In fruiting bodies however, the spheres do not convert back into rods. This may happen because the fruiting body environment provides additional signals preventing cells from re-elongating or it could be due to the lack of nutrients. The latter could explain the strongly reduced viability of starvation-induced spores. If the cells cannot finish spore formation but stay in a non-dormant state or try to grow out without nutrients, they could use up their energy sources and finally die.

3.3 Nfs-expression during starvation-induced development is C-signal dependent and controlled by FruA

The Δ*nfs* and *exo* mutants display similar phenotypes both in starvation- and glycerol-induced sporulation. To test whether the gene products function in the same process during spore formation, we first examined whether both mutants share the same dependency on developmental marker genes during starvation-induced sporulation. To be able to quantify the activity of the *nfs* promoter in various developmental mutant backgrounds, we fused the putative *nfs* promoter region to *mcherry* as a reporter.

The quantitative fluorescence measurements of developing cultures suggest that *nfs* expression during starvation-induced development is entirely dependent on *csgA* and therefore on C-signaling. The *csgA*-mutant is blocked early in development; it does not aggregate or sporulate. In the *dev* mutant background however, *nfs* promoter-driven gene expression was detected, but less than in the wild type. The *dev*-mutant does not form mature fruiting bodies and the number of spores is strongly reduced (Boysen *et al.*, 2002). This result suggests that *nfs*-expression depends partially on the *dev* locus. In the *exo* mutant background, wild type levels of *nfs* expression were detected suggesting that *nfs* regulation is independent of *exo*.

fruA is also a non-developing mutant. The FruA-protein is a transcription factor with a central role during starvation-induced development. The protein is thought to be phosphorylated and this modified form is proposed to allow the developmental program to proceed by differential control of gene expression (**Figure 1-6**) (Ellehauge *et al.*, 1998). Unexpectedly, we saw a strong and early increase of *nfs* promoter-driven fluorescence in the *fruA* mutant compared to wild type. This result was confirmed by Nfs immunoblot on time-course samples form an independent *fruA* mutant strain (data not shown). Interestingly, unpublished results (X. Shi & L. Søgaard-Andersen) suggest that *exo* is likewise transcribed in the non-developing *fruA* mutant. A possible explanation is that *nfs* as well as *exo*-expression during starvation-induced development is controlled by FruA and that FruA is involved in repression of these genes during early development (**Figure 3-1**).

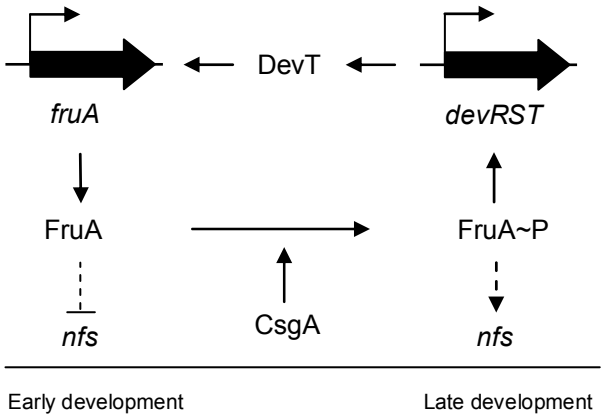

Figure 3-1 Schematic model of *nfs* expression control. During early stages of development, unphosphorylated FruA represses *nfs* expression directly or indirectly. CsgA triggers FruA phosphorylation. Phosphorylated FruA induces *devT* expression and DevT stimulates *fruA*-expression. High levels of FruA~P relive repression of late developmental genes such as *nfs*.

However, fluorescence measurements cannot provide direct evidence for accumulation of the Nfs-proteins in spore forming cells. Accumulation of the signal does not necessarily reflect increasing promoter activity since the Mcherry protein may have different stability properties than the Nfs-proteins. An important next step to investigate whether *nfs* and *exo* participate in the same process is to generate a Δ*nfs exo* double mutant. Analysis of glycerol- and starvation- induced Δ*nfs*, *exo* and Δ*nfs exo* mutants as well as wild type by electron microscopy should reveal if there are similar defects or missing layers in the spheres.

3.3.1 The Nfs proteins likely participate in a cell envelope-associated functional complex

The observation that the single *nfs* in-frame deletion mutants display phenotypes similar to deletion of the entire locus suggests that the proteins function together. This assumption is supported by the reduced stability of the Nfs proteins in single gene deletion backgrounds.

The Nfs proteins are detectable by immunoblot 30 minutes after addition of glycerol. At this time, gene expression levels are already at maximum. After two hours, all six detectable proteins accumulate to highest levels but only NfsA and B are stably detected until twelve hours. Analysis of protein stabilities in the single gene deletion backgrounds have shown that stability of NfsD to H strongly depends on presence of NsfA, B and C. However, if NfsD to H are missing, NfsA, B, to C levels are only reduced. These results could mean that the Nfs proteins do not form one large tight complex but two interacting complexes consisting of NfsA, B, C and of NfsD to H. Alternatively, NfsA, B and C may constitute a specific part of the complex that localizes to a different compartment (such as the outer membrane) and is therefore more stable (i.e. protected from degradation) than the remaining Nfs proteins. This possibility is supported by CELLO localization predictions that suggest that the first three proteins localize to the outer membrane.

NfsA and H likely are beta-barrel fold containing proteins. Beta-barrel structures are a characteristic motif of outer membrane proteins. NfsD contains a predicted N-terminal transmembrane domain. Therefore, the protein probably localizes to the cytoplasmic membrane. For NfsG, psiBlastp alignments suggest that this protein is related to ABC-transporters or ATP binding proteins. Additionally, Phobius prediction suggests that the N-terminal part is cytoplasm-exposed (containing the FHA-domain) and the C-terminal part localizes to the periplasm. Both parts are separated by a hydrophobic segment. Therefore, the protein likely also localizes to the cytoplasmic membrane. NfsE contains a lipid attachment site. Based on the amino acid sequence (+2 D sorting rule, (Seydel *et al.*, 1999)), the protein likely localizes to the outer membrane. For NfsB, C and F no clear prediction for a membrane anchoring structure or modification exists. Detection of NfsB and C in the cell envelope fraction by immunoblot suggests that those proteins are in a complex with the membrane anchored Nfs-proteins. NfsB and C share the protein stability pattern with NfsA suggesting that those proteins are in an outer membrane associated complex. NfsF contains a predicted signal peptide but no structural motif. The protein was not detectable by immunoblot. Therefore, localization and putative interaction partners for the small protein are not certain.

Based on the available data, we propose the following organization of the Nfs-proteins in the cell envelope (**Figure 3-2**):

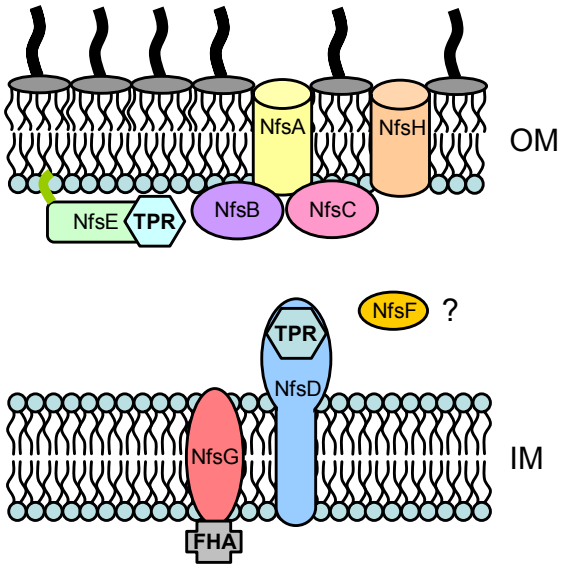

Figure 3-2 Schematic model of subcellular Nfs protein localization. OM: Outer membrane, IM: Inner membrane.

The predicted association of NfsA, B, C, E and H with the outer membrane and NfsD and G with the inner membrane needs to be confirmed by immunoblot of each separated membrane. To prove the assumed complex formation of the Nfs-Proteins, cross-linking and co-immunoprecipitation can be applied. To determine the stoichiometry of the proteins in the putative complex, quantitative immunoblot or *in vitro* complex formation analyses need to be performed. *In vivo* interaction can indirectly be shown by co-localization (fluorescent labelling or immunofluorescence) and directly by FRET-experiments with fluorescent markers that are known to function in the cell envelope such as Mcherry or Gfp and its derivatives when exported by the Tat-system.

During starvation-induced development, only two Nfs proteins were detected due to the strongly decreasing protein content of a developing culture and the fact that only a small proportion of cells convert into spores. To confirm that the Nfs proteins accumulate similarly during starvation-induced sporulation, the immunoblot analyses have to be carried out on samples of the spore-forming subpopulation. Recently, the experimental conditions for separation of cell subpopulations have been determined (B. Lee & P. Higgs, unpublished). This approach should improve immunoblot results since it specifically enriches *nfs* expressing cells (only spore forming cells activate the *nfs* promoter as shown by fluorescence microscopy).

The reason for the inability to delete *nfsC* is intriguing. The protein contains a predicted domain of unknown function and may be related to prenylyltransferases. It is unlikely that the protein is essential since the entire locus can be deleted without apparent influence on vegetative growth. The inabilities to even recombine in either the up- or downstream region of the gene may suggest that this particular genomic region is difficult to access by DNA-recombination approaches.

3.3.2 The Nfs-proteins are probably involved in cell envelope modifications

Position specific iterative Blastp searches suggested that the Nsf-proteins could be related to glycosyl- and glucosamintransferases. One interesting result of the array analysis supporting the psiBlastp results is that the four mutants *fdgA*, Ω7536 (*exo*), *Mxan_1101* and *Mxan_3026* defective in glycerol- and, in case of *exo* and *fdgA* also starvation-induced spore formation, contain mutations in genes belonging to the GO-functional sub-category 'Biosynthesis and degradation of surface polysaccharides and lipopolysaccharides'. Five of the ten up-regulated genes in this category are annotated as glycosyltransferases or N-acetylglucosamine epimerases which matches the psiBlastp results for NfsC, D and E. Glycosyltransferases form a large family of enzymes that catalyze the transfer of sugars or aminosugars to various substrates including proteins, lipids and peptidoglycan (Lairson *et al.*, 2008) (Mohammadi *et al.*, 2007). Therefore, putative functions of the Nfs proteins could be glycosylation of spore-specific proteins or their target could be the cell wall, i.e. they could be involved in coordinated cell wall modification or degradation during spore formation. If the peptidoglycan sacculus is not properly disassembled during spore formation but, for example, stays present either completely or as patches of cell envelope associated murein, spore formation could be perturbed. Interestingly, in *E. coli*, aberrant branched and spiral-like cell shapes have been reported to be associated with patches of inert peptidoglycan (de Pedro *et al.*, 2003) and inhibition of penicillin binding proteins (Varma & Young, 2004). To analyze if the Δ*nfs* mutant is defective in these putative functions, both protein glycosylation and peptidoglycan synthesis of the Δ*nfs* mutant were investigated.

Most studies about protein glycosylation have been carried out in eukaryotic systems. Here, glycosylation is one of the most important post-translational protein modifications. However, there exist an increasing number of glycosylated bacterial proteins. Interestingly, in bacteria surface exposed proteins are frequently glycosylated such as pilins, adhesins, S-layer proteins (Ku *et al.*, 2009, Voisin *et al.*, 2005, Steiner *et al.*, 2007, Messner *et al.*, 2008) as well as cortex and exosporium proteins of *Bacillus*

spores. Apparently, glycosylation of surface proteins utilizes different modules of the biosynthesis routes of lipopolysaccharide O-antigens. The sugar moieties are transferred from an activated precursor either as mono- or as oligosaccharide to the target protein by glycosyltransferases. In *E. coli*, this reaction has been shown to take place in the periplasm. Interestingly, in *S. parasanguinis,* a cluster of seven genes has recently been identified involved in biogenesis and glycosylation of a conserved surface glycoprotein and interaction of glycosyltransferases has also been shown (Bu *et al.*, 2008) coinciding with the assumed interaction of the Nfs proteins. In *M. xanthus,* at least one surface glycoprotein (VGP) has been described (Glufka & Maeba, 1991) suggesting that *M. xanthus* possesses the ability to modify exported proteins by glycosylation. Therefore, we reasoned that one possible function of the Nfs-proteins could be to glycosylate and facilitate export of spore coat associated target proteins.

Since all detectable Nfs-proteins migrate approximately at their calculated molecular mass in SDS-PA-gels, they are probably not extensively modified themselves by glycosylation. A hypothetical target protein is therefore likely not part of the *nfs* locus. However, clear differences in protein glycosylation patterns between wild type and Δ*nfs* were not detectable with the applied staining method. Techniques with better resolution such as chromatography and mass spectrometry could provide clearer results and samples of cells that have been induced for more than four hours should also be included because spore coat proteins may be synthesized and exported very late. Additionally, separated spore coats or outer membrane fractions of induced cells could be used for these analyses to enrich for the putative target protein(s).

Another cell envelope structure that is extensively modified both during spore formation and germination is the murein sacculus. In particular, upon spore germination, the peptidoglycan cell wall needs to be re-synthesized. To check if there are differences in cell wall synthesis during vegetative growth and germination in wild type and the Δ*nfs* mutant, staining of nascent peptidoglycan with Fluorescin labeled Vancomycin (VanFL) was applied. As expected, differences during vegetative growth were not observed consistent with the assumption that the Nfs proteins function specifically during spore formation. However, preparation of samples from outgrowing cells proved difficult because cells in this stage were very fragile. Therefore, modified fixing and staining methods should be applied. For instance, cells could be fixed on poly-L-lysine coated slides or treated on micropore filters to avoid mechanical forces. Nevertheless, some germinating cells displayed bright fluorescence signals at the tips of outgrowing spheres or patches of labeled peptidoglycan as expected suggesting that an optimized procedure could help to understand how outgrowing spores synthesize peptidoglycan *de novo* and organize it into a rod-shaped sacculus.

An additional possibility is that the Nfs proteins could be directly involved in synthesis of the carbohydrate containing spore envelope. Biogenesis and assembly of outer membrane components such as lipid A as well as the O-antigen carbohydrate chains and exopolysaccharides is accomplished by export from the inner leaflet of the cytoplasmic membrane, transport through the periplasm and insertion in the outer membrane. This process can involve a type I-like secretion system (Bos *et al.*, 2007). Type I secretion systems consist of an inner-membrane ABC-transporter, an outer membrane protein and a ‘membrane fusion protein’ which connects the inner- and outer membrane

components (Gentschev *et al.*, 2002, Gentschev *et al.*, 2004) (Faridmoayer *et al.*, 2007). The *M. xanthus* spore carbohydrate translocation and exporting machinery could be similarly organized and the cell envelope associated Nfs proteins may be part of this machinery. NfsG is a good candidate for an inner membrane transporter since it probably localizes to the cytoplasmic membrane, is related to ABC-transporters and possesses a cytoplasmic FHA domain that could mediate interaction with a precursor-delivering protein or nucleotide-activated sugar moiety. NfsA and H could represent the outer membrane part of the functional entity and the other Nfs proteins could mediate delivery of the carbohydrates through the periplasmic space.

It is still unknown whether the carbohydrates in the spore coat are cross-linked. If they are, the cross-linking enzymes need to localize in the cell envelope. A possible task of the Nfs proteins could therefore also be to crosslink the subunits of the spore coat. If the carbohydrates are synthesized and exported but not cross-linked, the subunits (i.e. glucose and galactosamine) may be found in the medium.

Additional evidence about the function of the Nfs proteins could also be obtained from an envelope analysis of the ovoids formed by the Δ*nfs* and *exo* mutants during glycerol induction and the spore-like entities formed inside fruiting bodies by electron microscopy. Furthermore, differences in the carbohydrate contents between Δ*nfs* and *exo* as well as wild type spores could help to reveal what the *M. xanthus* spore envelope consists of. Additionally, the phenotype of an *nfs* constitutively or overexpressing mutant could provide insights in the mechanism of how the Nfs proteins function. Therefore, the strong *pilA* promoter could be cloned in front of the *nfs*-locus. Providing this mutant is viable, an aberrant envelope of vegetative cells and cell shape defects are possible.

3.4 The fate of the rod-shape determining protein MreB depends on the sporulation pathway and plays a crucial role in spore germination

A key organizer of bacterial cell shape and cell wall synthesis is the actin-like protein MreB. *In vivo*, MreB is a cytoplasmic protein but it aggregates into membrane attached twisted, dynamic, spiral-like filaments that traverse the long-axis of the cell. Depletion of MreB in rod-shaped Gram-negative bacteria leads to defects in cell wall synthesis, formation of spheres, and then cell lysis whereas repletion reconstitutes rod-like cell shape (Figge *et al.*, 2004). MreB filaments are thought to indirectly position the cell wall synthesizing proteins (penicillin binding proteins – PPBs) and autolysins both during vegetative cell elongation and cell division (Divakaruni *et al.*, 2007, den Blaauwen *et al.*, 2008).

During spore formation, *M. xanthus* converts from rod-shaped cells into spherical spores and, during germination, back into rods suggesting extensive remodeling of the cytoskeleton as precondition for cell wall transformation. As mentioned above, it has been shown that *M. xanthus*' glycerol spores do not contain peptidoglycan (Bui *et al.*, 2008). Therefore, during sporulation, the peptidoglycan of vegetative cells must be degraded. Since the bacterial cell wall is essential to counteract the turgor pressure and

to prevent cell lysis in a hypoosmotic environment, the peptidoglycan has to be replaced by another structure simultaneously accompanied by cell shape change. This process needs to be tightly controlled to avoid leakage and cell lysis. During germination however, this exchange has to be reverted. In this case, the protective carbohydrate and protein coat must be degraded and replaced by a rod-shaped, evenly-growing murein sacculus in a similar tightly controlled manner.

To analyze the role of MreB during the shape change conversions *in vivo*, we first tried to generate a strain containing a fluorescently labeled version of MreB. We could only obtain mutants containing the N-terminal label suggesting that the C-terminal labeled version is lethal. However, specific fluorescence signals could not be observed. Similar results were reported from E. M. F. Mauriello & D. Zusman (personal communication). A possible reason for these results is that the modified version of MreB is not as efficiently assembled into filaments as the native form. Therefore, we tried to overexpress the labeled version by expressing it under control of the strong *pilA* promoter. Although overexpression of the labeled *mreB* led to detectable fluorescence signals, it also caused severe cell shape defects. In other organisms, where the MreB spirals could successfully visualized (such as *B. subtilis* and *E. coli*), the modified version of the gene was brought under control of an inducible promoter. Therefore, a similar way to fine-tune expression of *gfp-mreB* in *M. xanthus* could solve this issue. For that reason, an appropriate tightly-inducible promoter needs to be identified.

Our simultaneous second approach was to generate antibodies to MreB. After affinity purification of the antisera, antibodies of sufficient sensitivity and specificity could be obtained. Recent results suggest that MreB-spirals can successfully be detected by immunofluorescence in fixed vegetative *M. xanthus* cells (E. Cserti & P. Higgs, unpublished data). Localization and patterns of MreB during spore formation and germination should be analyzed.

Interestingly, our immunoblot analyses show that glycerol- and starvation-induced spores differ in their content of MreB. In glycerol spores, MreB is detectable throughout the whole spore formation process in similar amounts. During starvation-induced sporulation however, MreB decreases after 30 hours coinciding with the onset of spore formation suggesting controlled proteolysis of MreB. Since both types of spores are spherical, two different types of cytoskeleton re-arrangements need to be evoked. First, during starvation-induced development, MreB is likely degraded. Absence of MreB may allow formation of spherical cells (it is not yet known if starvation-induced spores contain peptidoglycan). Second, in the case of glycerol-induced spore formation, MreB is still present, but cells round up. MreB filaments could either be disassembled or the filaments are maintained but adapt their pitch to accommodate a spherical cell shape. In the latter case, the connection between MreB and cell wall synthesis likely becomes interrupted. This possibility is attractive since glycerol spores do not contain peptidoglycan. In glycerol spores, MreB still localizes to the cell envelope as shown by immunoblot on fractionated cell lysates. A similar observation was made in *Vibrio parahaemolyticus* when the cells enter the viable but nonculturable state and convert into small spheres (Chiu *et al.*, 2008). Therefore, it will be interesting to determine if the MreB in glycerol spores is still organized in a helical structure (as, for example in

spherical *E. coli* cells with inhibited PBP2, (Mohammadi *et al.*, 2007)) or in a diffuse, membrane attached pattern.

Addition of A22 to rod-shaped *M. xanthus* cells in CTT medium leads to formation of spheres and cell lysis suggesting that *M. xanthus* MreB is prone to A22 treatment. Interestingly, glycerol spores are prevented from outgrowth in the presence of A22. Starvation-induced spores brought back into rich medium synthesize MreB *de novo* but do also not elongate. Instead, both types of spores stay spherical and slowly loose refractivity suggesting that re-organization of the MreB cytoskeleton is an essential first step during germination. This assumption needs to be confirmed by MreB immunofluorescence on germinating spores. Simultaneous labeling of nascent peptidoglycan could show how MreB is involved in *de novo* synthesis of a rod-shaped cell wall.

3.5 Conclusion

The research in this thesis focused on the process of spore formation in the Gram-negative bacterium *M. xanthus*, i.e. on conversion of entire rod-shaped cells into spherical, resistant spores. As model for this process we applied glycerol-induced spore formation. Our transcriptome profiling data suggest that glycerol induction specifically activates the core sporulation genes and represents an appropriate system to analyze spore formation and cell shape change in *M. xanthus*.

We propose that synthesis and export of carbohydrates and assembly of a carbohydrate containing spore envelope is an important process to replace the peptidoglycan by a spore specific envelope structure and to generate resistant spores from vegetative cells. Considering the unusual spiral-like cell morphology of the Δ*nfs* strain during elongation, we speculate that this mutant degrades its peptidoglycan like the wild type but fails to replace it by a carbohydrate and protein coat. During conversion from enlarged ovoids back into rods, the re-establishing cytoskeleton governs peptidoglycan-synthesis without the protecting spore coat and the spiral-like morphology becomes visible.

The currently discussed models of bacterial cell wall growth require an existing peptidoglycan matrix. New cell wall material is incorporated by controlled hydrolysis of glycosidic and peptide bonds and insertion of precursors at specific sites leading to a continuously growing sacculus and preventing lysis (Vollmer *et al.*, 2008, Vollmer & Holtje, 2004). *M. xanthus* glycerol-induced spores however, do not contain a preexisting peptidoglycan matrix which means that emergence of a rod-shaped sacculus during germination is not explained by the current models of bacterial cell wall synthesis. Upon germination, the right cell shape and diameter has to be determined by another mechanism and translated into the emerging cell wall. Analysis of the Nfs proteins in combination with the rod-shape determining protein MreB both during spore formation and germination can therefore be utilized to study fundamental mechanisms of cell shape determination and cell wall morphogenesis in Gram-negative bacteria.

4 MATERIALS AND METHODS

4.1 Reagents, technical equipment and software

Common reagents, enzymes and antibiotics used in this study are listed in **Table 4-1** together with their suppliers. Specific chemicals are described in the text. Technical equipment and its manufacturers are listed in **Table 4-2** and specific software applied for data analysis is listed in **Table 4-3**.

Table 4-1 Sources of reagents, enzymes, antibiotics and kits

Reagent	**Vendor**
Media components, Agar-Agar	Roth (Karlsruhe) Merck (Darmstadt) Difco (Heidelberg)
Pure chemicals	Roth (Karlsruhe) Merck (Darmstadt)
SDS-PAGE size standards	MBI Fermentas (St. Leon-Rot)
Agarose gel electrophoresis size standards	New England Biolabs (Frankfurt a.M.) MBI Fermentas (St. Leon-Rot)
Oligonucleotides	MWG (Ebersberg) Invitrogen (Karlsruhe)
Rabbit Antisera	Eurogentec (Seraing, Belgium)
Enzyme	
Platinum®*Pfx* DNA-polymerase, Superscript™III reverse transcriptase	Invitrogen (Karlsruhe)
DnaseI (Rnase-free)	Ambion (Huntington, UK)
Other nucleic acid modifying enzymes (restriction endonucleases, T4 DNA ligase, antarctic phosphatase®, DNA polymerase I (Klenow) RnaseH)	New England Biolabs (Frankfurt a.M.) MBI Fermentas (St. Leon-Rot)
Proteinase K, Lysozyme	Sigma-Aldrich (Seelze)
Antibiotic	
Kanamycinsulfate, Chloramphenicol, Ampicillin sodiumsalt, Gentamycin, Spectinomycin, Oxytetracycline dihydrate	Roth (Karlsruhe)
Kit	
PCR purification, gel extraction, plasmid preparation, RNA purification	Quiagen (Hilden) Zymo research (Hiss diagnostics, Freiburg)
BigDye® Terminator v. 3.1 cycle sequencing, Cybr® Green PCR master mix	Applied Biosystems (Darmstadt)
Pro-Q® Emerald 300 glycoprotein gel stain	Invitrogen (Karlsruhe)
MasterPure™ DNA purification	Epicentre (Hess.-Oldendorf)

Table 4-2 Devices used in this study

Application	Device	Manufacturer
Centrifugation	RC 5B plus Ultra Pro 80	Sorvall / Thermo scientific (Dreieich)
	Multifuge 1 S-R Biofuge fresco Biofuge pico	Heraeus / Thermo scientific (Dreieich)
PCR	Mastercycler personal Mastercycler epgradient	Eppendorf (Hamburg)
Real time PCR	7300 Real time PCR system	Applied Biosystems (Darmstadt)
DNA sequencing	3130 Genetic analyzer	Applied Biosystems (Darmstadt)
Cell disintegration	French® pressure cell press	SLM instruments (Urbana, IL)
	FastPrep®24 cell and tissue homogenizer	MP Biomedicals (Illkirch, France)
Ultrasound sonification	Branson sonifier 250	Heinemann (Schwäbisch Gmünd)
HPLC protein purification	Äkta™ Unicorn™ 5.0	Amersham Bioscience (München)
Protein electrophoresis	Mini-PROTEAN® 3 Cell PROTEAN® II XI Cell	Bio-Rad (München)
Western blotting	TE42 Protein transfer tank TE62 Tank transfer unit	Amersham Bioscience (München)
	TE77 ECL semidry transfer unit	Amersham Bioscience (München)
Chemiluminescence detection	LAS-4000 luminescent image analyzer	Fujifilm Europe (Düsseldorf)
Microscopy	Zeiss Axio Imager.M1	Carl Zeiss (Jena)
	DM6000B microscope MZ 8 stereo microscope DME light microscope	Leica Microsystems (Wetzlar)
Micro array scanning	GenePix™4000B scanner	Axon Instruments (Union City, CA)
Fluorescence quantitation	Infinite M200 plate reader	Tecan (Gröding, Austria)
Electroporation	Gene pulser xcell	Bio-Rad (München)
Vacuum drying of nucleic acids and polyacrylamide gels	Univapo 100H with Unijet II refrigerated Aspirator and Unigeldryer 3545D	Uniequip (Martinsried)
Determination of optical densities and extinction of Coomassie Brilliant Blue stained protein solutions	Ultrospec 2100 pro	Amersham Bioscience (München)
Absorption of nucleic acid containing solutions	Nanodrop ND-1000 UV-Vis spectrophotometer	Nanodrop (Wilmington)

Table 4-2 continued

Application	Device	Manufacturer
DNA illumination and documentation	UVT 20 LE UV table	Herolab (Wiesloch)
	2 UV Transilluminator LM20E with BioDoc-IT-system and Mitsubishi P93 thermal video printer	UVP (Upland, CA)
Reaction incubation	Thermomixer compact	Eppendorf (Hamburg)
	Thermomixer comfort	
Incubation of bacterial cultures	Innova 4000® incubator shaker	New Brunswick Scientific (Nürtingen)
	Innova44® incubator shaker	
	B6420 incubator	Heraeus (Langenselbold)
	9020-0075 cooled incubator	Binder (Tuttlingen)
Steam sterilization	2540E	Tuttnauer (Breda, Netherlands)
	FVS MK 6,5	Fedegari Autoclavi (Albuzzano, Italy)
Heat sterilization	SFP800	Memmert (Schwabach)

Table 4-3 Software for data analysis

Application	Program	Vendor
Fluorescence microscopic image analysis	Metamorph® v. 7.5	Molecular Devices (Union City, CA)
Array scanning and data acquisition	GenePix™ Pro 6.0	Axon instruments (Union City, CA)
Array data administration and analysis	Acuity v. 4.0	Axon instruments (Union City, CA)
Statistical significance analysis of microarray data	SAM v. 2.23	Stanford University (CA)
Quantitation of chemiluminescence signals	MultiGauge	Fujifilm Europe (Düsseldorf)

4.2 Media

Culture media for *E. coli* were prepared as described (Sambrook *et al.*, 1989). All strains were cultivated aerobically. Antibiotics and X-Gal were added if selection for antibiotics resistance or blue-white screening was intended.

Table 4-4 Growth media for E. coli

Medium	Composition
Luria-Bertani (LB)	1% (w/v) tryptone, 0.5% (w/v) yeast extract, 1% (w/v) NaCl
Salt free LB	1% (w/v) tryptone, 0.5% (w/v) yeast extract
LB agar plates	LB-Medium, 1% (w/v) Agar-Agar

Table 4-5 Additives

Additive	Final concentration	Dissolved in
Ampicillin-Sodiumsalt	100 µg/ml	H_2O
Chloramphenicol	50 µg/ml	99.9% Ethanol
Gentamycinsulfate	10 µg/ml	H_2O
Kanamycinsulfate	100 µg/ml	H_2O
Oxytetracyclin-Dihydrate	10 µg/ml	0,1M HCl
X-Gal	40 µg/ml	DMF

M. xanthus strains were grown in 1% CTT, in CTTYE or CYE medium.

Table 4-6 Growth media for M. xanthus

Medium	Compostition
1% CTT	1% (w/v) Bacto™ Casitone, 10 mM Tris-Cl, pH 8.0, 1 mM potassiumphosphate buffer, pH 7.6, 8 mM $MgSO_4$
1% CTT agar plates	1% CTT-medium, 1.5% (w/v) Agar
CTT soft agar	1 % CTT-medium, 0.75% (w/v) agar
CTTYE	1% CTT-Medium, 0.2% (w/v) yeast extract
Casitone yeast extract (CYE) (Campos & Zusman, 1975)	1% (w/v) Bacto™ Casitone, 0.5% (w/v) yeast extract, 10 mM MOPS pH 7.6, 8 mM $MgSO_4$
CYE agar plates	CYE medium, 1.5% (w/v) agar

For *M. xanthus* developmental assays, nutrient limitation or strict starvation media were prepared as follows:

Table 4-7 Media for M. xanthus developmental assays

Medium	Composition
Clone fruiting (CF) agar plates (Hagen *et al.*, 1978) Prepared at least 24h before use	10 mM Tris-Cl, pH 8.0, 1 mM potassiumphosphate buffer, pH 7.6, 8 mM $MgSO_4$, Added after autoclaving: 0.015% (v/v) CTT medium, 0.02% (w/v) $(NH_4)_2SO_4$, 0.1% (w/v) Na-pyruvate, 0.2% (w/v) Na-citrate, 1.5% (w/v) agar
TPM agar plates (Kuner & Kaiser, 1982) Prepared at least 24h before use	10 mM Tris-Cl, pH 7.6, 1 mM potassium phosphate buffer, pH 7.6, 8 mM $MgSO_4$, 1.5% (w/v) agar
MMC-buffer for submerged culture	10 mM MOPS, pH 7.0, 4 mM $MgSO_4$, 2 mM $CaCl_2$

4.3 Microbiological Methods

4.3.1 Bacterial strains and plasmids

Table 4-8 *M. xanthus* strains, *E. coli* strains and plasmids used in this study

Strain	Genotype or characteristics	Reference or source
DK1622	Wild type	(Kaiser, 1979)
nfs deletion / insertion		
PH1200	DK1622 Δ*Mxan_(3371 – 3378)*	This study
PH1201	DK1622 Δ*Mxan_3371*	This study
PH1202	DK1622 Δ*Mxan_3372*	This study
PH1204	DK1622 Δ*Mxan_3374*	This study
PH1205	DK1622 Δ*Mxan_3375*	This study
PH1206	DK1622 Δ*Mxan_3376*	This study
PH1207	DK1622 Δ*Mxan_3377*	This study
PH1208	DK1622 Δ*Mxan_3378*	This study
PH1210	DK1622::pFM20 Km^R	This study
PH1211	DK1622::pFM21 Km^R	This study
PH1212	DK1622::pFM22 Km^R	This study
PH1214	DK1622::pFM24 Km^R	This study
PH1215	DK1622::pFM25 Km^R	This study
PH1216	DK1622::pFM26 Km^R	This study
PH1217	DK1622::pFM27 Km^R	This study
PH1218	DK1622::pFM28 Km^R	This study
nfs-promoter-reporter constructs		
PH1220	DK1622 *attB*::pAL4, Km^R	This study
PH1221	DK1622 *attB*::pFM16, Km^R	This study
PH1222	DK1622 *attB*::pFM18, Km^R	This study
PH1223	DK5279 *devR*::Ω4414 *attB*::pFM17 Km^R, Tc^R	(Thony-Meyer & Kaiser, 1993) This study
PH1224	DK11063 *fruA*::Ω7540 Tn5*lacZ* *attB*::pFM17, Km^R, Tc^R	(Søgaard-Andersen *et al.*, 1996), This study
PH1225	PH1244 (*exo*::pCR®2.1 TOPO) *attB*::pFM17, Km^R, Tc^R	This study
PH1226	DK5208 *csgA*::Tn5-132 ΩLS205 *attB*::pAL4, Km^R, Tc^R	(Kroos & Kaiser, 1987, Søgaard-Andersen *et al.*, 1996), This study
pCR®2.1 TOPO insertions		
PH1231	DK1622::pFM31, Km^R	This study
PH1232	DK1622::pFM32, Km^R	This study
PH1233	DK1622::pFM33, Km^R	This study
PH1234	DK1622::pFM34, Km^R	This study

PH1236	DK1622::pFM36, Km^R	This study
PH1237	DK1622::pFM37, Km^R	This study
PH1239	DK1622::pFM39, Km^R	This study
PH1240	DK1622::pFM40, Km^R	This study
PH1241	DK1622::pFM41, Km^R	This study
PH1242	DK1622::pFM42, Km^R	This study
PH1243	DK1622::pFM43, Km^R	This study
PH1244	DK1622::pFM44, Km^R	This study
In-vivo fluorescent labelling of MreB		
PH1250	DK1622 *attB*::pFM5 (*mreB*$_{Pr}$-*gfp-mreB*) Km^R	This study
PH1251	DK1622 *attB*::pSL8 (*pilA*$_{Pr}$-*gfp*) Km^R	This study
PH1252	DK1622 *attB*::pFM9 (*pilA*$_{Pr}$-*gfp-mreB*) Km^R	This study
PH1253	DK1622 *attB*::pFM7 (*mreB*$_{Pr}$-*venus-mreB*) Km^R	This study
PH1254	DK1622 *attB*::pFM3 (*mreB*$_{Pr}$-*gfp*) Km^R	This study
Mxan_6788 insertion / deletion		
PH1258	DK1622::pFM55, Km^R	This study
PH1259	DK1622 Δ*Mxan_6788*	This study
***E. coli* strains**		
TOP10	Host for cloning F^- *endA1 recA1 galE15 galK16 nupG rpsL* Δ*lacX74* Φ80*lacZ*ΔM15 *araD*139 Δ(*ara, leu*)7697 *mcrA* Δ(*mrr-hsdRMS-mcrBC*) λ^-	Invitrogen
BL21λDE3	F^- *ompT gal dcm lon hsdS*$_B$(r_B^- m_B^-) λ(DE3) [*lacI lacUV5*-T7 gene 1 *ind1 sam7 nin5*]	Novagen
DH5α	F^-, φ80d*lacZ*ΔM15, Δ(*lacZYA*$^-$ *argF*)U169, *deoR*, *recA*1, *endA*1, *hsdR*17(rk^-, mk^+), *phoA*, *supE*44, λ^-, *thi*-1, *gyrA*96, *relA*1 pBJ114, Km^R	Invitrogen
GJ1158	*ompT hsdS gal dcm* Δ*malAp510 malP*::(proUp-T7 RNAP) *malQ*::*lacZ*hyb11 Δ(*zhf*-900::Tn10dTet)	(Bhandari & Gowrishankar, 1997)
Plasmids		
General and backbone vectors		
pET32a+	Expression vector, T7-Promoter, His6-tag (N- and C- terminal), Ap^R	Novagen
pLysS	T7 lys, Cm^R	Novagen
pCR® 2.1 TOPO	Vector for insertion mutagenesis, Km^R	Invitrogen
pSL8	Derivative of pSWU30, *pilA*-promoter-*gfp*	S. Leonardy & L. Søgaard-Andersen, Marburg

pVENN-2	Source for *venus* gene and backbone for *mreB*::*venus* fusion	Prof. Dr. Martin Thanbichler
pXCHYN-1	Source for *mcherry* gene	Prof. Dr. Martin Thanbichler
pBJ114	pUC119 with Km^R and *galK*; derivative of pKG2, backbone for in-frame deletions	(Wu & Kaiser, 1996), (Julien *et al.*, 2000)
pSWU30	Derivative of pBGS18, Mx8 *attP*, Tc^R, Vector with Mx8 phage integrase gene, backbone vector for Mx8 site specific integrations	(Wu & Kaiser, 1996)
pFM10	pSWU30 derivative, Km^R	This study
Promoter-reporter constructs		
pAL4	nfs_{Pr}-*mcherry,* Km^R	This study
pFM16	$pilA_{Pr}$-*mcherry,* Km^R	This study
pFM17	nfs_{Pr}-*mcherry,* Tc^R	This study
pFM18	Backbone for Mx8 *att* integrations; Km^R, empty control vector	This study
nsf insertion / deletion		
pFM20	pBJ114Δ(*Mxan_3371-3378*)	This study
pFM21	pBJ114Δ*Mxan_3371*	This study
pFM22	pBJ114Δ*Mxan_3372*	This study
pFM23a	pBJ114Δ*Mxan_3373*	This study
pFM23b	pBJ114Δ*Mxan_3373*	This study
pFM24	pBJ114Δ*Mxan_3374*	This study
pFM25	pBJ114Δ*Mxan_3375*	This study
pFM26	pBJ114Δ*Mxan_3376*	This study
pFM27	pBJ114Δ*Mxan_3377*	This study
pFM28	pBJ114Δ*Mxan_3378*	This study
pCR®2.1 TOPO derivatives (containing internal gene fragments of 300 – 500 bp for insertion mutagenesis)		
pFM30	pCR®2.1-TOPO *Mxan_0110*	This study
pFM31	pCR®2.1-TOPO *Mxan_0434*	This study
pFM32	pCR®2.1-TOPO *Mxan_0524*	This study
pFM33	pCR®2.1-TOPO *Mxan_0646*	This study
pFM34	pCR®2.1-TOPO *Mxan_0690*	This study
pFM35	pCR®2.1-TOPO *Mxan_0781*	This study
pFM36	pCR®2.1-TOPO *Mxan_0862*	This study
pFM37	pCR®2.1-TOPO *Mxan_0888*	This study
pFM38	pCR®2.1-TOPO *Mxan_0912*	This study
pFM39	pCR®2.1-TOPO *Mxan_0994*	This study
pFM40	pCR®2.1-TOPO *Mxan_1065*	This study
pFM41	pCR®2.1-TOPO *Mxan_1092*	This study
pFM42	PCR®2.1-TOPO *Mxan_1101*	This study

pFM43	pCR®2.1-TOPO *Mxan_3026*	This study
pFM44	pCR®2.1-TOPO *Mxan_3327*	This study
pFM45	pCR®2.1-TOPO *mreB*	This study
mreB expression		
pFM50	pET32a^{+} *mreB*	This study
In-vivo fluorescent labelling of MreB		
pFM2	3' end of *mreB*-spacer-*venus*, Km^{R}	This study
pFM3	*mreB*$_{Pr}$-*gfp*, Km^{R}	This study
pFM5	*pilA*$_{Pr}$-*gfp-mreB*, Km^{R}	This study
pFM7	*mreB*$_{Pr}$-*venus-mreB*, Km^{R}	This study
pFM9	*pilA*$_{Pr}$-*gfp-mreB*, Km^{R}	This study
Mxan_6788 insertion / deletion		
pFM55	pBJ114Δ*Mxan_6788*	This study

4.3.2 Media and cultivation of bacteria

Media and solutions were autoclaved for 20 minutes at 121°C and 1 bar over pressure. Heat sensitive liquids as antibiotic- or carbohydrate-containing solutions were filtered using 0.22 or 0.45 µm pore size filters (Millipore, Schwalbach) and added after media have cooled to 60°C. Other equipment (such as glass ware, metal tools and ceramics) was sterilized at 180°C for three hours.

M. xanthus was cultivated aerobically at 32°C on 1% CTT agar in the dark. *M. xanthus* liquid cultures were inoculated by dispersion of single colonies by pipetting in an 1.5 ml Eppendorf tube containing 1 ml liquid medium. After dispersion, particles were pelleted briefly and the supernatant was transferred in an Erlenmeyer flask containing growth medium. Liquid cultures were grown on horizontal shakers at 240 rpm. Optical densities of *M. xanthus* liquid cultures were monitored at 550 nm (OD_{550}) using 1 cm path length.

E. coli was incubated aerobically on Luria-Bertani (LB-) agar at 37°C. *E. coli* liquid cultures were inoculated directly from single colonies into liquid medium and cultivated on horizontal shakers at 37°C and 240 rpm. The optical density was determined as above.

4.3.3 Storage of transformed *M. xanthus* and *E. coli* strains

M. xanthus and *E. coli* cultures on solid media were stored up to four weeks at 18 or 4°C, respectively. For long term storage, 10 ml cultures of *M. xanthus* were harvested at OD_{550} = 0.8 by centrifugation and resuspended in 1 ml medium. *E. coli* strains were not concentrated but supplemented with 10 M glycerol (2 M final concentration) directly before shock freezing in liquid nitrogen and stored at -70°C.

4.3.4 Cultivation of *M. xanthus* for development

For starvation induced development, *M. xanthus* strains were grown to an OD_{550} of 0.5 - 0.8 and harvested by centrifugation at 4.620 x g for 10 min at rt. The cell pellet was rinsed with MMC starvation buffer, centrifuged again for 5 min and resuspended in MMC buffer to a calculated OD_{550} of 7.0. Development was assayed on CF (Hagen *et al.*, 1978) and TPM agar plates (Kuner & Kaiser, 1982) by applying 10 µl drops of cell suspension on the agar surface. After drying, the cultures were incubated at 32°C in the dark. For development in submerged culture, the cell suspension was diluted 1:8 with MMC buffer and 400 µl were pipetted in each well of a 24-well microtiter plate. For development in large (145 mm diameter) petri dishes, 40 ml cell suspension was added per dish. Aggregation and fruiting body formation was monitored with a Leica MZ8 stereo microscope (Leica, Herrbrug) at 10- and 40-fold magnification. Images were taken after 24 h, 48 h, 72 h and 120 h.

4.3.5 Total protein isolation

For protein isolation, liquid cultures were transferred into centrifuge tubes and kept on ice. Developing submerged cultures were harvested from Petri dishes and transferred into centrifuge tubes. The dishes were rinsed once with MMC buffer and the buffer combined with the sample. After centrifugation (4.620 x g, 10 min, 4°C) supernatants were removed and the pellets were stored at -20°C or processed directly on ice.

Cell pellets were resuspended in 1/100 vol. ice cold buffer (10 mM HEPES, 150 mM NaCl) supplemented with mammalian protease inhibitor cocktail (Sigma, Taufkirchen). Up to 600 µl sample were transferred into 2 ml screw cap tubes filled with 0.6 g 0.1 mm zirconia/silica beads (BioSpec, Bartlesville, OK). Cells were mechanically disintegrated using a FastPrep®-24 tissue and cell homogenizer (MP Biomedicals, Illkirch, France) six times for 45 s each at 6.5 m/s speed. The supernatant was recovered, the bead matrix washed once with the same volume of buffer and the supernatants combined.

For protein recovery from samples of equal initial cell numbers, supernatants were not removed after cell lysis. Instead, equal volumes of 2 x LSB (0.125 M Tris-HCl pH 6.8, 20% (v/v) glycerol, 4% (v/v) SDS, 10% (v/v) betamercaptoethanol, 0.02% (w/v) coomassie G-250) were directly added to the tubes containing lysed cells with bead matrix and heated to 99°C for 10 min.

4.3.6 Cell fractionation

Cell lysates were separated into their soluble and insoluble fractions by ultracentrifugation at 100,000 x g and 4°C for 30 min (Sorvall Ultra Pro 80). The soluble fraction containing supernatant was recovered and the insoluble fraction containing pellet was washed twice and resuspended in an equal volume of 2 x LSB.

4.3.7 Determination of protein concentrations

Protein concentrations were determined after Bradford (Bradford, 1976) using the Bio-Rad protein assay kit (Bio-Rad, München) according to the instructions of the

manufacturer. Standard curves were obtained using dilutions of protein standard (bovine serum albumin). All sample protein concentrations were determined in triplicate with 50, 20 and 5 µl of a 1:10 dilution in 1 ml reaction volume. Absorbance was measured at 595 nm with an Ultrospec 2100 pro spectrophotometer (Amersham). Protein concentrations were calculated based on the slope value of the standard curve.

4.3.8 *M. xanthus* sporulation efficiency and spore viability

Sporulation efficiency of developing and glycerol induced cultures was determined by spore counting. After harvesting, cells were resuspended in 1 ml sterile water and spores were isolated from vegetative and non-resistant cells by heating (2 h at 50°C) followed by sonication at 30 kHz and 30 W output for 30 s in ice water. 10 µl of the treated samples were applied to a Thoma cell counting chamber (Hawksley, Lancing, UK). Spore numbers were calculated as per cent of wt.

Spore viability was determined by germination assays. 10-fold serial dilutions of heat- and sonication-treated cells were plated in CTT soft agar and incubated for two weeks. Colonies were counted after 5, 10 and 14 days. Colony numbers were calculated as per cent of wt.

4.4 Molecular biological methods

4.4.1 Oligonucleotides and plasmids

Oligonucleotides used as primers to amplify gDNA and cDNA templates are listed in the Appendix, **Table A-1**. Plasmids and expression vectors generated are listed in **Table 4-8**.

4.4.2 Construction of plasmids

Purified *M. xanthus* genomic DNA was used as template to amplify chromosomal regions for cloning.

pFM20 - 28 (in-frame deletion of *nfs* genes): Those plasmids are pBJ114 derivatives and used for markerless in-frame deletion of specific genomic regions as described in **Section 4.4.4**. The corresponding *E. coli* clones were selected on LB plates containing kanamycin, X-Gal and IPTG. Isolated plasmids were sequenced to confirm the inserts were error-free and subsequently introduced into *M. xanthus* DK1622 to generate strains PH1200 - 1208.

pFM30 - 44 (insertion mutagenesis by plasmid integration): Approximately 500 bp internal fragments of the genes to be disrupted were PCR-amplified, purified and directly cloned into pCR®2.1 TOPO (Invitrogen). The corresponding *E. coli* colonies were selected on LB plates containing kanamycin, X-Gal and IPTG. Isolated plasmids were sequenced to confirm correctness of the insert and subsequently introduced into *M. xanthus* DK1622 to generate strains PH1231 - 1244 by homologous recombination (**Figure 4-1**).

pFM50: This plasmid was constructed for heterologous over expression of *M. xanthus mreB* in *E. coli*. The gene was amplified and cloned into pET32a^{+} (Novagen) to generate pFM50. The corresponding *E. coli* clones were selected on LB agar containing ampicillin. The plasmid was sequenced to confirm the sequence was error-free and in-frame with tags and transferred into several expression strains.

pAL4 and its derivatives pFM16, pFM17, pFM18: These plasmids were used to fuse the putative *nfs* promoter region to *mcherry* as reporter. First, the *nfs* promoter region and *mcherry* were amplified with primers that allow for subsequent fusion of both fragments by overlap extension PCR and cloning into pFM10 (Mx8 *attP*, Km^{R}). The inserts were sequenced and introduced into *M. xanthus* strains.

PFM3 - 9 (fluorescent labelling of MreB): The *M. xanthus mreB*-gene was amplified by PCR and 5'-fused to *gfp* and *egfp* separated by a 16 and 12 amino acids spacer maintaining the reading frame. This fragment was cloned behind the putative mreB promoter region as well as behind the *pilA* promoter (for overexpression) and introduced into *M. xanthus* DK1622.

4.4.3 Generation of *M. xanthus* insertion mutants

Genes were disrupted by site directed insertion of a plasmid via homologous recombination and selection for antibiotics resistance as shown in **Figure 4-1**. The vector used cannot replicate in *M. xanthus*. Therefore, only insertion events give rise to resistant colonies. Insertion mutants were selected on kanamycin and verified by PCR using oligonucleotides specific for the pCR®2.1 TOPO plasmid and a neighboring region up- or downstream of the target gene. At least two independent colonies were used for further studies.

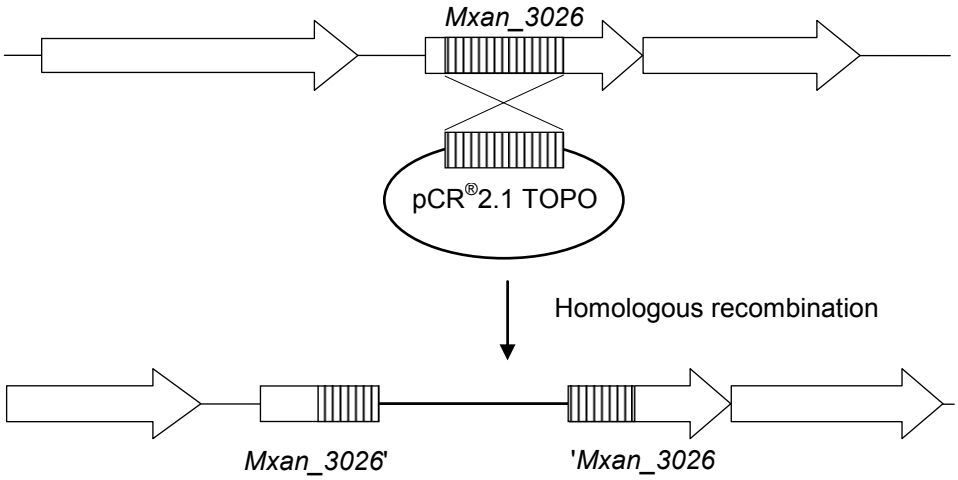

Figure 4-1 Generation of insertion mutants. A central part of the target gene of approximately 500 bp length was amplified by PCR. The purified PCR product was cloned into the pCR®2.1 TOPO plasmid. The plasmid was propagated in *E. coli* and after re-isolation electroporated into *M. xanthus* where homologous recombination leads to disruption of the target gene.

4.4.4 Construction of *M. xanthus* in-frame deletion mutants

In-frame deletions of specific genomic regions were generated applying the technique of (Ueki *et al.*, 1996) and (Sun & Shi, 2001). Therefore, approximately 500 bp fragments directly up- and downstream of the target region were amplified by PCR. The inner primers were designed to possess compatible ends which allow fusing the 500 bp fragments in a second PCR to a 1 kB contig maintaining the reading frame. This contig was cloned into pBJ114 and sequenced. Plasmids with error-free inserts were electroporated into *M. xanthus*.

pBJ114 cannot replicate in *M. xanthus* but provides for kanamycin resistance. Thus, growing *M. xanthus* colonies possess an plasmid insertion likely up- or downstream of the target region. Insertions were mapped by PCR and both, up- and downstream insertion mutants were isolated, if possible.

pBJ114 also contains the counterselectable marker *galK* (*E. coli* galactokinase gene) which converts galactose into its phosphorylated form. Since *M. xanthus* cannot metabolize galactose phosphate, the compound accumulates to toxic levels when cells are grown on galactose containing media. Thus, only cells that have undergone a second recombination to excise the plasmid are viable. However, only 50% of the growing mutants will have lost the vector and the genomic region, the remaining 50% will have lost only the vector and restore the original genomic situation providing the target gene is not essential (**Figure 4-2**).

The insertion mutants were grown in CTT medium to an optical density of 0.5. 200 µl of this culture were added to 3 ml CTT soft agar and plated on CTT agar containing 1% (w/v) galactose. Emerging colonies were transferred to CTT medium containing galactose or kanamycin. Colonies growing on galactose but not on kanamycin were used to verify deletions by PCR.

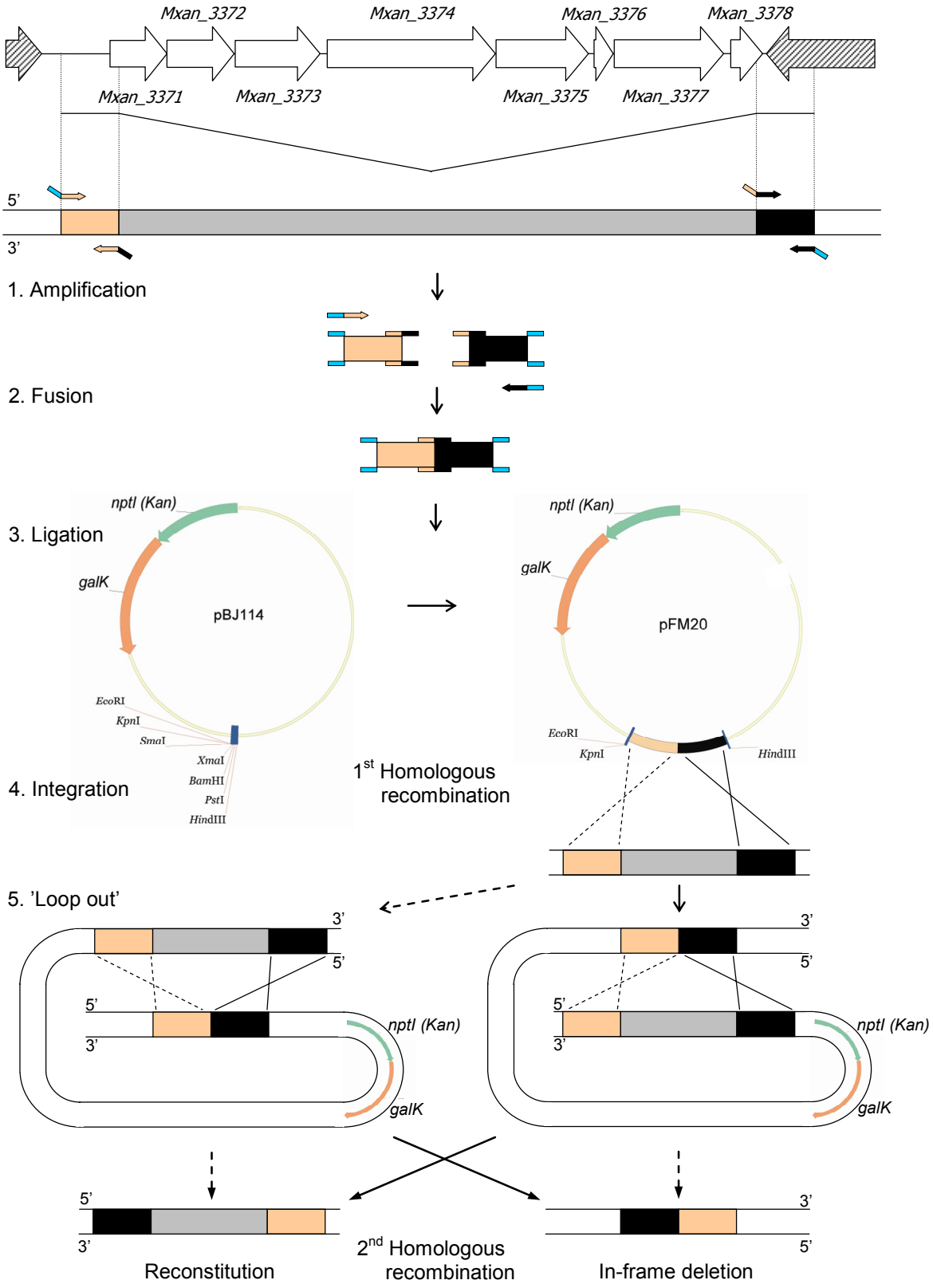

Figure 4-2 Scheme of markerless in-frame deletion mutagenesis. The first homologous recombination leads to plasmid integration up- or downstream of the genomic region to be deleted. The second recombination event eliminates only the vector (reconstitution) or the vector with the target region (in-frame deletion).

4.4.5 DNA preparation from *E. coli* and *M. xanthus*

Plasmid-DNA from *E. coli* was isolated using the QIAprep Spin Miniprep-Kit (Qiagen). *M. xanthus* genomic DNA was prepared using the Master Pure DNA purification kit (Epicentre) according to the instructions of the manufacturer. Concentration and purity was determined with the Nanodrop ND-1000 spectrophotometer (Nanodrop, Wilmington).

Quick DNA preparations to verify the presence of insertions by PCR were done by boiling cell samples for 10 min in 50 µl sterilized deionized water followed by cooling on ice and brief sedimentation of cell debris.

4.4.6 Polymerase chain reaction (PCR)

Amplification of specific DNA-fragments was carried out in 25 or 50 µl reaction volumes in FailSafe™ PCR PreMix J (Epicentre) with *Taq* DNA polymerase or with Platinum® *Pfx* DNA polymerase (Invitrogen) if sequence fidelity was required.

Table 4-9 PCR reaction mix (25 µl)

Component	Volume	Final concentration
2 x FailSafe™ PCR PreMix J	12.5 µl	1 x
10 µM primer	1 µl each	0.4 µM
Genomic or plasmid DNA	1 µl	10 pg - 200 ng
DNA Polymerase (2.5 U/µl)	0.5 µl	0.05 units
Sterile water	9 µl	-

A standard PCR reaction is shown (**Table 4-10**). The reaction conditions were modified based on predicted primer annealing temperatures, expected product sizes and DNA-polymerase.

Table 4-10 Standard PCR program

Step	Temperature	Time	
Initial denaturation	95°C	3 min	
Denaturation	95°C	30 s	x 29
Primer annealing	5 to 8°C below predicted melting temperature	15 s	
Polymerization	72°C	1 min per kb	
Final elongation	72°C	5 min	
Hold	4°C	∞	

PCR products were purified with the QIAquick® PCR Purification Kit (Qiagen) or the DNA clean and concentrator™ Kit (Zymo Research) or extracted from agarose gels.

4.4.7 Agarose gel electrophoresis

Nucleic acid fragments were separated by size with agarose gel electrophoresis at 9 Volt per cm in TAE buffer. Ethidiumbromide was added to agarose in a final concentration of 0.01% (v/v). 6 x sample loading buffer (30% (v/v) glycerol, 50 mM EDTA, 10 mM Tris-HCl pH 7.5, 0.44 µM bromphenolblue, 0.28 µM xylencyanol, 8.8 µM orange G) was combined with samples to 1 x final concentration. After electrophoresis, agarose gels were imaged using a 2UV-Transilluminator (UVP-Bio-Doc-IT-System, UniEquip) at 365 nm wavelength and documented with an electronic P93E thermoprinter (Mitsubishi). DNA fragments were isolated from agarose gels by cutting out and purification with the QIAquick® Gel Extraction Kit.

4.4.8 Restriction und ligation of DNA fragments

Restriction of DNA was carried out by incubation of 5 - 10 µg DNA with restriction endonucleases for 2 h according to specific requirements for the enzyme. Restricted DNA was purified with the QIAquick® PCR Purification Kit (Qiagen) or the DNA clean and concentrator™ Kit (Zymo Research). Fragments of specific size were isolated by agarose gel extraction.

Ligation reactions were performed with T4 DNA ligase. DNA fragments were ligated into vectors applying a 2.5-fold molar excess of insert-DNA. Usually, 20 fmol insert and 50 fmol vector DNA were ligated for 2 h at room temperature (complementary ends) or with PEG added at 18°C over night (blunt ends) followed by heat inactivation of the enzyme at 65°C for 15 min.

4.4.9 Preparation of electrocompetent *E. coli* cells

Over night cultures of *E. coli* strains were used to inoculate 200 ml LB-medium. Cells were grown at 37°C shaking at 240 rpm to an OD_{550} of 0.6 and harvested by centrifugation at 5,000 x g for 20 min, 4°C. The cell pellet was resuspended in 200 ml ice cold sterile 10% (v/v) glycerol and centrifuged again. The washing steps were repeated with 100 ml, 50 ml and 10 ml volumes. Finally, the cell pellet was resuspended in 0.4 ml 10% sterile glycerol and 50 µl aliquots were shock frozen in liquid nitrogen and stored at -70°C for later use.

4.4.10 Preparation of chemically competent *E. coli* cells

Over night cultures of *E. coli* strains were grown as above in 20 ml LB-medium. At OD_{550} = 0.6 the culture was immediately cooled on ice and harvested by centrifugation at 5,000 x g for 10 min at 4°C. The cell pellet was resuspended in 2 ml ice cold sterile TSS pH 6.5 (1% (w/v) tryptone 0.5% (w/v) yeast extract, 1% (w/v) NaCl, 10% (v/v) PEG (3350 or 8000 g/mol) 5% (v/v) DMSO, 50 mM $MgCl_2$ (Chung *et al.*, 1989)). 100 µl aliquots were shock frozen in liquid nitrogen and stored at -70°C.

4.4.11 Transformation of electrocompetent *E. coli* cells

2 - 5 µl heat inactivated ligation reaction were added to 50 µl electrocompetent *E. coli* cells on ice. The suspension was transferred into an electroporation cuvette and pulsed with 1.8 kV, 25 µF and 200 Ω. 500 µl LB medium were added, the suspension transferred into a sterile plastic tube and incubated for 1 h at 37°C shaking at 240 rpm. 5, 20 and 200 µl aliquots were then plated on LB agar containing appropriate antibiotics. The plates were incubated at 37°C over night, colonies transferred onto fresh agar plates and screened for the presence of the plasmid by PCR.

4.4.12 Transformation of chemically competent *E. coli* cells

100 µl aliquots of chemically competent *E. coli* cells were transformed on ice by adding 1 - 5 µl plasmid DNA, gently mixing followed by incubation on ice for 30 min. Cells were then heat shocked at 42°C for 2 min. After addition of 0.5 ml LB, cells were incubated at 37°C shaking at 240 rpm for 1 h. 20, 50 and 200 µl were plated on LB agar containing appropriate antibiotics and incubated over night at 37°C. Colonies were transferred on fresh LB agar and screened for the presence of the plasmid by PCR.

4.4.13 Transformation of *M. xanthus* cells

M. xanthus strains were grown in 100 ml CYE medium to an OD_{550} of 0.4 and harvested by centrifugation at 4.620 x g for 10 min at rt. The cell pellet was resuspended in 50 ml sterile deionized water and centrifuged as above. This washing step was repeated three times. The pellet was then resuspended in 150 µl sterile water and the suspension divided into 50 µl aliquots and either shock frozen in liquid nitrogen or used directly for electroporation.

3 - 8 µl plasmid DNA (corresponding to calculated 1 µg DNA) were transferred to the suspension of electrocompetent cells. The suspension was transferred into a 0.1 cm electro-poration cuvette and pulsed with 650 V, 25 µF and 400 Ω. 1 ml CYE medium was added immediately, the culture transferred into a fresh plastic tube and incubated at 32°C and 240 rpm in the dark for 5 h. Then, 50, 200 and 500 µl aliquots were added to 3 ml top agar, vortexed and used to overlay a CYE agar plate containing appropriate antibiotics. The plates were incubated at 32°C for 5 to 14 days and colonies transferred to fresh CTT agar plates.

Site specific recombination was verified by PCR. To verify plasmid integration at the *M. xanthus attB* phage attachment site, three PCR reactions with primers specific for the genomic *attB* locus and the plasmid specific *attP* site were performed (Magrini *et al.*, 1999). The length of PCR products was determined by agarose gel electrophoresis.

4.4.14 DNA sequencing

DNA sequencing was performed applying the chain termination method after Sanger. Sequencing reactions were set up using the Big Dye® Terminator™ Cycle Sequencing Kit (Applied Biosystems, Darmstadt) according to the instructions of the manufacturer in a 20 µl reaction volume and incubated as shown in **Table 4-11**. Reaction products were

purified either by DNA precipitation or with the BigDye® XTerminator™ Purification Kit (Applied Biosystems).

For precipitation, 10 µl 125 mM EDTA, 9 µl 3 M sodium acetate (pH 4,6), 80 µl HPLC-H_2O and 400 µl 96% ethanol were added to the reaction and incubated for 30 min at rt. DNA precipitates were pelleted by centrifugation at 15,000 x g for 30 min at 20 °C. The supernatant was removed and the pellet washed twice with freshly prepared 70% ethanol followed by 5 min centrifugation at 15,000 x g each. Finally, the ethanol was removed and the pellet air dried. For sequencing, the pellet was dissolved in 20 µl formamide. DNA sequences were analysed with the Vector NTI software suite 9.

Table 4-11 Incubation times and temperatures for DNA sequencing reactions

Step	Temperature	Time	
Initial denaturation	96°C	1 min	
Denaturation	96°C	10 s	x 29
Primer annealing and elongation	60°C	4 min	
Hold	10°C	∞	

4.4.15 Quantitative real time polymerase chain reaction

Quantitative real time polymerase chain reaction was applied to determine changes of single gene expression levels during time course experiments. For this purpose, target gene specific oligonucleotides were designed to amplify fragments of approximately 80 -100 bp length. Oligonucleotide pairs with equal predicted melting temperatures of approximately 61°C were preferred. To avoid formation of primer homo- and hetero-dimers, the derived sequences were checked using netprimer (http:// www.premierbiosoft.com/netprimer/netprlaunch/netprlaunch.html). Specificity of the oligonucleotides was tested on genomic DNA under standard PCR conditions (**Table 4-10**). One single PCR product of the expected size indicated specificity of each primer pair under these conditions.

Efficiency of each primer pair was determined using a 10-fold dilution series of genomic DNA (10 ng, 1 ng, 100 pg and 10 pg) as template. The reactions were performed as duplicates in 26 µl volumes with a 7300 Real Time PCR System using the SYBR® Green PCR Master Mix (Applied Biosystems).

Table 4-12 Real time PCR reaction mix (26 µl)

Component	Volume	Final concentration
SYBR® Green PCR Master Mix	13 µl	1 x
5 µM oligonucleotide	1 µl each	0.2 µM
Template (cDNA or gDNA)	1 µl	0,4 ng – 0,4 pg
Sterile water	10 µl	-

Table 4-13 Real time PCR program

Step	Temperature	Time	
Initial denaturation	95°C	10 min	
Denaturation	95°C	15 s	
Primer annealing and elongation	60°C	1 min	x 40
Denaturation	95°C	15 s	
Recording of dissociation curve	60°C 95°C	30 s 15 s	
Hold	10°C	∞	

Primer efficiencies were calculated by plotting values for the threshold cycle (C_t) over the logarithm of the relative template copy number. The slope value *m* of the obtained regression curve was used to determine the primer efficiency *E* as

$$E = 10^{-\frac{1}{m}}.$$

Only primer pairs with efficiencies near two were considered for further experiments.

cDNA was generated from DnaseI treated, purified total RNA extracts (**Section 4.8**). Priming was performed by adding 2 µl random hexamers ($pd(N)_6$, 100 ng/µl, Amersham), 1 µg total RNA (<10 µl), 1 µl dNTP mix (10 mM, Fermentas) and Rnase-free H_2O to a final volume of 13 µl. The reagents were incubated at 70°C for 5 min to denature secondary structures and then chilled on ice.

Reverse transcription was initiated by adding 4 µl 5 x RT buffer (Invitrogen), 1 µl SUPERase Rnase inhibitor (20 U/µl, Ambion), 1 µl SuperScript III reverse transcriptase (200 U/µl, Invitrogen) and 1 µl 0.1 M DTT. The reaction was incubated at 25°C for 5 min, 55°C for 50 min and 70°C for 15 min. For each time point, a control reaction without added reverse transcriptase was carried to check for absence of contaminating gDNA.

The optimal cDNA concentration for each target gene was determined by running real time PCR reactions on a series of cDNA dilutions. cDNA concentrations that resulted in exceeding the C_t after 25-30 cycles were chosen. Additionally, the melting curves were screened to exclude primer dimer formation and to confirm overlap of the dissociation curves.

All real time PCR reactions with the determined optimal primer pairs, cDNA concentrations and controls were performed in duplicate. Control reactions contained no cDNA (no reverse transcriptase) and H_2O (no template) as negative controls and gDNA as positive control.

Data were analyzed by first averaging the C_t values of the duplicate samples. Then, the ΔC_t values were determined by subtracting the C_t value for each time point from the C_t value of the t = 0 h sample. Thus, the ΔC_t value of t = 0 h was zero and the ΔC_t values

for the single time points reflect the relative change in template copy numbers at each time point.

The relative amount of transcript T_{rel} was quantified using the correlation

$$T_{rel} = E^{\Delta C_t}.$$

4.5 Biochemical methods

4.5.1 Heterologous overexpression and purification of *M. xanthus* MreB in *E. coli*

M. xanthus mreB was expressed in three *E. coli* strains. Various conditions were tested to optimize the yield in soluble protein.

The gene was cloned into plasmid pET32a$^+$ (Novagen) (designated pFM50) which is optimized for inducible protein over expression in *E. coli* and provides fusion tags to facilitate protein purification. The gene for MreB was amplified and cloned in-frame with both a N- and C-terminal his-tag. Sequencing confirmed that the inserted gene was error-free and the vector transferred into *E. coli* BL21λDE3 (with and without pLysS) and *E. coli* GJ1158.

Over night cultures were used to inoculate 600 ml LB medium supplemented with either ampicillin (100 µg ml^{-1} for BL21λDE3 and GJ1158) or ampicillin and chloramphenicol (100 µg ml^{-1} for BL21λDE3 pLysS) and incubated at 37°C shaking at 240 rpm. At an OD_{550} = 0.6, 1 ml culture was harvested by centrifugation and resuspended in 2 x LSB. For the remaining culture, *mreB* expression was induced by incubation with 1 mM IPTG (for BL21λDE3 and BL21λDE3 pLysS) or 0.3 M NaCl (for GJ1158) and the culture was grown for 2 h at 37°C. Alternatively, induction was carried out with 0.5 mM IPTG and growth at 18°C over night or with heat shock at 42°C followed by incubation with 0.5 mM IPTG at 37°C for 2 h or using the overnight autoinduction system (Novagen) solutions according to manufacture's instructions. After incubation, the cells were harvested by centrifugation at 4°C. All cultures were grown aerobically and aerated by constant shaking. Protein production was monitored by SDS-PAGE.

4.5.2 Protein purification

Overexpressed *mreB* was purified by affinity chromatography. Cell pellets were resuspended in binding buffer (10 mM HEPES, 150 mM NaCl, 10 mM imidazole, pH 7.4) and passed three times through a French Pressure Cell Press at 103.4 MPa. Inclusion bodies were separated from the lysate by centrifugation at 600 x g for 30 min at 4°C. The supernatant was filtered through a 0.45 µm pore size filter and further purified by affinity chromatography using Ni-NTA-Agarose resin (Qiagen). The resin was washed and equilibrated with binding buffer, the supernatant added to the resin and incubated for 1 h at 4°C slowly rotating to allow binding of the tagged protein. The suspension was then transferred to a Poly Prep chromatography column (Bio-Rad) and the chromatography was started by collecting the flow through followed by washing the

column with 10 volumes of binding buffer. Elution was carried out with 5 column volumes of elution buffer with increasing imidazole concentrations (50 -500 mM). Samples of each fraction were combined with equal volumes of 2 x LSB and loaded on a SDS-PA gel to visualize success of the purification. To remove imidazole, the samples were dialyzed against 10 mM HEPES, 150 mM NaCl, pH 7.4.

Fractions enriched in the target protein were further purified by anion exchange chromatography using the Äkta™ Unicorn™ 5.0 HPLC system (Amersham biosciences). For this purpose, samples were dialyzed against 50 mM Tris pH 7.6 and loaded on a MonoQ column. Elution was performed applying a gradient of 0 – 50 % of a 2 M NaCl solution in 50 mM Tris pH 7.6. Fractions were screened for their protein content spectrophotometrically and by loading samples on a SDS-PA gel.

4.5.3 Harvesting of inclusion bodies

E. coli BL21λDE3 pLysS pFM50 was grown at 37°C and induced in 1 mM IPTG for 2 h. Cells were harvested by centrifugation (20 min, 10.000 x g, 4°C). The cell pellet was resuspended in lysis buffer (10 mM HEPES, 150 mM NaCl, pH 7.4) supplemented with 5 µg/ml DnaseI, 2.5 mM $MgCl_2$ and 0.5 mg/ml lysozyme and incubated on ice for 30 min. The suspension was then homogenized using a syringe and passed 3 times through a French Pressure Press Cell. Inclusion bodies were separated from the cell lysates by centrifugation (600 x g, 30 min, 4°C). The pellet was washed three times with lysis buffer supplemented with increasing concentrations of triton X-100 (0, 1 and 2 %) to remove membrane associated proteins. Aliquots were taken each time to monitor the separation process by SDS-PAGE. After washing, the amount of protein was estimated as follows: The specific A_{220} absorption of the protein was computed based on the amino acid composition. The pellet was then solubilized in 2 x LSB without bromphenol blue and the absorbance of a 100-fold dilution was measured photometrically. The protein concentration was calculated based on the absorption value.

4.5.4 SDS Polyacrylamide Gel Electrophoresis (SDS-PAGE)

SDS-PAGE (Laemmli, 1970, Schägger & von Jagow, 1987) was performed to monitor heterologous protein expression, to separate and to purify proteins under denaturing conditions. To denature proteins, samples were combined with equal volumes of 2 x Laemmli sample buffer (LSB; 0.125 M Tris-HCl pH 6.8, 20 % (v/v) glycerol, 4 % (w/v) SDS, 10 % (v/v) β-mercaptoethanol, 0.02 % (w/v) bromphenol blue) and heated at 96°C for 5 min prior to loading the gel. PageRuler™ prestained protein ladder (Fermentas) was used to estimate the molecular weight of proteins. Electrophoresis was performed in Bio-Rad electrophoresis chambers (Bio-Rad, München) at 120 – 150 V in 1 x Tris-glycine-SDS running buffer (25 mM Tris, 190 mM glycine, 0,1% (w/v) SDS). The electrophoresis was stopped when the bromphenol blue dye front passed the bottom of the resolving gel. Proteins were visualized by soaking the gel in staining solution (25% (v/v) methanol, 10% (v/v) acetic acid, 0.25% (w/v) Coomassie brilliant blue R250) for 30 min and in destaining solution (28% (v/v) methanol, 10% (v/v) acetic acid) until protein bands became clearly visible.

Table 4-14 Composition of a 13% resolving and a 5 % stacking gel

Component	Resolving gel (10 ml)		Stacking gel (5 ml)	
	Volume	Final concentration	Volume	Final concentration
water	3 ml	-	2.9 ml	-
1.5 M Tris-HCl (pH 8.8)	2.5 ml	375 mM	-	-
10% (w/v) SDS	0.1 ml	0.1%	0.1 ml	0.1%
0.5 M Tris-HCl (pH 6.8)	-	-	1.25 ml	125 mM
30% acrylamide/ bisacrylamide	4.3 ml	12.9%	0.825 ml	4.95%
TEMED	6 µl	0.06%	3.75 µl	0.75%
10% (w/v) APS	80 µl	0.08%	50 µl	0.1%

4.6 Immunoblot analysis

4.6.1 MreB antibody generation

Purified MreB inclusion bodies from *E. coli* cell lysates were run on a preparative SDS gel in a Protean®II XI Cell (Biorad). 200 µg protein were loaded per lane. The gel was run at 4°C for 15 h at 11 mA in a TE62 tank transfer unit (Amersham). After the run, the gel was stained with autoclaved Coomassie in water for 30 min and then destained. The protein bands were cut out with a sterile scalpel and sent to Eurogentec (Seraing, Belgium) to immunize rabbits for antibody production.

4.6.2 Nfs antibody generation

Antibodies for Nfs-protein detection were generated by Eurogentec (Seraing) as peptide antibodies based on epitope prediction. The peptide sequences and their localization in each protein sequence are provided in the Appendix section (**Table 5-14**).

4.6.3 Affinity purification of MreB antibodies

The generated antisera displayed unspecific binding properties and needed to be affinity purified. Therefore, an adapted version of a protocol from Michael Koelle lab (Yale University) was applied: For purification of 2 ml serum, approximately 1 mg of the inclusion body fraction (containing the antigen MreB) was loaded on a SDS-PA gel and blotted on a PVDV membrane by electrophoretic tank transfer under standard conditions. The membrane was stained with Ponceau S in ddH_2O to visualize the protein and to mark its position on the membrane. Then, membrane and proteins were destained in ddH_2O, the MreB containing part of the membrane cut out and soaked in ddH_2O to remove remaining stain. Weakly bound protein was removed by soaking the membrane in acidic glycine buffer (100 mM glycine, pH to 2.5 with HCl) for 5 min. The membrane was washed and neutralized by soaking twice in TBS buffer (500 mM NaCl, 20 mM Tris pH 7.4, 0.05% (v/v) tween-20) for 2 min each and blocked in TBS-B

(3% (w/v) bovine serum albumin fraction V in TBS buffer) for 1 h with gentle rocking at rt. After blocking, the membrane was washed twice in TBS for 5 min each. Two ml serum were added to 8 ml TBS and incubated with the membrane for at 4°C over night slowly rolling to bind the antibodies. The membrane was recovered and soaked twice in TBS for 5 min. Bound antibodies were eluted by adding 1 ml of acidic glycine buffer (Harlow & Lane, 1988) and incubation at room temperature for 10 min with occasional vortexing. The antibody containing eluate was combined with 1 M Tris pH 8.0 leading to an antibody solution of pH 7.0. The elution step was repeated and the eluates unified. Purified antisera were stored at 4°C with 5 mM sodium azide and 1 mg ml^{-1} bovine serum albumin to prevent degradation.

4.6.4 Immunoblot analysis

M. xanthus cells were harvested from submerged cultures, glycerol induced cultures or CTT broth cultures as described above, pelleted at 4°C and frozen at –20°C or processed directly on ice. The pellets were resuspended in 1 ml ice cold MMC buffer supplemented with mammalian protease inhibitor cocktail (Sigma) and total protein was released by disintegration with a FastPrep®-24 instrument (**Section 4.3.5**). Protein concentrations were determined as described (**Section 4.3.7**). Samples of 5 or 10 µg $µl^{-1}$ protein or of equal initial cell numbers were loaded on a SDS-PA gel. Depending on the calculated molecular weight of the target protein; 8, 11, 13 or 15% PA gels were prepared (**Table 4-14**). Proteins were blotted on methanol activated polyvinylidene fluoride (PVDF) membranes using a tank transfer system (Hoeffer) in transfer buffer (25 mM Tris, 192 mM glycine, 10% methanol, 0.1% SDS, pH 8.3). After blotting, the membranes were briefly soaked in methanol and air dried. For blocking, the membranes were re-activated in methanol, washed in ddH_2O and incubated in blocking buffer (PBS-T, 137 mM NaCl, 10 mM phosphate, 2.7 mM KCl, 5% (w/v) non-fat milk powder, 0.1% (v/v) tween-20, pH 7.4) for 1 h at rt or at 4°C over night gently shaking. Western blot analysis was performed using the primary antibody dilutions listed in **Table 4-15**. Secondary anti-rabbit IgG horseradish peroxidase (HRP) coupled antibodies (Pierce, Bonn) were added to a 1:20,000 dilution and incubated for 1 – 2 h at rt. After washing in PBS, chemiluminescence substrate (Pierce) was added and signals were detected by exposure to CL-Xposure Film (Pierce) or using the LAS-4000 luminescent image analyzer (Fuji).

Table 4-15 Dilutions of primary antibodies used for immunodetection.

Antibody	MreB	NfsA-2	NfsB-2	NfsC-1	NfsD-2	NfsE-2	NfsF-1 / -2	NfsG-2	NfsH-1 / -2	HthA[a]	pilT[b]
Fold dilution	2,000	400	1,000	100	100	500	100	500	100	1,000	1,000

[a] Gift from A. Treuner-Lange, Gießen
[b] Gift from S. Leonardy & L. Søgaard-Andersen, Marburg

4.7 Sources for bioinformatics analyses of nucleotide and amino acid sequences

M. xanthus DNA- and protein sequences were obtained online from TIGR (http://www.tigr.org/cmr) or NCBI (http://www.ncbi.nlm.nih.gov/) and analyzed using the Blastn (against nonredundant database), Blastp and psiBlastp algorithms from NCBI or the SMART algorithm from EMBL (http://smart.embl-heidelberg.de/). Predictions pf subcellular protein localizations were carried out with SignalP (http://www.cbs.dtu.dk/services/SignalP/), the CELLO subcellular localization predictor (http://cello.life.nctu.edu.tw/), the subcellular localization prediction tool Psortb (http://www.psort.org/psortb/), the combined transmembrane topology and signal peptide predictor Phobius (http://phobius.cbr.su.se/) and the Subloc tool (http://www.bioinfo.tsinghua.edu.cn/SubLoc/). Prediction of lipoproteins and signal peptides was carried out with LipoP v. 1.0 (http://www.cbs.dtu.dk/services/LipoP/), Psortb and Phobius. To detect conserved domain structures, the TMHMM-Server (http://www.cbs.dtu.dk/services/TMHMM-2.0/) and the TMpred-Server (http://www.ch.embnet.org/software/TMPRED_form.html) were used. Protein 3-D structures were predicted using the protein fold recognition server Phyre (http://www.sbg.bio.ic.ac.uk/~phyre/index.cgi). The RED-TMBB-Server (http://bioinformatics2.biol.uoa.gr/PRED-TMBB/index.jsp) was used to predict beta barrel strutures. Related protein sequences in prokaryotic genomes were detected by Blastp and psiBlastp from NCBI and FastBlast from the Virtual Institute for Microbial Stress and Survival (http://www.microbesonline.org/). Sequence alignments and vector maps were generated using the Vector NTI Suite 9 (InforMax, Oxford, UK).

4.8 Microarray experiments

4.8.1 Experimental setup

Microarray time course experiments were performed for global transcriptional profiling of glycerol induced spore formation. All experiments were done in three independent biological replicates. A schematic overview of the experimental setup is shown (**Figure 4-3**).

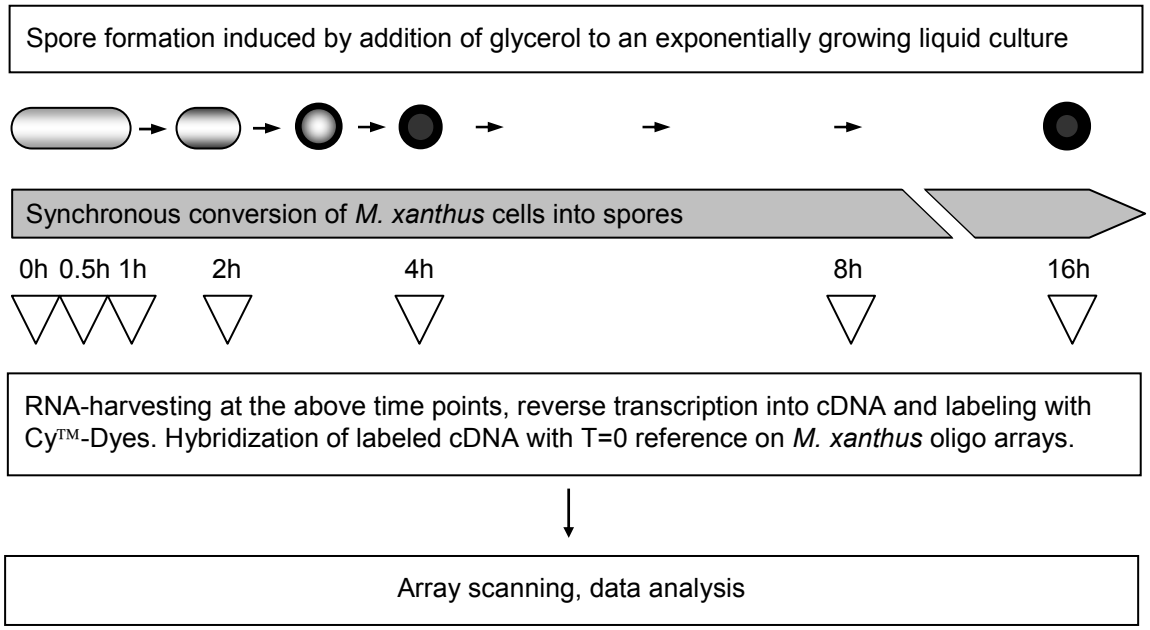

Figure 4-3 Schematic flow of a glycerol spore induction time course for micro array analysis.

A liquid culture of *M. xanthus* DK1622 was grown in CTT medium to an OD_{550} of 0.5. Subsequently, half of the culture was added in 45 ml aliquots to 5 ml stop solution (5% saturated phenol pH < 7 in ethanol) and harvested by centrifugation at 4°C, snap frozen in liquid nitrogen and stored at -70°C until later use. The remaining culture was induced by addition of glycerol to a final concentration of 0.5 M. Samples were harvested at 0.5, 1, 2, 4, 8 and 16 h after induction and treated as the samples of uninduced cells. Spore formation was monitored microscopically.

4.8.2 Sample preparation, probe generation and hybridization

Total RNA was isolated from cell pellets using the hot phenol method (Overgaard *et al.*, 2006, Maniatis, 1982, Müller & Jakobsen, 2008). Cells were lysed by resuspending the frozen pellets in 2.5 ml ice cold solution 1 (0.3 M sucrose, 0.01 M NaAc, pH 4.5) and transfer into a 15 ml tube containing 2.5 ml hot (65°C) solution 2 (2% SDS, 0.01 M NaAc, pH 4.5). The suspension was mixed gently by inversion and immediately used for hot phenol extraction. For this purpose, 5 ml hot phenol (65°C) were added and the solution mixed gently by inversion followed by incubation at 65°C for 5 min. The

samples were chilled in liquid nitrogen for ~10 s, kept on ice and centrifuged at 4,500 x g for 5 min, 4°C. The aqueous layer was transferred to a fresh 15 ml tube containing 5 ml hot (65°C) phenol. The samples were mixed gently by inversion and incubated 5 min at 65°C, chilled in liquid nitrogen for ~10 s and centrifuged as above. For phenol/chloroform/isoamylalcohol extraction, the aqueous layer was transferred to a fresh 15 ml tube containing 5 ml phenol:chloroform:isoamylylcohol (25:24:1, pH 6.6), mixed gently by inversion and centrifuged as above. The samples were chloroform/isoamylalcohol extracted by transfer of the aqueous layer to a 15 ml tube containing 5 ml chloroform:isoamylalcohol (24:1), mixed gently by inversion and centrifuged at 4,500 x g for 5 min, 4°C. Nucleic acids were precipitated by transfer of the aqueous layer to a fresh 15 ml tube containing 400 µl 3M NaAc pH 4.5 and 9 ml 96% EtOH. The samples were inverted several times and incubated at –70°C for 30 min or at –20°C over night. Precipitates were pelleted by centrifugation at 4,500 x g for 30 min at 4°C. The pellets were washed twice with freshly prepared ice cold 70% ethanol, air dried and finally dissolved in 1 ml Rnase-free H_2O and stored at –70°C.

The RNA was further treated with DnaseI (Ambion) followed by Qiagen RNeasy® column purification according to manufacture's instructions to remove genomic DNA. Quality of isolated RNA was verified by agarose gel electrophoresis, absence of contaminating genomic DNA was confirmed by PCR.

Probes were prepared as follows: Random priming was carried out by addition of 10 µg random hexamers ($pd(N)_6$, Amersham) to 25 µg purified RNA in a final volume of 15.5 µl followed by incubation at 70°C for 10 min and chilling on ice. Reverse transcription was initiated by addition of 4.5 µl RNase free water, 3 µl 0.1 M dithiothreitol (DDT), 0.5 µl RNase inhibitor (20 U/µl, Ambion), 0.6 µl 50 x deoxynucleoside triphosphate mix (25 mM dATP, 25 mM dCTP, 25 mM dGTP, 10 mM dTTP, 15 mM aminoallyl-dUTP), 3 µl reverse transcriptase (50 U/µl, Stratagene) and incubation at 37°C for 10 min, 42°C for 1 h 40 min and 50°C for 10 min.

RNA was hydrolyzed by addition of 10 µl 1 N NaOH and 10 µl 0.5 M EDTA followed by incubation at 65°C for 15 min. Samples were purified with Zymo DNA clean and concentrator™ spin columns (Zymo research) using freshly prepared phosphate wash buffer (5 mM KPO_4, 80% EtOH, pH 8.0) and elution buffer (4 mM KPO_4, pH 8.5). The samples were vacuum concentrated to ~1 µl and recovered in 7 µl 0.1 M fresh sodium bicarbonate pH 9.3. Then, NHS-ester dyes Cy™3 or Cy™5 (Amersham) were coupled to the amino groups of incorporated aminoallyl-dUTP. For this purpose, the lyophilized dyes were dissolved in 10 µl DMSO and 2 µl were added and samples were incubated for 2 h at room temperature in the dark. After purification with Zymo spin columns, labeling efficiency was determined photometrical and the labeled probes were either used directly for hybridization or stored at -20°C.

Prehybridization of arrays was performed by submerging the slides in a well dissolved, filtered (0.22 µm) solution of 5 x SSC buffer (pH 7.0), 0.1% SDS and 1% (w/v) BSA fraction V at 42°C for 2 hours. The slides were washed five times two minutes each in autoclaved ddH_2O at room temperature on a shaker, submerged in isopropanol for 2 min and finally dried by low speed centrifugation with a flat plate-holder adaptor for 10 min.

Probes were prepared for hybridization as follows: 22 µl of hybridization buffer (50% formamide, 5 x SSC buffer, 0.1% SDS, 60 µg salmon sperm DNA) were added to the labeled probes. Then, Cy™3- and Cy™5-labeled probes (representing reference and sample of one particular time point) were unified and heated at 95°C for three minutes.

After cooling to rt, the probes were applied to the prehybridized arrays, covered with a LifterSlip™ (Erie scientific) and mounted into a hybridization chamber. To avoid drying during incubation, 50 µl of hybridization buffer were added to the chamber. Sealed hybridization chambers were incubated submerged in a water bath for 16 h at 42°C.

After hybridization, arrays were washed three times 10 min each in buffers providing increasing stringency conditions (buffer 1: 2 x SSC pH 7.0, 0.1% SDS, buffer 2: 0.1 x SSC, 0.1% SDS, buffer 3: 0.1 x SSC) in the dark and dried by low speed centrifugation. Thereafter, arrays were scanned with a GenePix™4000B microarray scanner controlled by GenePix™ Pro 6.0 image analysis software (Axon instruments) at 532 nm (Cy3™) and 632 nm (Cy5™) wavelengths simultaneously.

4.8.3 Data analysis

Image analysis (block and spot finding, background detection) and data acquisition were performed with GenePix™ Pro 6.0 image analysis software. Each slide was checked manually for correct positioning of the grid and detection of each spot. Normalization and data analysis were carried out with Acuity 4.0 software package (Axon instruments) applying the following criteria: Normalization: Ratio based (mean ratio of medians = 1)

Substance name ≠ EMPTY
Substance name ≠ NULL
F532 Median – B532 ≥ 100 OR F635 Median – B635 ≥ 100 in at least one time point.

These pre-filtered datasets were analyzed with the Significance Analysis of Microarrays (SAM) software version 2.23 (Stanford University) to screen for significantly regulated genes. The three biological replicate time course experiments were analyzed separately as one class time courses. The signed area was considered for calculation. A false discovery rate (FDR) of 5% was applied to call a gene significantly regulated.

The sets of regulated genes were exported to Acuity and combined by averaging the values for each gene at each time point. Genes that display a log ratio < 1 or > 1 in at least one time point (corresponding to 2-fold up- or down regulation) and where data are present for all time points were called “genes regulated above threshold”.

The self-organizing map clustering algorithm of the Acuity software was applied to group significantly regulated genes based on their expression pattern. Yellow colors indicate upregulation, blue colors indicate downregulation.

The microarray data will be deposited in NCBIs Gene Expression Omnibus (http://www.ncbi.nlm.nih.gov/projects/geo/).

4.9 Plate reader experiments

Strains were grown in liquid to an OD_{550} = 0.5, harvested and developed in submerged culture in MMC buffer as described above in black 24-well glass bottom plates (Greiner Bio-One). At indicated time points, fluorescence signal intensity was measured at 615 nm wavelength in a plate reader (Tecan Infinite M200) controlled by i-control 1.4 software. Signals from cell-free, buffer containing wells were subtracted from signals of developing cultures to calculate absolute fluorescence intensities. Proper development was checked at each time point using a stereo microscope. All experiments were carried out in triplicate.

4.10 Labeling of nascent peptidoglycan with fluorescent vancomycin

Cells were grown in liquid. 1 ml samples were harvested by centrifugation (5000 x g, 10 min, 4°C) and fixed for 10 - 15 min by resuspension in 2.5 mM formaldehyde, 2.5% (w/v) paraformaldehyde, 30 mM NaH_2PO_4 pH 7.4. The fixed samples were split and one part was incubated with 3 µg/ml fluorescin conjugated vancomycin (VanFL) for 10 min in the dark. Cells were sedimented by centrifugation (3000 x g, 5 min, rt) and the pellet rinsed with fixing solution. The supernatant was discarded; the cells were carefully resuspended and spotted on an agar pad (1% Agarose in A50 Puffer) for microscopy. Fluorescence signals were detected at 515 nm wave length.

4.11 Microscopic methods

For fluorescence microscopy, *M. xanthus* cells were spotted on Agar pads (1% (w/v) agarose in A50 starvation buffer (10 mM MOPS, pH 7.2, 1 mM $CaCl_2$, 1 mM $MgCl_2$, 50 mM NaCl) covered with a cover slip and placed under the microscope. Phase contrast, DIC and fluorescence images were taken with 600- and 1000-fold magnification. Gfp and vancomycin specific signals were detected at 515 nm and Mcherry specific fluorescence signals were detected at 670 nm wavelength. The microscopes (**Table 4-2**) were controlled by Metamorph ver7.5 software. Images were taken with the camera types EM-CCD Cascade 1K (Photometrics, Tucson) or Leica DFC 350FX. Image processing was carried out with Metamorph ver7.5.

A APPENDIX

A.1 Oligonucleotides

All oligonucleotide primers used in this study were synthesized by MWG (Ebersberg) or Invitrogen (München). Underlined sequences indicate restriction sites used for cloning. Bolded sequences indicate complementary sequences that were used to fuse PCR products.

Table A-1 Primers used to generate in-frame deletion constructs and to screen in-frame deletion mutants. Primers del A and del 1 were used to generate the upstream fragment; primers del D and del 2 were used to generate the downstream fragment. Primers del A and del D were finally used to generate the fusion used for cloning. The chk primers were used to screen colonies for loss of the gene.

Primer	Sequence (5' → 3')
nfs del 1	**GTA CTT CAC ATG AAC TCC** CCG AGC CAC GGA GTC C
nfs del 2	**GGA GTT CAT GTG AAG TAC** ACG TTC TGA AGC CCG CAT ACA CG
nfs del A	CGTA GGT ACC CGA ACA AGA AGA TGC CCG GTC ACT ACG
nfs del D	GACT AAG CTT GAC GGC TAC GAG CCG TGG TTC G
nfs del chk up	CGC CGG AGG AGG CTG CCT CC
nfs del chk dwn	GGT CCA CGA GCC CAT GGA GCT GC
3371 del 1	**GAA GGT GTA ATG AAC TCC** CCG AGC CAC GGA GTC C
3371 del 2	**GGA GTT CAT TAC ACC TTC** TCC TTC TAG GTC CAC CTG ACT ATG
3371 del A	C GTA GGT ACC CGA ACA AGA AGA TGC CCG GTC ACT ACG
3371 del D	G ACT AAG CTT GTC CCC ACG GTG GGC GCG G
3371 del chk up	CGC CGG AGG AGG CTG CCT CC
3371 del chk dwn	CTG AGC ACC ACG CTG AAC TGC GCG
3372 del 1	**TCA GAA GAG GGA CAG GAA** CGG TCG CAT AGT CAG GTG
3372 del 2	**TTC CTG TCC CTC TCC TGA** TGC GCA GGA AGG CCT G
3372 del A	CGTA GGT ACC CCG ACG AGC TGG AAG ACC TCT GGC
3372 del D	GACT AAG CTT GTA CAC GCG ACT GTC CTG GGG GAC
3372 del chk up	GCT GCA GAC ACA CCT GAC GGC GC
3372 del chk dwn	GAA GGG CTC CAG TTG CCG CTC C
3373 del 1	**CTA CGG CTG TCG TTT CAT** GGC GGT TCA GGC CTT CCT G
3373 del 2	**ATG AAA CGA CAG CCG TAG** GTT CAC GAG CGA CGC
3373 del A	C GTA GGT ACC CAA CAA CTC GCT CGC GCA GTT CAG CG
3373 del D	G ACT AAG CTT GTC CGG GAT GCG GGG CAG CTC
3373 del chk up	CGG TGC CCT CCG CCG AGC C
3373 del chk dwn	GCG CGT CAT CTC CAA CTG GTA GAG G
3373 del 1 int	**GCG TCC GTT CGT CGG TGT** AGG CCT GGT TGA GG
3373 del 2 int	**ACA CCG ACG AAC GGA CGC** TGG CGC GGT ACG
3373 del A int	C GTA GGT ACC GCC GCT ACG AGA AGT TCG ACG GC
3373 del D int	G ACT AAG CTT TCT GGA TTG AGA AGT GGC GGT GGA ACG G
3374 del 1	**TCA TCG CAG AGC ACC CAC** TGA CGA GGG ACG ACG
3374 del 2	**GTG GGT GCT CTG CGA TGA** AGC TGT TTC GCA TCG ATT CC
3374 del A	C GTA GGT ACC GCA GTC CAC CGC GTC GCT CG
3374 del D	G ACT AAG CTT GGC GTC TTC AGC GCC CGC TGG
3374 del chk up	GGC TTC GCG CGC TTT CAG AAC GAG G
3374 del chk dwn	TCG GAC TCG TCC AGC TTT CCG GC

Table A-1 continued

Name	Sequence (5' → 3')
3375 del 1	**TCA CTT GCC CAG CTT CAT** CGC AGC ACC TCC CC
3375 del 2	**ATG AAG CTG GGC AAG TGA** GGC GGC TTC GCT TG
3375 del A	C GTA GGT ACC GAC CTG GCG GCG AAG CAG AAG G
3375 del D	G ACT AAG CTT GAC TGC CGC CGC CCG CTG C
3375 del chk up	GAG GCG GCC CGG GCG TTC G
3375 del chk dwn	CAC ATC CCC GGG GTT GAG CGC
3376 del 1	**CTA GAG GTT CAT GCT CAA** CCT CCC AAT GCA CAG CG
3376 del 2	**TTG AGC ATG AAC CTC TAG** CGG CAG CGG GCG
3376 del A	C GTA GGT ACC AGG TCC AGG GCC TGC AGA ACA TGC
3376 del D	G ACT AAG CTT TGG GAA CCA GGT TCG GCA GGT CC
3376 del chk up	GCC GAG CGC TCC TTC GGA AAG G
3376 del chk dwn	AGC AGG GTG TCG CCC CAC AGC
3377 del 1	**TCA CCC TCC CGC CGC CAT** GAG GAT TTT CCC TCT TC
3377 del 2	**ATG GCG GCG GGA GGG TGA** GCG ACG GTA GCG
3377 del A	C GTA GGT ACC CATCGGGGCCACCTGGCACC
3377 del D	G ACT AAG CTT CGG TCC ATG ACG CGC ACG TGG
3377 del chk up	GAA GGC GAT GGC GCT CCG GC
3377 del chk dwn	CTG GGG CGC TCA CGG GGC
3378 del 1	**GTA CTT CAC CTT CTT CAC** GGG TCC TCC CGA CAG
3378 del 2	**GTG AAG AAG GTG AAG TAC** ACG TTC TGA AGC CCG CAT ACA CG
3378 del A	C GTA GGT ACC GTG GCA AGT CCA TCA CCA AGG TCA TCC
3378 del D	G ACT AAG CTT GAC GGC TAC GAG CCG TGG TTC G
3378 del chk up	GGA CAA GAG CAA GAA GGA GAA GGA CCG
3378 del chk dwn	GTC CCC ACG GTG GGC GCG G
6788 del 1	**CGC GGG CTC CCC ATA GAC** GAG GAA TCT TGA AAG CAC
6788 del 2	**GTC TAT GGG GAG CCC GCG** CCC ATC CCC TGA
6788 del A	CCG GAA TTC AAG GCG GAA ATC AGC GGC AAC ATC AAC G
6788 del D	GCG GGA TCC AGG GGA TGC CGA TGA TGA TGC GCG
6788 del chk up	CAC CGC TCG CGA GAT TGG CGC C
M13 f long [a]	CAC GAC GTT GTA AAA CGA CGG CCA G
M13 r long [a]	GGA TAA CAA TTT CAC ACA GGA AAC AGC TAT GAC

[a] M13 f long and M13 r long are primers for sequencing of the fused fragments in pBJ114 and to check the insertion after the first homologous recombination.

Table A-2 Primers used for real time PCR.

Name	Gene	Sequence (5' → 3')
3370f	*rplC*	GGT GAC CAT CGG TTT TGG TG
3370r		ACG CGG AAT TCC TTC AGG TG
5543f	*Mxan_5543*	AGG GGC TCA CGC GCT ACT AC
5543r		CCT GCA CGT CCA GTT CGA G
0403f new	*atpE*	GGG TGC CGG TCT CTC CAT C
0403r new		AAA CGA CCA GCG CGA ACA G
3885f new	*prU*	ACC TGA ACG TCA CCG CCA AC
3885r new		TGC CGA ACA GGT CGA TGC
3227f	*exo*	ATG AAC CTC TATCCG GAC ATC GT[a]
3227r		AGC TCG AAG GCC GTC TCA[a]
6969f	*mspC*	AGA AGC TCA TCG CCG CAG TC
6969r		GAT GCC TGT CAC GTC CTT GG
7264f	*devR*	GCC TCA CCG AGG GAA ACA TC
7264r		TGG CTC CTG CTC ATT CAA GC

Table A-2 continued

Name	Gene	Sequence (5' → 3')
5432f	*tps*	GGT CGA TCT GAA GCC TGA CG
5432r		ATC TGG TCG CCG GTG AAA TC
3357f	*sigB*	ATC CGC CTC ATC TCC TAC GC
3357r		CGG GCC AGA CTG AAG AAC AG
6209f	*sigC*	TCA ACC AGT ACC CGC TGC TC
6209r		CTT CAT CAG GCC GAT GTT CG
3371f	*nfsA*	CTG CGT CTT TGC TTC GTT GG
3371r		ACC GAC CCC GAA GGA CAT C
3374r	*nfsD*	CGC GGT GCT CAT CAC TGG
3374f		AGC CTT CTC CTC TGC CTT GC
3378r	*nfsH*	TCT ACT CCA ACG CCC AGA CG
3378f		AGG TTG AAG AAG GCC ATG GTG

[a] Primers 3227f and 3227r were designed by J. S. Jakobsen.

Table A-3 Primers used to map transcriptional units of the *nfs* locus.

Name	Region	Sequence (5' → 3')
3372 del D	*nfsB - nfsC*	GAC TAA GCT TGT ACA CGC GAC TGT CCT GGG GGA C
3373 del A		CGT AGG TAC CCC GAC GAG CTG GAA GAC CTC TGG C
3373 - 74 f	*nfsC - nfsD*	AGT CGC TGT ATC GCC CGA AG
3373 - 74 r		GCA ATC CAG CAC CCA CTG AC
3375 - 76 f	*nfsE - nfsF*	CTG GGC AGG GCA CTG ATG
3375 - 76 r		CAT GCT CAA CCT CCC AAT GC
3377 del 2	*nfsG - nfsH*	ATG GCG GCG GGA GGG TGA GCG ACG GTA GCG
3377 del D		GAC TAA GCT TCG GTC CAT GAC GCG CAC GTG G
3378 - 79 f	*nfsH - Mxan_3379*	GGC CCA ACA TCA CCT CCT TC
3378 - 79 r		AGG TGA CGC CCA AGT CCA TC
nfs del 2	*nfsH - Mxan_3379*	GGA GTT CAT GTG AAG TAC ACG TTC TGA AGC CCG CAT ACA CG
nfs del D		GAC TAA GCT TGA CGG CTA CGA GCC GTG GTT CG

Table A-4 Primers used for insertion mutagenesis and to screen insertion mutants[a].

Name	Gene	Sequence (5' → 3')
0110 f	*Mxan_0110*	GGT GAT TCC CGC GCT GGC GG
0110 r		GCA CCA GCA CCC GCA CGT CC
0110 chk		CGC TCC CAA TCA CCG GCA TGA CC
0434 f	*Mxan_0434*	CGC CTC CGC GTA CAG GTC CG
0434 r		TGC CGG GCC TGG AGC CAG GC
0434 chk		GGC CAG CAG GTT GCG CTT CTG
0524 f	Mxan_0524	GCG CGT GCT CGT GGT GGA CG
0524 r		GGA CCT TCC CCT TGC TCG GCT TG
0524 chk		GCC CGA TGG CCC GCA CAA GG
0646 f	*Mxan_0646*	GGC TCG TCA CCG GTC AGC CC
0646 r		GGC GTT GGC GTC GCT GGA CC
0646 chk		AGG CGT GAT GAG CGT CTT GCC GC
0690 f	*Mxan_0690*	CAG TGA TGG GAC CTC CGT GGG C
0690 r		TCC CAG AAG GTG AAG ACC CCC ACG
0690 chk		CCC GGT TTC GGA CCG GAG AGG

Table A-4 continued

Name	Gene	Sequence (5' → 3')
0781 f		GTT GAC CTC GAT GTT CCC CAC GCC
0781 r	*Mxan_0781*	GCG GCG CTG AGT CCT CAT CTC G
0781 chk		CGC CAG GTG CTT GAG CAG TCG C
0862 f		CGT CCT TGT CCT CGA AGC GCA CG
0862 r	*Mxan_0862*	GCC TTT CAC GTC ATC GTC GAG TCT CC
0862 chk		CGT CGC GCT CCA GCT TCT TCA TGC
0888 f		CCG AGC AAG GAA GCG TCG GCG
0888 r	*Mxan_0888*	GCC CCT TCA GTG GCT TTC GGG C
0888 chk		CAC ACC AGG TCG GAG CGC AAC G
0912 f		CTT GTA GAG CTG AAT CTG GTC GGC CG
0912 r	*Mxan_0912*	CGC CGA CAA CCT CAC CTT CGA CG
0912 chk		CGC TGG TGA GGA GGC GGT CG
0994 f		GGA TGG ACG CCA GCG CTT GAA GG
0994 r	*Mxan_0994*	CGT GCC GTC GAA GGC GAT GGG
0994 chk		CTG CCC CAC GTC TTC GGC GC
1065 f		CCT AGG AGG CAG CCA CGC ATG C
1065 r	*Mxan_1065*	GTT GTT CAT CAG GTT CAT CTG CAT CAC CGC
1065 chk		GTT CCT CGC CTC GGA TGA GTC CC
1092 f		GCG TCC GCG AGG ACG TCA CG
1092 r	*Mxan_1092*	CAG CAC ACC CTG CTC GTA GCG AG
1092 chk		GGT CGC CGT GGA CCC CAT TGG
1101 f		CTG CCC CGG ACG TCC ATC TGG
1101 r	*Mxan_1101*	CAG CGT GCA CAC CGC GTA GCC
1101chk		CAC TGG CCA GCG CGG CTC C
3026 f		GCG TCC GTC GGG TGG TCC G
3026 r	*Mxan_3026*	CGC CAG ACG CCA CAG CCA GC
3026 chk		GTC CCG TAG GAA TTT CAG TCC GGG GC
exo ins f		GAT GAC GGC AGA CCA GCT TCT GGG
exo ins r	*Mxan_3227*	GGA CTC CAT GCC CTT CTC CGA AAC G
exo chk		CGC CGT CCG TTT GGT GGT GAC GC
mreB ins f		GCA AGA AGG TCC TCG CGG TGG
mreB ins r	*Mxan_6789*	CAT CTT GAT GAG CTC CGC CGT GC
mreB ins chk		CCC CGC TAT GAC GGG GAA ATT CC

[a]chk primers were used with the pCR®TOPO 2.1 vector specific M13 f long and M13 r long primers.

Table A-5 Primers used to verify integration at the Mx8 *att* locus.

Name	Description	Sequence (5' → 3')
attB rechts	Genome specific attB forward primer	GGA ATG ATC GGA CCA GCT GAA
attB links	Genome specific attB downstream primer	CGG CAC ACT GAG GCC ACA TA
attP rechts	Plasmid specific attP forward primer	GCT TTC GCG ACA TGG AGG A
attP links	Plasmid specific attP reverse primer	GGG AAG CTC TGG GTA CGA A

Table A-6 Primers used to clone and express *M. xanthus mreB* in *E. coli*.

Name	Sequence (5' → 3')
mreB f	CAG GAA TTC TTT GAC TGG CTT CAC ACC CTC TTC TCG CG
mreB r	TA CTC GAG GCC CGG CTG GCA GAC CTGC

Table A-7 Primers used to amplify and fuse *mreB* N-terminal to *gfp*.

Name	Description	Sequence (5' → 3')
mreB prom f	Amplification of the *mreB* promoter region	TAG ATC GAA TTC CCG CCC TGC TGT TCG AGC CCG
mreB prom r		**GGC CAT ACT AGA CAT ACG GGG GCG** GGA ACT TTC GG
gfp mreB prom f	Amplification of *gfp* for *mreB* promoter fusion	**CGC CCC CGT ATG TCT AGT ATG GCC** AAG GGC GAG GAG
gfp mcs r		GAC GTT GTA AAA CGA CGG CCA GTG CC
mreB 4	To clone *mreB* downstream of *gfp* and *venus*	T CAG GAT ATC ATG TTT GAC TGG CTT CAC ACC CTC TTC TCG
mreB 2		TA GGT ACC TCA GCC CGG CTG GCA GAC CTG C

Table A-8 Primers used to amplify and fuse *mreB* N-terminal to *venus*.

Name	Description	Sequence (5' → 3')
Venus 1	Amplification of the *mreB* promoter region	A TGC TAG GAA TTC CCG CCC TGC TGT TCG AGC CCG
Venus 2		**GCC CTT GCT CAC CAT ACG GGG GCG** GGA ACT TTC GG
Venus 3	Amplification of *venus* for *mreB* promoter fusion	**CGC CCC CGT ATG GTG AGC AAG GGC** GAG GAG CTG TTC
Venus 4		AG CTA GGA TCC CTC CGG AGC TCG AGA TCT TAA GGT ACC

Table A-9 Primers used to fuse *mreB* C-terminal to *venus* in pVENC2[a].

Name	Description	Sequence (5' → 3')
mreB 5	Upstream primer	ATG CTA GGC GCC CTC GCC GGC ATC GTG TTC GCC
mreB 6	Downstream primer	ATC GTA GGT ACC GCC CGG CTG GCA GAC CTG C

[a]pVENC2 was provided by Prof. Dr. Martin Thanbichler

Table A-10 Primers used to construct pAL4 (mcherry under *nfs* promoter) and its derivatives. The introduced stop codon is bolded.

Name	Description	Sequence (5' → 3')
nfs prom f	To amplify the *nfs* promoter region	G TAG TCA AAG CTT TTC GCT GCT GAG CGT TTG AAC GCT CG
nfs prom r		G TCA CAT ATG GTC CGC GTC ACC CGA CGC TCA G
mch f	To amplify *mcherry* from pXCHYN-1[a]	GAG ACG AC CAT ATG GTG AGC AAG GGC
mch r2		T ATC CAT ATG **TTA** GGC TCT AGA TAG TGG ATC CCC CGG GCT GCA GC

[a]pXCHYN-1 was provided by Prof. Dr. Martin Thanbichler

Table A-11 Primers used to construct pFM16 (*mcherry* under *pilA*-promoter).

Name	Description	Sequence (5' → 3')
pilA prom f	To amplify the *pilA* promotor from pSL8[a] and fuse it to *mcherry*	T ACT AAG CTT AG CCC GGG A GCG CTT CGG ATG
pilA prom r mch		**CTT GCT CAC CAT GGG GGT** CCT CAG AGA AGG TTG C
mch f pilA	To amplify *mcherry* from pAL4 and fuse it to the *pilA* promoter	**ACC CCC ATG GTG AGC AAG** GGC GAG GAG GAT AAC ATG G
mch r		CAC CGC ATA TGT TAG GCT CTA GAC TCC G

[a]pSL8 was provided by S. Leonardy & L. Søgaard-Andersen, Marburg. pSL8 is a pSWU30 derivative.

Table A-12 Primers used to construct pFM17 (pAL4 where Km^r is replaced by Tc^r). The oligonucleotides bind to flanking regions of the Tc^r-cassette of pSWU30. Since there was a interfering *ClaI* site in the intended region, the Tc^r cassette was amplified in two parts and fused by PCR allowing for deletion of the *ClaI* site. *Italicized* are mismatching positions that delete a *ClaI* recognition site.

Name	Description	Sequence (5' → 3')
tet f1	To amplify the first fragment	AT GCT AAG CTT AAA TCA ATC TAA AGT ATA TAT GAT TAA ACT TGG
tet r1		**TAA AGC TA*A TCT ATG ATA AGC*** TGT CAA ACA TGA G
tet f2	To amplify the second fragment	**GCT TAT C*AT AGA T*TA GCT TTA** ATG CGG
tet f2		A TGC ATC GAT GGA GTG GTG AAT CCG TTA GCG

Table A-13 General sequencing primers.

Name	Description	Sequence (5' → 3')
M13 f	For pCR®2.1 TOPO plasmids	GTA AAA CGA CGG CCA G
M13 r	For pCR®2.1 TOPO plasmids	CAG GAA ACA GCT ATG AC
gfp seq f	Internal *gfp* primer	CTG CCC GAC AAC CAC TAC CTG TCC
gfp seq r	Internal *gfp* primer	CCG TCC TCC TTG AAG TCG ATG CCC
mch seq f	Internal *mcherry* primer	CGT AAT GCA GAA GAA GAC CAT GGG CTG G
venus seq f	Internal *venus* primer	GGT GAA CCG CAT CGA GCT GAA GGG
pal seq f	Primer to sequence inserts of pAL4 and its derivatives	GAA GCG GAA GAG CGC CTG ATG CG
mreB seq f	Internal mreB sequencing primer	GGG CCT GCC CGT GTT CCT CG

A.2 Nfs protein sequences and antigenic peptides

Table A-14 Peptides used as antigens to generate Nsf-antibodies and their localization in the protein amino acid sequences (underlined).

Protein	Sequence (N → C) and antigenic peptides (underlined)
NsfA	VARGVHCTPAHGGPSHGPGRIMIARTLCVFASLAVSLAAPVAAAQDDENVLDKVVVRNRLYEPGGKLEMSFG VGLPLQTHLTAHYVFNAGVAYNLFNSFAVEARAGYAASRHTG**LARSISESFLNREDK**RVTDELEDLWQMNLH GVAGVRWAPIYGKLSLLSDLPVHFQAYVWAGGGLASFKRNSVIQCTQVVNRE**LGICDNRTSVDDRGS**ATQNF WVNESRVAPVVSAAVGFRFFILDKHGVRLELRDWAFRDNYRVNLERDAWEAGQATGEPARSPGLTHLVQFD LGYTFSF
NfsB	MRPFLSLALLVATATQAAPRVPAPAFALAQVQQVPAPGAETSVPPPSTQSQSLPEAPVGPASRPEPLVPAEA TEAFAPPAGVRPNAAPAQGS**DEVPASEPSRVDDTAP**VPSAEPAPTVGTDPAPATTGMAGQEAPPVPDDAPM LAS**DLGSDAPRTTDAQQ**QRLVNGAPLYNPNVSVHIVQKKRFADEGRHELTVYPATVQVNGKYTDHAGTAAH YTYHLQENFALQVMGQYNWYSNESAFNLELIDKVREQAQAASSLLLVWGAHAGVEVTPLYGKFAFLNNSLAQ FSVVLSGGAGVGSTRHLIRPAVTNDVEGESFRVPARFGDTGTKFMGSVGGGFRLQFGESYALRVEVRDLIYT ARVDRVDGCNLADFEALEAARSTNQDFASLNLSGSCRYEKFDGIDPKTKKNYREDIILGRDLVVEPSSDVLNN VSFYAGFSVLF
NfsC	MKRLLSLFVALAPLAVSAQPDSGGYNRALAAFNAGDMDTAAPLFFELAESASDAEVKGKAEYFLGQSLAQKG LPVAAFITYAAIVNAGPSHPSYLKAVEGLVDMQQQLDEHNLIPSILNQAYTDEVRDRWVTLPKEVLARINYLVG TVSQRKSRFEEARSLLEAVPQDSRVYAKSRYLLGVVLADPRFPGRPSEASVLDKDALAAFNAVLAAKEGQLD LRATQHLALIALGRLHYRRGEYT**DASAAYERVPRYSRY**WDQALFENGFARFQNEDFGGALGSLQALHAPQF AGAFQPESWILKATVYYYSCLYDEVKTTLAAFDEIYAPMERQLEPFTGEDVPLVQSFNLVAAENRRLPRPVYL WLRNNERIREVMRMLER**VDDEKRALTNGRWRG**TPLAAQSTASLEEVRGTLLQVGGTLAQSRIREAADNLRT FSDQAEIIRVQTALDEKDLLQAGVDQKALLTRQSLYRPKMPSAAWNYWKFQGEFWIDEIGYYQYTLKRGCPA KTAEQQP

Table A-14 continued

Protein	Sequence (N → C) and antigenic peptides (bolded)
NfsD	VGAGLPACRVGFTAGARMKVVLRFGALAVGAVLITGGVGEAAETQARKGGKKPAAASASKTSGASSKAGGK KKSAKAQVDRKAEEKAPPPGVAPEDVRQGPARVQPASAKFAELPRIPDAKRDALADKKRDEAIAAFKR**LIPKL RDGNPQKAEM**LYRLSELYWEKSKYLYQLEMTRFLAAEKEYDAAVARGEKVEPPKKNHADSERYRTETMGIY EDILRAYPDYPQRDEVLFSMGYNYYELGRREDAVARYEELIRDFPKSQFVPDAYIQLGNHYFENNKLIPAKEN YEKARDSGVPKIYGYAVYKLSWCDYNTGDYELGLKKLHEVVDYAAKSPELGDLRTEALNDLTVFYVQLDQPK EAIAYFKEKAPAQRVGRLLAKTAAGLVDAGHFDSAILAYRTLVDDEPMGANAPEYQQAIVRAHEGLRQRQLVR KEMKRMVDLYSPGGGWWKANEGKTAVLRNAFNVTEEAMRVMVTEYHQEAQKTRQVETYRLARDIYKQYVD AFASNANPDFVADSAFNLRFFYAEILWALEEWEAAAAEYDAVVAF**KIPDRDTAREVSNEAY**RKSAGYNAILAY DKLVKIERGQLAKSDLRDGQKVDEKKDKGDVAKQKIVKRDAKDRQEEALTKFEDRLVAACDVYVKLYPNTQD EIDLRYQAAVILYDRSHFVDAARRFGEIIEKFPEERRSRDAADLTMYVLESREEWLELNTLSKKFLENKKLAKP GTDFAVRVSRVVEGSQYKWVDEVVYKKEKNPKKAAEEFLRFVSDFPKSENADRALTYAMVIAQEAGEIDKGL AAGERFLKEYPRSPFELKARYSLAGLYEKVAEYRKAAVMAESLVASYDAAMKADDANGKRKATKAAAKVSVA PGAEDAESKRERVAAERKALLEEAGGWMADAQFNAGVWWEGAGEPQKAVAAYNTYVSRFKDRKDVPQVA FAAALAWEKEKKWSEAARAFGAFAETYGRDSRSSSAQVYQARYHELLAYEHLRNAREQERVQGELVRAWN RLPESARKDAAVLNAYGHARFLSLEPAWKRYVGIRFSRVSTIRRDLAAKQKEIQRLEKEYLAVLSTGSGDWGI AALTRIGLAYADFARNIMDSPDPSGLDEEQLAMYRSELENLALPLEDKAAEALEKALEKAYELGVYSPWTLAA QDQVNRLRPGAYAQVRQVDYRGSDTLVRSDLVRVLEGATATTPAPADSSKPSDDEAQAPTAARGEVLR
NfsE	MKLFRIDSFQVGAGKTQMTWFRSLLVGSLAFTAACA**SGPQKKQTAAPEVTP**PAAQQPAPEQKPVPPPAQKS GSAQSAFAAALQSYEAGDLDGARKGFEAVVDELPQSLNAQFNLG**VIAERQGRPDDARVAY**EKVLLLDPAHVP AVVNLGVMYRAQGRLDEAIALFQRALKTPGREYDASLLNSLSITYRVAGKLDESEAAARRVLVRNKDDPGAYK NLAHVAYAREKYRLAELLAGTARKHSENDPALYNLLGMVYLKLDDRARALVQFQKAISLDAKFTPGYLNLGAL ALSYRDYVGAERSFGKAVELEPGSPDATLYLAWALDGQKGRDPKKGLAAGEAFEKVLATRADLPEAVCGAG WAYASDRAGWQKAIAFLDRCKGLETTTDNDKQMITAKVQGLQNMLKAPPPEAAPATAEGEGDGAPADEAIG GGGAQPAGGAEGVAPGQGSDVAPEGDATGGAGAHPGQGTDAMPADDATGGVGSGAPLAPGGKGTPAGK
NfsF	LSMRRLVSAVVVLGLWAAPSVAMS**QEPRDTVKIVQEEDR**TVVRKKTVIDFTDVAVEGELTKPEGSYVLHRKKT DFQSLI**KVRDNFDPELQKSVD**NL
NfsG	MAAAKNNGLTLR**ITGPDGSTAEAVSEA**ESVIVGSGAQAAVKIQDPRVSNLHVMLKVDKDGSVTAIDLGSEGGT EVRGQRLVLPTALNPGDVLMVGGSQVEVLFGATQPERPLPAGARVAGPVFQGPVATPPPPRGMQMQTQTR ADLPNLVPTPPPPMRQVSTALGNRVERVASPGVIPVEPP**RQVPPGLQPRTTPSSA**RTSTPNVANTATPRRTV APHLQEPLPPEAMPTPEARVLQVALLWGDTLLEVQHFKDGVPVTIGEAKQNFFNVFAPSVGKSHVLAVSKKD VLEVRAPAGSRAFVTNQGNVRTKDALRAAGALSGQAGDDAEQRFTLGLHDRVEVSLGTVSFVARYVKPSPVI TAASLKDSDFTFFKITSICMLAGLAVVLTMVLTPRPELPQSADIFESQQRVAKFLIAPEKRLEAKKLQLSAPEEG AKAKDEEGKFGKEEAKQQEAAPSKPGTPVVDKSKKEKDRQAVGKAGLLGAFKGMKGGASDVFGPGGFGTG INDALGGLKGGAAMGDAQGVGGVGSRGTGKGGGGTALGIGGLGTQGTGRGTGGSGGIDLGGRGKSITKVIP GKTTVVGGLDKDVIAKVIRRHQGEIKYCYESELNKDPSLAGKVAVSFVIDPAGAVSDASVSETTLNNAAAERC MLSRIRRWKFPEPKGGGVVSVTYPWLFAPAGAGG
NfsH	VKKSQLIAALALLSSPVLAATPPEGVAF**EPRRGFFTETDIGVF**FTVGGENVYSNAQTYLQLGVGYDLTEKLSLG AHFGLGSSAQNCFAGYLPGTETCALSDNFTMAFFNLSAAYHVRVMDRLFLTPKVVAGYTRL**DPAPVDPDEGD PGRAV**NAPNAGLGFGVEYATGMDHFSVGADLLARYIIGPNITSFAIFPKVKYTF

A.3 Micro array data analysis results

Table A-15 List of regulated genes with annotation (TIGR) and GO main role (TIGR) sorted by *Mxan_*-numbers. Criteria: Regulation is significant based on SAM analysis (FDR 5%); data present for all time points; threshold: log-ratio 532/632 nm ≥ 1 (= 2-fold up- or down-regulated) in at least one time point. Most genes mentioned in the text are bolded.

Mxan-no.	Log ratio				Gene name	Annotation	GO mainrole
	0.5 h	1 h	2 h	4 h			
Mxan_0008	0.411	0.361	2.268	0.515		hypothetical protein	
Mxan_0009	-0.726	-1.07	-1.013	-0.452		major facilitator family transporter	Transport and binding
Mxan_0012	0.353	0.531	3.657	1.062		DoxD-like family protein	Unknown function
Mxan_0021	1.774	1.459	0.673	-0.301		hypothetical protein	
Mxan_0022	2.691	2.673	2.024	0.351		lipoprotein, putative	
Mxan_0034	1.625	1.854	0.871	0.552		hydrolase, haloacid dehalogenase-like family	Unknown function
Mxan_0035	3.586	4.216	3.199	1.159		ABC transporter, substrate-binding protein, aliphatic sulfonates family	Transport and binding
Mxan_0036	2.2	3.114	5.008	0.966		aliphatic sulfonates ABC transporter, permease protein, putative	Transport and binding
Mxan_0037	1.591	2.732	4.184	1.213		aliphatic sulfonates ABC transporter, ATP-binding protein, putative	Transport and binding
Mxan_0039	-0.452	-0.211	-1.084	-0.782		hypothetical protein	
Mxan_0040	1.114	1.423	1.479	-0.088		glucose 1-dehydrogenase, putative	Energy metabolism
Mxan_0041	3.16	4.161	3.01	0.414		glycosyl hydrolase, family 15	Energy metabolism
Mxan_0042	0.654	1.31	0.94	0.224		hypothetical protein	
Mxan_0046	-0.315	-0.607	-1.307	-0.696		hypothetical protein	
Mxan_0047	-0.635	-0.882	-1.227	-0.741		hypothetical protein	
Mxan_0048	-0.526	-0.743	-1.01	-0.603		hypothetical protein	
Mxan_0049	-0.81	-1.034	-1.22	-0.759		hypothetical protein	
Mxan_0052	1.246	0.818	0.341	0.556		conserved hypothetical protein	Hypothetical proteins
Mxan_0054	2.442	3.122	2.686	0.892		hypothetical protein	
Mxan_0056	3.201	2.643	1.476	0.348	*ppk*	polyphosphate kinase	Central intermediary
Mxan_0059	2.927	3.893	3.36	0.719		putative lipoprotein	Cell envelope
Mxan_0061	0.296	0.954	1.183	0.315		metallo-beta-lactamase family protein	
Mxan_0062	2.034	1.691	1.449	0.646		conserved hypothetical protein	Hypothetical proteins
Mxan_0064	0.933	1.367	1.323	0.748		conserved hypothetical protein, UPF0027 family	Hypothetical proteins
Mxan_0065	5.14	5.951	5.512	1.98		hypothetical protein	
Mxan_0068	0.772	0.759	1.082	-0.188		DNA-binding regulatory protein, putative	Regulatory functions
Mxan_0089	-0.539	-0.729	-1.093	-0.313		glutathione S-transferase domain protein	Unknown function
Mxan_0093	-0.878	-1.452	-1.829	-0.843		conserved hypothetical protein	Hypothetical proteins
Mxan_0094	-0.789	-1.295	-1.69	-0.699		amidohydrolase family protein	Unknown function
Mxan_0105	1.736	1.258	1.511	1.321		drug resistance transporter, EmrB/QacA family	Transport and binding
Mxan_0109	3.624	3.888	3.095	0.42		hypothetical protein	
Mxan_0110	3.148	3.421	0.941	-0.179	*cls*	cardiolipin synthase	Fatty acid and
Mxan_0120	1.706	1.532	1.029	0.591		hypothetical protein	
Mxan_0133	-0.418	-0.963	-1.715	-1.166		hypothetical protein	
Mxan_0141	-0.563	-1.06	-1.062	-0.56		SWIM zinc finger domain protein	Unknown function
Mxan_0144	-0.759	-1.089	-0.803	-0.511		hypothetical protein	
Mxan_0147	0.591	0.675	1.367	1.076		acetyltransferase, putative	Unknown function
Mxan_0149	0.238	0.619	3.767	0.649		Ser/Thr protein phosphatase family protein	
Mxan_0171	0.635	0.908	1.928	1.532		cation-binding protein, hemerythrin HHE family	Transport and binding
Mxan_0187	2.334	2.366	2.227	-0.15		fibril protein, degenerate	Disrupted reading
Mxan_0192	0.529	1.336	2.046	0.139		hypothetical protein	
Mxan_0197	0.728	1.057	0.676	0.32		sensor histidine kinase	Regulatory functions
Mxan_0201	-0.724	-1.233	-1.171	-0.876		hydrolase, alpha/beta fold family	Unknown function
Mxan_0206	0.616	1.05	0.901	0.349		peptidase, S8A (subtilisin) subfamily	Protein fate
Mxan_0207	0.327	1.033	0.62	-0.111		hypothetical protein	
Mxan_0210	0.711	1.075	0.204	0.178		transglycosylase SLT domain protein	
Mxan_0217	-0.418	-1.183	-1.558	-0.825		lipoprotein, putative	Cell envelope
Mxan_0234	0.567	0.843	1.044	0.495		actD protein, degenerate	Regulatory functions
Mxan_0237	1.549	1.568	0.564	-0.241		hypothetical protein	
Mxan_0239	0.941	1.007	2.292	0.667		conserved hypothetical protein	Hypothetical proteins
Mxan_0241	0.575	1.228	2.738	0.57		hypothetical protein	
Mxan_0248	1.32	1.339	0.778	0.196		hypothetical protein	
Mxan_0250	1.034	1.264	0.944	0.124		ABC transporter, ATP-binding protein	Transport and binding
Mxan_0258	0.733	0.73	1.084	0.363		ATPase domain protein	
Mxan_0259	0.488	1.332	0.858	0.065		response regulator	Regulatory functions
Mxan_0278	0.737	1.138	1.178	0.154		mercuric reductase, truncation	Cellular processes
Mxan_0279	3.027	2.718	2.011	1.51		putative ribosome-binding factor A	Transcription
Mxan_0280	2.047	1.857	1.759	1.475		conserved hypothetical protein	Hypothetical proteins
Mxan_0287	0.611	0.961	1.801	0.318		hypothetical protein	
Mxan_0293	0.779	0.082	1.233	0.17		conserved hypothetical protein	Hypothetical proteins
Mxan_0317	-1.421	-2.283	-1.615	-0.601		fatty acid desaturase family protein	Fatty acid and
Mxan_0330	0.709	1.348	1.147	0.108		hypothetical protein	
Mxan_0334	0.588	0.519	1.324	1.048		conserved domain protein	Hypothetical proteins
Mxan_0341	-0.538	-0.862	-1.119	-0.265	*kup*	potassium uptake protein	Transport and binding
Mxan_0347	1.774	2.315	1.151	0.199		sensory box histidine kinase	Regulatory functions

Mxan-no.	Log ratio				Gene name	Annotation	GO mainrole
	0.5 h	1 h	2 h	4 h			
Mxan_0348	4.2	5.002	3.536	0.601		hypothetical protein	
Mxan_0359	-0.864	-1.918	-2.363	-0.933		type 4 pilus biogenesis operon protein	
Mxan_0360	-0.826	-1.86	-2.345	-0.954		type 4 pilus biogenesis operon protein	
Mxan_0361	-0.818	-1.909	-2.189	-0.762		type 4 pilus biogenesis operon protein	
Mxan_0362	-1.575	-1.646	-1.876	-0.515		putative pilus biogenesis operon protein	Cell envelope
Mxan_0363	-1.533	-1.534	-1.87	-0.508		hypothetical protein	
Mxan_0364	-0.924	-1.077	-1.598	-0.236		hypothetical protein	
Mxan_0367	0.488	1.639	0.652	0.343		hypothetical protein	
Mxan_0372	5.318	5.875	4.717	0.985		lipoprotein, putative	Cell envelope
Mxan_0373	4.166	4.526	3.646	0.282		hypothetical protein	
Mxan_0380	1.411	1.858	1.547	2.214		hypothetical protein	
Mxan_0383	0.175	1.125	0.355	0.115		hypothetical protein	
Mxan_0390	1.888	2.191	2.08	0.549		regulator of ribonuclease activity A, putative	Transcription
Mxan_0391	2.155	2.372	1.805	0.393		oxidoreductase, aldo/keto reductase family	Unknown function
Mxan_0402	**-1.405**	**-1.365**	**-0.698**	**0.205**	***atpB***	**ATP synthase F0, A subunit**	**Energy metabolism**
Mxan_0403	**-1.152**	**-1.894**	**-1.215**	**-0.039**	***atpE***	**ATP synthase F0, C subunit**	**Energy metabolism**
Mxan_0404	**-1.233**	**-1.547**	**-0.994**	**-0.017**	***atpF***	**ATP synthase F0, B subunit**	**Energy metabolism**
Mxan_0405	-1.265	-1.295	-0.887	0.027	*ychF*	GTP-binding protein YchF	Unknown function
Mxan_0412	-0.813	-1.194	-1.364	-0.64		conserved hypothetical protein TIGR00266	Hypothetical proteins
Mxan_0414	1.517	0.567	0.62	0.18		Ser/Thr protein phosphatase family protein	Unknown function
Mxan_0415	-1.075	-1.733	-1.81	-0.857	*pilT*	twitching mobility protein	Cell envelope
Mxan_0416	-0.285	-0.722	-1.167	-0.261		conserved domain protein	Hypothetical proteins
Mxan_0419	1.933	2.483	1.046	0.044		conserved hypothetical protein	Hypothetical proteins
Mxan_0423	1.37	1.888	1.54	1.824		SPFH domain/band 7 family domain protein	Unknown function
Mxan_0430	2.16	3.663	3.471	0.142		hypothetical protein	
Mxan_0431	0.956	2.101	2.56	-0.028		lipoprotein, putative	Cell envelope
Mxan_0432	1.401	1.959	3.194	0.887		metallo-beta-lactamase family protein	Unknown function
Mxan_0433	1.328	0.913	0.585	-0.047		hypothetical protein	
Mxan_0434	3.609	3.627	3.372	0.293	*glgX*	glycogen debranching enzyme GlgX	Energy metabolism
Mxan_0435	0.914	0.997	1.747	-0.232		hypothetical protein	
Mxan_0436	1.651	2.399	3.58	1.681		hypothetical protein	
Mxan_0439	1.129	1.329	3.439	0.401		Erp domain protein	Unknown function
Mxan_0440	-0.028	0.203	1.508	-0.331		membrane protein, putative	Cell envelope
Mxan_0443	1.703	2.211	3.212	1.465		hypothetical protein	
Mxan_0451	-1.068	-1.317	-0.897	-0.456		PAP2 family protein	Unknown function
Mxan_0452	-1.046	-1.371	-0.964	-0.121		myo-inositol-1-phosphate synthase, putative	Energy metabolism
Mxan_0453	0.331	0.598	2.855	0.426		general stress protein 26, putative	Cellular processes
Mxan_0457	-1.822	-1.89	-0.497	-0.456		sigma 54 modulation protein, putative	Transcription
Mxan_0466	3.332	4.154	2.569	0.392		hypothetical protein	
Mxan_0471	0.635	0.901	4.65	2.272		hypothetical protein	
Mxan_0472	0.211	0.518	2.52	0.377		GIY-YIG catalytic domain protein	Unknown function
Mxan_0473	-0.008	0.278	1.794	0.16		conserved domain protein	Hypothetical proteins
Mxan_0480	0.256	1.172	1.042	0.046	*gloA*	lactoylglutathione lyase	Energy metabolism
Mxan_0502	1.201	0.97	0.741	0.133		transcriptional regulator, AsnC family	Regulatory functions
Mxan_0522	-1.537	-2.3	-2.129	-0.078		lipoprotein, putative	Cell envelope
Mxan_0524	4.91	4.477	2.975	1.025		response regulator	Regulatory functions
Mxan_0525	0.627	1.044	1.294	0.996		serine/threonine protein kinase, putative	
Mxan_0526	4.99	5.439	3.985	1.397		hypothetical protein	
Mxan_0527	2.859	2.82	3.912	0.743		efflux transporter, RND family, MFP subunit	Transport and binding
Mxan_0528	2.173	2.969	3.741	0.462		efflux transporter, AcrB/AcrD/AcrF family, inner membrane component	Transport and binding
Mxan_0529	1.458	2.12	1.96	0.354		4-alpha-glucanotransferase	Energy metabolism
Mxan_0531	-0.188	-0.634	-1.036	-0.591		aminotransferase, class I	
Mxan_0538	-0.769	-1.007	-0.58	0.569		lipoprotein, putative	Cell envelope
Mxan_0539	0.323	0.89	2.647	0.488		hypothetical protein	
Mxan_0541	0.684	1.749	1.082	-0.084	*treZ*	malto-oligosyltrehalose trehalohydrolase	Energy metabolism
Mxan_0542	0.4	1.267	1.253	0.64		F5/8 type C domain protein	
Mxan_0543	-1.196	-0.488	0.073	-0.16		peptidase, M20 (glutamate carboxypeptidase) family	Protein fate
Mxan_0545	-1.516	-1.081	-0.476	-0.191		hypothetical protein	
Mxan_0572	-0.857	-1.024	-0.898	-0.549		hypothetical protein	
Mxan_0575	-1.151	-1.579	-1.38	-0.372		arsenate reductase, putative	Cellular processes
Mxan_0581	-0.457	-0.312	-1.067	-1.11	*infC*	translation initiation factor IF-3	Protein synthesis
Mxan_0582	-0.48	-0.855	-1.025	-0.376		conserved hypothetical protein	Hypothetical proteins
Mxan_0585	-0.559	-1.525	-1.287	-0.878		conserved hypothetical protein	Hypothetical proteins
Mxan_0598	0.511	1.357	1.124	0.269		hypothetical protein	
Mxan_0605	-0.905	-0.941	-1.071	-0.974		hypothetical protein	
Mxan_0607	1.157	1.228	1.28	0.258		aldehyde dehydrogenase family protein	Energy metabolism
Mxan_0609	0.522	1.049	1.08	-0.246		PAP2 family protein	Unknown function
Mxan_0610	0.109	0.861	1.01	0.26		histone deacetylase family protein	
Mxan_0613	1.253	1.456	1.256	0.223		alkaline ceramidase	Fatty acid and
Mxan_0614	0.631	1.858	1.42	0.283		serine/threonine protein kinase	Regulatory functions
Mxan_0616	0.816	1.127	0.337	-0.231		carbohydrate kinase, thermoresistant glucokinase family	Energy metabolism
Mxan_0617	1.041	0.859	0.452	-0.25		carbonic anhydrase, putative	Central intermediary
Mxan_0640	0.64	1.426	1.715	0.379		conserved hypothetical protein	Hypothetical proteins
Mxan_0641	3.757	3.444	3.578	0.454		TspO/MBR family protein	Unknown function
Mxan_0642	0.815	1.502	1.333	0.179		hypothetical protein	

Mxan-no.	Log ratio				Gene name	Annotation	GO mainrole
	0.5 h	1 h	2 h	4 h			
Mxan_0644	0.217	1.047	1.007	-0.013		peptidase, M1 (aminopeptidase N) family	
Mxan_0646	3.214	2.687	2.159	0.757		endonuclease/exonuclease/phosphatase family protein	Unknown function
Mxan_0658	-1.252	-1.123	-1.013	-0.836		hypothetical protein	
Mxan_0659	-0.922	-0.911	-1.002	-0.767		lipoprotein, putative	Cell envelope
Mxan_0660	0.674	1.364	1.05	0.332		lipoprotein, putative	Cell envelope
Mxan_0661	0.897	1.603	1.218	0.305		rhomboid family protein	Unknown function
Mxan_0662	-0.624	-1.149	-1.374	-0.892		hypothetical protein	
Mxan_0663	-0.702	-0.664	-1.069	-0.328	*rnz*	ribonuclease Z	Transcription
Mxan_0670	-2.027	-2.039	-1.17	-0.662		hypothetical protein	
Mxan_0672	-0.855	-1.224	-2.195	-1.573	*cspC*	cold-shock protein CspC	Cellular processes
Mxan_0674	0.279	0.286	2.034	0.171		conserved hypothetical protein	Hypothetical proteins
Mxan_0682	-1.924	-1.106	-0.653	-0.443		conserved hypothetical protein	Hypothetical proteins
Mxan_0683	-1.215	-0.587	-0.55	-0.517		cytochrome P450 family protein	Central intermediary
Mxan_0687	-1.722	-1.702	-1.67	-0.424		ferric siderophore ABC transporter, periplasmic ferric siderophore-binding	Transport and binding
Mxan_0689	1.02	1.141	1.37	1.058		conserved hypothetical protein	Hypothetical proteins
Mxan_0690	2.213	4.235	4.285	1.419		lipoprotein, putative	Cell envelope
Mxan_0692	1.054	2.865	2.766	0.697		hypothetical protein	
Mxan_0693	0.822	0.653	1.164	0.137		hypothetical protein	
Mxan_0695	0.578	1.381	1.135	0.199		radical SAM domain protein	Unknown function
Mxan_0713	0.987	1.042	0.929	0.647		methyltransferase, CheR family	
Mxan_0716	0.643	1.116	1.483	0.639		hypothetical protein	
Mxan_0717	0.61	0.885	1.341	0.353		hypothetical protein	
Mxan_0721	1.314	1.636	0.901	0.109		heme ABC transporter, ATP-binding protein	Cellular processes
Mxan_0722	1.198	1.35	0.594	0.255		membrane protein, putative	Cell envelope
Mxan_0724	1.179	1.838	2.087	0.522		serine/threonine protein kinase, putative	
Mxan_0725	0.628	0.752	1.25	0.24		ABC1 domain protein	Unknown function
Mxan_0744	0.117	0.074	1.134	-0.124		hypothetical protein	
Mxan_0754	-0.899	-1.031	-1.048	-0.433		hypothetical protein	
Mxan_0762	-1.456	-1.037	-1.234	-0.669		conserved hypothetical protein	Hypothetical proteins
Mxan_0763	-0.994	-1.028	-1.267	-0.568		response regulator	Regulatory functions
Mxan_0766	0.464	1.064	1.23	0.259	*gyrA*	DNA gyrase, A subunit	DNA metabolism
Mxan_0776	0.981	1.023	0.254	0.348		von Willebrand factor type A domain protein	Unknown function
Mxan_0777	0.525	0.745	1.042	0.485		transcriptional regulator, MerR family	Regulatory functions
Mxan_0779	0.234	0.427	1.517	0.178		SPFH/band 7 domain protein	Unknown function
Mxan_0781	0.419	0.458	3.367	0.679		glycosyl transferase, group 1 family protein	Cell envelope
Mxan_0782	0.102	0.16	1.45	0.521		conserved hypothetical protein FRAMESHIFT	
Mxan_0792	-0.538	-1.138	-1.111	-0.819		peptidase, M16 (pitrilysin) family	
Mxan_0794	0.02	0.148	1.817	0.343		conserved hypothetical protein	Hypothetical proteins
Mxan_0795	0.572	1.054	1.886	0.687		conserved domain protein	Hypothetical proteins
Mxan_0798	0.842	1.796	1.519	0.359		hypothetical protein	
Mxan_0800	-0.066	0.351	2.154	0.061		hypothetical protein	
Mxan_0802	0.404	0.564	1.466	1.237		hypothetical protein	
Mxan_0807	0.646	2.213	3.57	0.557		conserved hypothetical protein	Hypothetical proteins
Mxan_0808	0.572	1.223	2.433	0.24		hypothetical protein	
Mxan_0809	0.791	1.129	0.6	0.446		hypothetical protein	
Mxan_0814	2.022	2.383	0.796	0.1		conserved domain protein	Hypothetical proteins
Mxan_0825	-0.913	-1.041	-1.289	-0.818		conserved hypothetical protein	Hypothetical proteins
Mxan_0850	0.412	1.086	1.021	0.333		oxidoreductase, molybdopterin-binding	
Mxan_0853	-1.606	-2.534	-2.211	-1.492		3-oxoacyl-(acyl-carrier-protein) synthase, putative	Fatty acid and
Mxan_0854	2.858	2.41	2.057	-0.241		conserved hypothetical protein	Hypothetical proteins
Mxan_0860	-0.066	0.37	1.069	0.34		conserved hypothetical protein	Hypothetical proteins
Mxan_0861	1.961	1.968	1.376	0.302		CHAD domain protein	Unknown function
Mxan_0862	3.908	3.479	2.744	1.234	*ppa*	inorganic pyrophosphatase	Central intermediary
Mxan_0866	4.114	4.961	5.547	2.028		Dps family protein	Cellular processes
Mxan_0873	-1.536	-1.64	-1.446	-0.68		adenylate/guanylate cyclase domain protein	
Mxan_0879	0.006	0.171	1.102	-0.45		conserved hypothetical protein	Hypothetical proteins
Mxan_0882	1.502	1.781	0.109	-0.022		serine/threonine protein kinase	Regulatory functions
Mxan_0885	0.761	0.483	0.939	1.062		conserved hypothetical protein	Hypothetical proteins
Mxan_0887	4.303	4.098	3.259	0.723		transcriptional regulator, TetR family	Regulatory functions
Mxan_0892	1.297	1.593	1.388	0.617		NAD dependent epimerase/dehydratase family	Energy metabolism
Mxan_0893	0.985	1.371	1.233	0.415		hypothetical protein	
Mxan_0907	-0.08	0.154	1.368	0.602		sigma-54 dependent transcriptional regulator, Fis family	Regulatory functions
Mxan_0909	0.498	0.817	1.058	-0.037		hypothetical protein	
Mxan_0912	1.312	1.723	2.393	-0.155	*glnA*	glutamate--ammonia ligase	Amino acid
Mxan_0922	1.439	1.371	0.486	0.467		lipoprotein, putative	Cell envelope
Mxan_0924	-0.913	-0.993	-1.128	-0.471		hypothetical protein	
Mxan_0927	1.028	1.873	3.765	1.122		cysteine dioxygenase, type I	Energy metabolism
Mxan_0929	0.609	1.849	1.275	0.175		hypothetical protein	
Mxan_0939	0.849	0.232	0.885	1.121		conserved hypothetical protein	Hypothetical proteins
Mxan_0944	0.563	0.784	2.32	2.817		hypothetical protein	
Mxan_0958	0.418	0.502	0.512	1.09	*sbcD*	nuclease SbcCD, D subunit, FRAMESHIFT	DNA metabolism
Mxan_0962	-1.379	-1.702	-1.618	-1.074		lipoprotein, putative	Cell envelope
Mxan_0977	-2.329	-2.399	-1.381	0.031		di-haem cytochrome-c peroxidase	Energy metabolism
Mxan_0980	0.462	-0.036	2.601	0.335		cytochrome c family protein	
Mxan_0986	-1.099	-0.941	-0.39	-0.504		hypothetical protein	
Mxan_0994	4.282	4.148	2.788	1.438		hypothetical protein	

Mxan-no.	Log ratio				Gene name	Annotation	GO mainrole
	0.5 h	1 h	2 h	4 h			
Mxan_0998	0.496	2.069	1.463	-0.022		peptidase, S8A (subtilisin) subfamily	
Mxan_0999	0.684	1.678	1.987	1.127		hypothetical protein	
Mxan_1001	-1.202	-1.318	-1.389	-0.27		hypothetical protein	
Mxan_1002	-0.28	-0.613	-1.092	-0.33		lipoprotein, putative	Cell envelope
Mxan_1003	-0.843	-1.234	-1.504	-0.475		Tat (twin-arginine translocation) pathway signal sequence domain protein	Unknown function
Mxan_1007	2.299	3.31	4.131	1.081		conserved hypothetical protein	Hypothetical proteins
Mxan_1008	1.672	2.73	4.368	1.125		hypothetical protein	
Mxan_1011	0.11	0.986	1.379	-0.376		hypothetical protein	
Mxan_1038	0.748	1.834	1.854	0.299		hypothetical protein	
Mxan_1039	0.103	0.084	1.29	0.161	*glkA*	glucokinase	Energy metabolism
Mxan_1048	-1.73	-1.766	-1.5	-0.497		UDP-glucose 6-dehydrogenase	
Mxan_1053	0.705	0.676	2.756	0.703		conserved hypothetical protein	Hypothetical proteins
Mxan_1056	0.301	0.891	1.126	0.548	*astB*	succinylarginine dihydrolase	Energy metabolism
Mxan_1061	3.347	2.971	1.181	-0.152	*rpoN*	RNA polymerase sigma-54 factor	Transcription
Mxan_1062	1.577	1.175	0.169	-0.122		acetyltransferase, GNAT family	
Mxan_1065	0.53	1.411	2.379	1.741	*yfiA*	ribosomal subunit interface protein	Protein synthesis
Mxan_1070	0.924	1.778	1.342	0.105	*dacB*	D-alanyl-D-alanine carboxypeptidase/D-alanyl-D-alanine-endopeptidase	Cell envelope
Mxan_1080	**-1.214**	**-2.105**	**-1.527**	**-0.344**		**NADH dehydrogenase I, N subunit**	**Energy metabolism**
Mxan_1081	**-1.169**	**-1.829**	**-1.32**	**-0.162**		**NADH dehydrogenase I, M subunit**	**Energy metabolism**
Mxan_1082	**-1.124**	**-1.746**	**-1.398**	**-0.194**		**NADH dehydrogenase I, L subunit**	**Energy metabolism**
Mxan_1083	**-1.356**	**-1.718**	**-1.33**	**-0.092**		**NADH dehydrogenase I, K subunit**	**Energy metabolism**
Mxan_1084	**-1.372**	**-1.715**	**-1.267**	**-0.163**		**NADH dehydrogenase I, J subunit**	**Energy metabolism**
Mxan_1085	**-1.359**	**-1.703**	**-1.163**	**-0.012**		**NADH dehydrogenase I, F subunit**	**Energy metabolism**
Mxan_1086	**-1.054**	**-1.364**	**-1.21**	**-0.045**		**NADH dehydrogenase I, E subunit**	**Energy metabolism**
Mxan_1089	-1.01	-0.809	-0.68	-0.335	*serB*	ACT domain protein/phosphoserine phosphatase SerB	Amino acid
Mxan_1091	0.234	0.573	1.245	0.718		conserved hypothetical protein	Hypothetical proteins
Mxan_1092	2.259	1.776	2.104	0.714		heat shock protein, HSP20 family.	Protein fate
Mxan_1095	-0.77	-1.033	-0.745	-0.031	*kdsA*	3-deoxy-8-phosphooctulonate synthase	Cell envelope
Mxan_1101	**6.964**	**6.732**	**5.121**	**2.009**		**UDP-N-acetylglucosamine 2-epimerase**	**Cell envelope**
Mxan_1102	2.627	2.273	1.118	0.091		RNA pseudouridine synthase family protein	Protein synthesis
Mxan_1103	0.05	0.423	1.219	0.514	*purF*	amidophosphoribosyltransferase	Purines, pyrimidines,
Mxan_1110	-1.153	-0.911	-0.704	-0.467		biotin/lipoic acid binding domain protein	Unknown function
Mxan_1112	0.532	0.577	1.88	0.864		hypothetical protein	
Mxan_1113	-1.134	-0.489	-0.603	-0.731	*pccB*	propionyl-CoA carboxylase, beta subunit	Energy metabolism
Mxan_1115	0.936	0.711	2.842	1.257		SREBP protease/CBS domain	Unknown function
Mxan_1117	-0.37	-0.457	-1.063	-0.766		lipoprotein, putative	Cell envelope
Mxan_1125	1.279	1.104	0.232	0.458		hypothetical protein	
Mxan_1126	3.223	3.411	3.383	0.13		hypothetical protein	
Mxan_1132	1.229	1.58	5.496	2.897		hypothetical protein	
Mxan_1136	-1.086	-1.139	-0.99	-0.786		conserved hypothetical protein	Hypothetical proteins
Mxan_1140	0.669	1.581	1.257	0.396		lipoprotein, putative	Cell envelope
Mxan_1146	0.589	1.283	1.167	0.623		conserved hypothetical protein	Hypothetical proteins
Mxan_1147	0.162	1.023	0.708	0.363		hypothetical protein	
Mxan_1148	0.333	1.175	1.027	0.429		hypothetical protein	
Mxan_1159	0.01	0.152	2.905	0.139		peptidase, C56 (PfpI) family	Protein fate
Mxan_1179	0	0.618	1.294	0.429		conserved hypothetical protein	Hypothetical proteins
Mxan_1182	-1.198	-1.211	-0.769	-0.694		conserved hypothetical protein	Hypothetical proteins
Mxan_1186	-0.509	-0.694	-1.25	-0.99		lipoprotein, putative	Cell envelope
Mxan_1188	0.91	1.051	0.313	0.2		hypothetical protein	
Mxan_1192	2.445	2.298	1.254	-0.194	*otsAB*	alpha,alpha-trehalose-phosphate synthase/trehalose-phosphatase	Cellular processes
Mxan_1197	-0.878	-1.02	-0.661	-0.601		peptidase, M1 (aminopeptidase N) family	Protein fate
Mxan_1223	0.693	1.053	0.713	0.765		phage tail assembly chaperone	Mobile and
Mxan_1234	-1.167	-0.963	-0.477	-0.141		serine/threonine kinase family protein	Protein fate
Mxan_1238	1.323	1.753	0.831	0.747		conserved hypothetical protein	Hypothetical proteins
Mxan_1247	0.739	0.413	1.262	0.358		conserved hypothetical protein	Hypothetical proteins
Mxan_1250	2.901	2.416	0.455	-0.14		RibD domain protein	Unknown function
Mxan_1253	0.055	0.25	0.334	1.061		chitinase, degenerate	Cell envelope
Mxan_1254	-0.024	1.059	0.366	0.164		hypothetical protein	
Mxan_1262	-0.565	-1.069	-1.221	-0.084		receptor family ligand-binding protein	
Mxan_1265	2.633	3.381	1.605	0.349		transporter, putative	Transport and binding
Mxan_1276	0.505	0.793	1.293	0.343		glutamate-cysteine ligase	Biosynthesis of
Mxan_1279	1.071	1.387	1.213	0.648		response regulator	Regulatory functions
Mxan_1280	0.819	1.388	1.403	0.342		histidine kinase family protein	
Mxan_1282	-0.622	-0.984	-1.094	-0.219		3-isopropylmalate dehydratase, large subunit, putative	Amino acid
Mxan_1284	-1.619	-1.336	-1.248	-0.197		2-isopropylmalate synthase/homocitrate synthase family protein	Unknown function
Mxan_1285	-2.576	-2.367	-2.03	-0.416		tryptophan halogenase	Cellular processes
Mxan_1286	-1.728	-2.828	-2.622	-0.91	*abcA*	ABC transporter, ATP-binding/permease protein	Transport and binding
Mxan_1287	-0.706	-0.995	-1.219	-0.215		conserved domain protein	Hypothetical proteins
Mxan_1288	-0.809	-1.666	-1.664	-0.619		carbamoyltransferase family protein	
Mxan_1289	-0.542	-1.483	-1.345	-0.777		phytanoyl-CoA dioxygenase	Energy metabolism
Mxan_1290	-0.675	-1.157	-1.015	-0.589		phosphotransferase	
Mxan_1291	-1.072	-1.019	-1.076	-0.233		non-ribosomal peptide synthetase	Cellular processes
Mxan_1292	-0.997	-1.068	-1.077	-0.267		hypothetical protein	
Mxan_1299	-0.992	-1.092	-1.287	-0.384		hypothetical protein	
Mxan_1311	2.209	2.042	0.652	-0.138	*aat*	leucyl/phenylalanyl-tRNA--protein transferase	Protein fate
Mxan_1314	-1.256	-1.11	-1.191	-0.46		hypothetical protein	

Mxan-no.	Log ratio				Gene name	Annotation	GO mainrole
	0.5 h	1 h	2 h	4 h			
Mxan_1316	-1.268	-1.263	-1.407	-0.298		tonB dependent receptor, putative	Transport and binding
Mxan_1317	-1.593	-1.807	-1.47	-0.275		lipoprotein, putative	Cell envelope
Mxan_1318	-1.506	-1.828	-1.53	-0.294	*hemS*	hemin transport protein HemS	Transport and binding
Mxan_1320	-0.425	-1.216	-1.042	-0.517	*hemU*	hemin ABC transporter, permease protein	Transport and binding
Mxan_1326	-0.272	-0.935	-1.043	-0.51		lipoprotein, putative	Cell envelope
Mxan_1328	-0.934	-1.58	-1.205	-0.424		conserved hypothetical protein	Hypothetical proteins
Mxan_1329	-0.704	-1.094	-0.826	-0.316		conserved hypothetical protein	Hypothetical proteins
Mxan_1334	-1.058	-1.454	-1.155	-0.108		thrombospondin type 3 repeat family protein	Unknown function
Mxan_1337	-0.379	-0.685	-1.156	-0.377		lipoprotein, putative	Cell envelope
Mxan_1338	-1.193	-1.682	-1.048	-0.484		lipoprotein, putative	Cell envelope
Mxan_1342	-0.911	-1.075	-0.713	-0.484		lipoprotein, putative	Cell envelope
Mxan_1344	0.221	1.508	1.642	-0.193		conserved hypothetical protein	Hypothetical proteins
Mxan_1347	0.844	3.787	6.544	2.447		hypothetical protein	
Mxan_1359	-0.787	-1.22	-1.382	-0.379		conserved hypothetical protein	Hypothetical proteins
Mxan_1360	-1.558	-2.193	-2.074	-0.655		conserved hypothetical protein	Hypothetical proteins
Mxan_1361	-1.032	-1.014	-1.158	-0.496		FHA domain protein	
Mxan_1364	-0.56	-1.283	-0.819	-0.441		conserved hypothetical protein	Hypothetical proteins
Mxan_1365	-0.835	-1.025	-0.431	-0.221		hypothetical protein	
Mxan_1366	-1.13	-1.301	-0.59	-0.303		hypothetical protein	
Mxan_1367	-1.119	-1.133	-0.491	-0.06		prepilin-type N-terminal cleavage/methylation domain protein	Cell envelope
Mxan_1368	-0.719	-1.156	-0.74	-0.365		putative prepilin-type N-terminal cleavage/methylation domain protein	Cell envelope
Mxan_1369	-0.885	-1.138	-0.4	-0.206		prepilin-type N-terminal cleavage/methylation domain protein	Cell envelope
Mxan_1482	-0.046	-0.232	-1.03	-0.193		polysaccharide deacetylase domain protein	Unknown function
Mxan_1485	0.841	1.398	0.653	0.971		cytochrome c, putative	Energy metabolism
Mxan_1486	2.685	2.512	2.013	3.017		HNH endonuclease domain protein	
Mxan_1500	1.108	1.857	1.818	1.486		hypothetical protein	
Mxan_1503	3.767	3.834	2.994	0.437	*nfi*	endonuclease V	DNA metabolism
Mxan_1504	1.116	0.87	0.363	-0.06		oxidoreductase, GMC family	Unknown function
Mxan_1508	1.383	1.964	0.831	1.305		hypothetical protein	
Mxan_1509	1.836	1.907	1.954	3.058		Ser/Thr protein phosphatase family protein	
Mxan_1521	0.907	1.155	0.625	0.903		conserved hypothetical protein	Hypothetical proteins
Mxan_1523	1.534	1.857	0.74	-0.052		acetyltransferase, GNAT family	
Mxan_1524	2.776	2.858	1.127	-0.107	*glgC*	glucose-1-phosphate adenylyltransferase	Energy metabolism
Mxan_1527	-0.68	-1.338	-0.918	-0.156		NAD dependent epimerase/dehydratase family protein	Energy metabolism
Mxan_1528	-0.783	-1.205	-1.006	-0.229		long-chain-fatty-acid CoA ligase, putative	Fatty acid and
Mxan_1529	-1.076	-1.35	-0.863	-0.181		hypothetical protein	
Mxan_1530	-0.905	-1.226	-0.871	0.105		HAD-superfamily subfamily IB hydrolase, TIGR01490	Unknown function
Mxan_1533	3.51	3.69	2.724	1.326	*treY*	maltooligosyltrehalose synthase	Energy metabolism
Mxan_1534	1.248	1.473	0.422	-0.201	*glgX*	glycogen debranching enzyme GlgX	Energy metabolism
Mxan_1535	-0.538	-0.408	-1.057	-0.506		membrane protein, TerC family	Cell envelope
Mxan_1539	-1.151	-1.269	-1.375	-0.555		lipoprotein, putative	Cell envelope
Mxan_1546	0.822	0.824	1.341	-0.06		conserved hypothetical protein	Hypothetical proteins
Mxan_1552	1.154	1.784	1.722	0.354		response regulator	
Mxan_1553	0.716	1.385	1.367	0.331		sensory box histidine kinase	Regulatory functions
Mxan_1554	0.605	1.272	4.396	1.375		iron-sulfur cluster-binding protein, Rieske family	Energy metabolism
Mxan_1555	0.534	1.533	3.19	0.234		cation-binding protein, hemerythrin HHE family	Transport and binding
Mxan_1556	0.131	0.503	2.023	-0.222		DNA-3-methyladenine glycosylase, putative	DNA metabolism
Mxan_1560	-0.611	-0.817	-1.1	-0.509		aminotransferase, class I	Unknown function
Mxan_1561	1.035	0.935	1.113	0.84		lipoprotein, putative	Cell envelope
Mxan_1562	1.166	0.861	1.094	0.895		Dps family protein	Cellular processes
Mxan_1570	1.427	1.6	1.306	0.351		aminotransferase, class V	Unknown function
Mxan_1577	-2.327	-3.749	-4.007	-4.08		serine/threonine protein kinase	Regulatory functions
Mxan_1578	-3.524	-5.416	-5.933	-6.892		metallo-beta-lactamase family protein	Unknown function
Mxan_1581	3.927	4.148	3.75	0.487		membrane protein, putative	
Mxan_1582	-0.486	-0.852	-1.194	-0.728		hypothetical protein	
Mxan_1591	-1.414	-0.557	0.134	-1.05		hypothetical protein	
Mxan_1597	-1.086	-1.049	-0.674	-0.541		ABC transporter, ATP-binding protein	Transport and binding
Mxan_1602	-0.871	-0.884	-1.241	-1.677		O-methyltransferase, putative	
Mxan_1604	-0.904	-1.016	-1.182	-0.87		permease, putative	
Mxan_1605	-0.427	-0.615	-1.08	-0.833		permease, putative	
Mxan_1606	-0.666	-1.103	-1.158	-0.7		hypothetical protein	
Mxan_1612	-0.573	-1.062	-1.238	-0.605		hypothetical protein	
Mxan_1613	-0.504	-0.833	-1.278	-0.583		hypothetical protein	
Mxan_1622	-0.954	-1.1	-0.483	-0.448		hypothetical protein	
Mxan_1624	-0.58	-1.091	-0.35	-0.322		peptidase, M16 (pitrilysin) family	Protein fate
Mxan_1627	-0.928	-1.385	-1.9	-1.36		hypothetical protein	
Mxan_1637	0.878	1.103	0.202	0.295		hypothetical protein	
Mxan_1642	-0.05	0.02	1.26	0.097		lipoprotein, putative	Cell envelope
Mxan_1651	-0.375	-0.83	-1.289	-0.703		hypothetical protein	
Mxan_1656	0.111	1.158	0.964	0.037		lipoprotein, putative	Cell envelope
Mxan_1657	0.215	1.001	0.882	-0.198		lipoprotein, putative	Cell envelope
Mxan_1659	-0.654	-0.711	-1.213	-0.918		PemK family protein	Unknown function
Mxan_1671	-1.91	-2.448	-1.96	-0.548		V-type H(+)-translocating pyrophosphatase	Transport and binding
Mxan_1672	-0.6	-1.497	-0.891	-0.163		hypothetical protein	
Mxan_1674	-0.283	-0.895	-1.128	-0.505		NAD dependent epimerase/dehydratase family protein	Energy metabolism
Mxan_1675	-0.568	-1.414	-1.624	-0.662		hypothetical protein	

Mxan-no.	Log ratio				Gene name	Annotation	GO mainrole
	0.5 h	1 h	2 h	4 h			
Mxan_1676	-1.06	-1.344	-1.747	-0.549		oxidase, FAD binding	Unknown function
Mxan_1678	-0.814	-1.166	-1.511	-0.452		deoxyhypusine synthase family protein	Protein fate
Mxan_1688	-1.517	-1.436	-0.834	-0.089		tonB family protein	
Mxan_1689	-1.037	-1.388	-1.404	-0.197		conserved hypothetical protein	Hypothetical proteins
Mxan_1690	-1.784	-1.649	-1.281	-0.349		esterase, putative	
Mxan_1695	1.129	0.909	0.675	0.627		permease, putative	Transport and binding
Mxan_1699	0.444	0.533	1.056	-0.038		hydrolase, alpha/beta fold family	Unknown function
Mxan_1702	0.338	0.556	1.061	0.127		hypothetical protein	
Mxan_1711	0.124	0.192	1.201	-0.146		transcriptional regulator, LysR family	Regulatory functions
Mxan_1721	0.75	1.599	1.34	0.442		lipoprotein, putative	Cell envelope
Mxan_1725	2.418	2.039	0.474	-0.359		hypothetical protein	
Mxan_1742	-0.545	-0.988	-1.006	-0.522		fatty acid desaturase family protein	Fatty acid and
Mxan_1743	-0.88	-1.081	-0.818	-0.326		cytochrome P450 family protein	Cellular processes
Mxan_1744	-1.479	-1.486	-0.994	-0.449		lipoxygenase family protein	
Mxan_1752	0.328	1.046	0.896	0.114	*iorB*	isoquinoline 1-oxidoreductase, beta subunit	Energy metabolism
Mxan_1795	0.381	0.721	2.55	2.258		lipoprotein, putative	Cell envelope
Mxan_1799	0.623	0.505	1.215	-0.099		transposase, IS5 family, degenerate	Disrupted reading
Mxan_1812	0.347	1.143	0.697	-0.226		hypothetical protein	
Mxan_1834	1.419	1.602	2.175	-0.313		hypothetical protein	
Mxan_1846	1.139	0.805	0.438	0.264		hypothetical protein	
Mxan_1856	0.02	1.058	0.437	0.147		hypothetical protein	
Mxan_1863	0.43	1.121	0.435	0.098		hypothetical protein	
Mxan_1864	1.657	1.588	1.319	0.349		N6 adenine-specific DNA methyltransferase	
Mxan_1876	0.356	0.823	1.254	0.391		DNA polymerase III, alpha subunit, Gram-positive type, putative	DNA metabolism
Mxan_1894	-1.199	-0.949	-0.868	-0.615		DNA-binding protein	Unknown function
Mxan_1901	-0.801	-1.024	-0.796	-0.051		transposase, IS5 family	Mobile and
Mxan_1917	0.288	0.657	1.049	0.566		hypothetical protein	
Mxan_1925	-0.906	-0.686	-1.013	-0.182	*mglA*	gliding motility protein MglA	Cellular processes
Mxan_1926	-0.958	-0.797	-1.105	-0.151	*mglB*	gliding motility protein MglB	Cellular processes
Mxan_1931	-1.138	-0.584	-1.016	-0.707		conserved hypothetical protein TIGR00103	Hypothetical proteins
Mxan_1941	1.377	1.199	0.565	0.263	*serS*	seryl-tRNA synthetase	Protein synthesis
Mxan_1946	1.305	1.281	0.336	-0.048		acyltransferase domain protein	Unknown function
Mxan_1957	2.15	3.08	1.622	0.448		lipoprotein, putative	Cell envelope
Mxan_1963	-0.826	-1.078	-0.745	-0.365		hypothetical protein	
Mxan_1964	0.7	1.348	3.447	1.05		hypothetical protein	
Mxan_1965	0.058	0.115	2.143	-0.056		lipoprotein, putative	Cell envelope
Mxan_1972	0.546	1.094	1.023	0.509		hypothetical protein	
Mxan_1974	0.842	0.967	1.261	0.257		conserved hypothetical protein	Hypothetical proteins
Mxan_1975	3.916	5.405	4.987	2.478		hypothetical protein	
Mxan_1981	2.137	4.24	3.936	1.145		hypothetical protein	
Mxan_1989	0.187	-0.065	1.065	0.739		hypothetical protein	
Mxan_1994	-1.383	-0.909	-0.3	0.001	*rpsI*	ribosomal protein S9	Protein synthesis
Mxan_2010	0.338	0.628	2.316	1.109		phage recombination protein Bet	Mobile and
Mxan_2015	2.472	2.172	1.257	0.227	*clpX*	ATP-dependent Clp protease, ATP-binding subunit ClpX	Protein fate
Mxan_2016	-0.249	-0.844	-1.129	-0.031	*pep*	prolyl endopeptidase precursor Pep	Protein fate
Mxan_2024	-0.837	-1.193	-0.53	-0.114		glutaredoxin homolog	Unknown function
Mxan_2031	0.429	1.374	0.781	-0.079		conserved domain protein	Hypothetical proteins
Mxan_2037	-0.449	-0.861	-1.95	-1.066		hypothetical protein	
Mxan_2081	-0.747	-0.856	-1.073	-0.572		lipoprotein, putative	Cell envelope
Mxan_2084	3.717	4.471	4.417	0.57		peptidase, S1C (protease Do) subfamily	Protein fate
Mxan_2092	0.094	0.941	1.015	0.081		peptidase, M16 (pitrilysin) family	Protein fate
Mxan_2094	-1.095	-1.11	-1.029	-0.592		conserved hypothetical protein	Hypothetical proteins
Mxan_2096	-0.854	-0.953	-1.188	-0.911		conserved hypothetical protein	Hypothetical proteins
Mxan_2099	-0.749	-1.488	-1.469	-1.148		conserved hypothetical protein	Hypothetical proteins
Mxan_2100	-0.354	-1.074	-0.921	-0.875		conserved hypothetical protein	Hypothetical proteins
Mxan_2107	0.908	1.283	-0.041	0.687		lipoprotein, putative	Cell envelope
Mxan_2117	1.77	3.077	2.966	0.947		hypothetical protein	
Mxan_2118	0.653	1.163	0.22	-0.009		hypothetical protein	
Mxan_2125	-0.825	-1.487	-1.445	-0.285		hypothetical protein	
Mxan_2127	-1.627	-2.218	-2.36	-0.372		peptidase, M12A (astacin) subfamily	Protein fate
Mxan_2137	0.09	0.21	1.865	0.282		oxidoreductase, aldo/keto reductase family	Unknown function
Mxan_2144	1.201	0.944	0.053	0.038		NmrA-like family protein	Unknown function
Mxan_2146	2.289	2.388	1.577	0.798		binding protein, putative	
Mxan_2147	2.382	2.818	1.437	0.651		lipoprotein, putative	Cell envelope
Mxan_2152	0.694	0.418	1.811	1.687		oxidoreductase, zinc-binding dehydrogenase family	Unknown function
Mxan_2180	0.96	0.904	1.191	0.206		NADP oxidoreductase coenzyme F420-dependent	Energy metabolism
Mxan_2183	2.403	4.091	3.78	1.748		lipoprotein, putative	Cell envelope
Mxan_2185	-0.036	0.268	1.303	0.528		4-carboxymuconolactone decarboxylase domain protein	
Mxan_2187	0.111	0.656	1.294	0.88		conserved domain protein	Hypothetical proteins
Mxan_2191	1.155	1.618	0.442	0.087		hypothetical protein	
Mxan_2208	-0.587	-0.856	-1.006	-0.896		conserved hypothetical protein	Hypothetical proteins
Mxan_2217	-0.108	-0.912	-1.376	-1.441		membrane protein, putative	Cell envelope
Mxan_2223	-0.682	-1.106	-1.445	-0.439		conserved hypothetical protein	Hypothetical proteins
Mxan_2231	1.223	0.771	0.608	0.343		lipoprotein, putative	Cell envelope
Mxan_2245	1.373	0.749	0.638	-0.222		hypothetical protein	
Mxan_2246	1.948	2.575	2.612	0.565		oxidoreductase, FAD-dependent	

Mxan-no.	Log ratio				Gene name	Annotation	GO mainrole
	0.5 h	1 h	2 h	4 h			
Mxan_2264	-0.855	-1.082	-0.965	-0.521	*mutA*	methylmalonyl-CoA mutase, beta subunit	Central intermediary
Mxan_2268	0.396	0.83	1.356	0.863		permease, putative	Transport and binding
Mxan_2269	**1.811**	**1.857**	**1.034**	**0.455**	***mspA***	**hypothetical protein**	
Mxan_2273	-0.971	-1.09	-0.921	-0.261		ribosome-associated GTPase, putative	Unknown function
Mxan_2276	-0.688	-1.525	-1.264	-0.753		hypothetical protein	
Mxan_2277	-1.095	-1.91	-1.681	-0.888		lipoprotein, putative	Cell envelope
Mxan_2280	-1.293	-1.568	-1.321	-0.408		phosphate transporter family protein	Transport and binding
Mxan_2281	-1.03	-1.352	-1.118	-0.294		conserved hypothetical protein	Hypothetical proteins
Mxan_2286	-0.671	-0.786	-1.188	-0.77	*dcp*	peptidyl-dipeptidase Dcp	Protein fate
Mxan_2290	-1.475	-1.253	-1.47	-0.736		lipoprotein, putative	Cell envelope
Mxan_2292	1.754	2.748	5.126	1.636		lipoprotein, putative	Cell envelope
Mxan_2299	3.942	5.056	4.907	0.936		lipoprotein, putative	Cell envelope
Mxan_2304	1.435	1.493	0.732	0.122		cytochrome P450 family protein	Central intermediary
Mxan_2312	-0.656	-0.849	-1.173	-0.823		hypothetical protein	
Mxan_2314	0.34	1.437	1.49	0.375		oxidoreductase, zinc-binding dehydrogenase family	Unknown function
Mxan_2318	1.117	1.435	0.941	-0.093	*gor*	glutathione-disulfide reductase	Biosynthesis of
Mxan_2319	0.687	1.573	0.728	-0.042		conserved hypothetical protein	Hypothetical proteins
Mxan_2320	1.26	1.407	1.111	0.11		conserved hypothetical protein	Hypothetical proteins
Mxan_2322	2.334	0.986	0.764	0.797		hypothetical protein	
Mxan_2326	3.404	4.051	3.064	1.326		aldehyde dehydrogenase family protein	Energy metabolism
Mxan_2335	0.214	0.371	1.632	1.385	*cysJ*	sulfite reductase [NADPH] flavoprotein, alpha-component	Central intermediary
Mxan_2339	0.24	1.036	2.18	1.822		siroheme synthase N-terminal domain protein	Biosynthesis of
Mxan_2342	-0.044	0.665	2.521	0.202		hypothetical protein	
Mxan_2352	1.032	1.287	2.406	0.878	*thrS*	threonyl-tRNA synthetase	Protein synthesis
Mxan_2364	0.541	1.126	1.054	0.821		beta-lactamase	Cellular processes
Mxan_2367	0.502	1.238	1.01	-0.029		acetyltransferase, GNAT family	
Mxan_2370	-1.129	-1.227	-1.481	-1.047		GAF domain protein	Unknown function
Mxan_2371	0.935	1.5	1.456	0.552	*mug*	G/U mismatch-specific DNA glycosylase	DNA metabolism
Mxan_2374	1.517	1.206	1.265	-0.03		conserved hypothetical protein	Hypothetical proteins
Mxan_2381	-0.685	-1.126	-0.487	-0.462		hypothetical protein	
Mxan_2406	-0.779	-1.06	-0.75	-0.894		hypothetical protein	
Mxan_2417	-0.187	-0.124	2.142	-0.044		conserved hypothetical protein	Hypothetical proteins
Mxan_2419	0.577	0.201	1.097	0.331	*pbpC*	penicillin-binding protein 1C	Cell envelope
Mxan_2420	1.308	2.539	3.44	1.862		putative lipoprotein	Cell envelope
Mxan_2421	0.134	0.286	2.088	0.44		conserved hypothetical protein	Hypothetical proteins
Mxan_2423	-1.105	-0.88	-0.488	-0.537		lipoprotein, putative	Cell envelope
Mxan_2425	1.26	1.698	5.14	2.008		hypothetical protein	
Mxan_2426	-0.549	-1.049	-0.712	-0.165		hypothetical protein	
Mxan_2427	-0.858	-1.307	-0.707	-0.031		hypothetical protein	
Mxan_2428	-0.768	-1.431	-0.733	-0.174		conserved hypothetical protein	Hypothetical proteins
Mxan_2429	-1.678	-1.809	-0.78	-0.012		ABC transporter, permease protein	Transport and binding
Mxan_2430	-1.568	-1.7	-1.006	-0.169		ABC transporter, ATP-binding protein	Transport and binding
Mxan_2433	-0.629	-0.73	-1.094	-0.691		hypothetical protein	
Mxan_2434	-1.011	-1.161	-1.079	-0.865		hypothetical protein	
Mxan_2435	-1.302	-1.307	-0.917	-0.427		TPR domain protein	
Mxan_2436	-1.287	-1.276	-1.125	-0.927		hypothetical protein	
Mxan_2438	-1.138	-1.065	-1.092	-0.798		type III secretion apparatus protein, YscI/HrpB family	Cellular processes
Mxan_2439	-1.577	-1.47	-1.496	-0.991		type III secretion apparatus lipoprotein, YscJ/HrcJ family	Cellular processes
Mxan_2454	-1.183	-1.336	-1.084	-0.709		hypothetical protein	
Mxan_2455	-1.542	-1.366	-1.642	-1.177		hypothetical protein	
Mxan_2468	0.474	0.61	1.161	0.758		PBS lyase HEAT-like repeat/cyclic nucleotide-binding domain protein	
Mxan_2470	-1.182	-0.974	-0.516	-0.196		5'-nucleotidase family protein	Unknown function
Mxan_2498	-0.954	-1.065	-0.904	-0.367		conserved hypothetical protein	Hypothetical proteins
Mxan_2500	0.91	1.027	0.497	0.492		RNA polymerase sigma-70 factor, ECF subfamily	Transcription
Mxan_2502	-0.348	-1.09	-0.913	-0.418		hypothetical protein	
Mxan_2503	-0.558	-1.177	-1.077	-0.643		hypothetical protein	
Mxan_2504	-0.527	-1.391	-1.285	-0.701		general secretion pathway protein L, putative	Protein fate
Mxan_2508	-0.048	-1.001	-0.662	-0.407		prepilin-type N-terminal cleavage/methylation domain protein	
Mxan_2509	-0.507	-1.49	-1.053	-0.551		conserved hypothetical protein	Hypothetical proteins
Mxan_2510	-0.651	-1.51	-1.185	-0.592	*gspG*	general secretion pathway protein G	Protein fate
Mxan_2512	-0.506	-1.204	-0.911	-0.295	*gspF*	general secretion pathway protein F	Protein fate
Mxan_2514	-0.629	-1.527	-0.572	-0.087	*gspD*	general secretion pathway protein D	Protein fate
Mxan_2515	-1.165	-1.502	-0.739	-0.107	*gspC*	general secretion pathway protein C	Protein fate
Mxan_2517	0.914	1.225	1.068	0.305		conserved domain protein	Hypothetical proteins
Mxan_2523	3.516	4.154	2.096	1.223		tetratricopeptide repeat protein	Unknown function
Mxan_2531	1.243	1.513	0.93	0.484		conserved domain protein	Hypothetical proteins
Mxan_2537	1.285	1.88	1.47	0.467		von Willebrand factor type A domain protein	Unknown function
Mxan_2538	-1.055	-0.865	-0.891	-0.448	*agmO*	adventurous gliding motility protein AgmO	Cellular processes
Mxan_2539	-1.761	-2.214	-1.588	-0.492		conserved hypothetical protein	Hypothetical proteins
Mxan_2540	-1.049	-1.525	-1.202	-0.52		conserved hypothetical protein	Hypothetical proteins
Mxan_2541	-1.611	-2.187	-1.951	-0.77		tetratricopeptide repeat protein	Unknown function
Mxan_2562	-1.105	-1.711	-0.806	-0.333		hypothetical protein	
Mxan_2565	0.864	1.289	1.805	0.594		hypothetical protein	
Mxan_2575	0.51	0.612	2.836	-0.002		lipoprotein, putative	Cell envelope
Mxan_2579	1.937	3.602	4.414	1.323		Ser/Thr protein phosphatase family/PKD domain protein	
Mxan_2580	1.82	4.815	5.753	1.166		lipoprotein, putative	Cell envelope

Mxan-no.	Log ratio				Gene name	Annotation	GO mainrole
	0.5 h	1 h	2 h	4 h			
Mxan_2581	2.17	3.471	5.163	1.49		hypothetical protein	
Mxan_2582	1.39	2.028	3.724	0.349		thymidylate kinase, putative	Purines, pyrimidines,
Mxan_2583	0.501	1.696	3.771	0.465		hypothetical protein	
Mxan_2584	1.158	3.992	5.789	1.927		hypothetical protein	
Mxan_2598	0.482	0.43	1.043	0.196		hypothetical protein	
Mxan_2610	1.539	2.963	2.349	0.385		lipoprotein, putative	Cell envelope
Mxan_2618	-1.428	-1.025	-0.565	-0.295	*purA*	adenylosuccinate synthetase	Purines, pyrimidines,
Mxan_2620	2.25	2.602	2.809	0.706		hypothetical protein	
Mxan_2622	0.857	1.468	3.422	0.394		conserved hypothetical protein	Hypothetical proteins
Mxan_2623	0.623	1.565	4.059	0.691		conserved domain protein	Hypothetical proteins
Mxan_2625	4.833	5.115	4.276	1.282		hypothetical protein	
Mxan_2626	0.848	1.399	1.648	1.542		DNA internalization-related competence protein ComEC/Rec2	Cellular processes
Mxan_2627	-0.205	0.631	1.411	0.514		transcriptional regulator, CarD family	Regulatory functions
Mxan_2634	2.124	1.496	0.384	-0.424		conserved hypothetical protein	Hypothetical proteins
Mxan_2635	3.376	3.668	2.462	0.546		hypothetical protein	
Mxan_2637	2.315	1.854	1.156	0.094		hypothetical protein	
Mxan_2638	2.841	3.202	2.546	0.574		hypothetical protein	
Mxan_2639	3.686	2.936	0.986	0.156		conserved hypothetical protein	Hypothetical proteins
Mxan_2644	-1.183	-1.055	-0.215	-0.027		peptidylprolyl cis-trans isomerase	Protein fate
Mxan_2652	1.218	1.497	0.709	0.063	*trx*	thioredoxin	Energy metabolism
Mxan_2659	-0.993	-2.361	-2.632	-0.736		hypothetical protein	
Mxan_2660	-1.494	-2.164	-1.978	-0.386		lipoprotein, putative	Cell envelope
Mxan_2661	-1.492	-2.067	-1.887	-0.33		5'-nucleotidase family protein	Unknown function
Mxan_2666	-0.893	-1.318	-0.601	-0.054	*pdhA*	pyruvate dehydrogenase complex, E1 component, pyruvate	Energy metabolism
Mxan_2667	-0.845	-1.404	-0.623	-0.111	*pdhB*	pyruvate dehydrogenase complex, E1 component, pyruvate	Energy metabolism
Mxan_2668	-0.505	-1.257	-0.599	-0.031	*pdhC*	pyruvate dehydrogenase complex , E2 component, dihydrolipoamide	Energy metabolism
Mxan_2680	-1.022	-0.521	-0.41	-0.319		serine/threonine protein kinase	
Mxan_2687	1.971	1.272	2.619	0.786		sensor histidine kinase	Regulatory functions
Mxan_2688	**5.947**	**6.57**	**5.9**	**1.949**		**conserved hypothetical protein**	**Hypothetical proteins**
Mxan_2689	**3.173**	**3.727**	**4.848**	**0.063**		**lipopolysaccharide biosynthesis protein**	**Cell envelope**
Mxan_2690	**1.753**	**2.784**	**3.222**	**-0.002**		**TldD/PmbA family protein**	**Unknown function**
Mxan_2695	-1.091	-0.399	-0.498	-0.201	*rpmB*	ribosomal protein L28	Protein synthesis
Mxan_2702	-1.102	-1.198	-1.727	-0.499		cyclic nucleotide-binding domain protein	Unknown function
Mxan_2703	-0.524	-0.946	-1.03	-0.129		cAMP phosphodiesterases class-II, putative	Unknown function
Mxan_2706	1.502	1.189	0.708	0.487		conserved hypothetical protein	Hypothetical proteins
Mxan_2710	-1.465	-1.802	-1.34	-0.184		lipoprotein, putative	Cell envelope
Mxan_2714	1.033	1.696	4.161	0.634		hypothetical protein	
Mxan_2715	0.941	1.131	3.357	0.315		endonuclease/exonuclease/phosphatase family protein	
Mxan_2716	3.886	3.662	2.334	0.865		conserved domain protein	Hypothetical proteins
Mxan_2717	3.896	4.001	2.581	0.942		conserved domain protein	Hypothetical proteins
Mxan_2718	4.17	4.387	2.773	0.908		hypothetical protein	
Mxan_2719	3.93	4.344	2.796	0.866		hypothetical protein	
Mxan_2720	2.62	3.287	1.862	0.389		hypothetical protein	
Mxan_2721	0.792	1.081	0.77	0.154		hypothetical protein	
Mxan_2726	**-0.519**	**-1.054**	**-0.809**	**-0.009**		**NADH dehydrogenase I, I subunit**	**Energy metabolism**
Mxan_2727	**-0.707**	**-1.472**	**-1.009**	**-0.286**		**NADH dehydrogenase I, H subunit, putative**	**Energy metabolism**
Mxan_2729	**-1.071**	**-1.109**	**-0.778**	**-0.081**		**NADH dehydrogenase I, D subunit**	**Energy metabolism**
Mxan_2731	0.346	1.021	0.57	0.237		sulfatase domain protein	Unknown function
Mxan_2741	0.805	1.466	2.483	0.812		conserved domain protein	Hypothetical proteins
Mxan_2742	-0.449	-0.982	-1.366	-0.589	*speA*	arginine decarboxylase	Central intermediary
Mxan_2752	1.589	1.169	0.635	0.051		hypothetical protein	
Mxan_2753	1.34	1.249	0.425	0.082		conserved hypothetical protein	Hypothetical proteins
Mxan_2770	1.072	0.449	0.155	0.141	*gvpa*	gas vesicle structural protein GvpA	Cellular processes
Mxan_2790	0.588	0.665	0.95	1.352	*prtA*	protease A	Protein fate
Mxan_2791	-0.011	0.481	1.152	1.336	*prtB*	protease B	Protein fate
Mxan_2798	-0.711	-0.892	-1.083	-0.513		polyketide/non-ribosomal peptide synthetase	Cellular processes
Mxan_2807	-0.952	-1.041	-0.688	-0.324		GSPII_E domain/HD domain/response regulator	Regulatory functions
Mxan_2809	0.519	1.031	2.502	0.285		conserved hypothetical protein	Hypothetical proteins
Mxan_2810	1.053	1.09	1.352	-0.026		hypothetical protein	
Mxan_2811	-1.344	-2.139	-2.101	-2.217		oxidoreductase, FAD-dependent	Unknown function
Mxan_2815	1.114	1.47	1.073	-0.061	*gapA*	glyceraldehyde-3-phosphate dehydrogenase 1	Energy metabolism
Mxan_2816	1.331	1.502	1.03	-0.038	*pgk*	phosphoglycerate kinase	Energy metabolism
Mxan_2817	0.797	1.051	0.912	-0.067	*tpiA*	triosephosphate isomerase	Energy metabolism
Mxan_2842	-0.943	-0.633	-1.107	-1.319		transcriptional regulator, LysR family	Regulatory functions
Mxan_2868	0.381	0.648	1.133	0.747		conserved hypothetical protein	Hypothetical proteins
Mxan_2883	-1.335	-2.088	-1.884	0.298		lipoprotein, putative	Cell envelope
Mxan_2884	0.559	1.237	1.798	1.356		tetratricopeptide repeat protein	Unknown function
Mxan_2891	-0.793	-1.175	-0.902	-0.668		WGR domain protein	Unknown function
Mxan_2892	-1.366	-1.581	-1.491	-0.894		WGR domain protein	Unknown function
Mxan_2905	1.213	1.725	1.07	0.69		dofA protein	Unknown function
Mxan_2906	-0.833	-1.299	-1.769	-1.068		penicillin acylase family protein	Cellular processes
Mxan_2908	3.062	3.986	2.992	0.414		lipoprotein, putative	Cell envelope
Mxan_2909	3.975	4.372	2.969	0.451		hypothetical protein	
Mxan_2926	-0.49	-1.195	-1.149	-0.315		ferredoxin, 2Fe-2S	Energy metabolism
Mxan_2927	-0.63	-0.722	-1.097	-0.818		glycosyl hydrolase, family 18	Energy metabolism
Mxan_2932	0.811	0.496	1.412	0.23		lipoprotein, putative	Cell envelope

Mxan-no.	Log ratio				Gene name	Annotation	GO mainrole
	0.5 h	1 h	2 h	4 h			
Mxan_2943	0.437	1.172	0.24	0.12		hypothetical protein	
Mxan_2944	0.823	0.672	1.17	0.77		conserved hypothetical protein	Hypothetical proteins
Mxan_2957	0.144	0.657	1.053	0.742	*sigD*	RNA polymerase sigma-D factor, authentic frameshift	Transcription
Mxan_2961	2.79	1.866	1.275	0.402		sensor histidine kinase	Regulatory functions
Mxan_2967	-0.415	-1.217	-0.963	-0.448		efflux transporter, AcrB/AcrD/AcrF family, inner membrane component	Transport and binding
Mxan_2968	-0.553	-1.147	-1.084	-0.54		efflux transporter, RND family, MFP subunit	
Mxan_2971	2.174	1.873	0.944	0.329		conserved hypothetical protein	Hypothetical proteins
Mxan_2972	3.906	4.322	3.067	1.004		hypothetical protein	
Mxan_2973	-1.105	-0.798	-0.454	0.031	*rrmJ*	ribosomal RNA large subunit methyltransferase J	Protein synthesis
Mxan_2974	-0.501	-0.945	-1.031	-0.015		conserved hypothetical protein	Hypothetical proteins
Mxan_2975	0.241	0.393	1.038	0.433		hypothetical protein	
Mxan_2977	3.979	3.858	3.667	0.823		conserved hypothetical protein TIGR00282	Hypothetical proteins
Mxan_2978	3.331	3.358	3.157	0.612		5-formyltetrahydrofolate cyclo-ligase family protein	
Mxan_2981	0.387	0.247	1.253	0.429		conserved domain protein	Hypothetical proteins
Mxan_2982	0.231	0.498	1.897	0.578		hypothetical protein	
Mxan_2985	-1.17	-1.357	-1.102	-0.233		Fic family protein	Unknown function
Mxan_2988	1.747	1.158	1.441	0.142		patatin-like phospholipase family protein	Unknown function
Mxan_2990	2.903	2.952	1.313	0.389		hypothetical protein	
Mxan_2993	1.1	1.453	1.481	0.553		conserved domain protein	Hypothetical proteins
Mxan_2994	0.979	1.253	1.233	0.375		glycosyl hydrolase, family 57	Energy metabolism
Mxan_2995	2.833	2.485	2.255	0.541		peptidase, S1C (protease Do) subfamily	Protein fate
Mxan_2996	1.705	1.682	1.487	0.239		GDSL-like lipase/acylhydrolase	
Mxan_3001	-0.486	-0.533	-1.012	-0.345		LysM domain protein	Unknown function
Mxan_3003	-0.755	-1.145	-1.276	0.056		MotA/TolQ/ExbB proton channel family protein	Transport and binding
Mxan_3004	-0.749	-1.103	-1.014	0.334		TolR-like protein	Unknown function
Mxan_3006	0.429	2.052	5.485	2.258		DksA homolog	Unknown function
Mxan_3026	**3.487**	**4.505**	**3.605**	**1.378**		**O-antigen polymerase family protein**	**Cell envelope**
Mxan_3027	4.909	6.612	5.91	4.318		glycosyl transferase, group 1	
Mxan_3038	-1.007	-0.851	-0.741	-0.277		hypothetical protein	
Mxan_3041	-1.055	-0.584	-0.311	-0.266	*gcvH*	glycine cleavage system H protein	Energy metabolism
Mxan_3044	0.972	1.029	0.802	0.269		tonB domain protein	Unknown function
Mxan_3046	0.16	1.157	1.362	0.61		lipoprotein, putative	Cell envelope
Mxan_3049	-0.095	0.449	0.997	1.083		conserved domain protein	Hypothetical proteins
Mxan_3051	-1.276	-1.042	-1.289	-0.741		ferrodoxin, 4Fe-4S	Energy metabolism
Mxan_3060	-1.3	-1.107	-0.845	-0.071	*cglB*	adventurous gliding motility protein CglB	Cellular processes
Mxan_3069	-1.434	-1.393	-0.744	-0.045	*rpmG*	ribosomal protein L33	Protein synthesis
Mxan_3071	-0.939	-1.087	-0.453	0.153		hypothetical protein	
Mxan_3072	-1.19	-0.928	-0.437	0.164	*nusG*	transcription termination/antitermination factor NusG	Transcription
Mxan_3073	-1.102	-0.915	-0.34	-0.022	*rplK*	ribosomal protein L11	Protein synthesis
Mxan_3074	-1.208	-1.165	-0.545	-0.137	*rplA*	ribosomal protein L1	Protein synthesis
Mxan_3075	-1.11	-1.446	-0.983	0.069	*rplJ*	ribosomal protein L10	Protein synthesis
Mxan_3076	-0.976	-1.41	-0.893	0.074	*rplL*	ribosomal protein L7/L12	Protein synthesis
Mxan_3079	-0.128	0.98	1.119	0.335		conserved hypothetical protein	Hypothetical proteins
Mxan_3098	0.278	1.122	0.717	0.158		sensory box histidine kinase	Regulatory functions
Mxan_3105	-2.337	-2.99	-2.926	-0.828		Type IV leader peptidase family protein	Protein fate
Mxan_3106	-2.266	-2.861	-2.918	-0.712		protein transporter, outer bacterial membrane secretin (secretin) family	Protein fate
Mxan_3108	-1.417	-1.458	-0.922	-0.511		FHA domain/tetratricopeptide repeat protein	
Mxan_3110	3.233	4.007	3.196	1.918		hypothetical protein	
Mxan_3117	0.755	2.111	2.7	0.533	*fruA*	fruA protein	Regulatory functions
Mxan_3127	1.083	0.849	0.888	0.262		hypothetical protein	
Mxan_3128	-0.259	-0.788	-1.093	-0.304		hypothetical protein	
Mxan_3129	-0.677	-1.15	-1.055	-0.426		peptidase, S9A (prolyl oligopeptidase) subfamily	Protein fate
Mxan_3133	0.294	0.504	1.134	0.757		putative membrane protein	Cell envelope
Mxan_3134	0.083	0.895	1.164	0.796		hypothetical protein	
Mxan_3137	0.328	0.701	4.305	1.063		hypothetical protein	
Mxan_3153	0.515	1.847	2.191	0.715		ethanolamine ammonia-lyase, large subunit/small subunit	
Mxan_3154	-0.648	-0.867	-1.213	-0.663	*menB*	naphthoate synthase	Biosynthesis of
Mxan_3155	-0.815	-1.054	-0.988	-0.534		lipoprotein, putative	Cell envelope
Mxan_3156	0.395	1.079	0.954	-0.009		channel protein, hemolysin III family	Cellular processes
Mxan_3159	-1.073	-0.813	-0.779	-0.587		hypothetical protein	
Mxan_3162	-1.151	-0.969	-0.574	-0.276	*fumB*	fumarate hydratase, class I	Energy metabolism
Mxan_3164	1.034	0.883	0.568	0.909		hypothetical protein	
Mxan_3169	-1.281	-1.528	-1.337	-0.807		putative membrane protein	Cell envelope
Mxan_3175	-0.569	-3.005	-4.621	-0.954		hypothetical protein	
Mxan_3188	2.779	2.047	1.138	0.186		PhoH family protein	Unknown function
Mxan_3189	2.341	1.745	0.679	0.054		hypothetical protein	
Mxan_3190	1.737	1.356	0.444	0.081		hypothetical protein	
Mxan_3192	0.854	0.844	1.073	0.637	*dnaK*	chaperone protein DnaK	Protein fate
Mxan_3201	-1.026	-0.869	-0.364	-0.376		FHA domain protein	Unknown function
Mxan_3212	**1.982**	**1.862**	**1.583**	**0.368**		**conserved hypothetical protein**	**Hypothetical proteins**
Mxan_3213	**1.871**	**2.22**	**1.898**	**0.703**	***actA***	**C-signal regulator ActA**	**Cellular processes**
Mxan_3214	**3.176**	**4.132**	**4.539**	**2.098**	***actB***	**sigma-54 activator protein ActB**	**Cellular processes**
Mxan_3216	0.529	0.642	1.098	0.271		ActD FRAMESHIFT	
Mxan_3223	0.17	0.319	1.269	0.318		conserved hypothetical protein	Hypothetical proteins
Mxan_3225	**3.223**	**3.624**	**3.383**	**0.963**	***fdgA***	**polysaccharide biosynthesis/export protein**	**Cell envelope**
Mxan_3226	**5.281**	**6.124**	**5.817**	**3.047**		**hypothetical protein**	

Mxan-no.	Log ratio				Gene name	Annotation	GO mainrole
	0.5 h	1 h	2 h	4 h			
Mxan_3227	**4.56**	**5.842**	**5.125**	**1.673**	***exo***	**chain length determinant family protein**	**Cell envelope**
Mxan_3228	**5.686**	**7.268**	**6.031**	**2.503**		**putative protein-tyrosine kinase**	**Regulatory functions**
Mxan_3229	**3.058**	**4.446**	**4.285**	**0.771**		**bacterial sugar transferase**	
Mxan_3230	**3.61**	**3.659**	**3.47**	**0.973**		**conserved hypothetical protein**	**Hypothetical proteins**
Mxan_3231	**6.288**	**6.194**	**5.713**	**1.399**		**conserved hypothetical protein**	**Hypothetical proteins**
Mxan_3232	**5.241**	**5.46**	**5.226**	**2.524**		**aminotransferase, DegT/DnrJ/EryC1/StrS family**	**Unknown function**
Mxan_3233	**4.039**	**5.172**	**3.8**	**0.938**		**conserved hypothetical protein**	**Hypothetical proteins**
Mxan_3236	0.701	0.634	0.657	1.342		macrolide 2'-phosphotransferase	Cellular processes
Mxan_3243	-0.646	-0.4	-1.616	-1.147		hypothetical protein	
Mxan_3252	-0.725	-1.078	-0.993	-0.429	*dsbE*	thiol:disulfide interchange protein DsbE	Energy metabolism
Mxan_3253	-0.563	-1.237	-0.871	-0.36	*ccmF*	cytochrome c-type biogenesis protein CcmF	Energy metabolism
Mxan_3254	-1.232	-1.354	-0.848	-0.343	*ccmE*	cytochrome c-type biogenesis protein CcmE	Energy metabolism
Mxan_3255	-1.215	-1.412	-0.789	-0.23		conserved hypothetical protein	Hypothetical proteins
Mxan_3256	-0.74	-1.043	-0.546	-0.245	*ccmC*	heme exporter protein CcmC	Protein fate
Mxan_3258	0.109	-0.905	-1.201	-0.26	*ccmA*	heme ABC exporter, ATP-binding protein CcmA	Transport and binding
Mxan_3259	**2.165**	**4.55**	**7.363**	**3.903**		**polysaccharide deacetylase family protein**	**Energy metabolism**
Mxan_3260	**1.71**	**2.689**	**5.359**	**2.792**		**putative membrane protein**	**Cell envelope**
Mxan_3261	**4.124**	**4.393**	**5.365**	**2.295**		**transferase hexapeptide repeat family protein**	
Mxan_3262	**4.408**	**5.065**	**5.58**	**1.492**		**glycosyltransferase 1 family protein**	**Cell envelope**
Mxan_3263	**4.999**	**5.897**	**6.366**	**2.666**		**putative glycosyltransferase**	**Cell envelope**
Mxan_3271	**4.176**	**6.182**	**7.254**	**2.647**		**lipoprotein, putative**	**Cell envelope**
Mxan_3283	-0.601	-0.866	-1.032	-0.289		hypothetical protein	
Mxan_3285	1.437	1.156	0.963	0.866		peptidase, S8A (subtilisin) subfamily	
Mxan_3286	1.105	1.039	0.731	0.446		conserved hypothetical protein	Hypothetical proteins
Mxan_3290	0.72	1.296	1.301	0.534		sensor histidine kinase/response regulator	Signal transduction
Mxan_3293	0.902	1.297	0.945	0.298		conserved hypothetical protein	Hypothetical proteins
Mxan_3295	**-1.149**	**-1.179**	**-0.745**	**0.164**	***rpsL***	**ribosomal protein S12**	**Protein synthesis**
Mxan_3296	**-1.247**	**-0.846**	**-0.505**	**-0.133**	***rpsG***	**ribosomal protein S7**	**Protein synthesis**
Mxan_3300	**-1.047**	**-0.863**	**-0.471**	**-0.025**	***rplD***	**ribosomal protein L4**	**Protein synthesis**
Mxan_3303	**-0.929**	**-1.05**	**-0.394**	**-0.067**	***rpsS***	**ribosomal protein S19**	**Protein synthesis**
Mxan_3305	**-0.98**	**-1.06**	**-0.515**	**-0.128**	***rpsC***	**ribosomal protein S3**	**Protein synthesis**
Mxan_3306	**-0.818**	**-1.04**	**-0.411**	**0.012**	***rplP***	**ribosomal protein L16**	**Protein synthesis**
Mxan_3307	**-0.861**	**-1.028**	**-0.491**	**-0.091**	***rpmC***	**ribosomal protein L29**	**Protein synthesis**
Mxan_3308	**-1.047**	**-1.075**	**-0.524**	**-0.076**	***rpsQ***	**ribosomal protein S17**	**Protein synthesis**
Mxan_3309	**-1.128**	**-1.369**	**-0.513**	**-0.058**	***rplN***	**ribosomal protein L14**	**Protein synthesis**
Mxan_3310	**-0.988**	**-1.203**	**-0.633**	**-0.085**	***rplX***	**ribosomal protein L24**	**Protein synthesis**
Mxan_3312	**-1.257**	**-1.13**	**-0.281**	**0.188**	***rpsN***	**ribosomal protein S14**	**Protein synthesis**
Mxan_3314	**-1.376**	**-0.971**	**-0.298**	**0.09**	***rplF***	**ribosomal protein L6**	**Protein synthesis**
Mxan_3315	**-1.648**	**-1.309**	**-0.588**	**-0.119**	***rplR***	**ribosomal protein L18**	**Protein synthesis**
Mxan_3316	**-1.431**	**-1.359**	**-0.695**	**-0.162**	***rpsE***	**ribosomal protein S5**	**Protein synthesis**
Mxan_3317	**-1.536**	**-1.404**	**-0.758**	**-0.202**	***rpmD***	**ribosomal protein L30**	**Protein synthesis**
Mxan_3318	**-1.11**	**-1.061**	**-0.674**	**-0.256**	***rplO***	**ribosomal protein L15**	**Protein synthesis**
Mxan_3328	-0.73	-1.105	-0.744	-0.003		hypothetical protein	
Mxan_3329	-0.596	-1.04	-0.432	-0.102		tetratricopeptide repeat protein	Unknown function
Mxan_3344	1.896	2.67	1.747	0.587		transglycosylase SLT domain protein	Unknown function
Mxan_3356	-0.096	0.445	1.302	0.025		oligopeptide transporter, OPT family	Transport and binding
Mxan_3357	**4.518**	**5.314**	**5.657**	**3.74**	***sigB***	**RNA polymerase sigma-B factor**	**Cellular processes**
Mxan_3358	1.227	2.298	5.631	3.634		hypothetical protein	
Mxan_3361	3.135	3.287	2.215	0.374		ATPase, AAA family	
Mxan_3362	2.148	3.289	4.397	0.757		hypothetical protein	
Mxan_3363	3.355	4.31	4.524	2.666		transglycosylase SLT domain protein	Unknown function
Mxan_3365	4.065	4.176	4.121	1.471		hypothetical protein	
Mxan_3366	0.651	1.008	1.243	0.313		putative membrane protein	Cell envelope
Mxan_3367	1.772	1.485	0.869	0.223		hypothetical protein	
Mxan_3368	1.477	1.182	0.808	-0.339		hypothetical protein	
Mxan_3371	**7.259**	**7.064**	**4.995**	**2.911**	***nfsA***	**hypothetical protein**	
Mxan_3372	**4.071**	**4.084**	**2.487**	**1.076**	***nfsB***	**hypothetical protein**	
Mxan_3373	**5.267**	**6.286**	**4.263**	**1.567**	***nfsC***	**conserved hypothetical protein**	**Hypothetical proteins**
Mxan_3374	**4.82**	**5.717**	**3.333**	**0.211**	***nfsD***	**tetratricopeptide repeat protein**	**Unknown function**
Mxan_3375	**5.674**	**5.53**	**4.794**	**1.082**	***nfsE***	**adventurous gliding protein T, putative**[a]	**Cellular processes**
Mxan_3376	**5.869**	**6.436**	**4.961**	**2.289**	***nfsF***	**hypothetical protein**	
Mxan_3377	**5**	**6.001**	**4.372**	**1.481**	***nfsG***	**FHA/TonB domain protein**	**Unknown function**
Mxan_3378	**4.607**	**5.178**	**3.558**	**0.985**	***nfsH***	**hypothetical protein**	
Mxan_3383	1.25	0.827	0.299	0.159		hypothetical protein	
Mxan_3388	-1.126	-0.788	-0.619	0.223	*carB*	carbamoyl-phosphate synthase, large subunit	Purines, pyrimidines,
Mxan_3399	1.246	1.061	0.658	0.118		lipoprotein, putative	Cell envelope
Mxan_3402	0.774	1.335	1.31	0.967		D-alanyl-D-alanine carboxypeptidase family protein	Cell envelope
Mxan_3416	2.52	3.86	2.361	0.38		lipoprotein, putative	Cell envelope
Mxan_3421	0.556	2.268	1.3	0.079		conserved hypothetical protein	Hypothetical proteins
Mxan_3431	0.848	1.309	1.959	0.119		outer membrane efflux protein	Transport and binding
Mxan_3432	0.446	1.322	0.819	0.142		multicopper oxidase domain protein	Unknown function
Mxan_3445	-0.556	-1.066	-1.324	-0.518		hypothetical protein	
Mxan_3454	0.145	0.651	1.251	0.418		2-oxo acid dehydrogenase acyltransferase catalytic domain protein	Unknown function
Mxan_3459	2.357	1.59	1.521	0.308		conserved hypothetical protein	Hypothetical proteins
Mxan_3460	1.744	1.331	1.619	0.335		oxidoreductase, Gfo/Idh/MocA family	
Mxan_3465	-1.241	-1.142	-0.785	0.125	*hutH*	histidine ammonia-lyase	Energy metabolism

Mxan-no.	Log ratio				Gene name	Annotation	GO mainrole
	0.5 h	1 h	2 h	4 h			
Mxan_3469	3.162	4.699	3.838	0.649		glycosyl transferase, group 2 family protein	Cell envelope
Mxan_3479	1.458	2.391	1.759	0.746		lipoprotein, putative	
Mxan_3480	0.566	1.132	0.666	0.461		iron-sulfur cluster-binding protein, Rieske family	Energy metabolism
Mxan_3486	-1.031	-1.16	-0.808	-0.159		thioesterase domain protein	Unknown function
Mxan_3488	-2.246	-2.955	-2.693	-1.302		antibiotic biosynthesis protein, putative	Cellular processes
Mxan_3495	-1.024	-1.935	-2.121	-1.009		fatty acid desaturase family protein	Fatty acid and
Mxan_3507	3.033	2.616	1.741	0.088	*galE*	UDP-glucose 4-epimerase	Energy metabolism
Mxan_3508	3.69	3.506	2.408	1.289	*lepA*	GTP-binding protein LepA	Unknown function
Mxan_3517	-1.209	-0.791	-1.08	-0.026		hypothetical protein	
Mxan_3520	-0.407	-1.031	-1.371	-0.934		3-phosphoshikimate 1-carboxyvinyltransferase, putative	Amino acid
Mxan_3522	-1.045	-1.483	-1.625	-1.227	*aroC*	chorismate synthase	Amino acid
Mxan_3530	0.381	0.193	1.119	0.102	*menA*	1,4-dihydroxy-2-naphthoate octaprenyltransferase	Biosynthesis of
Mxan_3537	-1.334	-0.948	-0.572	-0.501	*icd*	isocitrate dehydrogenase, NADP-dependent	Energy metabolism
Mxan_3538	-1.182	-0.94	-0.597	-0.558	*mdh*	malate dehydrogenase	Energy metabolism
Mxan_3541	-1.255	-0.94	-0.849	-0.198	*sucC*	succinyl-CoA synthase, beta subunit	Energy metabolism
Mxan_3542	-1.152	-1.086	-0.865	-0.21	*sucD*	succinyl-CoA synthetase, alpha subunit	Energy metabolism
Mxan_3543	-0.847	-1.068	-0.981	-0.348	*ndk*	nucleoside diphosphate kinase	Purines, pyrimidines,
Mxan_3544	-0.652	-0.889	-1.012	-0.366		radical SAM enzyme, Cfr family	
Mxan_3564	-0.739	-1.912	-2.514	-1.184		peptidase, M36 (fungalysin) family	Protein fate
Mxan_3574	2.99	2.322	1.812	1.394		von Willebrand factor type A domain protein	Unknown function
Mxan_3580	0.907	-0.015	1.96	1.212		hypothetical protein	
Mxan_3581	-1.363	-1.66	-1.678	-0.612		peptidyl-dipeptidase A	Protein fate
Mxan_3583	1.886	1.458	0.906	0.784		conserved hypothetical protein	Hypothetical proteins
Mxan_3596	-0.787	-0.56	-1.033	-0.47	*ihfA*	integration host factor, alpha subunit	DNA metabolism
Mxan_3605	-1.479	-1.671	-1.661	-1.041		response regulator	
Mxan_3608	0.223	-0.039	1.016	0.761		hypothetical protein	
Mxan_3619	-1.13	-1.522	-1.341	-0.289		polyketide synthase type I	
Mxan_3621	-0.515	-1.063	-0.869	0.261		polyketide synthase type I	
Mxan_3638	-0.444	-1.036	-1.358	-0.434		peptidase, M19 family	Protein fate
Mxan_3639	-1.675	-1.587	-1.287	-0.034		iron-chelator utilization protein	
Mxan_3640	-0.455	-1.669	-0.787	0.447		siderophore biosynthesis aminotransferase	Biosynthesis of
Mxan_3643	-1.048	-1.141	-0.664	0.415		non-ribosomal peptide synthase MxcG	
Mxan_3644	-0.851	-1.021	-0.896	0.208		isochorismatase	Biosynthesis of
Mxan_3645	-1.353	-1.654	-0.922	0.135		2,3-dihydroxybenzoate-AMP ligase	Biosynthesis of
Mxan_3646	-1.97	-1.48	-0.626	0.408		isochorismate synthase	Biosynthesis of
Mxan_3647	-1.396	-1.165	-0.759	0.293		2,3-dihydro-2,3-dihydroxybenzoate dehydrogenase	Biosynthesis of
Mxan_3673	-0.632	-1.175	-0.981	-0.048		hypothetical protein	
Mxan_3677	0.883	1.033	1.022	1.085		major facilitator family transporter	Transport and binding
Mxan_3681	2.371	2.171	0.573	0.449		hypothetical protein	
Mxan_3682	0.816	1.702	2.09	0.665	*glgB*	1,4-alpha-glucan branching enzyme	Energy metabolism
Mxan_3683	0.847	1.905	2.329	0.743		sugar phosphotransferase, putative	Energy metabolism
Mxan_3684	**2.132**	**3.253**	**3.239**	**1.33**	***treS***	**trehalose synthase**	**Energy metabolism**
Mxan_3685	1.878	2.817	3.059	1.231		conserved hypothetical protein	Hypothetical proteins
Mxan_3695	-1.068	-1.063	-1.475	-0.451		hypothetical protein	
Mxan_3697	3.391	2.887	2.522	0.383		conserved hypothetical protein	Hypothetical proteins
Mxan_3698	-0.979	-1.164	-0.884	-0.262		lipoprotein, putative	Cell envelope
Mxan_3720	-1.11	-1.181	-0.864	0.127		kinase, pfkB family	Unknown function
Mxan_3734	2.047	3.363	2.709	0.691		response regulator	
Mxan_3735	3.354	4.316	4.23	2.272		response regulator - FRAMESHIFT	Signal transduction
Mxan_3743	2.414	2.645	1.601	0.021		hypothetical protein	
Mxan_3745	1.524	1.104	0.383	-0.365		hypothetical protein	
Mxan_3758	5.54	5.957	5.534	3.494		hypothetical protein	
Mxan_3765	-1.254	-0.825	-1.416	-0.658	*era*	GTP-binding protein Era	Cellular processes
Mxan_3767	-1.049	-1.166	-1.205	-0.119		hypothetical protein	
Mxan_3771	1.034	1.301	1.351	0.291		conserved hypothetical protein	Hypothetical proteins
Mxan_3776	-1.52	-1.731	-1.079	0.006		hypothetical protein	
Mxan_3781	1.294	0.441	0.478	0.515		DedA family protein	Unknown function
Mxan_3808	0.28	0.556	1.035	0.24	*sppA*	signal peptide peptidase SppA	Protein fate
Mxan_3816	0.952	1.268	1.174	0.8		hypothetical protein	
Mxan_3830	-0.884	-1.647	-1.564	-0.416		hypothetical protein	
Mxan_3843	0.252	0.617	1.11	0.776		hypothetical protein	
Mxan_3849	1.197	0.509	0.832	0.318		hypothetical protein	
Mxan_3850	1.457	1.211	1.282	0.334		general stress protein GsiB, putative	Cellular processes
Mxan_3851	0.83	0.505	1.11	0.219		membrane protein, putative	Cell envelope
Mxan_3860	1.163	0.932	0.627	0.04		NADH-ubiquinone/plastoquinone oxidoreductase family protein	Energy metabolism
Mxan_3862	1.12	1.35	0.902	0.389		Na+/H+ ion antiporter	
Mxan_3863	1.221	1.281	0.621	0.184		monovalent cation/proton antiporter, MrpF/PhaF family	
Mxan_3864	1.224	1.208	0.727	0.41		monovalent cation/proton antiporter, MnhG/PhaG family	
Mxan_3875	0.7	0.576	2.192	1.512		oxidoreductase, iron-sulfur binding subunit	
Mxan_3881	2.414	3.24	3.275	0.701	*pyc*	pyruvate carboxylase	Energy metabolism
Mxan_3884	0.138	1.355	5.077	2.998		hypothetical protein	
Mxan_3885	**0.54**	**1.933**	**6.547**	**3.77**	***prU***	**hypothetical protein**	
Mxan_3888	0.943	1.813	1.739	1.807		hypothetical protein	
Mxan_3892	1.522	2.023	1.863	1.005		maltose O-acetyltransferase	Energy metabolism
Mxan_3914	-0.661	-1.047	-1.153	-0.15		membrane protein, putative	Cell envelope
Mxan_3915	-1.094	-1.429	-1.523	-0.339		tonB family protein	Transport and binding

Mxan-no.	Log ratio				Gene name	Annotation	GO mainrole
	0.5 h	1 h	2 h	4 h			
Mxan_3919	1.213	1.606	1.017	0.65	*rnk*	regulator of nucleoside diphosphate kinase	Regulatory functions
Mxan_3930	-1.055	-0.888	-0.413	-0.116	*lspA*	signal peptidase II	Protein fate
Mxan_3951	-0.399	-0.97	-1.033	-0.93		metallo-beta-lactamase family protein	Unknown function
Mxan_3953	0.335	0.815	1.213	0.401		hypothetical protein	
Mxan_3954	3.017	3.283	2.894	0.675		hypothetical protein	
Mxan_3958	-1.044	-0.846	-0.267	0.224	*truD*	tRNA pseudouridine synthase D	Protein synthesis
Mxan_3960	1.245	1.156	0.589	0.01		hypothetical protein	
Mxan_3961	1.407	1.091	0.668	0.04		hypothetical protein	
Mxan_3966	-4.135	-4.124	-3.359	-5.792		universal stress family protein	Cellular processes
Mxan_3967	-1.493	-2.181	-2.758	-3.011		putative membrane protein	Cell envelope
Mxan_3971	-1.925	-2.58	-2.31	-0.521		lipoprotein, putative	Cell envelope
Mxan_3976	-1.141	-0.782	-0.288	-0.16		conserved hypothetical protein	Hypothetical proteins
Mxan_3979	0.724	1.144	0.87	0.339		hypothetical protein	
Mxan_3985	0.11	1.901	3.727	2.333		hypothetical protein	
Mxan_3993	2.364	2.234	1.109	0.175	*lon*	ATP-dependent protease La	Protein fate
Mxan_3996	0.92	0.059	0.439	1.207		hypothetical protein	
Mxan_4008	1.121	1.219	-0.051	0.202		hypothetical protein	
Mxan_4026	0.372	0.292	0.138	1.016	*mutL*	DNA mismatch repair protein MutL	DNA metabolism
Mxan_4033	2.008	1.964	0.19	0.554		hypothetical protein	
Mxan_4041	2.542	2.575	0.178	-0.198		arsenical pump-driving ATPase	Cellular processes
Mxan_4042	**4.365**	**3.63**	**0.905**	**0.285**	***nla6***	**sigma-54 dependent DNA-binding reponse regulator Nla6**	**Cellular processes**
Mxan_4043	4.574	3.928	1.803	0.843		sensor histidine kinase, putative	Regulatory functions
Mxan_4046	0.67	1.376	0.901	0.116		hypothetical protein	
Mxan_4051	-1.277	-1.175	-0.956	-0.469	*leuS*	leucyl-tRNA synthetase	Protein synthesis
Mxan_4054	1.909	1.735	1.192	0.042	*clpX*	ATP-dependent Clp protease, ATP-binding subunit ClpX	Protein fate
Mxan_4058	-0.693	-0.947	-1.146	-0.024		hypothetical protein	
Mxan_4061	-0.894	-0.858	-1.083	-0.234		lipoprotein, putative	Cell envelope
Mxan_4064	-1.199	-1.132	-0.362	-0.111		adenylylsulfate kinase, putative	Central intermediary
Mxan_4077	0.381	0.456	1.48	-0.118		polyketide synthase type I	Cellular processes
Mxan_4084	-1.013	-0.975	-0.857	-0.583		cyclic nucleotide-binding domain protein	
Mxan_4092	2.181	2.694	2.873	0.103		hypothetical protein	
Mxan_4093	1.967	2.869	2.947	0.261		membrane protein, putative	
Mxan_4095	-1.017	-0.653	-0.668	-0.73		hypothetical protein	
Mxan_4096	0.243	0.092	2.429	0.569	*dmpA*	D-aminopeptidase	Protein fate
Mxan_4102	-0.551	-0.81	-1.189	-0.756		ABC transporter, ATP-binding protein	Transport and binding
Mxan_4107	-0.977	-1.833	-0.679	-0.701		lipoprotein, putative	
Mxan_4109	-1.14	-1.133	-1.189	-0.561		hypothetical protein	
Mxan_4111	3.204	2.823	2.894	0.315		pirin family protein	Unknown function
Mxan_4119	0.798	1.169	0.437	-0.243		hypothetical protein	
Mxan_4132	1.707	2.702	1.718	0.215		conserved domain protein	Hypothetical proteins
Mxan_4133	4.086	4.083	3.17	0.463		hypothetical protein	
Mxan_4136	1.408	1.583	0.855	0.195	*phrB*	deoxyribodipyrimidine photolyase	DNA metabolism
Mxan_4140	-1.432	-1.227	-0.877	-0.583	*frzE*	gliding motility regulatory protein	Cellular processes
Mxan_4141	-1.226	-1.095	-0.638	-0.356		frzcd protein	Cellular processes
Mxan_4150	-0.973	-1.17	-0.842	-0.506		hypothetical protein	
Mxan_4156	0.468	0.42	1.411	0.282		conserved domain protein	Hypothetical proteins
Mxan_4159	-1.225	-1.423	-1.571	0.041	*udk*	uridine kinase	Purines, pyrimidines,
Mxan_4168	-0.989	-1.134	-0.951	-0.636		hypothetical protein	
Mxan_4183	-0.849	-0.939	-1.058	-0.89		hypothetical protein	
Mxan_4184	-1.002	-1.134	-1.224	-1.045		hypothetical protein	
Mxan_4190	1.123	0.964	0.841	1.354		MutS2 family protein	DNA metabolism
Mxan_4193	0.986	1.04	0.861	0.638		hypothetical protein	
Mxan_4203	0.787	0.854	1.974	0.381		sensor histidine kinase	
Mxan_4208	-1.453	-0.915	-0.789	-0.355		tetratricopeptide repeat protein	Unknown function
Mxan_4209	1.524	1.634	0.427	0.12		hypothetical protein	
Mxan_4210	1.891	1.789	0.475	-0.207	*rnr*	ribonuclease R	Transcription
Mxan_4211	-0.63	-0.922	-1.111	-0.649		hypothetical protein	
Mxan_4223	0.741	0.541	1.204	0.386		putative histidinol-phosphate phosphatase	Amino acid
Mxan_4224	0.694	0.556	1.19	0.652	*hisF*	imidazoleglycerol phosphate synthase, cyclase subunit	Amino acid
Mxan_4225	0.575	0.753	1.067	0.368	*hisB*	imidazoleglycerol-phosphate dehydratase	Amino acid
Mxan_4226	0.753	0.437	1.558	0.618		phosphoribosylformimino-5-aminoimidazole carboxamide ribotide	Amino acid
Mxan_4228	0.857	0.803	2.165	0.61	*hisC*	histidinol-phosphate aminotransferase	Amino acid
Mxan_4229	1.315	1.26	2.523	1.02	*hisD*	histidinol dehydrogenase	Amino acid
Mxan_4230	0.917	0.889	2.556	1.122	*hisG*	ATP phosphoribosyltransferase	Amino acid
Mxan_4236	-2.446	-2.276	-2.72	-3.792		CBS domain protein	Unknown function
Mxan_4237	-2.641	-3.42	-3.394	-4.017		sodium:sulfate symporter	Transport and binding
Mxan_4238	-1.639	-1.541	-1.137	-1.523		hypothetical protein	
Mxan_4239	-1.661	-1.925	-1.697	-2.653		hypothetical protein	
Mxan_4240	-2.182	-2.766	-2.557	-3.155		sigma-54 dependent DNA-binding response regulator	Regulatory functions
Mxan_4245	-1.328	-1.462	-1.123	-1.16		response regulator	Regulatory functions
Mxan_4246	-2.382	-2.393	-1.983	-1.888		sensor histidine kinase	Signal transduction
Mxan_4250	0.482	0.63	2.859	1.17		phosphoribosyl transferase domain protein	Unknown function
Mxan_4259	0.066	0.541	1.545	-0.415		hypothetical protein	
Mxan_4274	0.455	0.806	0.592	1.816		hypothetical protein	
Mxan_4277	1.035	2.06	0.727	0.432		peptidase, S1A (chymotrypsin) subfamily	Protein fate
Mxan_4288	-1.008	-0.265	-0.55	-0.596		hypothetical protein	

Mxan-no.	Log ratio				Gene name	Annotation	GO mainrole
	0.5 h	1 h	2 h	4 h			
Mxan_4290	-1.687	-1.092	-0.125	-0.288		thioesterase, putative	Unknown function
Mxan_4291	-1.357	-1.178	-0.182	-0.352		conserved hypothetical protein	Hypothetical proteins
Mxan_4292	-0.404	-0.94	-2.639	-1.109		polyketide synthase	Cellular processes
Mxan_4293	-0.44	-0.736	-2.727	-1.186		hypothetical protein	
Mxan_4294	-0.374	-0.799	-2.835	-1.191		arsenical pump-driving ATPase	Cellular processes
Mxan_4295	-0.431	-0.945	-2.864	-1.064		patatin-like phospholipase family protein	Unknown function
Mxan_4296	-0.109	-1.238	-1.457	-0.728		non-ribosomal peptide synthetase	Cellular processes
Mxan_4297	-0.033	-1.697	-1.918	-0.76		polyketide synthase	
Mxan_4298	-0.287	-0.966	-1.248	-0.687		polyketide synthase type I	
Mxan_4299	-0.462	-1.602	-1.833	-0.657		non-ribosomal peptide synthase/polyketide synthase	Cellular processes
Mxan_4300	-1.042	-1.39	-1.424	-0.344		polyketide synthase type I	Cellular processes
Mxan_4301	-1.471	-1.472	-1.395	-0.178		polyketide synthase type I	Cellular processes
Mxan_4305	-1.108	-1.059	-0.722	-0.168		amino acid adenyltransferase	Central intermediary
Mxan_4325	-1.031	-1.034	-0.983	-0.019		hypothetical protein	
Mxan_4327	-1.159	-1.219	-1.093	-0.373		Glu/Leu/Phe/Val dehydrogenase family protein	Energy metabolism
Mxan_4331	1.551	1.994	1.312	0.507		co-chaperone GrpE, putative	Protein fate
Mxan_4332	1.606	2.693	2.578	1.4		hypothetical protein	
Mxan_4333	1.552	1.379	1.193	0.391	*ftsH*	ATP-dependent metalloprotease FtsH	Cellular processes
Mxan_4338	0.855	1.409	0.492	0.156		serine/threonine-protein kinase, degenerate	Regulatory functions
Mxan_4351	1.533	0.569	0.094	0.181	*pdxJ*	pyridoxal phosphate biosynthetic protein PdxJ	Biosynthesis of
Mxan_4361	0.809	1.092	0.744	0.91		hypothetical protein	
Mxan_4362	-1.032	-0.681	-0.101	-0.084		hypothetical protein	
Mxan_4363	1.219	0.802	0.711	0.206		hypothetical protein	
Mxan_4368	-0.07	0.331	1.441	0.019		hypothetical protein	
Mxan_4370	-0.405	-0.66	-1.836	-0.832		NAD dependent epimerase/dehydratase family protein	Energy metabolism
Mxan_4387	-1.325	-1.15	-0.895	-0.654		hypothetical protein	
Mxan_4388	-1.505	-1.322	-1.016	-0.511	*kamD*	D-lysine 5,6-aminomutase, alpha subunit	Energy metabolism
Mxan_4389	3.863	3.248	1.46	0.825	*katB*	catalase KatB	Cellular processes
Mxan_4390	1.026	0.644	0.521	0.523		ankyrin repeat protein	
Mxan_4394	-1.184	-1.915	-2.383	-1.272		thioesterase domain protein	Unknown function
Mxan_4407	0.991	1.323	1.575	0.915		conserved domain protein	Hypothetical proteins
Mxan_4411	-0.544	-1.38	-0.647	-0.203		JmjC domain protein	Unknown function
Mxan_4419	-1.423	-1.116	-0.216	-0.464		beta-hydroxylase, aspartyl/asparaginyl family	Unknown function
Mxan_4421	-0.718	-1.244	-1.688	-0.877		lipoprotein, putative	Cell envelope
Mxan_4432	1.671	1.545	1.376	0.883		response regulator/sensor histidine kinase, putative	Signal transduction
Mxan_4442	-0.718	-0.931	-1.115	-0.552		hypothetical protein	
Mxan_4453	1.001	0.808	0.092	0.155		hypothetical protein	
Mxan_4454	3.123	2.391	0.618	-0.389		cyclase/dehydrase, putative	Unknown function
Mxan_4455	3.241	2.5	0.886	-0.328	*glpX*	fructose-1,6-bisphosphatase, class II	Energy metabolism
Mxan_4475	-1.833	-1.76	-2.144	-1.705		ATP-dependent helicase, DEAD/DEAH box family	Transcription
Mxan_4479	-0.475	-1.008	-1.06	-0.433		serine/threonine protein kinase, putative	Regulatory functions
Mxan_4488	0.951	1.113	1.124	1.153		hypothetical protein	
Mxan_4500	0.019	0.636	1.06	0.731		conserved domain protein	Hypothetical proteins
Mxan_4524	0.648	2.854	3.757	2.655		hypothetical protein	
Mxan_4530	-1.026	-1.236	-1.153	-0.422		polyketide synthase type I	
Mxan_4531	-0.659	-1.452	-1.029	-0.403		conserved hypothetical protein	Hypothetical proteins
Mxan_4535	-0.738	-0.836	-1.305	-0.432		RNA polymerase sigma-70 factor, putative	Transcription
Mxan_4538	-0.833	-0.823	-1.291	-0.616		hypothetical protein	
Mxan_4541	-1.719	-1.906	-1.336	-0.992		hypothetical protein	
Mxan_4543	1.13	1.142	0.572	0.073		YceI-like family protein	Unknown function
Mxan_4546	0.592	1.851	1.796	0.19		hypothetical protein	
Mxan_4547	2.469	3.805	4.213	1.735		molybdenum cofactor carrier protein, putative	Biosynthesis of
Mxan_4552	-0.471	-0.831	-1.213	-0.854		hypothetical protein	
Mxan_4559	-0.872	-1.325	-1.162	-0.372		tonB dependent receptor, putative	Transport and binding
Mxan_4560	-0.821	-1.177	-1.097	-0.492		hypothetical protein	
Mxan_4568	3.008	3.197	2.044	0.923		lipoprotein, putative	Cell envelope
Mxan_4578	0.844	1.008	3.929	1.81		conserved hypothetical protein	Hypothetical proteins
Mxan_4579	0.698	0.613	1.275	0.001		sensor histidine kinase	Signal transduction
Mxan_4580	-0.009	0.201	1.297	0.183		sigma-54 dependent DNA-binding response regulator	Regulatory functions
Mxan_4581	0.059	0.157	1.378	0.048		peptidoglycan-associated lipoprotein (Pal) family protein	Cell envelope
Mxan_4588	0.385	1.242	3.747	0.316		ribonuclease BN family protein	Transcription
Mxan_4591	0.177	-0.842	-1.201	-0.148	*pkn1*	serine/threonine-protein kinase PKN1	Regulatory functions
Mxan_4626	-0.447	-0.622	-1.198	-0.651	*pgsA*	CDP-diacylglycerol--glycerol-3-phosphate 3-phosphatidyltransferase	Fatty acid and
Mxan_4636	-1.201	-0.984	-0.624	-0.363		conserved hypothetical protein	Hypothetical proteins
Mxan_4641	-1.271	-0.771	-0.631	-0.103		hypothetical protein	
Mxan_4651	-1.129	-0.854	-0.471	-0.034		type II secretion system protein F domain protein	Protein fate
Mxan_4653	0.6	1.359	1.87	0.865		lipoprotein, putative	Cell envelope
Mxan_4687	1.696	2.508	3.652	1.127		YHS domain protein	
Mxan_4689	1.646	1.648	2.325	3.112		hypothetical protein	
Mxan_4690	-1.108	-1.203	-1.207	-0.369	*secF*	protein-export membrane protein SecF	Protein fate
Mxan_4691	-0.874	-1	-1.021	-0.303	*secD*	protein-export membrane protein SecD	Protein fate
Mxan_4724	-0.654	-1.004	-1.093	-0.3	*lpxA*	acyl-[acyl-carrier-protein]--UDP-N-acetylglucosamine O-acyltransferase	Cell envelope
Mxan_4726	-0.582	-1.11	-1.176	-0.157	*lpxD*	UDP-3-O-[3-hydroxymyristoyl] glucosamine N-acyltransferase	Cell envelope
Mxan_4727	-0.903	-1.076	-0.869	-0.14		outer membrane protein, OmpH family	Cell envelope
Mxan_4732	-0.151	0.639	1.38	0.352		hypothetical protein	
Mxan_4733	-0.146	1.09	2.35	1.222		RNA polymerase sigma-70 factor, ECF subfamily	Transcription

Mxan-no.	Log ratio				Gene name	Annotation	GO mainrole
	0.5 h	1 h	2 h	4 h			
Mxan_4746	-1.064	-2.044	-1.731	-1.423		TonB-dependent receptor	Cell envelope
Mxan_4747	-0.789	-2.147	-1.935	-1.435		lipoprotein, putative	Cell envelope
Mxan_4748	1.043	1.394	2.143	0.697		3-hydroxyisobutyrate dehydrogenase family protein	Unknown function
Mxan_4765	-0.845	-1.027	-1.11	-0.463		conserved hypothetical protein TIGR00244	Hypothetical proteins
Mxan_4766	-0.777	-0.931	-1.033	-0.425	*glyA*	serine hydroxymethyltransferase	Amino acid
Mxan_4769	-1.132	-0.819	-0.9	-0.237	*acpP*	acyl carrier protein	Fatty acid and
Mxan_4771	-0.853	-0.921	-1.163	-0.421	*fabD*	malonyl CoA-acyl carrier protein transacylase	Fatty acid and
Mxan_4780	0.146	0.609	1.006	0.44		phosphohistidine phosphatase, putative	Central intermediary
Mxan_4789	1.203	1.196	0.635	-0.224	*pstC*	phosphate ABC transporter, permease protein PstC	Transport and binding
Mxan_4790	1.052	1.294	0.669	0.248	*pstA*	phosphate ABC transporter, permease protein PstA	Transport and binding
Mxan_4800	-1.264	-1.194	-0.731	-0.644		Rhs element Vgr family protein	Unknown function
Mxan_4807	-0.892	-1.547	-1.481	-0.893		conserved hypothetical protein	Hypothetical proteins
Mxan_4808	-0.762	-1.623	-1.51	-0.956		conserved hypothetical protein	Hypothetical proteins
Mxan_4809	-0.599	-0.995	-1.655	-1.03		conserved hypothetical protein	Hypothetical proteins
Mxan_4810	-0.302	-0.898	-1.001	-0.572		conserved hypothetical protein	Hypothetical proteins
Mxan_4813	-0.895	-1.312	-0.992	-0.638	*clpB*	ATP-dependent chaperone protein ClpB	Protein fate
Mxan_4824	0.325	1.28	0.502	0.525		ClpA/B family protein	
Mxan_4825	0.846	1.534	0.961	0.83		ClpA/B family protein	
Mxan_4826	0.291	0.805	1.037	0.049	*sodB*	superoxide dismutase, Fe	Cellular processes
Mxan_4840	-1.433	-1.367	-1.313	-0.617		pirin family protein	Unknown function
Mxan_4841	-1.601	-1.27	-0.732	-0.294		serine/threonine protein kinase, putative	
Mxan_4849	-0.81	-1.252	-1.769	-0.509		conserved hypothetical protein	Hypothetical proteins
Mxan_4860	-0.698	-1.324	-1.165	-0.196		hypothetical protein	
Mxan_4864	-0.89	-1.12	-0.643	-0.461		hypothetical protein	
Mxan_4876	3.048	4.275	2.183	0.303		lipoprotein, putative	Cell envelope
Mxan_4882	0.385	1.495	4.498	0.537		Ser/Thr protein phosphatase family protein	Unknown function
Mxan_4896	1.823	1.294	0.747	0.237		glutaredoxin, GrxC family	Energy metabolism
Mxan_4897	2.32	1.808	1.98	0.559		hypothetical protein	
Mxan_4898	1.294	1.266	1.835	0.146		hypothetical protein	
Mxan_4909	0.536	0.461	1.576	0.746	*murA*	UDP-N-acetylglucosamine 1-carboxyvinyltransferase	Cell envelope
Mxan_4914	-0.39	-1.471	-2.022	-1.087		F5/8 type C domain protein	Unknown function
Mxan_4923	0.283	0.098	1.457	0.586		hypothetical protein	
Mxan_4932	-0.882	-0.762	-1.235	-1.107		hypothetical protein	
Mxan_4937	0.771	1.729	2.346	-0.211		EGF domain protein	Unknown function
Mxan_4955	-0.841	-1.071	-0.706	-0.437		conserved hypothetical protein	Hypothetical proteins
Mxan_4956	-1.102	-1.795	-1.698	-0.705		hypothetical protein	
Mxan_4960	0.854	1.158	1.991	-0.001		hypothetical protein	
Mxan_4961	0.807	1.1	2.656	0.151		membrane protein, putative	Cell envelope
Mxan_4964	3.529	4.308	4.47	0.493		lipoprotein, putative	Cell envelope
Mxan_4967	-0.82	-1.465	-1.777	-0.233	*lpxC*	UDP-3-O-acyl N-acetylglycosamine deacetylase	Cell envelope
Mxan_4979	1.038	1.427	1.07	0.58		hypothetical protein	
Mxan_5008	0.056	0.44	1.469	0.097		putative membrane protein	Cell envelope
Mxan_5023	-1.085	-0.547	-0.171	-0.064		tonB dependent receptor	Transport and binding
Mxan_5024	-1.829	-1.092	-0.456	-0.218		conserved domain protein	Hypothetical proteins
Mxan_5033	-0.811	-1.535	-1.904	-1.1		hypothetical protein	
Mxan_5041	0.955	1.589	0.933	1.312		sigma-54 dependent transcriptional regulator, Fis family	Regulatory functions
Mxan_5043	-0.285	-0.686	-1.255	-0.473		putative lipoprotein	
Mxan_5050	-0.757	-0.966	-1.152	-0.264		hypothetical protein	
Mxan_5057	2.551	1.381	-0.045	0.141		ribonucleoside-diphosphate reductase, alpha subunit	Purines, pyrimidines,
Mxan_5073	2.374	4.255	4.117	1.166		hypothetical protein	
Mxan_5078	-1.211	-0.855	-0.169	0.173	*rpsF*	ribosomal protein S6	Protein synthesis
Mxan_5079	-1.024	-1.077	-0.194	0.1	*rpsR*	ribosomal protein S18 - POINT MUTATION	Protein synthesis
Mxan_5080	-1.099	-1.205	-0.295	0.117	*rplI*	ribosomal protein L9	Protein synthesis
Mxan_5083	0.924	1.093	1.886	1.356		DNA-binding response regulator	Regulatory functions
Mxan_5092	1.773	1.821	1.232	0.335	*clpB*	ATP-dependent chaperone protein ClpB	Protein fate
Mxan_5102	-1.159	-1.006	-0.707	0.134		hypothetical protein	
Mxan_5116	-0.96	-0.887	-1.104	-0.377		serine/threonine protein kinase	Regulatory functions
Mxan_5123	0.119	1.033	0.993	0.453	*mrpA*	sensor histidine kinase MrpA	Cellular processes
Mxan_5124	0.567	1.126	1.583	0.871	*mrpB*	sigma-54 dependent DNA-binding response regulator MrpB	Cellular processes
Mxan_5125	2.712	1.772	0.597	0.884	*mrpC*	transcriptional regulator MrpC	Cellular processes
Mxan_5126	2.117	1.138	0.405	0.863		hypothetical protein	
Mxan_5127	-0.546	-1.503	-1.62	-1.912		aromatic amino acid hydroxylase, biopterin-dependent	Energy metabolism
Mxan_5131	-0.451	-1.145	-1.116	-0.356		Ser/Thr protein phosphatase family protein	Unknown function
Mxan_5132	0.747	1.072	1.175	0.591		hypothetical protein	
Mxan_5137	2.064	1.724	1.054	0.287		peptidase, M1 (aminopeptidase N) family	Protein fate
Mxan_5138	-0.818	-0.415	-1.028	-0.087		adenine-specific DNA methyltransferase, putative	DNA metabolism
Mxan_5149	1.7	0.705	0.278	0.625	*mcP1*	chemoreceptor McP1	Cellular processes
Mxan_5151	-1.12	-1.365	-0.888	0.181		chemotaxis coupling protein CheW	Cellular processes
Mxan_5152	-1.175	-1.792	-1.031	0.258		OmpA family protein	
Mxan_5155	0.599	0.515	1.78	2.149		aminotransferase, class V	Unknown function
Mxan_5166	0.22	1.466	2.207	1.471		bacterial leucyl aminopeptidase	Protein fate
Mxan_5169	-0.4	-0.58	-1.267	-1.439		hypothetical protein	
Mxan_5172	-1.015	-1.721	-1.362	-0.792		radical SAM domain protein	
Mxan_5179	1.872	2.249	3.903	2.441		tetratricopeptide repeat protein	Unknown function
Mxan_5181	0.439	0.281	1.188	0.427		penicillin-binding protein, 1A family	Cell envelope
Mxan_5185	1.393	1.026	0.962	0.662		O-methyltransferase, putative	Unknown function

Mxan-no.	Log ratio				Gene name	Annotation	GO mainrole
	0.5 h	1 h	2 h	4 h			
Mxan_5186	1.205	0.865	0.251	0.059		transporter, small multidrug resistance (SMR) family	Cellular processes
Mxan_5187	1.376	2.102	2.065	-0.569		hypothetical protein	
Mxan_5188	5.024	6.061	6.416	3.552	*yfiA*	ribosomal subunit interface protein	Protein synthesis
Mxan_5190	4.275	5.336	4.292	1.609		hypothetical protein	
Mxan_5193	-0.772	-0.897	-1.088	-0.183		treponemal membrane protein B precursor-like protein, putative	Cell envelope
Mxan_5194	-1.01	-1.28	-1.051	0.053		OmpA domain protein	Cell envelope
Mxan_5203	1.06	0.764	0.439	0.563	*dnaG*	DNA primase	DNA metabolism
Mxan_5220	1.924	4.379	2.118	-0.064		HhH-GPD domain protein	Unknown function
Mxan_5221	0.645	2.701	0.922	0.066		conserved hypothetical protein	Hypothetical proteins
Mxan_5222	3.492	5.066	4.405	-0.069	*frdB*	fumarate reductase, iron-sulfur protein	Energy metabolism
Mxan_5223	3.014	5.107	3.13	-0.021		4-carboxymuconolactone decarboxylase domain protein	
Mxan_5224	3.001	3.262	1.244	0.203	*frdA*	fumarate reductase, flavoprotein subunit	Energy metabolism
Mxan_5225	5.088	5.164	7.155	1.012	*frdC*	fumarate reductase, cytochrome b subunit	Energy metabolism
Mxan_5242	-0.853	-1.598	-2.284	-1.195		hypothetical protein	
Mxan_5244	1.341	1.349	0.706	0.595		conserved hypothetical protein	Hypothetical proteins
Mxan_5258	0.392	0.82	0.101	1.198		hypothetical protein	
Mxan_5266	0.661	1.013	0.109	0.801		hypothetical protein	
Mxan_5268	0.869	1.142	-0.047	1.345		hypothetical protein	
Mxan_5269	0.149	1.061	0.47	0.241		S1D (lysyl endopeptidase) subfamily C-terminal domain protein	
Mxan_5280	1.306	1.659	0.583	0.925		lipoprotein, putative	Cell envelope
Mxan_5286	1.037	1.741	1.193	0.312		hypothetical protein	
Mxan_5306	-1.072	-1.105	-1.114	-0.652		acetyltransferase, GNAT family	Unknown function
Mxan_5309	0.438	0.558	2.203	1.031		conserved hypothetical protein	Hypothetical proteins
Mxan_5311	0.9	0.921	2.039	0.935		hypothetical protein	
Mxan_5313	0.207	0.443	1.495	0.433		DNA-binding response regulator	Regulatory functions
Mxan_5314	0.34	0.371	1.146	0.069		sensor histidine kinase	Regulatory functions
Mxan_5315	-1.112	-1	-0.586	-0.002		lipoprotein, putative	Cell envelope
Mxan_5324	2.753	1.937	0.606	-0.457		hypothetical protein	
Mxan_5325	1.226	0.673	0.102	-0.162		5`-nucleotidase family protein	Unknown function
Mxan_5327	-1.166	-1.451	-1.499	-0.353	*gmd*	GDP-mannose 4,6-dehydratase	Cell envelope
Mxan_5336	-0.788	-1.155	-1.042	-0.259		conserved hypothetical protein	Hypothetical proteins
Mxan_5343	-1.034	-1.216	-0.81	-0.183	*tsf*	translation elongation factor Ts	Protein synthesis
Mxan_5344	-1.238	-1.496	-0.924	-0.125	*rpsB*	ribosomal protein S2	Protein synthesis
Mxan_5348	2.013	1.376	-0.006	0.161		M23 peptidase domain protein	Protein fate
Mxan_5351	0.305	0.801	1.529	0.747		SNF2/helicase domain protein	
Mxan_5352	-1.13	-0.819	-0.535	-0.444	*apt*	adenine phosphoribosyltransferase	Purines, pyrimidines,
Mxan_5366	1.075	0.864	0.711	0.569		response regulator/GGDEF domain protein	Regulatory functions
Mxan_5368	-0.568	-1.187	-0.973	-0.045		YdjC-like protein	Unknown function
Mxan_5371	0.36	1.049	1.939	0.82	*fadJ*	fatty oxidation complex, alpha subunit FadJ	Fatty acid and
Mxan_5372	0.76	1.288	1.928	0.933		fatty oxidation complex, beta subunit	Fatty acid and
Mxan_5376	0.97	1.48	1.702	0.653		glycosyl hydrolase, family 13	Energy metabolism
Mxan_5378	0.712	1.123	1.333	0.415		sugar ABC transporter, permease protein/periplasmic sugar-binding	Transport and binding
Mxan_5390	-0.574	-1.271	-1.949	-0.586		lipoprotein, putative	Cell envelope
Mxan_5391	1.536	3.118	3.386	1.811		hypothetical protein	
Mxan_5402	1.004	1.65	1.593	0.311		cytochrome c, putative	Energy metabolism
Mxan_5406	-1.011	-0.99	-1.008	-0.395		conserved hypothetical protein	Hypothetical proteins
Mxan_5424	0.87	1.484	4.72	0.732		conserved hypothetical protein	Hypothetical proteins
Mxan_5425	0.57	0.363	2.349	0.202		CapA family protein	Cell envelope
Mxan_5430	**0.543**	**0.98**	**1.41**	**0.27**	***ops***	**development-specific protein S FRAMESHIFT**	**Cellular processes**
Mxan_5432	**0.649**	**1.398**	**1.905**	**0.202**	***tps***	**development-specific protein S**	**Cellular processes**
Mxan_5450	-0.733	-1.076	-1.441	-0.987		lipoprotein, putative	Cell envelope
Mxan_5451	0.482	0.797	1.077	0.42		hypothetical protein	
Mxan_5462	-0.966	-1.198	-0.741	-0.166		hypothetical protein	
Mxan_5469	2.123	2.735	2.309	0.314		male sterility protein homolog	Unknown function
Mxan_5471	2.466	2.405	2.124	-0.005		glutathione S-transferase domain protein	Unknown function
Mxan_5477	0.215	1.126	1.163	0.324		lipoprotein, putative	Cell envelope
Mxan_5478	0.194	2.101	2.523	0.727		LysM domain protein	Unknown function
Mxan_5480	0.568	1.106	0.703	0.318		transcriptional regulator, LysR family	Regulatory functions
Mxan_5481	0.331	1.713	2.054	0.374		lipoprotein, putative	Cell envelope
Mxan_5487	-1.553	-1.78	-1.643	-0.277		Tat (twin-arginine translocation) pathway signal sequence domain protein	Unknown function
Mxan_5488	-1.004	-1.138	-1.578	-0.434		hypothetical protein	
Mxan_5489	0.394	0.977	1.508	0.541	*rpiA*	ribose-5-phosphate isomerase	Energy metabolism
Mxan_5490	-0.538	-0.507	-1.111	-0.568		conserved hypothetical protein	Hypothetical proteins
Mxan_5497	0.662	2.444	1.826	0.545		general secretion pathway protein E, N-terminal domain protein	Unknown function
Mxan_5500	1.727	0.685	0.39	-0.047		GDSL-like lipase/acylhydrolase domain protein	
Mxan_5504	-0.872	-1.112	-0.691	0.062		putative membrane protein	Cell envelope
Mxan_5505	-1.354	-1.299	-0.796	-0.193		response regulator	Regulatory functions
Mxan_5508	-0.525	-1.2	-1.312	-1.284		lipoprotein, putative	Cell envelope
Mxan_5520	-0.662	-1.17	-1.427	-0.961		conserved hypothetical protein	Hypothetical proteins
Mxan_5521	-0.899	-0.977	-1.358	-1.18		hypothetical protein	
Mxan_5522	-0.959	-1.287	-1.09	-1.164		lactonizing lipase	Fatty acid and
Mxan_5524	0.008	0.808	1.061	-0.024		conserved hypothetical protein	Hypothetical proteins
Mxan_5529	3.261	3.245	3.013	0.915		2,3-bisphosphoglycerate-dependent phosphoglycerate mutase, putative	Energy metabolism
Mxan_5531	-2.779	-3.007	-2.681	-2.551		conserved hypothetical protein	Hypothetical proteins
Mxan_5532	-2.745	-3.516	-3.968	-4.223	*hemN*	oxygen-independent coproporphyrinogen III oxidase	Biosynthesis of
Mxan_5535	-0.88	-1.148	-1.61	-1.08		hypothetical protein	

Mxan-no.	Log ratio				Gene name	Annotation	GO mainrole
	0.5 h	1 h	2 h	4 h			
Mxan_5542	-1.727	-1.99	-2.533	-3.236		hypothetical protein	
Mxan_5543	**-3.986**	**-4.77**	**-5.486**	**-5.699**		**ATPase, P-type (transporting), HAD superfamily, subfamily IC**	**Transport + Binding**
Mxan_5544	-1.267	-1.812	-2.002	-2.283		conserved hypothetical protein	Hypothetical proteins
Mxan_5549	0.746	0.698	0.799	1.185		enoyl-CoA hydratase/isomerase family protein	Fatty acid and
Mxan_5551	1.351	0.715	0.273	-0.059		SEC-C motif domain protein	Unknown function
Mxan_5555	1.352	0.781	0.574	3.339		conserved hypothetical protein	Hypothetical proteins
Mxan_5558	-3.312	-4.767	-5.035	-5.524		cytochrome c, putative	Energy metabolism
Mxan_5559	-2.866	-2.28	-2.368	-3.909		nitrate reductase, gamma subunit, putative	Energy metabolism
Mxan_5560	-4.496	-5.189	-5.601	-5.773		cytochrome c family protein	
Mxan_5562	-1.539	-1.449	-1.022	-0.89		cytochrome c peroxidase	
Mxan_5563	0.259	0.476	1.088	0.302		hypothetical protein	
Mxan_5577	-1.005	-0.723	-0.41	-0.283	*ppa*	inorganic pyrophosphatase	Central intermediary
Mxan_5592	-1.401	-1.02	-0.727	-0.228		DNA-binding response regulator	Regulatory functions
Mxan_5595	2.59	1.545	-0.066	0.172	*accC*	acetyl-CoA carboxylase, biotin carboxylase	Fatty acid and
Mxan_5597	-0.804	-0.893	-1.09	-0.441	*ftsZ*	cell division protein FtsZ	Cellular processes
Mxan_5620	0.922	1.11	1.507	1.158		serine/threonine protein kinase	Regulatory functions
Mxan_5626	-0.69	-1.154	-1.221	-0.809		hypothetical protein	
Mxan_5629	3.215	4.331	3.598	0.806		alcohol dehydrogenase, iron-containing	Energy metabolism
Mxan_5630	4.348	5.102	5.068	1.017		glutamine synthetase family protein	Central intermediary
Mxan_5635	2.052	2.088	1.555	0.14		hypothetical protein	
Mxan_5637	-1	-0.755	-0.663	-0.151	*ligA*	DNA ligase, NAD-dependent	DNA metabolism
Mxan_5658	-1.297	-1.237	-1.223	-0.623		hypothetical protein	
Mxan_5668	1.912	2.122	2.711	0.477		hypothetical protein	
Mxan_5670	2.119	1.817	0.975	0.62	*trxB*	thioredoxin	Energy metabolism
Mxan_5674	1.377	1.288	0.808	0.965		hypothetical protein	
Mxan_5688	-1.041	-0.595	-0.619	-0.189		response regulator	Regulatory functions
Mxan_5703	-0.78	-0.421	-0.914	-1.029		PspA/IM30 family protein	Unknown function
Mxan_5705	-1.059	-1.244	-0.83	-0.375		amidohydrolase domain protein	Unknown function
Mxan_5706	-1.071	-1.093	-0.877	-0.358	*cdd*	cytidine deaminase	Purines, pyrimidines,
Mxan_5707	-1.198	-1.23	-0.967	-0.528		hypothetical protein	
Mxan_5718	-1.106	-0.947	-0.601	-0.014		C4-type zinc finger domain protein, DksA/TraR family	Unknown function
Mxan_5719	-1.062	-1.01	-0.863	-0.268	*deoC*	deoxyribose-phosphate aldolase	Energy metabolism
Mxan_5724	-1.152	-0.54	-0.511	0.014		conserved domain protein	Hypothetical proteins
Mxan_5727	-1.273	-1.008	-0.788	-0.475		conserved hypothetical protein	Hypothetical proteins
Mxan_5729	0.48	0.563	0.495	1.345		type II restriction endonuclease, putative	DNA metabolism
Mxan_5730	1.298	1.055	0.825	0.261		putative reverse transcriptase	DNA metabolism
Mxan_5739	0.319	1.175	1.41	0.468		lipoprotein, putative	Cell envelope
Mxan_5740	-1.295	-1.668	-0.806	0.051		glycosyl transferase, group 2	Energy metabolism
Mxan_5742	-1.167	-1.378	-0.969	-0.076		lipoprotein, putative	Cell envelope
Mxan_5743	-1.011	-1.269	-0.879	-0.257		hypothetical protein	
Mxan_5750	-1.325	-1.692	-1.161	0.153	*carF*	carotenoid synthesis regulator CarF	Biosynthesis of
Mxan_5756	-0.587	-1.053	-0.983	0.03	*tolB*	tolB protein	Cellular processes
Mxan_5758	-1.043	-1.186	-0.943	-0.111	*cefD*	isopenicillin N epimerase	Cellular processes
Mxan_5768	-1.155	-0.896	-0.419	0.222	*accB*	acetyl-CoA carboxylase, biotin carboxyl carrier protein	Fatty acid and
Mxan_5769	-1.26	-0.834	-0.361	0.209	*efp*	translation elongation factor P	Protein synthesis
Mxan_5773	-1.131	-0.769	-0.627	0.011		lipoprotein, putative	Cell envelope
Mxan_5774	-1.443	-1.058	-0.671	-0.106	*pilO*	type IV pilus biogenesis protein PilO	Cell envelope
Mxan_5775	-1.42	-1.076	-0.6	-0.261	*pilN*	type IV pilus biogenesis protein PilN	Cell envelope
Mxan_5776	-1.027	-0.961	-0.89	-0.584	*pilM*	type IV pilus biogenesis protein PilM	Cell envelope
Mxan_5783	0.241	-0.582	-2.052	-0.675	*pilA*	pilin	Cell envelope
Mxan_5786	-1.051	-1.108	-1.095	-0.469	*pilC*	type 4 fimbrial assembly protein PilC	Cell envelope
Mxan_5787	-0.921	-1.299	-1.021	-0.52	*pilT*	twitching motility protein PilT	Cell envelope
Mxan_5788	-1.105	-0.76	-0.389	-0.175	*pilB*	type IV-A pilus assembly ATPase PilB	Cell envelope
Mxan_5796	-1.031	-1.646	-1.37	-0.441		HAMP domain protein	Unknown function
Mxan_5797	-1.055	-1.555	-1.231	-0.314		PBS lyase HEAT repeat-like domain protein	Unknown function
Mxan_5808	3.181	2.727	1.193	-0.052		carboxyl-terminal protease family protein	Protein fate
Mxan_5809	-0.738	-0.753	-1.05	-0.464		hypothetical protein	
Mxan_5814	-1.047	-0.779	-0.807	-0.401		putative transcriptional regulator	Regulatory functions
Mxan_5817	1.476	1.678	1.417	0.602		anion-transporting ATPase family protein	Transport and binding
Mxan_5818	0.949	1.106	1.044	0.451	*agmR*	anion-transporting ATPase	Transport and binding
Mxan_5819	0.806	1.365	2.403	1.149		conserved domain protein	Hypothetical proteins
Mxan_5820	0.675	0.915	1.576	0.822	*agmM*	peptidase, M48 (Ste24 endopeptidase) family, AgmM	Protein fate
Mxan_5826	2.099	2.223	1.236	0.175	*prkA*	PrkA protein	Regulatory functions
Mxan_5827	1.673	2.102	1.046	-0.063		conserved hypothetical protein	Hypothetical proteins
Mxan_5828	**2.077**	**2.501**	**1.263**	**0.047**	***cbgA***	**SpoVR homolog**	
Mxan_5836	1.645	1.084	0.518	-0.471		peptidase, M3 (thimet oligopeptidase) family	Protein fate
Mxan_5837	-0.858	-1.186	-0.898	-0.118		bacterial Ig-like domain (group 1)/fibronectin type III domain protein	Unknown function
Mxan_5844	1.364	1.007	0.217	-0.002	*dnaE*	DNA polymerase III, alpha subunit	DNA metabolism
Mxan_5845	0.391	0.879	2.362	1.021		conserved hypothetical protein	Hypothetical proteins
Mxan_5846	0.902	1.009	1.405	0.48		hypothetical protein	
Mxan_5855	1.405	2.219	2.2	1.332		hypothetical protein	
Mxan_5856	1.231	2.425	2.24	1.332	*acsA*	acetate--CoA ligase	Energy metabolism
Mxan_5857	0.849	2.107	2.088	1.041		conserved hypothetical protein	Hypothetical proteins
Mxan_5858	0.772	2.043	2.006	0.89		phenylacetic acid permease PaaL	Transport and binding
Mxan_5859	0.339	1.712	1.287	0.511		cation channel family protein	Transport and binding
Mxan_5860	0.52	0.701	2.201	0.239		metallo-beta-lactamase family protein	Unknown function

Mxan-no.	Log ratio				Gene name	Annotation	GO mainrole
	0.5 h	1 h	2 h	4 h			
Mxan_5873	-0.752	-0.701	-1.201	-0.645	*gdhA*	glutamate dehydrogenase	Amino acid
Mxan_5877	-0.229	-1.135	-1.161	-0.667		YceI-like family protein	
Mxan_5880	2.491	1.695	0.84	-0.107		hypothetical protein	
Mxan_5887	-0.056	0.058	1.053	-0.218		trypsin domain protein	Unknown function
Mxan_5888	0.349	0.426	2.614	0.441		conserved hypothetical protein	Hypothetical proteins
Mxan_5896	1.234	1.389	1.192	-0.12		oxidoreductase, short chain dehydrogenase/reductase family	Unknown function
Mxan_5897	1.004	1.414	0.949	0.108		Phosphotransferase enzyme family domain protein	Cellular processes
Mxan_5898	0.665	1.141	0.574	0.106		conserved hypothetical protein	Hypothetical proteins
Mxan_5900	1.01	1.513	1.163	0.57		conserved hypothetical protein	Hypothetical proteins
Mxan_5902	1.345	1.466	1.874	1.64		putative homoserine-O-acetyltransferase	Amino acid
Mxan_5908	1.185	1.145	0.628	-0.097		histone deacetylase family protein	
Mxan_5909	0.416	0.768	1.049	0.255		oxidoreductase, short chain dehydrogenase/reductase family	Unknown function
Mxan_5911	2.949	2.078	0.911	0.462		penicillin-binding protein, 1A family	Cell envelope
Mxan_5913	1.025	1.23	0.663	0.472		hypothetical protein	
Mxan_5919	2.921	2.921	1.393	-0.03	*etfA*	electron transfer flavoprotein, alpha subunit	Energy metabolism
Mxan_5920	2.773	2.871	1.306	-0.117	*etfB*	electron transfer flavoprotein, beta subunit	Energy metabolism
Mxan_5922	-1.002	-1.072	-1.236	-0.446		transaldolase, putative	Energy metabolism
Mxan_5935	1.021	0.336	0.989	1.737		phosphorylase, family 2	Unknown function
Mxan_5954	2.009	1.754	1.479	0.316		conserved hypothetical protein	Hypothetical proteins
Mxan_5955	0.581	1.016	0.332	0.381		membrane protein, putative	Cell envelope
Mxan_5956	1.159	1.921	1.383	0.511		MIP family channel protein	Transport and binding
Mxan_5964	1.128	0.533	0.131	0.643		putative membrane protein - POINT MUTATION	Cell envelope
Mxan_5970	-1.012	-1.071	-0.612	-0.285		peptidase, S8 (subtilisin) family	Protein fate
Mxan_5974	1.968	0.422	0.081	0.183		hydrolase, alpha/beta fold family	Unknown function
Mxan_5975	1.458	1.641	2.97	0.396		lipoprotein, putative	Cell envelope
Mxan_5976	-1.029	-0.826	-0.571	-0.892		serine/threonine protein kinase, putative	Regulatory functions
Mxan_5977	-1.448	-1.363	-1.613	-0.962		conserved hypothetical protein	Hypothetical proteins
Mxan_5981	-1.007	-0.625	-0.646	-0.568		putative ribonuclease D	Transcription
Mxan_5983	0.298	1.078	0.967	0.344		O-methyltransferase family protein	
Mxan_5984	4.674	4.427	2.805	1.159		hypothetical protein	
Mxan_5985	0.594	1.125	1.054	0.722		conserved domain protein	Hypothetical proteins
Mxan_5988	1.063	0.625	0.673	0.262		thermostable carboxypeptidase 1	
Mxan_5999	1.036	0.352	0.497	0.367		kelch domain protein	Unknown function
Mxan_6000	-1.829	-1.68	-1.102	-0.129		iron compound ABC transporter, periplasmic iron compound-binding	Transport and binding
Mxan_6008	-1.248	-1.28	-1.273	-1.263		chitinase, class II	Energy metabolism
Mxan_6011	0.412	0.686	1.176	0.209		peptidase, M20 (glutamate carboxypeptidase) family	Protein fate
Mxan_6014	1.28	1.327	1.367	0.854		hypothetical protein	
Mxan_6027	-0.595	-1.334	-1.114	-0.557		methyl-accepting chemotaxis protein	Cellular processes
Mxan_6029	-1.166	-1.575	-1.101	-0.401		chemotaxis sensor histidine kinase/response regulator	Regulatory functions
Mxan_6033	-1.048	-1.123	-1.014	-0.213		chemotaxis protein CheY, putative	
Mxan_6035	-1.059	-1.111	-0.579	-0.06	*sucA*	2-oxoglutarate dehydrogenase, E1 component	Energy metabolism
Mxan_6036	-0.973	-1.126	-0.661	-0.089	*sucB*	2-oxoglutarate dehydrogenase, E2 component, dihydrolipoamide	Energy metabolism
Mxan_6040	1.762	1.73	1.405	0.536		hypothetical protein	
Mxan_6061	-0.997	-1.12	-0.548	-0.114	*aroF*	phospho-2-dehydro-3-deoxyheptonate aldolase	Amino acid
Mxan_6065	-0.635	-1.044	-0.551	-0.333	*trpB*	tryptophan synthase, beta subunit	Amino acid
Mxan_6066	-0.802	-0.906	-1.013	-0.578	*trpA*	tryptophan synthase, alpha subunit	Amino acid
Mxan_6073	0.416	0.444	1.947	0.011		conserved hypothetical protein	Hypothetical proteins
Mxan_6078	-1.377	-1.413	-0.886	-0.078		cytochrome c, putative	Energy metabolism
Mxan_6079	-1.589	-1.541	-0.88	-0.113		molybdopterin oxidoreductase, iron-sulfur binding subunit, putative	Energy metabolism
Mxan_6080	-1.295	-1.592	-1.082	-0.328		polysulfide reductase, subunit C, putative	Energy metabolism
Mxan_6081	-1.274	-1.757	-1.171	-0.373		conserved hypothetical protein	Hypothetical proteins
Mxan_6082	-1.043	-1.6	-1.121	-0.318		cytochrome c family protein	Energy metabolism
Mxan_6083	-1.373	-1.875	-1.472	-0.586		putative membrane protein	Cell envelope
Mxan_6084	-1.21	-1.6	-1.187	-0.349		hypothetical protein	
Mxan_6085	-0.776	-1.097	-0.85	0.058		conserved hypothetical protein	Hypothetical proteins
Mxan_6086	**-1.03**	**-1.379**	**-1.074**	**-0.317**	***coxA***	**cytochrome c oxidase, subunit II**	**Energy metabolism**
Mxan_6087	**-0.708**	**-1.245**	**-0.907**	**-0.078**	***coxA***	**cytochrome c oxidase, subunit I**	**Energy metabolism**
Mxan_6088	**-0.759**	**-1.478**	**-1.16**	**-0.39**	***coxC***	**cytochrome c oxidase, subunit III**	**Energy metabolism**
Mxan_6089	**-0.563**	**-1.355**	**-1.176**	**-0.306**		**cytochrome c oxidase, subunit IV, putative**	**Energy metabolism**
Mxan_6090	-1.441	-2.42	-2.441	-0.704		hypothetical protein	
Mxan_6098	0.887	1.444	0.807	0		hypothetical protein	
Mxan_6100	-0.537	-0.888	-1.09	-0.359		hypothetical protein	
Mxan_6107	-0.468	-1.221	-1.18	-0.196		oxidoreductase, zinc-binding dehydrogenase family	
Mxan_6114	0.519	0.784	1.013	0.066		adenylate/guanylate cyclase domain protein	Unknown function
Mxan_6115	1.899	1.566	-0.211	0.481		hypothetical protein	
Mxan_6116	2.943	1.96	0.335	0.245		hypothetical protein	
Mxan_6117	3.045	2.373	0.198	-0.067		sensory box histidine kinase	Regulatory functions
Mxan_6121	-1.428	-1.686	-1.516	-0.673		hypothetical protein	
Mxan_6122	-0.374	-0.756	-1.063	-0.328	*gst*	glutathione S-transferase	Cellular processes
Mxan_6123	-0.196	-1.011	-1.14	-0.321		glyoxalase family protein	Unknown function
Mxan_6129	0.264	0.475	1.35	0.128		transcriptional regulator, LysR family	Regulatory functions
Mxan_6134	-0.67	-1.181	-0.92	-0.608		Ig-like domain/kelch domain protein	Unknown function
Mxan_6142	-0.968	-1.335	-1.198	-0.546		conserved hypothetical protein	Hypothetical proteins
Mxan_6185	-0.915	-1.302	-0.605	-0.167		hypothetical protein	
Mxan_6187	-0.631	-1.11	-1.155	-0.56		hypothetical protein	
Mxan_6188	2.393	4.676	4.952	1.891	*katE*	catalase HPII	Cellular processes

Mxan-no.	Log ratio				Gene name	Annotation	GO mainrole
	0.5 h	1 h	2 h	4 h			
Mxan_6190	-1.06	-1.231	-1.279	-0.498		sodium/solute symporter	Transport and binding
Mxan_6193	-0.356	-0.624	-1.192	-0.688		conserved hypothetical protein	Hypothetical proteins
Mxan_6194	-0.416	-1.23	-1.822	-0.784		conserved hypothetical protein	Hypothetical proteins
Mxan_6195	-0.188	-1.113	-1.588	-0.7		glycosyl transferase, group 1 family protein	Cell envelope
Mxan_6196	-0.787	-1.199	-1.58	-0.949		hypothetical protein	
Mxan_6197	-0.322	-0.921	-1.898	-1.347		hypothetical protein	
Mxan_6208	1.054	1.44	2.846	-0.162		hypothetical protein	
Mxan_6209	**7.016**	**7.134**	**6.771**	**6.559**	***sigC***	**RNA polymerase sigma-C factor**	**Transcription**
Mxan_6219	-0.478	-0.813	-1.841	-0.959		lipoprotein, putative	Cell envelope
Mxan_6220	-0.567	-0.56	-1.11	-0.716		isoleucyl-tRNA synthetase, mupirocin resistant, putative	Cellular processes
Mxan_6223	-1.083	-1.158	-0.905	-0.58		sensor histidine kinase	Regulatory functions
Mxan_6225	-0.86	-0.813	-1.002	-0.484		lipoprotein, putative	Cell envelope
Mxan_6236	2.006	2.179	0.389	0.518		polysaccharide-degrading enzyme, putative	Cell envelope
Mxan_6240	0.256	0.769	1.224	0.046		hypothetical protein	
Mxan_6242	-0.821	-1.343	-1.828	-1.267		hypothetical protein	
Mxan_6247	-1.295	-1.153	-1.291	-0.458		terpene synthase family protein	Cellular processes
Mxan_6248	-2.112	-3.049	-3.191	-0.944		cyclic nucleotide-binding domain protein	
Mxan_6249	-1.429	-2.348	-2.996	-0.792		cyclic nucleotide-binding domain protein	
Mxan_6258	0.622	0.823	2.35	0.219		hypothetical protein	
Mxan_6259	0.509	0.659	1.946	0.029	*agmJ*	adventurous gliding motility protein AgmJ	Cellular processes
Mxan_6261	-0.945	-0.61	-1.191	-0.751		RNA-directed DNA polymerase from retron mx65	DNA metabolism
Mxan_6264	0.126	0.629	2.667	0.522		conserved hypothetical protein	Hypothetical proteins
Mxan_6272	-0.945	-2.154	-2.48	-0.794		conserved hypothetical protein	Hypothetical proteins
Mxan_6274	0.156	0.242	1.03	0.403		polysaccharide deacetylase domain protein	Unknown function
Mxan_6280	0.369	1.109	1.74	1.228		hypothetical protein	
Mxan_6281	0.356	1.033	1.092	0.309		hypothetical protein	
Mxan_6306	-0.063	-1.452	-1.682	-1.349		fatty acid desaturase family protein	Fatty acid and
Mxan_6313	0.928	1.362	0.687	0.254		lipoprotein, putative	Cell envelope
Mxan_6315	2.356	2.532	1.91	0.458		sensor histidine kinase/response regulator	Regulatory functions
Mxan_6316	-1.203	-1.575	-1.319	0.03		GTP cyclohydrolase family protein	
Mxan_6323	0.218	0.73	2.841	0.273		oxidoreductase, zinc-binding dehydrogenase family	
Mxan_6325	0.515	1.161	-0.053	-0.057		oxidoreductase, short chain dehydrogenase/reductase family	
Mxan_6332	0.915	0.85	2.406	0.193		conserved hypothetical protein	Hypothetical proteins
Mxan_6335	0.975	1.152	1.159	0.403		sensor histidine kinase/response regulator	Regulatory functions
Mxan_6336	1.506	1.827	2.318	0.131		conserved hypothetical protein	Hypothetical proteins
Mxan_6339	-0.719	-1.101	-0.679	-0.16		vitamin K epoxide reductase family/thioredoxin domain protein	Unknown function
Mxan_6351	-1.03	-0.908	-1.037	-0.523		hypothetical protein	
Mxan_6352	-0.902	-1.177	-1.075	-0.325		conserved domain protein	Hypothetical proteins
Mxan_6362	1.002	0.682	1.165	0.47		conserved domain protein	Hypothetical proteins
Mxan_6366	1.595	1.778	1.523	-0.115		hypothetical protein	
Mxan_6367	0.997	1.489	1.489	-0.092		lipoprotein, putative	Cell envelope
Mxan_6368	3.315	2.593	1.357	0.188		hypothetical protein	
Mxan_6371	1.581	1.576	0.879	0.075	*nagB*	glucosamine-6-phosphate isomerase	Central intermediary
Mxan_6375	-1.067	-1.244	-1.484	-1.094		hypothetical protein	
Mxan_6382	0.698	0.9	1.08	1.377		FHA domain protein	Unknown function
Mxan_6399	-0.84	-1.584	-1.361	-0.971		3-oxoacyl-(acyl-carrier-protein) reductase, putative	
Mxan_6409	0.269	1.164	1.075	0.06		beta-lactamase, putative	Cellular processes
Mxan_6417	-1.078	-1.143	-1.195	-0.457	*exsB*	exsB protein	Unknown function
Mxan_6430	2.115	2.127	2.837	0.292		hypothetical protein	
Mxan_6431	1.564	1.795	3.889	0.49		cardiolipin synthetase domain protein	Unknown function
Mxan_6432	1.133	1.28	1.351	0.111		acyl-CoA dehydrogenase, putative	Fatty acid and
Mxan_6433	4.649	6.039	5.09	1.489		putative lipoprotein	Cell envelope
Mxan_6435	3.919	4.087	4.03	1.87		peptidase, M48 family	Protein fate
Mxan_6436	4.668	4.682	3.718	1.966		conserved domain protein	Hypothetical proteins
Mxan_6437	-0.538	-1.302	-1.805	-3.133		lipoprotein, putative	Cell envelope
Mxan_6438	1.738	2.028	1.665	0.244	*clpP*	ATP-dependent Clp protease, proteolytic subunit ClpP	Protein fate
Mxan_6439	1.111	1.324	1.351	0.395	*fumC*	fumarate hydratase, class II	Energy metabolism
Mxan_6441	**5.18**	**5.093**	**3.226**	**0.741**	***aceB***	**malate synthase A**	**Energy metabolism**
Mxan_6442	**6.11**	**6.978**	**5.2**	**1.352**	***aceA***	**isocitrate lyase**	**Energy metabolism**
Mxan_6444	0.367	0.443	1.443	0.079		hypothetical protein	
Mxan_6446	0.396	1.095	0.177	0.027		hypothetical protein	
Mxan_6457	0.116	1.052	0.527	-0.068		lipoprotein, putative	Cell envelope
Mxan_6458	2.038	1.599	0.704	0.446		DedA family protein	Unknown function
Mxan_6463	2.927	2.441	1.507	0.099	*malQ*	4-alpha-glucanotransferase	Energy metabolism
Mxan_6464	1.21	1.904	1.825	0.45		outer membrane protein, OMP85 family	Cell envelope
Mxan_6465	1.769	2.114	1.671	0.032		conserved hypothetical protein	Hypothetical proteins
Mxan_6467	-0.944	-1.465	-1.746	-1.116		lipoprotein, putative	Cell envelope
Mxan_6469	0.451	0.201	1.448	0.255	*trx*	thioredoxin	Energy metabolism
Mxan_6481	-0.026	0.94	2.067	0.468		conserved hypothetical protein	Hypothetical proteins
Mxan_6488	-1.07	-1.173	-0.957	-0.32		hypothetical protein	
Mxan_6491	1.647	2.193	2.248	0.352		cation-transporting ATPase, E1-E2 family	Transport and binding
Mxan_6496	1.56	1.724	0.642	0.059	*tpx*	thiol peroxidase	Cellular processes
Mxan_6500	1.324	1.87	1.24	-0.36		serine/threonine protein kinase	Regulatory functions
Mxan_6501	-1.329	-1.269	-1.201	-0.573		mannose-1-phosphate guanylyltransferase	Cell envelope
Mxan_6513	2.383	1.868	0.889	0.223		hydrolase, NUDIX family	Unknown function
Mxan_6516	-0.835	-0.996	-1.184	-0.672	*ahcY*	adenosylhomocysteinase	Energy metabolism

Mxan-no.	Log ratio				Gene name	Annotation	GO mainrole
	0.5 h	1 h	2 h	4 h			
Mxan_6520	-1.365	-1.087	-1.294	-0.646		membrane protein, putative	Cell envelope
Mxan_6538	-1.667	-3.082	-2.302	-2.875		hypothetical protein	
Mxan_6539	-1.627	-1.813	-1.252	-1.153		extracellular protease domain protein	
Mxan_6543	3.268	4.346	3.062	0.555		Ser/Thr protein phosphatase family protein	Unknown function
Mxan_6544	1.128	1.343	0.536	-0.162		hypothetical protein	
Mxan_6550	-0.343	-0.621	-1.067	-0.369		glycosyl hydrolase, family 15	Energy metabolism
Mxan_6563	-0.491	-0.881	-1.016	-0.419		lipoprotein, putative	Cell envelope
Mxan_6566	0.219	1.259	0.894	0.315		HIT domain protein	Unknown function
Mxan_6572	-0.698	-1.329	-1.977	-1.007		iron-sulfur cluster-binding protein, Rieske family	Energy metabolism
Mxan_6573	-0.545	-1.202	-1.809	-0.529		putative lipoprotein	
Mxan_6574	-0.427	-1.17	-1.656	-0.432		lipoprotein, putative	Cell envelope
Mxan_6580	3.441	3.958	1.795	0.41		FHA domain protein	Unknown function
Mxan_6589	-1.34	-1.229	-1.256	-0.665		peptidase, family C69	Protein fate
Mxan_6599	0.549	0.864	1.009	-0.115		conserved hypothetical protein	Hypothetical proteins
Mxan_6601	-1.304	-1.256	-1.408	-0.885		peptidase, S9C (acylaminoacyl-peptidase) subfamily	
Mxan_6609	3.334	3.21	3.392	0.788		putative lipoprotein	
Mxan_6623	-0.578	-0.956	-1.386	-0.707		hypothetical protein	
Mxan_6624	-0.971	-1.429	-1.504	-0.841		AhpC/TSA family protein	
Mxan_6625	-1.321	-1.206	-0.693	-0.37		hypothetical protein	
Mxan_6636	0.732	1.04	1.088	-0.194		AMP-binding protein	
Mxan_6639	1.194	1.73	1.384	0.424		chalcone/stilbene synthase family protein	Unknown function
Mxan_6640	-0.696	-0.851	-1.221	0.061		hypothetical protein	
Mxan_6641	-1.203	-1.244	-1.554	-0.392		hypothetical protein	
Mxan_6651	0.701	1.03	2.162	1.542		endonuclease/exonuclease/phosphatase family protein	Unknown function
Mxan_6657	0.997	1.006	1.82	0.39		conserved hypothetical protein	Hypothetical proteins
Mxan_6666	0.448	1.111	2.066	0.363		hypothetical protein	
Mxan_6668	0.386	0.936	4.1	1.005		conserved hypothetical protein	Hypothetical proteins
Mxan_6693	-1.047	-0.644	-1.054	-0.588	*difD*	fibril biogenesis regulator DifD	Cellular processes
Mxan_6694	-0.703	-0.726	-1	-0.288	*difC*	fibril biogenesis regulator DifC	Cellular processes
Mxan_6696	-0.727	-0.764	-1.004	-0.226	*difA*	methyl-accepting chemotaxis protein DifA	Cellular processes
Mxan_6699	0.621	0.501	1.08	0.398		lipoprotein, putative	
Mxan_6700	0.834	0.742	0.47	1.072		conserved hypothetical protein	Hypothetical proteins
Mxan_6712	1.3	1.694	2.697	0.45		hypothetical protein	
Mxan_6713	3.094	3.454	4.854	1.452		hypothetical protein	
Mxan_6718	1.385	1.796	1.285	0.019		hypothetical protein	
Mxan_6719	2.165	2.508	1.506	0.502		peptidase, M50 (S2P protease) family	Protein fate
Mxan_6720	-1.062	-1.004	-1.411	-0.528		lipoprotein, putative	Cell envelope
Mxan_6722	6.431	6.231	5.81	1.423		HAD-superfamily hydrolase, subfamily IA, variant 1	Unknown function
Mxan_6723	3.166	3.621	3.593	1.719		conserved hypothetical protein	Hypothetical proteins
Mxan_6724	4.097	4.216	3.729	1.892		conserved hypothetical protein TIGR00147	Hypothetical proteins
Mxan_6728	1.144	0.995	1.916	0.581		oxidoreductase, zinc-binding dehydrogenase family	Unknown function
Mxan_6734	1.113	1.275	0.862	0.19		response regulator/sensory box histidine kinase	Regulatory functions
Mxan_6735	-0.663	-1.051	-1.163	-0.582		sensor histidine kinase/response regulator	Regulatory functions
Mxan_6752	3.039	2.96	5.65	3.472		lipoprotein, putative	Cell envelope
Mxan_6753	3.787	3.289	3.034	1.841		phospholipase D family protein	Fatty acid and
Mxan_6755	-1.77	-1.2	-0.491	-0.056		hypothetical protein	
Mxan_6756	-1.491	-1.029	-0.468	-0.127		conserved hypothetical protein	Hypothetical proteins
Mxan_6759	-1.215	-1.073	-1.338	-0.652	*rpoE*	RNA polymerase sigma-E factor	Transcription
Mxan_6763	-0.753	-0.773	-1.141	-0.603		conserved hypothetical protein	Hypothetical proteins
Mxan_6764	2.362	1.696	1.277	0.218		hydrolase, alpha/beta fold family	Unknown function
Mxan_6770	0.428	0.619	4.599	0.416		hypothetical protein	
Mxan_6776	0.236	1.301	1.793	0.43		hypothetical protein	
Mxan_6780	0.636	0.526	1.754	0.554		hypothetical protein	
Mxan_6781	1.431	0.858	1.458	-0.112		hypothetical protein	
Mxan_6782	0.985	0.609	1.015	-0.356		conserved hypothetical protein, selenocysteine-containing	
Mxan_6788	3.283	2.576	1.667	0.543		conserved domain protein	Hypothetical proteins
Mxan_6790	0.442	1.285	1.482	0.212		conserved hypothetical protein	Hypothetical proteins
Mxan_6797	-0.347	-0.727	-1.294	-0.964		putative membrane protein	Cell envelope
Mxan_6802	1.017	1.188	0.563	0.31	*adh*	alcohol dehydrogenase, zinc-containing	Energy metabolism
Mxan_6805	**-1.509**	**-1.892**	**-1.933**	**-0.528**	***rpsD***	**ribosomal protein S4**	**Protein synthesis**
Mxan_6807	-0.952	-1.407	-1.557	-0.879		lipoprotein, putative	Cell envelope
Mxan_6815	1.196	1.876	1.512	1.003		hypothetical protein	
Mxan_6816	0.751	1.467	1.263	0.379		hypothetical protein	
Mxan_6819	1.244	0.778	0.362	1.111		hypothetical protein	
Mxan_6843	1.207	0.816	-1.427	0.952		putative membrane protein	Cell envelope
Mxan_6849	-0.037	0.937	1.024	-0.025		peptidyl-prolyl cis-trans isomerase, FKBP-type	Protein fate
Mxan_6850	1.366	1.617	1.64	0.78		hypothetical protein	
Mxan_6856	0.969	1.146	0.384	0.396		hypothetical protein	
Mxan_6857	0.475	1.179	1.276	0.134		putative membrane protein	Cell envelope
Mxan_6859	2.914	2.747	1.51	0.5	*gph*	phosphoglycolate phosphatase	Energy metabolism
Mxan_6860	2.263	2.024	0.651	0.029	*aglS*	adventurous gliding motility protein AglS	Cellular processes
Mxan_6861	2.828	2.6	1.087	0.213		biopolymer transport protein, ExbD/TolR family	
Mxan_6862	3.059	2.509	0.94	0.202		MotA/TolQ/ExbB proton channel family protein	
Mxan_6870	0.595	0.544	1.064	0.254		conserved hypothetical protein	Hypothetical proteins
Mxan_6873	0.349	0.571	1.016	0.686		conserved hypothetical protein	
Mxan_6874	0.434	0.668	0.792	1.018	*phaC*	poly(R)-hydroxyalkanoic acid synthase, class III, PhaC subunit	Fatty acid and

Mxan-no.	Log ratio				Gene name	Annotation	GO mainrole
	0.5 h	1 h	2 h	4 h			
Mxan_6880	2.163	1.459	0.532	0.557		hypothetical protein	
Mxan_6882	1.806	1.456	0.882	0.05		transcription elongation factor, GreA/GreB family	Transcription
Mxan_6883	0.273	1.159	1.237	-0.013		dienelactone hydrolase family protein	Energy metabolism
Mxan_6884	-1.258	-1.54	-1.484	-0.642		hypothetical protein	
Mxan_6888	0.476	0.729	1.119	0.176		hypothetical protein	
Mxan_6901	0.186	1.227	3.564	1.003		metallo-beta-lactamase family protein	Unknown function
Mxan_6911	-0.32	-0.572	-1.374	-0.431		TonB-dependent receptor	Transport and binding
Mxan_6913	-0.692	-1.517	-0.782	-1.814	*cydA*	cytochrome d ubiquinol oxidase, subunit I	Energy metabolism
Mxan_6914	2.14	2.15	4.864	2.175		hypothetical protein	
Mxan_6915	1.582	2.058	5.018	1.7		hypothetical protein	
Mxan_6921	**-1.382**	**-1.422**	**-1.055**	**-0.248**	***atpC***	**ATP synthase F1, epsilon subunit**	**Energy metabolism**
Mxan_6922	-1.415	-1.522	-1.055	-0.265		hypothetical protein	
Mxan_6923	**-1.438**	**-1.432**	**-0.533**	**0.275**	***atpD***	**ATP synthase F1, beta subunit**	**Energy metabolism**
Mxan_6928	0.204	0.508	2.539	1.142		hypothetical protein	
Mxan_6936	0.612	1.496	1.557	0.236		hypothetical protein	
Mxan_6937	2.312	3.88	4.621	1.502		CsbD-like family	Cellular processes
Mxan_6946	0.676	1.006	0.208	0.526		hypothetical protein	
Mxan_6950	1.034	1.092	0.711	-0.006		methyl-accepting chemotaxis protein	
Mxan_6953	0.85	1.107	0.665	0.084		sensory box histidine kinase	Regulatory functions
Mxan_6956	1.281	1.333	0.406	-0.201	*dotR*	response regulator DotR	Regulatory functions
Mxan_6959	0.921	1.192	0.19	0.22	*cheB*	protein-glutamate methylesterase	Cellular processes
Mxan_6960	0.522	1.19	0.673	0.088	*cheR*	chemotaxis protein methyltransferase CheR	Cellular processes
Mxan_6961	0.672	1.223	0.675	-0.057		PBS lyase HEAT-like repeat protein	Unknown function
Mxan_6962	1.17	1.382	1.122	-0.061		methyl-accepting chemotaxis protein	Cellular processes
Mxan_6963	0.944	1.22	0.927	0.047		chemotaxis protein CheW, putative	Cellular processes
Mxan_6965	1.382	1.468	1.198	0.459		chemotaxis protein CheY, putative	
Mxan_6966	1.091	1.732	1.5	0.569		response regulator/sensory box histidine kinase	Regulatory functions
Mxan_6968	3.587	3.607	3.175	1.344		response regulator	Regulatory functions
Mxan_6969	**4.934**	**5.416**	**7.665**	**4.884**	***mspC***	**hypothetical protein**	
Mxan_6970	0.918	2.156	2.99	0.433		hypothetical protein	
Mxan_6972	0.315	1.006	1.638	0.825		Ser/Thr protein phosphatase family protein	Unknown function
Mxan_6976	-1.589	-1.54	-0.67	0.574		hypothetical protein	
Mxan_6978	-1.744	-1.756	-0.928	0.339		lipoprotein, putative	Cell envelope
Mxan_6979	-0.798	-1.048	-0.899	0.033		sensor histidine kinase	Regulatory functions
Mxan_6981	-1.179	-1.086	-1.277	-0.47		conserved hypothetical protein	Hypothetical proteins
Mxan_6985	-0.296	-0.616	-1.251	-0.983		hypothetical protein	
Mxan_6986	-0.69	-0.956	-1.201	-0.595		aldehyde dehydrogenase family protein	Energy metabolism
Mxan_6987	-0.976	-0.716	-1.015	-0.499	*fadJ*	fatty oxidation complex, alpha subunit	Fatty acid and
Mxan_6991	-0.367	-0.858	-1.153	-0.921		hypothetical protein	
Mxan_6993	3.706	4.539	2.148	0.657		conserved hypothetical protein	Hypothetical proteins
Mxan_6995	0.557	0.993	1.292	0.625		hypothetical protein	
Mxan_6996	0.704	1.121	0.984	0.295	*asgD*	response regulator/sensor histidine kinase AsgD	Cellular processes
Mxan_6998	-1.483	-1.304	-1.489	-0.528		DNA-binding protein	
Mxan_6999	-0.903	-0.84	-1.137	0.056		hypothetical protein	
Mxan_7000	-0.769	-0.335	-1.247	-0.381		lipoprotein, putative	Cell envelope
Mxan_7001	2.465	2.878	1.829	0.903		response regulator	Regulatory functions
Mxan_7002	1.413	1.896	0.738	0.233		sensory box histidine kinase	Regulatory functions
Mxan_7006	1.285	2.06	1.748	1.392		hypothetical protein	
Mxan_7012	1.384	1.137	0.807	0.026		hypothetical protein	
Mxan_7021	1.309	1.885	1.904	0.583		putative esterase	Unknown function
Mxan_7023	1.043	1.477	0.662	-0.06		lipoprotein, putative	Cell envelope
Mxan_7024	1.476	1.979	1.355	0.333		response regulator	Regulatory functions
Mxan_7026	**-1.017**	**-1.122**	**-0.771**	**0.053**	***atpH***	**ATP synthase F1, delta subunit**	**Energy metabolism**
Mxan_7030	-0.709	-0.582	-1.061	-0.234		hypothetical protein	
Mxan_7035	1.705	2.459	2.425	0.427		conserved hypothetical protein	Hypothetical proteins
Mxan_7036	2.394	2.217	1.568	0.508		hypothetical protein	
Mxan_7037	-1.056	-1.335	-1.529	-0.45		chemotaxis MotB protein, putative	Cellular processes
Mxan_7039	-0.827	-1.139	-1.089	-0.179		lipoprotein, putative	Cell envelope
Mxan_7040	-0.795	-1.192	-1.227	-0.342		outer membrane protein P1, putative	Cell envelope
Mxan_7052	0.732	1.188	1.183	0.301		hypothetical protein	
Mxan_7053	0.673	1.056	1.982	0.857		NmrA-like family protein	Unknown function
Mxan_7054	1.121	1.147	2.41	0.31		hypothetical protein	
Mxan_7059	0.277	0.584	1.027	0.578		sensory box histidine kinase	Regulatory functions
Mxan_7072	0.009	0.376	1.017	0.748		transcriptional regulator, GntR family/aminotransferase, classes I and II	Regulatory functions
Mxan_7073	0.026	0.607	1.754	0.578		hypothetical protein	
Mxan_7082	0.206	0.748	1.062	0.446		serine/threonine protein kinase	Regulatory functions
Mxan_7084	-1.413	-1.082	-0.82	-1.007	*map*	methionine aminopeptidase, type I	Protein fate
Mxan_7085	-2.449	-2.391	-2.188	-2.272		hypothetical protein	
Mxan_7086	-1.939	-2.777	-3.089	-3.533		conserved domain protein	Hypothetical proteins
Mxan_7088	-0.984	-1.301	-0.85	-0.831		hypothetical protein	
Mxan_7089	-1.058	-1.623	-1.416	-0.782		lipoprotein, putative	Cell envelope
Mxan_7096	0.672	0.832	1.346	-0.228		conserved hypothetical protein	Hypothetical proteins
Mxan_7098	2.807	3.368	4.45	1.004		hypothetical protein	
Mxan_7099	1.993	2.392	3.884	0.629		hypothetical protein	
Mxan_7104	-0.792	-1.132	-1.269	-0.605		peptidase, M3 (thimet oligopeptidase) family	Protein fate
Mxan_7112	-1.344	-1.229	-1.119	-0.853		conserved hypothetical protein	Hypothetical proteins

Mxan-no.	Log ratio				Gene name	Annotation	GO mainrole
	0.5 h	1 h	2 h	4 h			
Mxan_7113	-0.93	-1.243	-1.368	-1.073		lipoprotein, putative	Cell envelope
Mxan_7124	1.245	0.629	0.08	0.397		iron-sulfur cluster-binding protein, Rieske family	Energy metabolism
Mxan_7132	0.553	0.287	0.213	1.23		conserved hypothetical protein	Hypothetical proteins
Mxan_7135	-0.519	-0.7	-1.064	-0.864		hypothetical protein	
Mxan_7149	1.215	1.516	1.132	0.282		conserved hypothetical protein	Hypothetical proteins
Mxan_7150	0.854	1.431	0.879	0.228		response regulator	
Mxan_7155	0.497	0.229	1.528	0.683		phosphoribosyl transferase domain protein	Unknown function
Mxan_7160	0.21	0.125	1.699	0.003	*alr*	alanine racemase	Cell envelope
Mxan_7162	0.976	0.362	0.439	1.017		serine/threonine kinase family protein	Protein fate
Mxan_7164	-3.74	-4.851	-4.304	-5.796		universal stress family protein	
Mxan_7165	-3.458	-5.126	-4.559	-5.914	*ldhA*	D-lactate dehydrogenase	Energy metabolism
Mxan_7166	1.067	0.427	1.196	-0.034		nicotinate phosphoribosyltransferase, putative	Biosynthesis of
Mxan_7173	-0.418	-1.079	-0.643	-0.511		hypothetical protein	
Mxan_7174	1.864	2.594	1.486	0.134		DNA-binding protein	
Mxan_7179	2.131	1.631	0.931	0.7		lipoprotein, putative	Cell envelope
Mxan_7193	-0.867	-1.593	-1.479	-0.72		hypothetical protein	
Mxan_7194	0.067	0.591	2.462	0.248		oxidoreductase, short chain dehydrogenase/reductase family	
Mxan_7196	-1.038	-1.469	-1.539	-0.317		hypothetical protein	
Mxan_7204	0.643	1.369	2.885	0.577		conserved hypothetical protein	Hypothetical proteins
Mxan_7205	0.463	0.595	1.466	0.923		phthalate dioxygenase reductase, putative	Energy metabolism
Mxan_7209	3.243	3.502	1.752	0.654		peptidase, S8A (subtilisin) subfamily	Protein fate
Mxan_7210	2.072	1.852	0.389	0.344		hypothetical protein	
Mxan_7212	1.874	2.168	0.762	-0.651		hypothetical protein	
Mxan_7213	2.362	2.183	0.658	-0.6		di-haem cytochrome-c peroxidase	Energy metabolism
Mxan_7229	0.766	0.726	1.693	0.402		hypothetical protein	
Mxan_7232	0.439	1.208	1.403	0.479		hydrolase, alpha/beta fold family	Unknown function
Mxan_7236	1.132	1.441	0.555	-0.112		hypothetical protein	
Mxan_7254	0.007	0.703	1.34	0.643		conserved hypothetical protein	Hypothetical proteins
Mxan_7257	0.694	0.503	1.046	0.884		pentapeptide repeat domain protein	Unknown function
Mxan_7260	0.857	1.241	0.218	0.006		CRISPR-associated fusion protein Cas4/Cas1	Mobile and
Mxan_7270	1.122	1.359	0.842	0.321		membrane protein, putative	Cell envelope
Mxan_7275	0.687	1.058	2.134	0.091		conserved hypothetical protein	Hypothetical proteins
Mxan_7282	1.107	0.576	0.222	0.112	*cmr1*	CRISPR-associated protein, TM1795 family	Mobile and
Mxan_7293	0.255	1.158	1.005	0.16		sugar ABC transporter, permease protein, putative	Transport and binding
Mxan_7295	0.48	1.006	0.879	0.353		sugar ABC transporter, periplasmic sugar-binding protein, putative	Transport and binding
Mxan_7296	0.316	1.395	1.543	0.674		hypothetical protein	
Mxan_7297	-0.471	-0.606	-1.189	-0.846		hypothetical protein	
Mxan_7299	0.203	-0.182	1.916	1.043		fatty acid desaturase family protein	Fatty acid and
Mxan_7301	1.288	1.38	0.882	0.622		conserved hypothetical protein	Hypothetical proteins
Mxan_7302	3.123	4.18	4.73	0.875		CDP-alcohol phosphatidyltransferase family protein	Fatty acid and
Mxan_7303	0.83	1.376	1.702	1.226		hypothetical protein	
Mxan_7306	-0.712	-1.017	-1.007	-0.687		conserved hypothetical protein	Hypothetical proteins
Mxan_7307	-1.124	-1.223	-1.115	-0.548		conserved hypothetical protein	Hypothetical proteins
Mxan_7310	-1.322	-1.363	-1.175	-0.446		oxidoreductase, short chain dehydrogenase/reductase family	Unknown function
Mxan_7319	1.077	1.056	0.589	0.139		transcriptional regulator, putative	Regulatory functions
Mxan_7320	2.081	1.881	1.204	0.229		FAD-binding monooxygenase, PheA/TfdB family	
Mxan_7330	-1.384	-1.758	-1.692	-0.381		hypothetical protein	
Mxan_7331	-1.088	-1.409	-1.312	-0.096		TonB-dependent receptor	Transport and binding
Mxan_7332	-0.701	-1.099	-2.132	-0.816		lipoprotein, putative	Cell envelope
Mxan_7333	-0.483	-1.086	-2.155	-0.778		lipoprotein, putative	Cell envelope
Mxan_7334	0.73	1.254	0.803	0.026		hypothetical protein	
Mxan_7335	3.177	2.748	0.678	-0.29		hypothetical protein	
Mxan_7336	3.12	2.169	0.111	0.086		conserved hypothetical protein	Hypothetical proteins
Mxan_7338	-0.433	-0.649	-1.157	-0.565		hypothetical protein	
Mxan_7339	0.427	1.381	0.812	0.623		SlyX homolog	Unknown function
Mxan_7368	0.196	1.172	0.809	0.345		sensory box histidine kinase	Regulatory functions
Mxan_7370	-1.355	-1.463	-1.372	-0.34		serine/threonine protein kinase	Regulatory functions
Mxan_7371	-1.63	-2.023	-1.858	-0.728		serine/threonine protein kinase, putative	Regulatory functions
Mxan_7374	0.511	1.912	3.371	0.894		hypothetical protein	
Mxan_7377	0.775	1.431	1.163	0.277	*rocD*	ornithine aminotransferase	Energy metabolism
Mxan_7380	0.448	0.912	3.686	0.522		CBS domain protein	Unknown function
Mxan_7384	0.404	0.482	2.475	0.271		conserved hypothetical protein	Hypothetical proteins
Mxan_7390	-1.087	-0.78	-1.196	-0.262		hypothetical protein	
Mxan_7392	2.369	3.764	1.817	0.584		hypothetical protein	
Mxan_7395	-0.763	-0.716	-1.171	-0.758		general secretion pathway protein, GspG family	Protein fate
Mxan_7399	0.227	1.193	0.898	0.033		hypothetical protein	
Mxan_7402	2.156	1.939	1.581	0.462		hypothetical protein	
Mxan_7403	0.591	0.3	3.924	1.222		hypothetical protein	
Mxan_7405	0.646	0.369	3.657	0.351		proline dehydrogenase	
Mxan_7406	0.8	1.035	1.374	0.256		glycosyl hydrolase, family 15	Energy metabolism
Mxan_7407	-0.848	-1.071	-1.187	-0.686		hypothetical protein	
Mxan_7408	-0.971	-1.027	-0.737	-0.488		hypothetical protein	
Mxan_7409	-1.439	-1.309	-0.862	-0.54		conserved hypothetical protein	Hypothetical proteins
Mxan_7424	3.581	3.378	3.156	2.785		conserved hypothetical protein	Hypothetical proteins
Mxan_7436	-2.099	-3.177	-1.643	0.207		outer membrane efflux protein	Transport and binding
Mxan_7437	-2.201	-3.168	-1.557	0.447		heavy metal efflux pump, CzcA family	Cellular processes

Mxan-no.	Log ratio				Gene name	Annotation	GO mainrole
	0.5 h	1 h	2 h	4 h			
Mxan_7438	-1.435	-2.664	-1.319	0.445		cobalt-zinc-cadmium resistance protein, putative	Cellular processes
Mxan_7444	1.578	2.397	0.865	-0.188		response regulator/sensory box histidine kinase	Regulatory functions
Mxan_7452	2.606	2.331	0.757	0.585		hypothetical protein	
Mxan_7468	0.743	1.266	3.156	0.074		hypothetical protein	
Mxan_7471	2.304	2.186	1.485	0.443		conserved hypothetical protein	Hypothetical proteins
Mxan_7474	-0.596	-1.043	-1.013	-0.46		lipoprotein, putative	Cell envelope
Mxan_7475	-1.035	-1.201	-1.427	-0.696		conserved hypothetical protein	Hypothetical proteins
Mxan_7495	-0.514	-0.746	-1.283	-0.883		drug resistance transporter, Bcr/CflA family	Cellular processes
Mxan_7507	1.196	0.482	0.507	0.481		hypothetical protein	
Mxan_7508	1.233	0.636	0.083	0.234		hypothetical protein	
Mxan_7513	-1.243	-1.926	-2.443	-2.239		hypothetical protein	
Mxan_7514	-0.598	-0.912	-1.378	-1.113		hypothetical protein	

[a]Annotation could not be confirmed

REFERENCES

Alm, E. J., K. H. Huang, M. N. Price, R. P. Koche, K. Keller, I. L. Dubchak & A. P. Arkin, (2005) The MicrobesOnline Web site for comparative genomics. *Genome Res* **15**: 1015-1022.

Altschul, S. F., T. L. Madden, A. A. Schaffer, J. Zhang, Z. Zhang, W. Miller & D. J. Lipman, (1997) Gapped BLAST and PSI-BLAST: a new generation of protein database search programs. **25**: 3389-3402.

Apelian, D. & S. Inouye, (1990) Development-specific sigma-factor essential for late-stage differentiation of *Myxococcus xanthus*. *Genes Dev.* **4**: 1396-1403.

Apelian, D. & S. Inouye, (1993) A new putative sigma factor of *Myxococcus xanthus*. *J. Bacteriol.* **175**: 3335-3342.

Ausmees, N., H. Wahlstedt, S. Bagchi, M. A. Elliot, M. J. Buttner & K. Flardh, (2007) SmeA, a small membrane protein with multiple functions in *Streptomyces* sporulation including targeting of a SpoIIIE/FtsK-like protein to cell division septa. *Mol Microbiol* **65**: 1458-1473.

Bacon, K., D. Clutter, R. H. Kottel, M. Orlowski & D. White, (1975) Carbohydrate accumulation during myxospore formation in *Myxococcus xanthus*. *J Bacteriol* **124**: 1635-1636.

Bagyan, I. & P. Setlow, (2002) Localization of the cortex lytic enzyme CwlJ in spores of *Bacillus subtilis*. *J Bacteriol* **184**: 1219-1224.

Barak, I., E. Ricca & S. M. Cutting, (2005) From fundamental studies of sporulation to applied spore research. *Mol Microbiol* **55**: 330-338.

Bendezu, F. O., C. A. Hale, T. G. Bernhardt & P. A. de Boer, (2008) RodZ (YfgA) is required for proper assembly of the MreB actin cytoskeleton and cell shape in *E. coli*. *EMBO J*.

Bennett-Lovsey, R. M., A. D. Herbert, M. J. Sternberg & L. A. Kelley, (2008) Exploring the extremes of sequence/structure space with ensemble fold recognition in the program Phyre. *Proteins* **70**: 611-625.

Berleman, J. E. & C. E. Bauer, (2004) Characterization of cyst cell formation in the purple photosynthetic bacterium *Rhodospirillum centenum*. *Microbiology* **150**: 383-390.

Bhandari, P. & J. Gowrishankar, (1997) An *Escherichia coli* host strain useful for efficient overproduction of cloned gene products with NaCl as the inducer. *J Bacteriol* **179**: 4403-4406.

Bos, M. P., V. Robert & J. Tommassen, (2007) Biogenesis of the gram-negative bacterial outer membrane. *Annu Rev Microbiol* **61**: 191-214.

Boysen, A., E. Ellehauge, B. Julien & L. Søgaard-Andersen, (2002) The DevT protein stimulates synthesis of FruA, a signal transduction protein required for fruiting body morphogenesis in *Myxococcus xanthus*. *J. Bacteriol.* **184**: 1540-1546.

Bradford, M. M., (1976) A rapid and sensitive method for the quantitation of microgram quantities of protein utilizing the principle of protein-dye binding. *Anal Biochem* **72**: 248-254.

Bretscher, A. P. & D. Kaiser, (1978) Nutrition of *Myxococcus xanthus*, a fruiting myxobacterium. *J. Bacteriol.* **133**: 763-768.

Bu, S., Y. Li, M. Zhou, P. Azadin, M. Zeng, P. Fives-Taylor & H. Wu, (2008) Interaction between two putative glycosyltransferases is required for glycosylation of a serine-rich streptococcal adhesin. *J Bacteriol* **190**: 1256-1266.

Bui, N. K., J. Gray, H. Schwarz, P. Schumann, D. Blanot & W. Vollmer, (2008) The peptidoglycan sacculus of *Myxococcus xanthus* has unusual structural features and is degraded during glycerol-induced myxospore development. *J Bacteriol*.

Caberoy, N. B., R. D. Welch, J. S. Jakobsen, S. C. Slater & A. G. Garza, (2003) Global mutational analysis of NtrC-like activators in *Myxococcus xanthus*: Identifying activator mutants defective for motility and fruiting body development. *J. Bacteriol.* **185**: 6083-6094.

Carballido-Lopez, R., (2006) Orchestrating bacterial cell morphogenesis. *Mol Microbiol* **60**: 815-819.

Carballido-Lopez, R. & A. Formstone, (2007) Shape determination in *Bacillus subtilis*. *Curr Opin Microbiol* **10**: 611-616.

Chater, K. F., (2001) Regulation of sporulation in *Streptomyces coelicolor* A3(2): a checkpoint multiplex? *Curr Opin Microbiol* **4**: 667-673.

Chater, K. F. & G. Chandra, (2006) The evolution of development in *Streptomyces* analysed by genome comparisons. *FEMS Microbiol Rev* **30**: 651-672.

Chiu, S. W., S. Y. Chen & H. C. Wong, (2008) Localization and expression of MreB in *Vibrio parahaemolyticus* under different stresses. *Appl Environ Microbiol* **74**: 7016-7022.

Chudakov, D. M., S. Lukyanov & K. A. Lukyanov, (2005) Fluorescent proteins as a toolkit for *in vivo* imaging. *Trends Biotechnol* **23**: 605-613.

Chung, C. T., S. L. Niemela & R. H. Miller, (1989) One-step preparation of competent *Escherichia coli*: transformation and storage of bacterial cells in the same solution. *Proc Natl Acad Sci U S A* **86**: 2172-2175.

Claessen, D., W. de Jong, L. Dijkhuizen & H. A. Wosten, (2006) Regulation of *Streptomyces* development: reach for the sky! *Trends Microbiol* **14**: 313-319.

Costa, T., L. Steil, L. O. Martins, U. Volker & A. O. Henriques, (2004) Assembly of an oxalate decarboxylase produced under sigmaK control into the *Bacillus subtilis* spore coat. *J Bacteriol* **186**: 1462-1474.

Coutinho, P. M., E. Deleury, G. J. Davies & B. Henrissat, (2003) An evolving hierarchical family classification for glycosyltransferases. *J Mol Biol* **328**: 307-317.

D'Andrea, L. D. & L. Regan, (2003) TPR proteins: the versatile helix. *Trends Biochem Sci* **28**: 655-662.

Dahl, J. L., F. K. Tengra, D. Dutton, J. Yan, T. M. Andacht, L. Coyne, V. Windell & A. G. Garza, (2007) Identification of major sporulation proteins of *Myxococcus xanthus* using a proteomic approach. *J Bacteriol* **189**: 3187-3197.

de Pedro, M. A., K. D. Young, J. V. Holtje & H. Schwarz, (2003) Branching of *Escherichia coli* cells arises from multiple sites of inert peptidoglycan. *J Bacteriol* **185**: 1147-1152.

den Blaauwen, T., M. A. de Pedro, M. Nguyen-Disteche & J. A. Ayala, (2008) Morphogenesis of rod-shaped sacculi. *FEMS Microbiol Rev* **32**: 321-344.

DeRisi, J. L., V. R. Iyer & P. O. Brown, (1997) Exploring the metabolic and genetic control of gene expression on a genomic scale. *Science* **278**: 680-686.

Divakaruni, A. V., C. Baida, C. L. White & J. W. Gober, (2007) The cell shape proteins MreB and MreC control cell morphogenesis by positioning cell wall synthetic complexes. *Mol Microbiol* **66**: 174-188.

Divakaruni, A. V., R. R. Loo, Y. Xie, J. A. Loo & J. W. Gober, (2005) The cell-shape protein MreC interacts with extracytoplasmic proteins including cell wall assembly complexes in *Caulobacter crescentus*. *Proc Natl Acad Sci U S A* **102**: 18602-18607.

Downard, J. S. & D. R. Zusman, (1985) Differential expression of protein S genes during *Myxococcus xanthus* development. *J Bacteriol* **161**: 1146-1155.

Durocher, D., I. A. Taylor, D. Sarbassova, L. F. Haire, S. L. Westcott, S. P. Jackson, S. J. Smerdon & M. B. Yaffe, (2000) The molecular basis of FHA domain:phosphopeptide binding specificity and implications for phospho-dependent signaling mechanisms. *Mol Cell* **6**: 1169-1182.

Dworkin, M. & S. M. Gibson, (1964) A system for studying microbial morphogenesis: rapid formation of microcysts in *Myxococcus xanthus*. *Science* **146**: 243-244.

Eisen, M. B., P. T. Spellman, P. O. Brown & D. Botstein, (1998) Cluster analysis and display of genome-wide expression patterns. *Proc Natl Acad Sci U S A* **95**: 14863-14868.

Elbein, A. D., Y. T. Pan, I. Pastuszak & D. Carroll, (2003) New insights on trehalose: a multifunctional molecule. *Glycobiology* **13**: 17R-27R.

Ellehauge, E., M. Norregaard-Madsen & L. Søgaard-Andersen, (1998) The FruA signal transduction protein provides a checkpoint for the temporal co-ordination of intercellular signals in *Myxococcus xanthus* development. *Mol Microbiol* **30**: 807-817.

Enguita, F. J., P. M. Matias, L. O. Martins, D. Placido, A. O. Henriques & M. A. Carrondo, (2002) Spore-coat laccase CotA from *Bacillus subtilis*: crystallization and preliminary X-ray characterization by the MAD method. *Acta Crystallogr D Biol Crystallogr* **58**: 1490-1493.

Errington, J., (2003) Regulation of endospore formation in *Bacillus subtilis*. *Nat Rev Microbiol* **1**: 117-126.

Faridmoayer, A., M. A. Fentabil, D. C. Mills, J. S. Klassen & M. F. Feldman, (2007) Functional characterization of bacterial oligosaccharyltransferases involved in O-linked protein glycosylation. *J Bacteriol* **189**: 8088-8098.

Figge, R. M., A. V. Divakaruni & J. W. Gober, (2004) MreB, the cell shape-determining bacterial actin homologue, co-ordinates cell wall morphogenesis in *Caulobacter crescentus*. *Mol Microbiol* **51**: 1321-1332.

Filer, D., S. H. Kindler & E. Rosenberg, (1977) Myxospore coat synthesis in *Myxococcus xanthus*: enzymes associated with uridine 5'-diphosphate-N-acetylgalactosamine formation during myxospore development. *J Bacteriol* **131**: 745-750.

Formstone, A. & J. Errington, (2005) A magnesium-dependent mreB null mutant: implications for the role of mreB in *Bacillus subtilis*. *Mol Microbiol* **55**: 1646-1657.

Gaona, G., C. Nunez, J. B. Goldberg, A. S. Linford, R. Najera, M. Castaneda, J. Guzman, G. Espin & G. Soberon-Chavez, (2004) Characterization of the *Azotobacter vinelandii algC* gene involved in alginate and lipopolysaccharide production. *FEMS Microbiol Lett* **238**: 199-206.

Gardy, J. L., M. R. Laird, F. Chen, S. Rey, C. J. Walsh, M. Ester & F. S. Brinkman, (2005) PSORTb v.2.0: expanded prediction of bacterial protein subcellular localization and insights gained from comparative proteome analysis. *Bioinformatics* **21**: 617-623.

Gentschev, I., G. Dietrich & W. Goebel, (2002) The *E. coli* alpha-hemolysin secretion system and its use in vaccine development. *Trends Microbiol* **10**: 39-45.

Gentschev, I., G. Dietrich, S. Spreng, B. Neuhaus, E. Maier, R. Benz, W. Goebel, J. Fensterle & U. R. Rapp, (2004) Use of the alpha-hemolysin secretion system of *Escherichia coli* for antigen delivery in the *Salmonella typhi* Ty21a vaccine strain. *Int J Med Microbiol* **294**: 363-371.

Glufka, R. & P. Maeba, (1991) Release of a cell surface protein during development of *Myxococcus xanthus*. *J Bacteriol* **173**: 7988-7991.

Gollop, R., M. Inouye & S. Inouye, (1991) Protein U, a late-developmental spore coat protein of *Myxococcus xanthus*, is a secretory protein. *J Bacteriol* **173**: 3597-3600.

Hagen, D. C., A. P. Bretscher & D. Kaiser, (1978) Synergism between morphogenetic mutants of *Myxococcus xanthus*. *Dev. Biol.* **64**: 284-296.

Hardisson, C. & M. B. Manzanal, (1976) Ultrastructural studies of sporulation in *Streptomyces*. *J Bacteriol* **127**: 1443-1454.

Harlow, E. & D. Lane, (1988) *Antibodies: A Laboratory Manual.* Cold Spring Harbor, NY: Cold Spring Harbor Laboratory.

Harris, B. Z. & M. Singer, (1998) Identification and characterization of the *Myxococcus xanthus argE* gene. *J Bacteriol* **180**: 6412-6414.

Henriques, A. O. & C. P. Moran, Jr., (2007) Structure, assembly, and function of the spore surface layers. *Annu Rev Microbiol* **61**: 555-588.

Hong, H., D. R. Patel, L. K. Tamm & B. van den Berg, (2006) The outer membrane protein OmpW forms an eight-stranded beta-barrel with a hydrophobic channel. *J Biol Chem* **281**: 7568-7577.

Horiuchi, T., M. Taoka, T. Isobe, T. Komano & S. Inouye, (2002) Role of *fruA* and *csgA* genes in gene expression during development of *Myxococcus xanthus*. Analysis by two-dimensional gel electrophoresis. *J. Biol. Chem.* **277**: 26753-26760.

Hua, S. & Z. Sun, (2001) Support vector machine approach for protein subcellular localization prediction. *Bioinformatics* **17**: 721-728.

Hugenholtz, P., B. M. Goebel & N. R. Pace, (1998) Impact of culture-independent studies on the emerging phylogenetic view of bacterial diversity. *J Bacteriol* **180**: 4765-4774.

Inouye, M., S. Inouye & D. R. Zusman, (1979a) Biosynthesis and self-assembly of protein S, a development-specific protein of *Myxococcus xanthus*. *Proc Natl Acad Sci U S A* **76**: 209-213.

Inouye, M., S. Inouye & D. R. Zusman, (1979b) Gene expression during development of *Myxococcus xanthus*: pattern of protein synthesis. *Dev. Biol.* **68**: 579-591.

Isticato, R., G. Esposito, R. Zilhao, S. Nolasco, G. Cangiano, M. De Felice, A. O. Henriques & E. Ricca, (2004) Assembly of multiple CotC forms into the *Bacillus subtilis* spore coat. *J Bacteriol* **186**: 1129-1135.

Iwai, H., N. Masaoka, T. Ishii & S. Satoh, (2002a) A pectin glucuronyltransferase gene is essential for intercellular attachment in the plant meristem. *Proc Natl Acad Sci U S A* **99**: 16319-16324.

Iwai, N., K. Nagai & M. Wachi, (2002b) Novel S-benzylisothiourea compound that induces spherical cells in *Escherichia coli* probably by acting on a rod-shape-determining protein(s) other than penicillin-binding protein 2. *Biosci Biotechnol Biochem* **66**: 2658-2662.

Julien, B., A. D. Kaiser & A. Garza, (2000) Spatial control of cell differentiation in *Myxococcus xanthus*. *Proc. Natl. Acad. Sci. USA* **97**: 9098-9103.

Kaiser, D., (1979) Social gliding is correlated with the presence of pili in *Myxococcus xanthus*. *Proc. Natl. Acad. Sci. USA* **76**: 5952-5956.

Kaiser, D., (2003) Coupling cell movement to multicellular development in myxobacteria. *Nature Rev. Microbiol.* **1**: 45-54.

Kaiser, D., (2004) Signaling in myxobacteria. *Annu Rev Microbiol* **58**: 75-98.

Kall, L., A. Krogh & E. L. Sonnhammer, (2007) Advantages of combined transmembrane topology and signal peptide prediction--the Phobius web server. *Nucleic Acids Res* **35**: W429-432.

Karczmarek, A., R. Martinez-Arteaga, S. Alexeeva, F. G. Hansen, M. Vicente, N. Nanninga & T. den Blaauwen, (2007) DNA and origin region segregation are not affected by the transition from rod to sphere after inhibition of *Escherichia coli* MreB by A22. *Mol Microbiol* **65**: 51-63.

Kim, H., M. Hahn, P. Grabowski, D. C. McPherson, M. M. Otte, R. Wang, C. C. Ferguson, P. Eichenberger & A. Driks, (2006) The *Bacillus subtilis* spore coat protein interaction network. *Mol Microbiol* **59**: 487-502.

Klobutcher, L. A., K. Ragkousi & P. Setlow, (2006) The *Bacillus subtilis* spore coat provides "eat resistance" during phagocytic predation by the protozoan *Tetrahymena thermophila*. *Proc Natl Acad Sci U S A* **103**: 165-170.

Komano, T., T. Furuichi, M. Teintze, M. Inouye & S. Inouye, (1984) Effects of deletion of the gene for the development-specific protein S on differentiation in *Myxococcus xanthus*. *J Bacteriol* **158**: 1195-1197.

Komano, T., S. Inouye & M. Inouye, (1980) Patterns of protein production in *Myxococcus xanthus* during spore formation induced by glycerol, dimethyl sulfoxide, and phenethyl alcohol. *J Bacteriol* **144**: 1076-1082.

Kottel, R. H., K. Bacon, D. Clutter & D. White, (1975) Coats from *Myxococcus xanthus*: characterization and synthesis during myxospore differentiation. *J Bacteriol* **124**: 550-557.

Kroos, L., (2007) The *Bacillus* and *Myxococcus* developmental networks and their transcriptional regulators. *Annu Rev Genet* **41**: 13-39.

Kroos, L. & D. Kaiser, (1987) Expression of many developmentally regulated genes in *Myxococcus* depends on a sequence of cell interactions. *Genes & Dev.* **1**: 840-854.

Kroos, L., P. J. Piggot & C. P. Moran, Jr., (2008) *Bacillus subtilis* Sporulation and Other Multicellular Behaviors. In: Myxobacteria. Multicellularity and Differentiation. D. E. Whitworth (ed). Washington, DC.: ASM Press, pp. 363 - 383.

Kruse, T., B. Blagoev, A. Lobner-Olesen, M. Wachi, K. Sasaki, N. Iwai, M. Mann & K. Gerdes, (2006) Actin homolog MreB and RNA polymerase interact and are both required for chromosome segregation in *Escherichia coli*. *Genes Dev* **20**: 113-124.

Kruse, T., S. Lobedanz, N. M. S. Berthelsen & L. Søgaard-Andersen, (2001) C-signal: A cell surface-associated morphogen that induces and coordinates multicellular fruiting body morphogenesis and sporulation in *M. xanthus*. *Mol. Microbiol.* **40**: 156-168.

Ku, S. C., B. L. Schulz, P. M. Power & M. P. Jennings, (2009) The pilin O-glycosylation pathway of pathogenic *Neisseria* is a general system that glycosylates AniA, an outer membrane nitrite reductase. *Biochem Biophys Res Commun* **378**: 84-89.

Kuner, J. M. & D. Kaiser, (1982) Fruiting body morphogenesis in submerged cultures of *Myxococcus xanthus*. *J. Bacteriol.* **151**: 458-461.

Laemmli, U. K., (1970) Cleavage of structural proteins during the assembly of the head of bacteriophage T4. *Nature* **227**: 680-685.

Lairson, L. L., B. Henrissat, G. J. Davies & S. G. Withers, (2008) Glycosyltransferases: structures, functions, and mechanisms. *Annu Rev Biochem* **77**: 521-555.

Letunic, I., R. R. Copley, B. Pils, S. Pinkert, J. Schultz & P. Bork, (2006) SMART 5: domains in the context of genomes and networks. *Nucleic Acids Res* **34**: D257-260.

Licking, E., L. Gorski & D. Kaiser, (2000) A common step for changing cell shape in fruiting body and starvation-independent sporulation in *Myxococcus xanthus*. *J. Bacteriol.* **182**: 3553-3558.

Lobedanz, S. & L. Søgaard-Andersen, (2003) Identification of the C-signal, a contact-dependent morphogen coordinating multiple developmental responses in *Myxococcus xanthus*. *Genes Dev.* **17**: 2151-2161.

Magge, A., A. C. Granger, P. G. Wahome, B. Setlow, V. R. Vepachedu, C. A. Loshon, L. Peng, D. Chen, Y. Q. Li & P. Setlow, (2008) Role of dipicolinic acid in the germination, stability, and viability of spores of *Bacillus subtilis*. *J Bacteriol* **190**: 4798-4807.

Magrini, V., C. Creighton & P. Youderian, (1999) Site-specific recombination of temperate *Myxococcus xanthus* phage Mx8: genetic elements required for integration. *J Bacteriol* **181**: 4050-4061.

Maniatis, T., E. F.Fritsch, and J. Sambrook, (1982) Molecular Cloning, A Laboratory Manual. *Cold Spring Harbor Laboratory Press, Cold Spring Habor, NY*.

March, J. C., G. Rao & W. E. Bentley, (2003) Biotechnological applications of green fluorescent protein. *Appl Microbiol Biotechnol* **62**: 303-315.

Mazza, P., E. E. Noens, K. Schirner, N. Grantcharova, A. M. Mommaas, H. K. Koerten, G. Muth, K. Flardh, G. P. van Wezel & W. Wohlleben, (2006) MreB of *Streptomyces coelicolor* is not essential for vegetative growth but is required for the integrity of aerial hyphae and spores. *Mol Microbiol* **60**: 838-852.

McBride, M. J. & D. R. Zusman, (1989) Trehalose accumulation in vegetative cells and spores of *Myxococcus xanthus*. *J Bacteriol* **171**: 6383-6386.

McCleary, W. R., B. Esmon & D. R. Zusman, (1991) *Myxococcus xanthus* protein C is a major spore surface protein. *J Bacteriol* **173**: 2141-2145.

Messner, P., (2004) Prokaryotic glycoproteins: unexplored but important. *J Bacteriol* **186**: 2517-2519.

Messner, P., K. Steiner, K. Zarschler & C. Schaffer, (2008) S-layer nanoglycobiology of bacteria. *Carbohydr Res* **343**: 1934-1951.

Mohammadi, T., A. Karczmarek, M. Crouvoisier, A. Bouhss, D. Mengin-Lecreulx & T. den Blaauwen, (2007) The essential peptidoglycan glycosyltransferase MurG forms a complex with proteins involved in lateral envelope growth as well as with proteins involved in cell division in *Escherichia coli*. *Mol Microbiol* **65**: 1106-1121.

Moir, A., (2006) How do spores germinate? *J Appl Microbiol* **101**: 526-530.

Moreno, S., R. Najera, J. Guzman, G. Soberon-Chavez & G. Espin, (1998) Role of alternative sigma factor *algU* in encystment of *Azotobacter vinelandii*. *J Bacteriol* **180**: 2766-2769.

Morrison, C. E. & D. R. Zusman, (1979) *Myxococcus xanthus* mutants with temperature-sensitive, stage-specific defects: evidence for independent pathways in development. *J Bacteriol* **140**: 1036-1042.

Müller, F.-D. & J. S. Jakobsen, (2008) Expression analysis. In: Myxobacteria. Multicellularity and Differentiation. D. E. Whitworth (ed). Washington, DC.: ASM Press, pp. 479 - 489.

Murzin, A. G., S. E. Brenner, T. Hubbard & C. Chothia, (1995) SCOP: a structural classification of proteins database for the investigation of sequences and structures. *J Mol Biol* **247**: 536-540.

Nariya, H. & M. Inouye, (2008) MazF, an mRNA interferase, mediates programmed cell death during multicellular *Myxococcus* development. *Cell* **132**: 55-66.

Nariya, H. & S. Inouye, (2006) A protein Ser/Thr kinase cascade negatively regulates the DNA-binding activity of MrpC, a smaller form of which may be necessary for the *Myxococcus xanthus* development. *Mol Microbiol* **60**: 1205-1217.

Nelson, D. R. & D. R. Zusman, (1983) Evidence for long-lived mRNA during fruiting body formation in *Myxococcus xanthus*. *Proc Natl Acad Sci U S A* **80**: 1467-1471.

Nielsen, M., A. A. Rasmussen, E. Ellehauge, A. Treuner-Lange & L. Sogaard-Andersen, (2004) HthA, a putative DNA-binding protein, and HthB are important for fruiting body morphogenesis in *Myxococcus xanthus*. *Microbiology* **150**: 2171-2183.

Nunez, C., S. Moreno, G. Soberon-Chavez & G. Espin, (1999) The *Azotobacter vinelandii* response regulator AlgR is essential for cyst formation. *J Bacteriol* **181**: 141-148.

O'Connor, K. A. & D. R. Zusman, (1991) Behaviour of peripheral rods and their role in the life cycle of *Myxococcus xanthus*. *Journal of Bacteriology* **173**: 3342-3355.

O'Connor, K. A. & D. R. Zusman, (1997) Starvation-independent sporulation in *Myxococcus xanthus* involves the pathway for beta-lactamase induction and provides a mechanism for competitive cell survival. *Mol Microbiol* **24**: 839-850.

O'Connor, K. A. & D. R. Zusman, (1999) Induction of beta-lactamase influences the course of development in *Myxococcus xanthus*. *J Bacteriol* **181**: 6319-6331.

Ogawa, M., S. Fujitani, X. Mao, S. Inouye & T. Komano, (1996) FruA, a putative transcription factor essential for the development of *Myxococus xanthus*. *Mol. Microbiol.* **22**: 757-767.

Orlowski, M., P. Martin, D. White & M. C. Wong, (1972) Changes in activity of glyoxylate cycle enzymes during myxospore development in *Myxococcus xanthus*. *J Bacteriol* **111**: 784-790.

Otani, M., S. Kozuka, C. Xu, C. Umezawa, K. Sano & S. Inouye, (1998) Protein W, a spore-specific protein in *Myxococcus xanthus*, formation of a large electron-dense particle in a spore. *Mol Microbiol* **30**: 57-66.

Overgaard, M., S. Wegener-Feldbrugge & L. Søgaard-Andersen, (2006) The orphan response regulator DigR is required for synthesis of extracellular matrix fibrils in *Myxococcus xanthus*. *J Bacteriol* **188**: 4384-4394.

Pereira, P. M., S. R. Filipe, A. Tomasz & M. G. Pinho, (2007) Fluorescence ratio imaging microscopy shows decreased access of vancomycin to cell wall synthetic sites in vancomycin-resistant *Staphylococcus aureus*. *Antimicrob Agents Chemother* **51**: 3627-3633.

Pichoff, S. & J. Lutkenhaus, (2007) Overview of cell shape: cytoskeletons shape bacterial cells. *Curr Opin Microbiol* **10**: 601-605.

Piggot, P. J. & D. W. Hilbert, (2004) Sporulation of *Bacillus subtilis*. *Curr Opin Microbiol* **7**: 579-586.

Piggot, P. J. & R. Losick, (2002) Sporulation genes and intercompartmental regulation. In: *Bacillus subtilis* and Its Closest Relatives: from Genes to Cells. R. Losick (ed). Washington, DC.: ASM Press, pp. 483-518.

Plamann, L. & H. B. Kaplan, (1999) Cell-Density Sensing during Early Development in *Myxococcus xanthus*. In: Cell-cell signaling in bacteria. G. M. Dunny & S. C. Winans (eds). Washington DC: ASM Press, pp. 67-82.

Power, P. M. & M. P. Jennings, (2003) The genetics of glycosylation in Gram-negative bacteria. *FEMS Microbiol Lett* **218**: 211-222.

Qualls, G. T., K. Stephens & D. White, (1978) Morphogenetic movements and multicellular development in the fruiting Myxobacterium, *Stigmatella aurantiaca*. *Dev Biol* **66**: 270-274.

Reichenbach, H., (1999) The ecology of the myxobacteria. *Env. Microbiol.* **1**: 15-21.

Reynolds, P. E., (1989) Structure, biochemistry and mechanism of action of glycopeptide antibiotics. *Eur J Clin Microbiol Infect Dis* **8**: 943-950.

Rolbetzki, A., M. Ammon, V. Jakovljevic, A. Konovalova & L. Søgaard-Andersen, (2008) Regulated secretion of a protease activates intercellular signaling during fruiting body formation in *M. xanthus*. *Dev Cell* **15**: 627-634.

Rosenbluh, A. & E. Rosenberg, (1989) Sporulation of *Myxococcus xanthus* in liquid shake flask cultures. *J Bacteriol* **171**: 4521-4524.

Sadler, W. & M. Dworkin, (1966) Induction of cellular morphogenesis in *Myxococcus xanthus*. II. Macromolecular synthesis and mechanism of inducer action. *J Bacteriol* **91**: 1520-1525.

Sambrook, J., E. F. Fritsch & T. Maniatis, (1989) *Molecular Cloning. A Laboratory Manual*. Cold Spring Harbor Laboratory Press, Cold Spring Harbor, N.Y.

Schaffer, C. & P. Messner, (2004) Surface-layer glycoproteins: an example for the diversity of bacterial glycosylation with promising impacts on nanobiotechnology. *Glycobiology* **14**: 31R-42R.

Schägger, H. & G. von Jagow, (1987) Tricine-sodium dodecyl sulfate-polyacrylamide gel electrophoresis for the separation of proteins in the range from 1 to 100 kDa. *Anal. Biochem.* **166**: 368-379.

Setlow, P., (2006) Spores of *Bacillus subtilis*: their resistance to and killing by radiation, heat and chemicals. *J Appl Microbiol* **101**: 514-525.

Seydel, A., P. Gounon & A. P. Pugsley, (1999) Testing the '+2 rule' for lipoprotein sorting in the *Escherichia coli* cell envelope with a new genetic selection. *Mol Microbiol* **34**: 810-821.

Sherlock, O., U. Dobrindt, J. B. Jensen, R. Munk Vejborg & P. Klemm, (2006) Glycosylation of the self-recognizing *Escherichia coli* Ag43 autotransporter protein. *J Bacteriol* **188**: 1798-1807.

Sigrist, C. J., L. Cerutti, N. Hulo, A. Gattiker, L. Falquet, M. Pagni, A. Bairoch & P. Bucher, (2002) PROSITE: a documented database using patterns and profiles as motif descriptors. *Brief Bioinform* **3**: 265-274.

Søgaard-Andersen, L., (2004) Cell polarity, intercellular signalling and morphogenetic cell movements in *Myxococcus xanthus*. *Curr. Opin. Microbiol.* **7**: 587-593.

Søgaard-Andersen, L., (2008) Contact-Dependent Signaling in *Myxococcus xanthus*: the Function of the C-Signal in Fruiting Body Morphogenesis. In: Myxobacteria: Multicellularity and Differentiation. D. E. Whitworth (ed). Washington, DC: ASM Press, pp. 77 - 91.

Søgaard-Andersen, L. & D. Kaiser, (1996) C factor, a cell-surface-associated intercellular signaling protein, stimulates the cytoplasmic Frz signal transduction system in *Myxococcus xanthus*. *Proc Natl Acad Sci U S A* **93**: 2675-2679.

Søgaard-Andersen, L., F. J. Slack, H. Kimsey & D. Kaiser, (1996) Intercellular C-signaling in *Myxococcus xanthus* involves a branched signal transduction pathway. *Genes Dev.* **10**: 740-754.

Sonenshein, A. L., J. A. Hoch & R. Losick, (1993) *Bacillus subtilis* and Other Gram-Positive Bacteria: Biochemistry, Physiology, and Molecular Genetics. *ASM Press*, Washington, DC.

Steiner, K., R. Novotny, K. Patel, E. Vinogradov, C. Whitfield, M. A. Valvano, P. Messner & C. Schaffer, (2007) Functional characterization of the initiation enzyme of S-layer glycoprotein glycan biosynthesis in *Geobacillus stearothermophilus* NRS 2004/3a. *J Bacteriol* **189**: 2590-2598.

Sudo, S. Z. & M. Dworkin, (1969) Resistance of vegetative cells and microcysts *of Myxococcus xanthus*. *J Bacteriol* **98**: 883-887.

Sun, H. & W. Shi, (2001) Analyses of *mrp* genes during *Myxococcus xanthus* development. *J. Bacteriol.* **183**: 6733-6739.

Sutherland, I. W. & C. L. Mackenzie, (1977) Glucan common to the microcyst walls of cyst-forming bacteria. *J Bacteriol* **129**: 599-605.

Tavazoie, S., J. D. Hughes, M. J. Campbell, R. J. Cho & G. M. Church, (1999) Systematic determination of genetic network architecture. *Nat Genet* **22**: 281-285.

Teintze, M., R. Thomas, T. Furuichi, M. Inouye & S. Inouye, (1985) Two homologous genes coding for spore-specific proteins are expressed at different times during development of *Myxococcus xanthus*. *J Bacteriol* **163**: 121-125.

Tengra, F. K., J. L. Dahl, D. Dutton, N. B. Caberoy, L. Coyne & A. G. Garza, (2006) CbgA, a protein involved in cortex formation and stress resistance in *Myxococcus xanthus* spores. *J Bacteriol* **188**: 8299-8302.

Terai, G., T. Takagi & K. Nakai, (2001) Prediction of co-regulated genes in *Bacillus subtilis* on the basis of upstream elements conserved across three closely related species. *Genome Biol* **2**: RESEARCH0048.

Thony-Meyer, L. & D. Kaiser, (1993) devRS, an autoregulated and essential genetic locus for fruiting body development in *Myxococcus xanthus*. *J Bacteriol* **175**: 7450-7462.

Titus, J. A., W. M. Reed, R. M. Pfister & P. R. Dugan, (1982) Exospore formation in *Methylosinus trichosporium*. *J Bacteriol* **149**: 354-360.

Tudor, J. J. & S. F. Conti, (1977a) Characterization of bdellocysts of *Bdellovibrio sp*. *J Bacteriol* **131**: 314-322.

Tudor, J. J. & S. F. Conti, (1977b) Ultrastructural changes during encystment and germination of *Bdellovibrio sp*. *J Bacteriol* **131**: 323-330.

Ueki, T. & S. Inouye, (2005) Identification of a gene involved in polysaccharide export as a transcription target of FruA, an essential factor for *Myxococcus xanthus* development. *J Biol Chem* **280**: 32279-32284.

Ueki, T., S. Inouye & M. Inouye, (1996) Positive-negative KG cassettes for construction of multi-gene deletions using a single drug marker. *Gene* **183**: 153-157.

Varley, A. W. & G. C. Stewart, (1992) The *divIVB* region of the *Bacillus subtilis* chromosome encodes homologs of *Escherichia coli* septum placement (*minCD*) and cell shape (*mreBCD*) determinants. *J Bacteriol* **174**: 6729-6742.

Varma, A. & K. D. Young, (2004) FtsZ collaborates with penicillin binding proteins to generate bacterial cell shape in *Escherichia coli*. *J Bacteriol* **186**: 6768-6774.

Vasquez, G. M., F. Qualls & D. White, (1985) Morphogenesis of *Stigmatella aurantiaca* fruiting bodies. *J Bacteriol* **163**: 515-521.

Viswanathan, P., T. Ueki, S. Inouye & L. Kroos, (2007) Combinatorial regulation of genes essential for *Myxococcus xanthus* development involves a response regulator and a LysR-type regulator. *Proc Natl Acad Sci U S A* **104**: 7969-7974.

Vobis, G. & C. Zimmermann, (1984) Fine structure of the knobby spore type of *Streptomyces torulosus. Arch Mikrobiol* **138**: 229-232.

Voisin, S., R. S. Houliston, J. Kelly, J. R. Brisson, D. Watson, S. L. Bardy, K. F. Jarrell & S. M. Logan, (2005) Identification and characterization of the unique N-linked glycan common to the flagellins and S-layer glycoprotein of *Methanococcus voltae*. *J Biol Chem* **280**: 16586-16593.

Vollmer, W., D. Blanot & M. A. de Pedro, (2008) Peptidoglycan structure and architecture. *FEMS Microbiol Rev* **32**: 149-167.

Vollmer, W. & J. V. Holtje, (2004) The architecture of the murein (peptidoglycan) in gram-negative bacteria: vertical scaffold or horizontal layer(s)? *J Bacteriol* **186**: 5978-5987.

Waller, L. N., N. Fox, K. F. Fox, A. Fox & R. L. Price, (2004) Ruthenium red staining for ultrastructural visualization of a glycoprotein layer surrounding the spore of *Bacillus anthracis* and *Bacillus subtilis*. *J Microbiol Methods* **58**: 23-30.

Whittenbury, R. & C. S. Dow, (1977) Morphogenesis and differentiation in *Rhodomicrobium vannielii* and other budding and prosthecate bacteria. *Bacteriol Rev* **41**: 754-808.

Whitworth, D. E., (2008) Myxobacteria: Multicellularity and Differentiation. *ASM Press*, Washington, DC.

Wu, S. S. & D. Kaiser, (1996) Markerless deletions of *pil* genes in *Myxococcus xanthus* generated by counterselection with the *Bacillus subtilis sacB* gene. *J. Bacteriol.* **178**: 5817-5821.

Yu, C. S., C. J. Lin & J. K. Hwang, (2004) Predicting subcellular localization of proteins for Gram-negative bacteria by support vector machines based on n-peptide compositions. *Protein Sci* **13**: 1402-1406.

Zilhao, R., M. Serrano, R. Isticato, E. Ricca, C. P. Moran, Jr. & A. O. Henriques, (2004) Interactions among CotB, CotG, and CotH during assembly of the *Bacillus subtilis* spore coat. *J Bacteriol* **186**: 1110-1119.

Zusman, D. R., A. E. Scott, Z. Yang & J. R. Kirby, (2007) Chemosensory pathways, motility and development in *Myxococcus xanthus*. *Nat Rev Microbiol* **5**: 862-872.

CURRICULUM VITAE

PERSONAL DATA

Name	Frank-Dietrich Müller
Date/Place of birth	1973-01-09, Zwickau, Germany

EDUCATION

1991 – 1994	Studies of Management Sciences
	University of Applied Sciences, Meissen, Germany
1994	Graduation: Diplom-Verwaltungswirt
1994 – 1995	Civilian service
1996 – 1999	Administration officer
1999 – 2001	Studies of Biology
	University of Bayreuth, Germany
2001	Vordiplom
2001 – 2004	Studies of Biology, Majors: Microbiology, Genetics and Ecology
	Friedrich-Schiller University Jena, Germany
2003 – 2004	Diploma thesis
	Centre for Environmental Research Leipzig-Halle,
	Dept. Environmental Microbiology, Germany
	Topic: Microbial diversity of an acidic mining lake and changes of community composition caused by *in situ* remediation.
2004	Graduation: Diplom-Biologe
2005 – 2009	Philipps University and Max Planck Institute for Terrestrial Microbiology, Marburg, Germany
	Dept. Ecophysiology
	Supervisor: Dr. Penelope I. Higgs

ERKLÄRUNG

Ich erkläre, dass ich meine Dissertation

„Analyse des Sporulationsprozesses in *Myxococcus xanthus*“

selbstständig, ohne unerlaubte Hilfe angefertigt und mich dabei keiner anderen als der von mir ausdrücklich bezeichneten Quellen und Hilfen bedient habe. Die Dissertation wurde in der jetzigen oder einer ähnlichen Form noch keiner anderen Hochschule eingereicht und hat noch keinen sonstigen Prüfungszwecken gedient.

Marburg, _____

Frank-Dietrich Müller